Electrochemical Society

GLC Anodes Are CUSTOM MADE for JEFFERSON CHEMICALS

The Jefferson Chemical Company Inc., chlor-alkali cell room at Port Neches, Texas

ACCELERATE your cost reduction program by putting GLC custom made anodes to work in your electrolytic cells.

OUR TECHNICAL PERSONNEL can help gear GLC anode characteristics to the goals of longer anode life, longer diaphragm life, reduced power and labor costs.

PRODUCTS ELECTRODE GLC DIVISION YOU CAN TRUST

GREAT LAKES CARBON CORPORATION

18 EAST 48TH STREET, NEW YORK 17, N.Y. OFFICES IN PRINCIPAL CITIES

EDITORIAL STAFF

C. L. Faust, Chairman, Publication Committee
Cecil V. King, Editor
Norman Hackerman, Technical Editor
Ruth G. Sterns, Managing Editor
U. B. Thomas, News Editor
H. W. Salzberg, Book Review Editor
Natalie Michalski, Assistant Editor

DIVISIONAL EDITORS

W. C. Vosburgh, Battery
Milton Stern, Corrosion
R. T. Foley, Corrosion
Louis J. Frisco, Electric Insulation
Seymour Senderoff, Electrodeposition
H. C. Froelich, Electronics
Ephraim Banks, Electronics
Ernest Paskell, Electronics—Semiconductors
Sherlock Swann, Jr., Electro-Organic
Stanley Wawzonek, Electro-Organic
John M. Blocher, Jr., Electrothermics and Metallurgy
J. H. Westbrook, Electrothermics and Metallurgy
N. J. Johnson, Industrial Electrolytic
C. W. Tobias, Theoretical Electrochemistry
A. J. deBethune, Theoretical Electrochemistry
R. M. Hurd, Theoretical Electrochemistry

ADVERTISING OFFICE

ECS

1860 Broadway, New York 23, N. Y.

ECS OFFICERS

Henry B. Linford, President
Columbia University, New York, N. Y.

F. L. LaQue, Vice-President
International Nickel Co., Inc., New York, N. Y.

W. J. Hamer, Vice-President
National Bureau of Standards, Washington, D. C.

Lyle I. Gilbertson, Vice-President
Air Reduction Co., Murray Hill, N. J.

Ernest G. Enck, Treasurer
Felicity Farm, Gwynedd Valley, Pa.

Iver E. Campbell, Secretary
National Steel Corp., Weirton, W. Va.

Robert K. Shannon, Executive Secretary
National Headquarters, The ECS, 1860 Broadway, New York 23, N. Y.

Manuscripts submitted to the Journal should be sent, in triplicate, to the Editorial Office at 1860 Broadway, New York 23, N. Y. They should conform to the revised Instructions to Authors, published on pp. 145C-146C of this issue. Manuscripts so submitted become the property of The Electrochemical Society and may not be published elsewhere, in whole or in part, unless permission is requested of and granted by the Editor.

The Electrochemical Society does not maintain a supply of reprints of papers appearing in its Journal. A photoprint copy of any particular paper, however, may be obtained by corresponding direct with the Engineering Societies Library, 29 W. 39 St., New York 18, N. Y.

Inquiries re positive microfilm copies of volumes should be addressed to University Microfilms, Inc., 313 N. First St., Ann Arbor, Mich.

Walter J. Johnson, Inc., 111 Fifth Ave., New York 3, N. Y., have reprint rights to out-of-print volumes of the Journal, and also have available for sale back volumes and single issues, with the exception of the current calendar year. Anyone interested in securing back copies should correspond direct with them.

Journal of the Electrochemical Society

JULY 1961 **VOL. 108 • NO. 7**

CONTENTS

Editorial

The Indianapolis Meeting 126C

Technical Papers

The Discharge Mechanism of Certain Oxide Electrodes. *H. B. Mark, Jr., and W. C. Vosburgh* 615
The Polarization of Metals in Boiling, Distilled Water. *J. E. Draley, F. E. DeBoer, and C. A. Youngdahl* 622
Hydrated Oxide Films on Aluminum. Their Growth and Their Importance in Electrolytic Capacitors. *D. Altenpohl and W. Post* 628
Immersion Plating of the Platinum Group Metals. *R. W. Johnson* 632
Electroluminescence in Zinc Sulfide as Due to Minority Carrier Injection. *W. A. Thornton* 636
Characteristics of the {111} Surfaces of the III-V Intermetallic Compounds, II. Surface Damage. *H. C. Gatos, M. C. Lavine, and E. P. Warekois* 645
Epitaxial Silicon Films by the Hydrogen Reduction of $SiCl_4$. *H. C. Theuerer* 649
The Preparation and Properties of Some II-V Semiconducting Compounds. *G. A. Silvey, V. J. Lyons, and V. J. Silvestri* 653
Desensitization of Zirconium Powder, Especially Zirconium Powder Used in Primers. *P. Karlowicz, G. Norwitz, and J. Cohen* 659
Anodic Polarization Curves in Molten Carbonate Electrolysis. *G. J. Janz and F. Saegusa* 663
Intermediate Temperature Fuel Cells. *G. V. Elmore and H. A. Tanner* 669
The Temperature Coefficients of Electrode Potentials, II. The Second Isothermal Temperature Coefficient. *G. R. Salvi and A. J. deBethune* 672
Analysis of Galvanostatic Transients and Application to the Iron Electrode Reaction. *J. O'M. Bockris and H. Kita* 676
Characteristic Functions and Parameters in the Theory of Hydrogen Overpotential, III. General Considerations. *G. W. Castellan* 686
The Influence of Ion-Pairs on Reaction Mechanism. The Bromoacetate-Thiosulfate Reaction. *G. Corsaro and M. C. Morris* 689
Limiting Currents for the Reduction of the Tri-iodide Ion at a Rotating Platinum Disk Cathode. *J. D. Newson and A. C. Riddiford* 695
The Kinetics of the Iodine Redox Process at Platinum Electrodes. *J. D. Newson and A. C. Riddiford* 699

Technical Notes

Barrel Plating by Means of Electroless Palladium. *R. N. Rhoda* 707
A Displacement Copper System for the Soldering of "Pure" Aluminum. *S. L. Matlow* 709
Measurement of Thickness of Electroplates Taking Advantage of the Inpedance Change in the Stripping. *U. H. Narayanan, K. Sundararajan, and M. S. Kasabekar* 710
On the Theory of Electroluminescence Deterioration. *P. M. Jaffe* 711
The Use of Thermoelectric Effects during Crystal Growth. *J. R. O'Connor* 713

Brief Communication

Germanium-Doped Gallium Arsenide Tunnel Diodes. *R. Solomon, R. Newman, and N. R. Kyle* 716

Feature Section

The Changing Pattern of Industrial Research—Presidential Address. *R. A. Schaefer* 129C

Current Affairs 133C-146C

Published monthly by The Electrochemical Society, Inc., from Manchester, N. H., **Executive Offices, Editorial Office** and **Circulation Dept.,** and **Advertising Office** at 1860 Broadway, New York 23, N. Y., combining the JOURNAL and TRANSACTIONS OF THE ELECTROCHEMICAL SOCIETY. Statements and opinions given in articles and papers in the JOURNAL OF THE ELECTROCHEMICAL SOCIETY are those of the contributors, and The Electrochemical Society assumes no responsibility for them. Subscription to members as part of membership service; subscription to nonmembers $24.00. Single copies $1.70 to members, $2.25 to nonmembers.

Copyright 1961 by The Electrochemical Society, Inc.

Entered as second-class matter at the Post Office at Manchester, N. H., under the act of August 24, 1912.

Editorial

The Indianapolis Meeting

THE Annual Spring Meeting held in May was eminently successful in attracting both members and non-members to the various sessions, symposia, and feature events. The Divisional Officers merit congratulations for their attractive programs, and the Indianapolis Local Committee for its expeditious handling of registration, information, crowded meeting rooms, lunches, and other facilities for many more people than really were expected to be present. The total registration of more than 1200 is not the record for a Spring Meeting—that record is held by the Washington Meeting of 1957— but some 30 fewer papers were scheduled for presentation than in Washington, and the sessions were finished in three days instead of the usual four.

More people were registered on Sunday than ever before, perhaps because of the three-day session limitation and the fact that the Monday morning talks were not to be missed. On Monday, the Insulation Division, which had asked for a room to accommodate 80 people, found 200 trying to get in. The Fuel Cell Symposium, with a maximum of 200 estimated, had an attendance closer to 300. The Electronics Division had its usual good attendance, and the Theoretical Division Symposium on Techniques was very popular. In fact, at no session did one see, as was common a few years ago, a dozen people in attendance at 9:00 A.M. with eight or ten more drifting in later.

An obvious reason for the high interest in the Meeting is to be found in the nature of the Symposia. Many of the papers presented were not concerned primarily with new research, although some new findings may have been included in them. They were reviews and surveys in various fields of the objectives and the techniques which have been used, with discussion of the theory and of future plans and possibilities. A good example is the Symposium on Modern Instrumentation and Techniques of Electrochemical Measurements. This type of program attracts newcomers and experienced workers as well, because it gives a quick background survey in each field, which would require several hours in the library otherwise. There is additional interest if experts from abroad can attend and present their methods and viewpoints, especially if they customarily publish in languages other than English.

Many of the papers so presented are, of course, not suitable for the JOURNAL, although their content of new experiments and theory will, no doubt, be incorporated in suitable future publications. It is here that the Extended Abstracts, or some form of preprinting, perhaps in even longer version than 1000 or 1500 words, play an important role. These booklets give the listener a record, better than any notes he can take, to look over later (as well as *before* the talks), complete with literature references. The Electronics Division underestimated the number of copies of their Abstracts needed; was sold out on Tuesday. The Theoretical Division had only a few copies left. These preprints fill an obvious wish and need, and must be encouraged.

—CVK

PIONEERING

AT BELL TELEPHONE LABORATORIES

In such an open field as this Dr. Karl Jansky of Bell Laboratories opened the way to radio astronomy. His search for a mysterious source of radio noise led him—and us—to the stars for our answer.

Today Bell scientists continue their pioneering in many fields—among them the transmission of human voices on beams of coherent light. Bell Laboratories' revolutionary Optical Maser foreshadows the use of light as a whole new medium of telephone, TV and data communications.

These are but two of the many fundamental advances which have come from breaking fresh ground at the world center of communications research and development.

ANACONDA PURE COPPER *Electranodes*

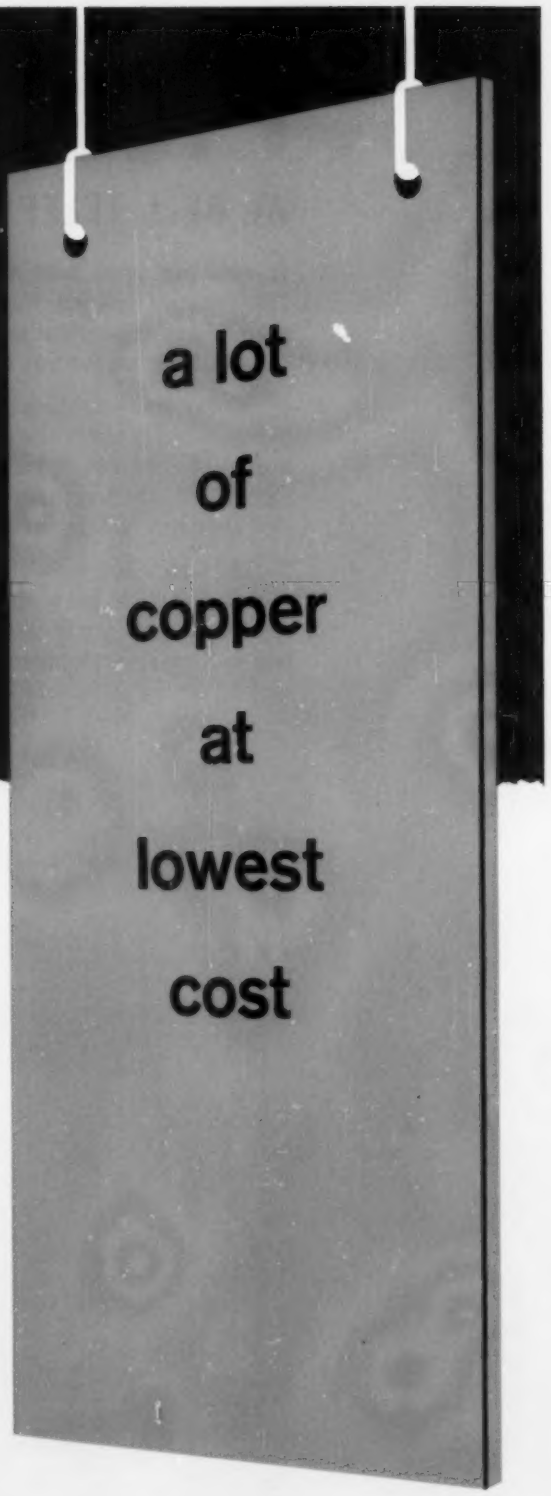

Now . . . pure copper anodes available in the lowest price range! Developed solely for the plating trade, Anaconda Electranodes are produced from full 1″ thick electro-deposited copper.

QUICK FACTS

Economical—in the lowest price range of any copper anodes of similar thickness.

Highest Commercial Purity—made from virgin metal of 99.925% minimum purity.

Ample Thickness—to drill and tap holes for insertion of suspension hooks.

Oxygen-Free—suitable for both acid and cyanide plating.

Dense Structure—no porosity.

Here, for the first time, is high-quality electrolytic copper available in full 1″ thickness that cuts handling time, lowers costs. Electranodes can be used in any plating operation where a flat anode will fill requirements. If you want an economy type anode, Electranodes offer you the finest quality at the lowest possible cost.

Write for Electranode Specification Form. We'll follow up with prompt price and delivery information on Electranodes to meet your specific needs. Address: Anaconda American Brass Company, Waterbury 20, Conn. In Canada: Anaconda American Brass Ltd., New Toronto, Ontario. 61-812

ANACONDA®

AMERICAN BRASS COMPANY

The Discharge Mechanism of Certain Oxide Electrodes

Harry B. Mark, Jr. and W. C. Vosburgh

Department of Chemistry, Duke University, Durham, North Carolina

ABSTRACT

The discharges of PbO_2, TiO_2, and Tl_2O_3 electrodes were studied and are compared with similar discharges of the MnO_2 electrode. The overpotentials of PbO_2 and TiO_2 electrodes at small current densities are linear functions of the current density, but Tl_2O_3 is like MnO_2 in having a square-root relation. It is considered that the first step in the electrode reaction is reduction to a lower oxide or hydroxide and that the subsequent disposal of this is rate-determining. The square-root relation is correlated with the existence of an unstable valence state between the initial and final products. A few experiments with $Ce(OH)_4$ and SnO_2 electrodes were carried out, but these were less satisfactory as current-producing electrodes than the others.

It is of interest to inquire how much alike various oxide electrodes are in their discharge processes. The discharge of the MnO_2 electrode in acid electrolytes has been studied in this laboratory and a theory of the process has been proposed (1, 2). The polarization is considered to be almost entirely a solid-state concentration polarization under the experimental conditions. In the present investigation, the discharge of three other oxide electrodes have been studied under similar conditions. The theory proposed for MnO_2 can be applied also to Tl_2O_3, PbO_2, and TiO_2 with minor alternations. A few experiments were carried out with $Ce(OH)_4$ and SnO_2 electrodes. All of these electrodes resemble MnO_2 in having a compound of intermediate valence as the product of the first reduction step rather than being reduced directly to a metal.

Preparation of Electrodes

Lead dioxide electrodes.—A Pt tube 5.0 mm in outside diameter and 51.5 mm long was sealed by glyptal cement to a Pyrex tube at the top and to a glass plug at the bottom. Electrical contact was made through the glass tube to the interior of the Pt tube. The Pt then was plated with rough-surfaced gold from a bath of $AuCl_3$ at room temperature. This electrode had very nearly the same dimensions and apparent surface area (8 cm^2) as the graphite electrodes used in previous work (3) for the preparation of MnO_2 electrodes. The PbO_2 was electrodeposited on the gold surface from a solution of 0.0057M $Pb(NO_3)_2$ and 0.12M HNO_3 with a current density of 10 ma/electrode (1.25 ma/cm^2) for 30 or 40 min at room temperature. With these conditions the deposit was probably β-PbO_2 (4, 5). The experience gained in seeking satisfactory conditions was compatible with the data of Shibasaki (6). A deposit with different discharge characteristics, and presumed to be α-PbO_2, was obtained from a bath of 1.5M NH_3 and 6.5M $NH_4C_2H_3O_2$ saturated with $Pb(C_2H_3O_2)_2$ with current density of 10 to 50 ma/electrode for 40 to 60 min, or from a bath of 100 g/l of $Pb(OH)_2$ and 200 g/l NaOH with current density of 10 ma/electrode for 40 min (4).

Titanium dioxide electrodes.—Electrodeposits of TiO_2 did not adhere well to the gold-plated electrodes, but were satisfactory on graphite. As in previous work (3) graphite rods of spectrochemical grade 4.8 mm in diameter were sealed by glyptal cement into short pieces of glass tube so that 52 mm projected at the bottom and enough at the top for electrical connections. The bottom portions of the rods were plated with TiO_2 from a solution of 0.01M $TiCl_3$ and 0.6M HCl with a current density of 1 ma/electrode for 6 to 24 hr. This was followed by anodic oxidation in 0.24M HCl until bubbles of oxygen were evolved. One electrode of a number plated in this way was blue in color while the others, which will be called normal, did not differ noticeably in appearance from the graphite. Blue TiO_2 could be prepared from a bath containing H_3AsO_4, but such electrodes were not reproducible in properties. Blue TiO_2 also could be prepared by heating normal TiO_2 electrodes in a vacuum for 1 to 3 days at 140°-200°C. Some TiO_2 electrodes were prepared with foreign cations in the plating bath. These were not blue, but were different from the normal.

Since the normal TiO_2 electrodes did not differ in appearance from unplated graphite a test was made to see whether they were in fact different. An unplated graphite electrode was given the anodic oxidation treatment and placed in a discharge cell in $TiCl_3$ electrolyte. The initial open-circuit potentials of both graphite and TiO_2 electrodes were much too high and were probably oxygen potentials. On passage of current the unplated electrode showed no discharge capacity, whereas normal TiO_2 electrodes after a short discharge attained reproducible open-circuit potentials and showed reasonable discharge capacities. The conversion of normal to blue TiO_2 is also evidence of a real deposit, since the blue TiO_2 was visible.

Thallium oxide electrodes.—A satisfactory dark-gray electrodeposit of Tl_2O_3 was obtained on gold-plated platinum from an electrolyte of 0.02M Tl_2SO_4 and 0.75M NaOH. The deposit was hard and adhered tightly to the gold.

Tin oxide and cerium hydroxide electrodes.—Electrodeposits of SnO_2 on graphite were obtained from an electrolyte of 0.1M $SnCl_2$ and 0.07M HCl with a current of 0.8 ma/electrode for 20 hr. The deposit was white and powdery and did not adhere well.

Electrodeposits which were probably $Ce(OH)_4$ (7) were obtained on gold-plated platinum from a neutral solution containing Ce(III). The deposit was greenish yellow and gelatinous and did not adhere well. It dissolved slowly in solutions of pH 3 or less.

Discharge Overpotential of Lead Dioxide Electrodes

Self-discharge.—Beck, Jones, and Wynne-Jones (8) in studying PbO_2 electrodes made by anodic oxidation of Pb found a rate of self-discharge equivalent to a current of 0.75 ma/cm^2. This was determined by measuring the electrical output of the electrode as a function of rate of discharge. Since correction of their overpotential data for self-discharge altered the relation of overpotential to current considerably, it was important to measure the rate of self-discharge of the electrodes used in the present investigation.

Discharge of PbO_2 electrodes in 0.1M H_2SO_4 electrolyte to zero potential measured against a Hg_2SO_4 reference electrode gave electrical outputs varying inversely with the current and considerably smaller than the theoretical capacity calculated from the data on preparation of the electrodes. Discharge conditions are described below and were similar to those previously used for MnO_2 electrodes (9). Electrodes prepared with a current of 10 ma/electrode for 30 min gave outputs varying from 116 to 182 ma-min as the current varied from 7 to 1 ma. However, considerable undischarged PbO_2 remained on the electrodes at the end of the discharge, as shown by liberation of I_2 from an acidified KI solution.

When the amount of PbO_2 on undischarged electrodes was determined by a colorimetric method (10) it was found to be 0.111 ± 0.007 milliequivalents instead of 0.188 as calculated for 100% charging efficiency. When the PbO_2 remaining after discharge was determined by the same colorimetric method, and this amount added to the PbO_2 calculated from the electrical output, the sum was within the experimental error of 0.111 milliequivalent for all current densities. The self-discharge was therefore too small to be measured by a discharge procedure.

The failure of PbO_2 electrodes to discharge completely and the variability of the amount of undischarged residue is worthy of note, because the same phenomena have been observed for MnO_2 electrodes discharging in acid electrolyte (11).

A more satisfactory measure of the self-discharge of PbO_2 was obtained by determination of the Pb(II) formed by a colorimetric procedure using dithizone (10). A freshly plated electrode was made the anode in the electrolysis of dilute HNO_3 until O_2 was evolved freely to insure absence of Pb(II). It then was placed in 20 ml of 0.15M $HClO_4$ and after a few days was removed, washed, and transferred to another portion of the $HClO_4$ solution, and later in the same way to a third, fourth, and fifth solution. The Pb(II) found in the $HClO_4$ solution was proportional to the time of contact with the electrode and averaged 0.15 mg in 10^5 sec, which is equivalent to a discharge current of 1.4×10^{-3} ma/electrode or 1.8×10^{-4} ma/cm^2.

In the overpotential measurements, discharge currents of 0.3-3 ma/electrode were used in the most important experiments, and currents of 0.05-0.4 ma/electrode in a less important series. Therefore, the self-discharge was considered negligible and no correction was made for it.

Overpotential measurements.—For discharge the electrode under test was mounted in a rubber stopper fitting a 300-ml electrolytic beaker so that the electrode was located centrally in the beaker. A cylindrical sheet-lead anode lined the inside of the beaker. A Luggin capillary with its end at a distance from the test electrode equal to about four times its diameter led to a reference electrode of Hg and Hg_2SO_4 in a 0.1M H_2SO_4 electrolyte. An inlet tube was provided for the introduction of a stream of nitrogen which provided the stirring.

Electromotive forces were measured by a L&N Speedomax recording potentiometer. For the larger overpotentials an instrument sensitive to about 1 mv was used. For the smaller, and for observation of the growth and decay of PbO_2 electrode polarization a recorder with a 10-mv range was combined with a Type K potentiometer. This recorder had a fast chart speed, 5 cm/min, and was sensitive to about 0.01 mv.

Currents for discharge were furnished by three dry cells in series with the appropriate resistance and measured by a calibrated milli- or microammeter. The current was maintained constant manually.

When an electrode in the discharge cell had come to open-circuit equilibrium, as shown by constancy of potential for 15 min, a current was passed until a constant closed-circuit potential was attained. Then the circuit was broken and the electrode allowed to reattain a constant open-circuit potential. The difference between the equilibrium open-circuit potential after discharge, E_o, and the steady-state closed-circuit potential, E_p, was taken as the overpotential. The open-circuit potential after discharge was chosen on the assumption that appreciable changes in open-circuit potential between the final closed-circuit measurement and the subsequent open-circuit measurement were improbable.

When the first overpotential measurement was completed a second was made, usually with a different current. Then a third and as many more as possible were made without a change in the characteristics of the electrode. To insure against errors from permanent changes in the electrode one of the early measurements always was repeated later. Only if the two overpotentials agreed within 3 mv was the series accepted as valid. In a long series of measurements the overpotentials usually increased eventually.

Since the apparatus was like that used previously for the similar study of MnO_2 electrodes, and since

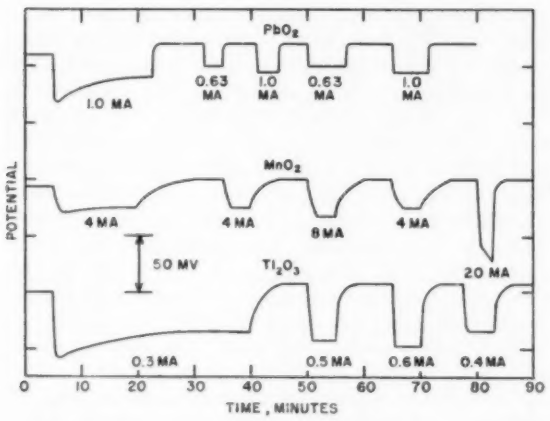

Fig. 1. Open- and closed-circuit potentials in successive short discharges of single electrodes of PbO_2, MnO_2, and Tl_2O_3 plotted against time. The PbO_2 and MnO_2 electrodes were discharged in acid electrolyte and the Tl_2O_3 electrode in alkaline.

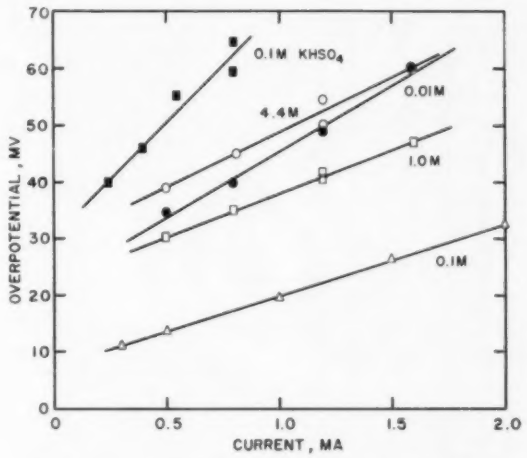

Fig. 2. Overpotentials of PbO_2 electrodes plotted against current per electrode of 8 cm^2 area; electrolytes: ●, 0.01M H_2SO_4; △, 0.1M H_2SO_4; □, 1.0M H_2SO_4; and O, 4.4M H_2SO_4, all with excess $PbSO_4$; and ■, 0.1M $KHSO_4$ and 0.1M K_2SO_4.

the electrolyte concentrations were comparable (1) and the currents small, the estimate of negligible corrections for iR and electrolyte concentration polarization should apply to the present work.

Figure 1 illustrates the results obtained. The upper curve is for a β-PbO_2 electrode; the electrode potential is plotted against total time elapsed. The beginning of current flow is indicated by an abrupt decrease in potential and the opening of the circuit by an abrupt increase. The discharge current in milliamperes per electrode is given for each discharge. The middle curve is the similar one for γ-MnO_2 discharging in 1M H_2SO_4 and 0.1M $MnSO_4$ (1). The lowest curve is for a Tl_2O_3 electrode discharging in 0.002M Tl_2SO_4 and 1.2M NaOH. A comparison of the overpotential magnitudes on the basis of the data of Fig. 1 is of little value because the true surface areas are unknown.

It is shown in Fig. 1 that in the first discharge of each of the three electrodes the potential passed through a minimum. Subsequent discharges do not show a minimum. However, for both β-PbO_2 and γ-MnO_2 the use of the more sensitive measuring instrument revealed slight minima in discharges after the first. If a β-PbO_2 electrode stood overnight after one or more discharges the first subsequent discharge showed an appreciable minimum, but it was not as large as in the original discharge.

From discharge curves such as shown in Fig. 1 the relation of the overpotential of β-PbO_2 to the current was obtained for currents between 0.038 and 0.38 ma/cm^2 (0.30 and 3.0 ma/electrode). The electrodes became unreliable when currents larger than 3 ma/electrode were passed. Some representative results for an electrolyte of 0.1M H_2SO_4 saturated with $PbSO_4$ and containing excess suspensed solid are given in Table I.

Different β-PbO_2 electrodes did not agree in overpotential, as shown in Table I. In Fig. 2 the data in Table I for electrode 1 are plotted, along with similar data for electrolytes of other concentrations of H_2SO_4 and one of $KHSO_4$ and K_2SO_4, all saturated with $PbSO_4$. A single electrode was used for 0.01, 1.0, and 4.4M H_2SO_4 electrolytes to minimize errors from the lack of reproducibility of different electrodes. If Table I is fairly representative of the variation of different electrodes, and of the 0.1M H_2SO_4 overpotential, it must be concluded that the overpotential is not any simple function of the H_2SO_4 concentration. Of the concentrations tried 0.1M H_2SO_4 gave the lowest overpotential and the $KHSO_4$ and K_2SO_4 solution the highest.

In all cases a plot of overpotential against current density, or current per electrode, was a straight line within the limit of error. Because of the limited range of currents, plotting against the square root of the current gave as good a straight line for electrode 2 (Table I) but only fairly satisfactory ones for the others. For MnO_2 electrodes discharging in acid electrolyte the overpotential is a linear function of the square root of the current density (2). For neither electrode is the relation of overpotential to the logarithm of the current density linear.

When currents greater than 3 ma/electrode were passed the closed-circuit potential did not become constant but decreased as in the discharge of the MnO_2 electrode at 20 ma (Fig. 1). Electrodes always were damaged by such a discharge, and subsequent discharges at lower currents gave overpotentials that were too large and not reproducible. The PbO_2

Table I. Variation of the overpotential of β-PbO_2 electrodes with current density in an electrolyte of 0.1M H_2SO_4 saturated with $PbSO_4$

Current, ma/cm^2	Overpotential, mv		
	Electrode 1	2	3
0.038	11, 11	—	—
0.063	14, 14	16	7, 8
0.094	—	21	—
0.125	20	24, 26	11, 12
0.188	27	30	16
0.25	33, 34	35	20
0.31	36	40	—
0.38	—	45	28

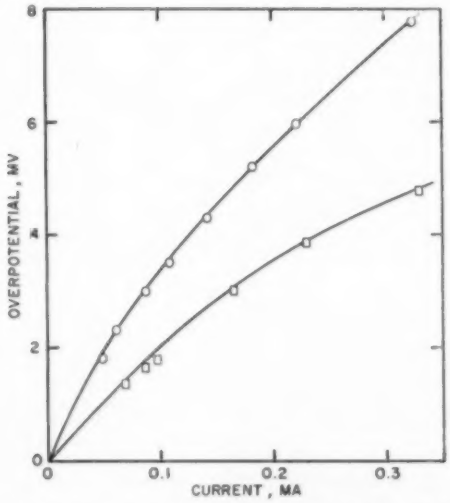

Fig. 3. Relation between the overpotential of the PbO_2 electrode and current per electrode in the region of small currents. The two curves represent two different electrodes.

deposit of damaged electrodes was loosened from the gold surface.

Discharge of a PbO_2 electrode in an electrolyte of 0.10M HNO_3 and 0.05M $Pb(NO_3)_2$ gave overpotentials as nearly like those in 0.1M H_2SO_4 as could be expected of different electrodes. In 0.15M $HClO_4$ and 0.10M $Pb(ClO_4)_2$, however, currents a tenth of those used for 0.1M H_2SO_4 electrolytes (Table I) gave overpotentials of the same order of magnitude as for the H_2SO_4. This was true also of 6M $HClO_4$ electrolyte, but in 1.0M $HClO_4$ and 0.1M $Pb(ClO_4)_2$ currents of 2-12 ma/electrode were required for overpotentials of this order of magnitude. Since the same electrode was used for the three $HClO_4$ electrolytes the large difference cannot be ascribed to the variation of electrodes.

To investigate the region of smaller currents and overpotentials two series of measurements were made with the 0.1M H_2SO_4 electrolyte by means of the more sensitive recording potentiometer with currents of 0.006-0.05 ma/cm^2 which gave overpotentials of 1-8 mv. Figure 3 shows the relation between overpotential and current, which is expressed by curved lines that can be extrapolated to the origin.

Growth and decay of polarization.—The time involved in the growth and decay of polarization of PbO_2 electrodes was observed in connection with the overpotential measurements with small currents. Figure 4 shows 3 growth curves for β-PbO_2 electrodes in different electrolytes and one for α-PbO_2. These were taken from curves made on the recording potentiometer with the faster chart speed and greater sensitivity. The discharges represented were not the first discharges of the respective electrodes.

The potentials of the β-PbO_2 electrodes all passed through minima like the minima found for γ-MnO_2 in discharges after the first (1). Small minima like that of curve 2, Fig. 4, were not detectable by the less sensitive recording potentiometer, and so are

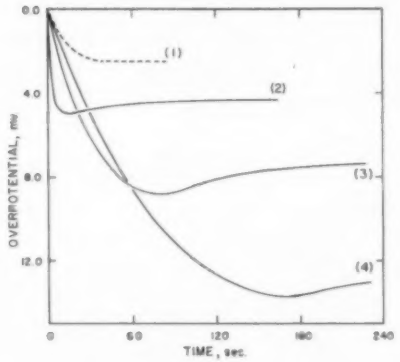

Fig. 4. Growth of polarization of PbO_2 electrodes; curve 1, α-PbO_2 in 0.1M H_2SO_4, 0.30 ma/electrode; curve 2, β-PbO_2 in 0.1M H_2SO_4, 0.050 ma/electrode; curve 3, β-PbO_2 in 0.01M H_2SO_4, 0.050 ma/electrode; curve 4, β-PbO_2 in 0.1M $KHSO_4$, 0.1M K_2SO_4, 0.050 ma/electrode; all electrolytes saturated with $PbSO_4$.

not shown in Fig. 1. The time required for the attainment of the minimum potential varied inversely with the acidity from 15 to 170 sec. Only a negligible part of the overpotential was established too rapidly to be followed by the recorder at the lower acidities.

The decay of polarization of a β-PbO_2 electrode is shown in Fig. 5 for three current densities. The initial potentials of the decay curves were the same within the limit of error as the steady-state potentials during current flow.

Experiments with α-PbO_2.—Overpotentials of α-PbO_2 electrodes were not reproducible and the open-circuit potentials were not constant. The overpotentials were considerably smaller than for β-PbO_2. No potential minimum in an α-PbO_2 discharge was observed. A representative α-PbO_2 discharge curve is shown in Fig. 4.

Discharge Overpotential of Titanium Dioxide Electrodes

For present purposes the discharge of a TiO_2 electrode is taken to mean the reduction of the TiO_2 by analogy with the PbO_2 electrode. For overpotential measurements the electrolyte was 0.03M $TiCl_3$ and 0.56M HCl. The anode consisted of 8 graphite rods surrounding the TiO_2 electrode. A saturated calomel electrode was used as the reference electrode.

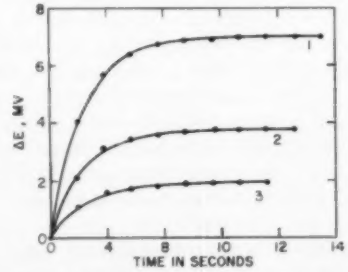

Fig. 5. Change of potential, ΔE, of a β-PbO_2 electrode with time on open circuit, starting with the steady-state closed-circuit potential. Curve 1, polarized at 0.225 ma; 2, at 0.109 ma; and 3 at 0.050 ma/electrode (8 cm^2). The points were taken from a recorder graph.

The open-circuit potentials of both normal and blue TiO_2 electrodes were much too high when they were first put into the electrolyte, but fell to constant values (−0.7 v and −0.5 v, respectively) in about an hour. The negative sign indicates that the TiO_2 electrode was negative with reference to the calomel electrode. When Mg^{++} was present in the plating bath the initial open-circuit potential was above + 0.6 v, and it decreased very slowly. A short discharge at 0.6 ma decreased the potential rapidly to below − 0.9 v, and subsequently on open circuit the potential became constant within the normal range. Similar abnormal electrodes were obtained when Al^{+++} and H_3PO_4 were in the plating bath, but with Mn^{++}, Zn^{++}, Ba^{++}, and Li^+ the TiO_2 produced seemed normal.

For overpotential measurements an electrode was kept on open circuit until its potential had remained constant for 15 min, then a series of short discharges and recoveries was begun, as for PbO_2 electrodes. The results obtained are illustrated in Fig. 6, which shows curves similar to those of Fig. 1, for normal and blue TiO_2. The overpotential of the normal TiO_2 electrode was much larger than that of β-PbO_2, but smaller than that of blue TiO_2.

Duplicate measurements at the same current density for the same normal electrode agreed within 2 mv, but different electrodes differed by about as much as did different PbO_2 electrodes. Figure 7 shows overpotential data for three normal TiO_2 electrodes and one blue electrode which was made by electrodeposition. The discharge overpotential of the TiO_2 electrode is a linear function of the current, but not of the square root of the current.

Discharge Overpotential of Thallium (III) Oxide Electrodes in Alkaline Electrolyte

The Tl_2O_3 electrodes in an electrolyte of 0.002M Tl_2SO_4 and 1.2M NaOH were quite reproducible in open-circuit potential. Against a reference electrode of Hg, Hg_2SO_4, and 0.1M Na_2SO_4, the potential was -0.520 ± 0.005 v, without correction for liquid junction potential.

For the overpotential measurements, current was passed between Tl_2O_3 electrodes and carbon anodes

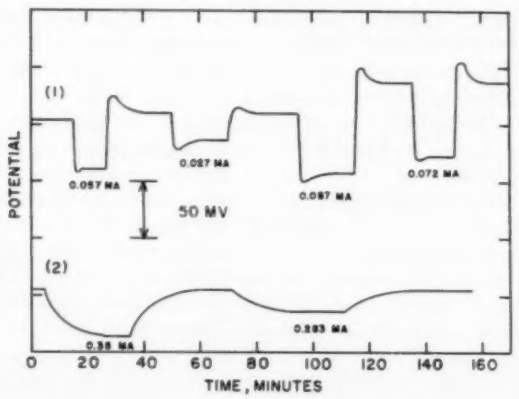

Fig. 6. Open- and closed-circuit potentials in successive discharges of single electrodes of: 1, blue TiO_2 and 2, normal TiO_2 in acid electrolyte containing $TiCl_3$.

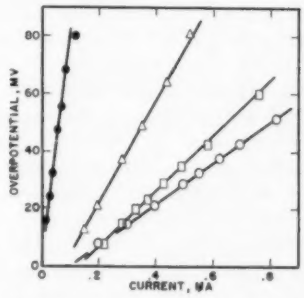

Fig. 7. Relation between the overpotential of normal TiO_2 electrodes (O, □, △) and a blue TiO_2 electrode (●) and the current per electrode (8 cm^2).

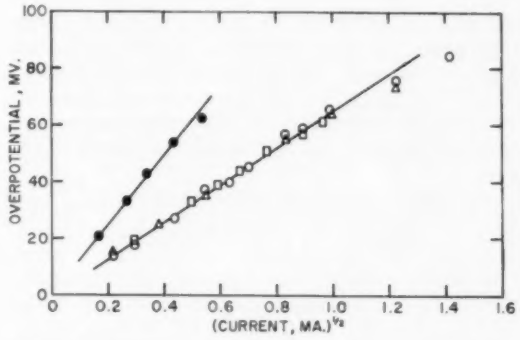

Fig. 8. Relation between the overpotential of Tl_2O_3 electrodes in alkaline electrolyte and the square root of the current per electrode.

(arranged as for TiO_2) in the direction to reduce the Tl(III). Alternate open- and closed-circuit measurements gave results such as shown in Fig. 1. The over-potentials of three electrodes agreed within 3 mv, but a fourth was different. The overpotentials are shown in Fig. 8 plotted against the square root of the current per electrode. Plotting against the first power of the current density gives a curve.

Cerium (IV) Hydroxide and Tin (IV) Oxide Electrodes

Overpotential measurements for $Ce(OH)_4$ electrodes in an electrolyte of $(NH_4)_2SO_4$ buffered at pH 5 with pyridine and pyridinium sulfate were unsatisfactory. Currents larger than 0.001 ma damaged the electrodes, and the overpotential at this current was 20-30 mv. Growth and decay of polarization were slow.

The growth and decay of polarization of SnO_2 electrodes were so slow that a series of measurements was not attempted. A fairly reproducible overpotential of 85 mv was measured for a current of 0.022 ma.

Discussion

The Overpotential.—It has been assumed previously that in the early part of the discharge of electrodeposited γ-MnO_2 electrodes in ammonium salt electrolyte at pH 7-8 the following reaction takes place (12, 13).

$$MnO_2 + H^+ + e^- \longrightarrow MnOOH \qquad [1]$$

The formula MnOOH is used here as the simplest representation of a Mn(III) reduction product formed within the MnO_2 lattice and to some extent on the surface exposed to the electrolyte. The electrode potential accordingly decreases. Part of the decrease is designated as overpotential and on opening the circuit the overpotential decays because of solid-state diffusion of the excess of MnOOH near the surface into the interior (14). The diffusion may involve the movement of only protons and electrons. At equilibrium the oxide has a lower available oxygen content than the original and gives a lower electrode potential. The open-circuit potential during part of the discharge is proportional to the amount of discharge (2).

Later in the discharge when the closed-circuit potential has fallen by 0.2 to 0.3 v a second reaction takes place, and Mn^{++} begins to appear in the electrolyte. This may be attributed to the following reaction [2] or [3], or perhaps both, combined with reaction [4]. The formula $Mn(OH)_2$ designates a Mn(II) compound on or below the surface of the oxide.

$$2MnOOH \longrightarrow MnO_2 + Mn(OH)_2 \qquad [2]$$

$$MnOOH + H^+ + e \longrightarrow Mn(OH)_2 \qquad [3]$$

$$Mn(OH)_2 + 2NH_4^+ \longrightarrow Mn^{++} + 2H_2O + 2NH_3 \qquad [4]$$

In the early part of the discharge the slow step in the electrode process must be the diffusion, which goes on for a long time (4-40 days) after the breaking of the circuit. Later in the discharge Mn^{++} is produced both during current flow and after its termination. Therefore, either reaction [2] or [4] must be slow. Diffusion must be involved, but whether it is rate-determining is not clear. There is evidence that the amount of lower oxide on the surface is a small fraction of the total (13).

As the pH of the electrolyte decreases there is no evidence of an abrupt change in mechanism. The portion of the discharge during which no Mn^{++} is formed decreases. In the more acid solutions the slow step may be considered to be

$$2MnOOH + 2H^+ \longrightarrow MnO_2 + Mn^{++} + 2H_2O \qquad [5]$$

Below pH 3 the mechanism leading to the formation of Mn^{++} accounts for all of the electrode reaction and the decay of overpotential; the open-circuit potential does not decrease as the discharge proceeds.

A quantitative relation of overpotential to current was derived on the basis of the above mechanism for discharges in electrolytes of pH less than 3. Reaction [5] was assumed to be the slow step and the overpotential was predicted to be proportional to the square root of the current density. This was in agreement with experiment except at very low overpotentials, where one of the assumptions was questionable.

It is of interest to inquire whether the discharge mechanism and the assumptions proposed for the MnO_2 electrode can be applied to the three similar electrodes of the present investigation. The overpotential of the Tl_2O_3 electrode is a linear function of $i^{1/2}$ like the MnO_2 electrode, but the TiO_2 electrode has a first-power relation. The PbO_2 electrode is somewhat uncertain, but probably has a first-power relation. Examination of the derivation (2) will show that, if a reaction similar to reaction [4] had been assumed as the slow step instead of reaction [5], the overpotential would have been proportional to the first power of the current. The difference is that the velocity of reaction [5] was assumed proportional to the square of the Mn(III) concentration, whereas that of reaction [4] can be assumed proportional to the concentration. Reactions similar to reaction [5] are possible only when the primary discharge product is an unstable product intermediate in valence between the initial and final products. There can be no such substance in the partial reduction of TiO_2 since the final product is a Ti(III) compound. Therefore, the disposal of a Ti(III) oxide or hydroxide is the slow step and the theory predicts a first-power relation, in accordance with Fig. 7.

Since the overpotential of the Tl_2O_3 electrode is proportional to the square root of the current (Fig. 8), the theory requires an unstable intermediate form between the Tl(III) and Tl(I) states. A Tl(II) valence state has been postulated in kinetic studies (15-17) and is mentioned by Latimer (18). It may be postulated here that a Tl(II) oxide or hydroxide is formed within the Tl_2O_3 structure and in the steady state of polarization disproportionates as fast as formed to give the soluble TlOH.

The assumption of direct reduction of PbO_2 to a Pb(II) compound would imply that electrons are added in pairs. On the other hand, if Pb(III) exists it must be only a transitory state. The slow step in the discharge of the PbO_2 electrode may be either the charge transfer or the slow reaction of $Pb(OH)_2$ within the PbO_2 lattice with acid. In the former case a linear relation of overpotential to current would be expected if the true current density is small. The effect of the acidity of the electrolyte on the overpotential is best understood in terms of its effect on the rate of reaction of $Pb(OH)_2$ with acid. If this reaction is the slow step, the PbO_2 electrode resembles the TiO_2 electrode, and a first-power relation of overpotential and current would be expected. Only if a slowly reacting Pb(III) intermediate were formed could we expect a square-root relation.

The semiconductivity of the oxides and the electrode characteristics.—It is essential to the theory of oxide electrodes given above that the oxide be an electronic semiconductor so that the electrons can pass through it. While no precise values for the conductances of particular oxides can be given without measurements, some of the oxides used in this investigation differ so much that a qualitative comparison can be made on the basis of literature values. The best semiconductor is PbO_2 with unusually large conductivity (19, 20). Next best are Tl_2O_3, MnO_2 and blue TiO_2, which are fairly good conductors (20-22) while TiO_2, CeO_2, and SnO_2 are much poorer than these (23, 22, 20). The $Ce(OH)_4$ and SnO_2 electrodes would pass only very small currents and had large overpotentials and slow growth

and decay of polarization. It is uncertain whether electrodeposited TiO_2 is more like the blue TiO_2 or the TiO_2 for which the semiconductivity was measured.

The minimum in the discharge curve.—It has been noticed previously (24, 1) that in the discharge of β-PbO_2 and γ-MnO_2 electrodes in acid electrolytes the electrode potential passes through a minimum before the attainment of a steady state. In the present investigation minima were found in the discharges of β-PbO_2 in all electrolytes, Tl_2O_3 (in alkaline electrolyte) and blue TiO_2, and were not observed for normal TiO_2 and α-PbO_2. When γ-MnO_2 is discharged in NH_4Cl or $(NH_4)_2SO_4$ electrolyte there is a minimum if the *p*H is 4 or 5, but none at *p*H 7-8 (25, 26). On the other hand α-MnO_2 shows no minimum in either acid or $(NH_4)_2SO_4$ electrolyte (26).

Nucleation has been suggested as an explanation of the minimum in the PbO_2 discharge curve (24). While nucleus formation could be expected to lead to such a phenomenon, it is difficult to see what nuclei are formed in the β-PbO_2 discharge in HNO_3 and $HClO_4$ electrolytes and on this basis why no minima are observed for α-PbO_2, α-MnO_2, and normal TiO_2.

Another phenomenon that may be connected with the minimum is the expansion of the crystal lattice on discharge which was observed for MnO_2 by Brenet (27) and Neuman and Fink (28), provided that it can be demonstrated that the other oxides act likewise. Brenet found the expansion less pronounced for α-MnO_2 than for γ-MnO_2 in agreement with the data on the minima. The loosening of electrodeposited PbO_2 from its cylindrical support by excessive current and the similar damage to γ-MnO_2 can be understood on this basis.

Acknowledgment

This work was supported in part by the Office of Ordnance Research.

Manuscript received July 8, 1960; revised manuscript received March 8, 1961. Part of this paper was prepared for delivery before the Columbus Meeting, Oct. 9-13, 1959. Based on a thesis submitted to the graduate faculty of Duke University in partial fulfillment of the requirements for the degree of Doctor of Philosophy by H. B. Mark, Jr.

Any discussion of this paper will appear in a Discussion Section to be published in the June 1962 JOURNAL.

REFERENCES

1. S. Yoshizawa and W. C. Vosburgh, *This Journal*, **104**, 399 (1957).
2. W. C. Vosburgh and J. H. DeLap, *ibid.*, **107**, 255 (1960).
3. D. T. Ferrell, Jr., and W. C. Vosburgh, *ibid.*, **98**, 335 (1951).
4. A. I. Zaslavskii, Yu. D. Kondrashov, and S. S. Tolkachev., *Doklady Akad. Nauk S.S.S.R.*, **75**, 559 (1950); *Chem. Abstracts*, **45**, 2739 (1951).
5. H. Bode and E. Voss, *Z. Elektrochem.*, **60**, 1053 (1956).
6. Y. Shibasaki, *This Journal*, **105**, 624 (1958).
7. D. M. Yost, H. Russell, Jr., and C. S. Garner, "The Rare-Earth Elements and Their Compounds," p. 60, John Wiley & Sons, Inc., New York (1947).
8. W. H. Beck, R. Jones, and W. F. K. Wynne-Jones, *Trans. Faraday Soc.*, **50**, 1249 (1954).
9. A. M. Chritzberg, Jr., D. R. Allenson, and W. C. Vosburgh, *This Journal*, **102**, 557 (1955).
10. F. D. Snell and C. T. Snell, "Colorimetric Methods of Analysis," 3rd ed., Vol. II, p. 43, D. Van Nostrand Co., New York (1949).
11. S. Hills, Ph. D. Thesis, Duke University, 1956, p. 49.
12. W. C. Vosburgh, *This Journal*, **106**, 839 (1959).
13. W. C. Vosburgh and P. S. Lou, *ibid.*, **108**, 485 (1961).
14. A. B. Scott, *ibid.*, **107**, 941 (1960).
15. K. G. Ashurst and W. C. E. Higgonson, *J. Chem. Soc.*, **3044** (1953).
16. F. R. Duke and B. Bornong, *J. Phys. Chem.*, **60**, 1015 (1956).
17. J. Bednar, *Collection Czechoslov. Chem. Communs.*, **24**, 1240 (1959); *Chem. Abstracts*, **53**, 11081 b (1959).
18. W. M. Latimer, "Oxidation Potentials," 2nd ed., p. 163, Prentice-Hall, Inc., New York (1952).
19. U. B. Thomas, *Trans. Electrochem. Soc.*, **94**, 42 (1948).
20. M. LeBlanc and H. Sachse, *Physik. Z.*, **32**, 887 (1931).
21. R. Glicksman and C. K. Morehouse, *This Journal*, **103**, 149 (1956).
22. M. Foëx, *Bull. soc. chim.*, [5], **11**, 6 (1944).
23. P. W. Bridgman, *Proc. Am. Acad. Arts Sci.*, **79**, 127 (1951).
24. W. H. Beck, R. Lind, and W. F. K. Wynne-Jones, *Trans. Faraday Soc.*, **50**, 147 (1954).
25. A. M. Chritzberg, Jr., and W. C. Vosburgh, *This Journal*, **104**, 1 (1957).
26. A. Kozawa and W. C. Vosburgh, *ibid.*, **105**, 63 (1958).
27. J. Brenet, Proc. Intern. Comm. Electrochem. Thermodynam. and Kinetics, 8th Meeting, Madrid, 1956, p. 394.
28. K. Neumann and W. Fink, *Z. Elektrochem.*, **62**, 114 (1958).

The Polarization of Metals in Boiling, Distilled Water

J. E. Draley, F. E. DeBoer, and C. A. Youngdahl[1]

Argonne National Laboratory, Argonne, Illinois

ABSTRACT

A survey of the polarization behavior (both cathodic and anodic) of sixteen metals in boiling, distilled water is presented. For the current densities used, no simple relation such as the Tafel plot described the dependence of E on I. For many metal-water systems reliable and reproducible data have been obtained, although in some of these systems the poor reproducibility is not reassuring. Thus, several systems lend themselves to more thorough study.

The elucidation of the mechanism of the reaction of a metal with water is of wide and basic interest. This reaction, *per se*, is of practical interest in the corrosion of high efficiency power plants, water-cooled nuclear reactors, and in a few other instances. It is of interest in all aqueous corrosion systems since water is the species present in greatest concentration. It seems obvious, then, that the reaction of water with the metal should be studied both for its intrinsic value and as a reference base for aqueous solution studies.

Several aspects of the reactions of metals with pure, liquid water have been studied (1). Since most of these reactions are, or probably are, electrochemical in nature, it appears that some electrochemical measurements should be profitable. It is believed likely that the most valuable result of studying the polarization, or E *vs.* I, curve for a reaction will be the determination of its slope, which we propose to call retardance.[2] The variation of this retardance as a function of current should be interpretable in terms of reaction mechanism.

A search of the literature disclosed only a few previous papers dealing with polarization in pure water: Draley *et al.* (2) have described a method of measurement in the first paper of this series. It is probable that the paper of Tomashov and Mikhailovskii (3) is not of immediate relevance since the adsorbed water film used was probably contaminated by the salt from the salt bridge. Draley and Ruther (4) have reported a few results for aluminum alloys at 200° and 290°C. There have been, of course, many polarization studies in acid, salt, and alkaline solutions.

Under these circumstances, it seems reasonable to survey the behavior of several metal-water systems in order to have a background for more intensive study. This has been done for a number of common metals and the results are reported here.

In many corroding systems, and in particular for a number of metals in pure water, it is difficult to obtain polarization data having mechanistic significance. The basic problem originates in the nature of the reactions occurring. Often corrosion product films formed have a high resistance to penetration by the ions and electrons transferred in the reaction. These films frequently rupture from stress or the liberation of hydrogen beneath them, hydrate, dehydrate, or are reduced sporadically during the reaction. Local pH changes occur in the solution next to the surface. The over-all topography changes as the reaction proceeds, exposing new kinds of surface and altering the resistive properties of the films formed. Differences in film composition occur, changing their properties.

As far as is known there has been no adequate theoretical treatment of these phenomena, so that there is no basic equation relating rates for the corrosion reactions (involving these complex mixed processes) with the solution potential. In order to deal with such a situation, one approach is to take all these things as they are and determine empirically the relationship between solution potential and over-all current. The next step in the analysis is to break down the combined curves into contributions from the various mixed processes occurring. The results given here are part of an effort to show how the first step, the determination of meaningful over-all polarization curves, might be obtained.

There are many cases in which it is not possible to obtain meaningful steady-state potential values by either galvanostatic or potentiostatic methods. The application of a current or potential changes the balance between the processes occurring so that when some relatively unchanging condition is reached it is no longer representative of the situation which was present without external polarization. A simple illustration points up the problem. If a small constant anodic current is applied to aluminum in pure water, the potential becomes more positive at approximately a constant rate (depending on the current used) to roughly + 1 v *vs.* the saturated calomel electrode. At this point oxygen evolution occurs and the potential almost ceases to change. There is obviously no steady-state potential derivable from this measurement which is meaningful in terms of the reactions occurring during corrosion. Equally illustrative are the cases where

[1] Present address: Particle Data Laboratory Inc., 196 Clinton St., Elmhurst, Ill.

[2] The term retardance is chosen, rather than resistance, impedance, etc., because it does not suggest any specific electrical analogy, but it is similar to these electrical terms and has the same units. Furthermore, its meaning is obvious: retardance is a measure of that which holds back a reaction. Thus it also is of general kinetic meaning.

the application of anodic current decreases the corrosion current and the application of cathodic current increases the corrosion rate. Galvanostatic or potentiostatic, potential-current diagrams for such situations do not provide direct information about the processes occurring during corrosion because the processes changed during polarization.

It is observed that the basic cause of the changes which do occur is the electricity passed in the measurement. Presumably, if no electricity were passed, the surface and the reactions would not be changed. It is thus suggested that if sets of measurements were made so that at each current different amounts of electricity, Q, were passed, it should be possible to extrapolate to the "zero Q" case to obtain the datum desired. The method chosen in the present investigation is to apply continuously increasing polarizing currents at different constant rates, and to extrapolate for each current to the infinitely fast application rate.

It is immediately apparent that if the scanning rate is high, some of the polarizing current will be used in non-faradaic (or capacitative) processes. To avoid this, scanning rates are kept low in an effort to maintain approximate steady-state conditions throughout.

Experimental

The experimental techniques and apparatus are essentially the same as reported previously (2). Two differences should be noted: (*A*) The test cell has been redesigned, Fig. 1, because the auxiliary electrode introduced an error into the potential measurement. This error was found to be caused by a difference of potential between the water layer just in front of the auxiliary electrode and the layer just behind it, during the measuring period. This potential difference was presumably due to the difference in polarization caused by different current densities on the two sides during passage of the polarizing current. When the auxiliary electrode was put outside the chamber, as shown in Fig. 1, no further interference could be detected. (*B*) It has been found that the small amount of pre-electrolysis that was applied in the original procedure had no effect on the aluminum cathodic polarization curve. For the present work, the water was not pre-electrolyzed. A thorough test of pre-electrolysis would involve about 15 l of low conductivity water. Effective pre-electrolysis often involves less than a liter of 1*N* solution electrolyzed at about 0.01 amp/cm^2 for 24 hr (5). Bicelli and La Vecchia (6) use an even higher level of pre-electrolysis; they pass 50-60 coul/ml at $I = 0.05$ amp. It is obvious that a comparable level of pre-electrolysis would be difficult to accomplish with the solutions used here.

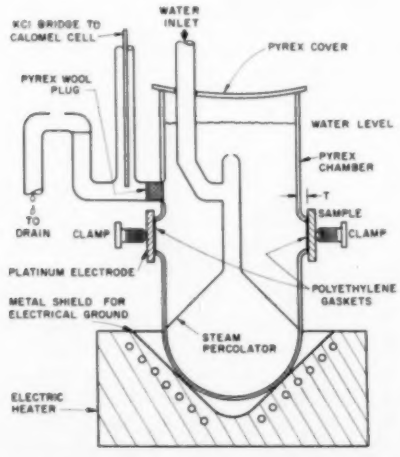

Fig. 1. Chamber used for polarization studies of metals in boiling, refreshed water.

The water was triply distilled, with one intermediate cation exchange process, and had a resistivity of about 1.1-1.3 megohm-cm at 25°C. Although it was not normally done, water resistivity could be doubled by prolonged outgassing, indicating the presence of CO_2 from the air. The oxygen content of the water entering the cell was found to be 6.0 ± 0.2 ppm (using an Industrial Instruments Inc. Dissolved Oxygen Analyser). It may be noted that the pertinent data, the oxygen content and the variation of the oxygen content in the boiling water of the cell, are not available. This variation may account for some of the variation of the polarization results. Typical analyses for metallic impurities showed only the presence of a few parts per billion of common metals (Al, Ca, Cu, Fe, K, Mg, and Na).

Another check on water quality is the rate of increase of current, which is a measure of the water resistivity, during a run under standardized conditions. On one occasion it was observed that the 100°C resistivity, measured in this way, was lower than normal even though the room temperature resistivity was normal and that a few polarization curves were different as a result; curves determined in this way are not reported here.

The cell water was refreshed at about 10 ml/min (4% refreshment/min) in order to sweep away corrosion product in the water and to prevent contamination by the KCl of the salt bridge (in one test 0.2-0.4 ppm KCl changed the Al polarization curve markedly). The water was kept boiling for experimental ease. The reference electrode (saturated calomel) was at room temperature except for the cases Ag, Au, Co, Cr, Fe, Pt, Sn, and Y, for which the temperature was about 55°C; the variation in reference potential is about 20 mv, or less than the average deviation of the open-circuit potential in each case.

The sample was prepared by wet grinding (240 grit paper); it was then washed, clamped in place and sealed to the cell, and left in contact with boiling water for about 20 hr. It has been shown experimentally that neither the sealing process (in a 150° oven for 3 min) nor the polyethylene gasket affects the polarization curve. Samples were left for about 20 hr since most reached a steady-state open-circuit potential in this time. A polarization curve was then run by continuously increasing the current at a constant rate for about 10 min, during which the potential was measured about 10 times/sec, using the interrupter. For subsequent curves the metal was reground, etc., so that there was no effect of previous tests. Since the hole in the cell,

through which contact of the water to the sample was made, had an area of 1 cm², all the results reported refer to 1 cm² geometric area.

The current was interrupted 10 times/sec for 5 msec each interruption. The voltmeter continuously records the potential existing between the sample and reference electrode at the times corresponding to the top of the interrupted pulses (2). After each run the wave form presented to the voltmeter was examined; if the potential decayed more than 10 mv in the last 3 msec of the interruption, the run was discarded. Also, the a-c pickup was measured after each run; the results were corrected for this influence. Periodic checks to insure that the equipment was functioning well were made. The more important of these were (*a*) that the output voltage change equaled the input voltage change (daily), (*b*) that there was no effect of input impedance below about 5 megohms (monthly), and (*c*) a mock cell was tested (monthly).

All the metals were of a purity that would correspond to research grade chemicals or better. The Cr, Ni, Cu, and Sn were the purest available; the Al was 99.998%; and the Fe was electrolytic iron which had been vacuum melted and rolled. There are no data to indicate how sensitive the polarization is to impurities or to alloying elements in the metal.

Results

Polarization curves for sixteen metals have been obtained at three rates of current application. Each was run several times, and the average curves are shown in Fig. 2 (a-p). These were obtained by suitable addition of average polarization voltages to the average open-circuit potential. (The original data are continuous recorder traces; they were averaged at several arbitrary currents, and therefore no points show on the plots.) Reproducibilities of these potentials and polarizations are indicated in Table I.

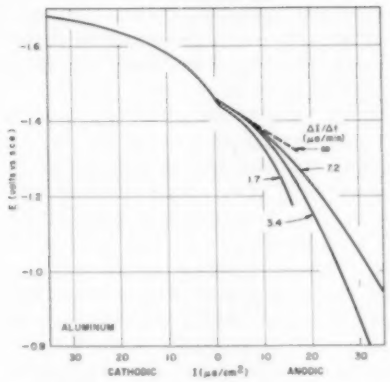

Fig. 2a-p. Polarization curves of 16 metals in pure, boiling water at various rates of current application. The curves are all taken after 22 hr exposure to the boiling water.

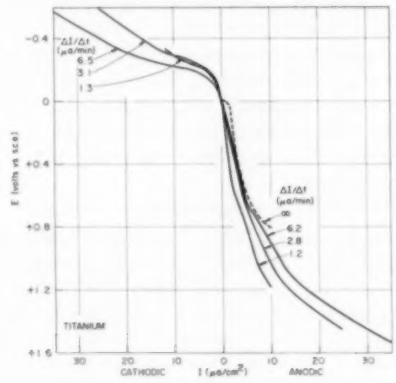

Fig. 2b

Because of the variability and irregularity of the curve shapes, linear, rectangular coordinates are used. There were only a few instances in which it appeared instructive to plot potential as a function

Table I. Maximum average deviation of potential

Metal	OCSP, v vs. S.C.E.	Maximum average deviation of potential: Cathodic in mv	Cathodic % of overpotential	Cathodic Current of max. dev., μa	Cathodic No. of curves	Anodic in mv	Anodic % of overpotential	Anodic Current of max. dev., μa	Anodic No. of curves
Al	−1.461 ± 0.015	12	6	25	20	12	6	35	8
Ti	−0.004 ± 0.022	83[a]	14	25	5	50	7	5	4
V	−0.357 ± 0.030	40	11	30	22	10	6	35	16
Cr	−0.196 ± 0.065	84	14	35	8	67	10	35	6
Fe	−0.462 ± 0.049	70	35	30	14	29	[c]	35	8
Co	+0.004 ± 0.026	22	6	30	4	13[b]	15	5	8
Ni	−0.204 ± 0.023	38	9	30	6	24	5	10	4
Cu	+0.059 ± 0.017	35	23	35	4	10	12	30	6
Y	−0.504 ± 0.098	120	18	20	6	61[b]	9	5	5
Nb	−0.078 ± 0.044	60	9	35	7	47	7	5	8
Mo	−0.310 ± 0.018	16	12	35	4	11	18	35	6
Ag	+0.073 ± 0.022	290	53	30	4	5	~5	5-35	4
Sn	−0.233 ± 0.077	70	13	30	4	127	11	15	4
Ta	−0.010 ± 0.032	92	12.5	35	4	60	5	35	4
Pt	+0.235 ± 0.030	160	25	35	10	30	4	35	6
Au	+0.097 ± 0.037	150	23	35	4	65	6	35	4

[a] The average deviation increases markedly above 20 μa; at 20 μa the average deviation is 24 mv, 5% of the overpotential.
[b] The anodic curves reverse and the deviations become quite large; the values listed are at currents less than those at which the reverses occur.
[c] Since this current is beyond the point, about 1 μa/cm², where the curve has reversed, this number has very little pertinence.

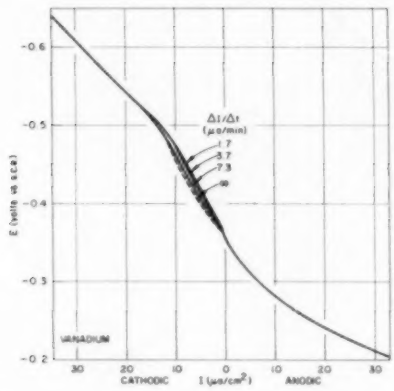

Fig. 2c

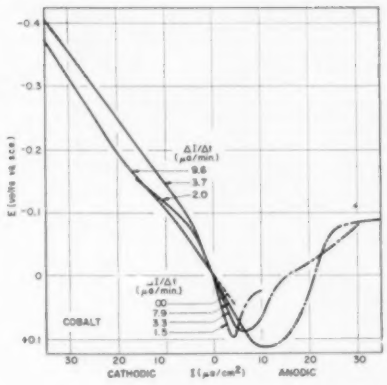

Fig. 2f

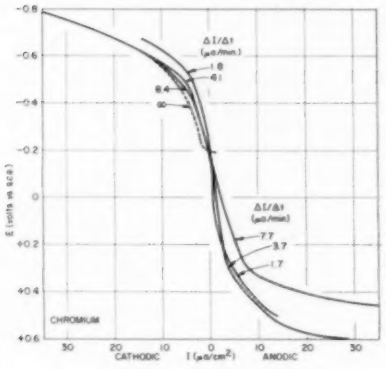

Fig. 2d

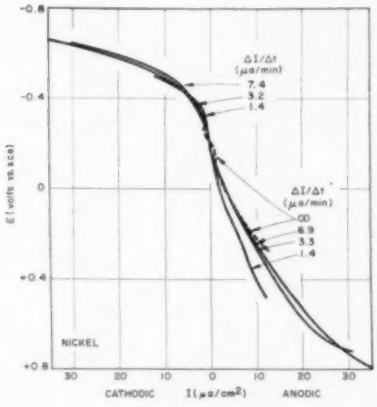

Fig. 2g

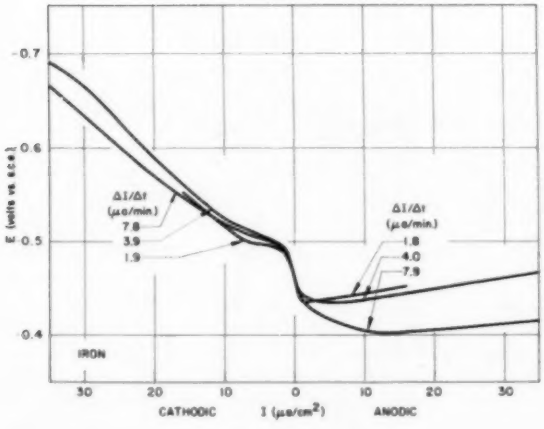

Fig. 2e

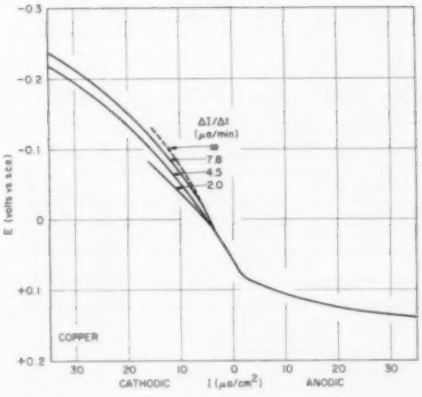

Fig. 2h

of the logarithm of the current. For these cases, rather straight lines were produced on such a plot for roughly the highest 2/3 of the current applied, indicating some relatively simple control of the electrochemical reaction.

The three curves available for each were extrapolated to the situation where no coulombs had been passed in the measurements, as follows: At a number of currents, the quantity of electricity passed in each determination of polarized potential was calculated. The potential was then plotted as a function of Q (or of $\Delta t/\Delta I$, the reciprocal of the rate of application of current, which is proportional to Q at any given current)[3] and extrapolated to zero. The resultant "zero Q" polarization curves are shown on the plots of Fig. 2 as dashed lines.

Two examples of this extrapolation are shown in Fig. 3. The E *vs.* Q plots of the following systems were straight lines similar to those of aluminum

[3] Having the x-axis values the same on the plot (Fig. 3) allows consistent extrapolation and a comparison of the extrapolation for the different currents chosen. Since, with a constant rate of current increase, $Q = \frac{1}{2} I' \frac{\Delta t}{\Delta I}$, Q is proportional to $\Delta t/\Delta I$ at any given current. At different values of I only the proportionality factor is changed.

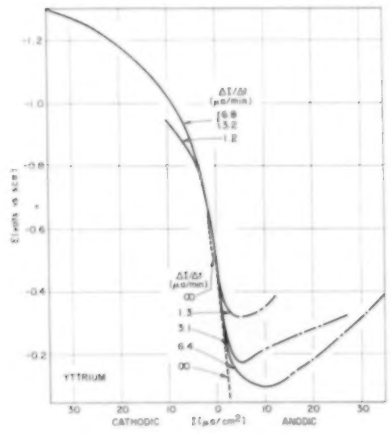

Fig. 2i

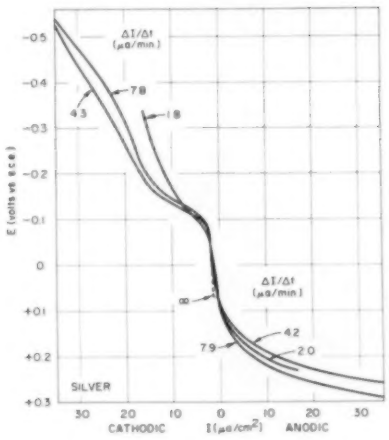

Fig. 2l

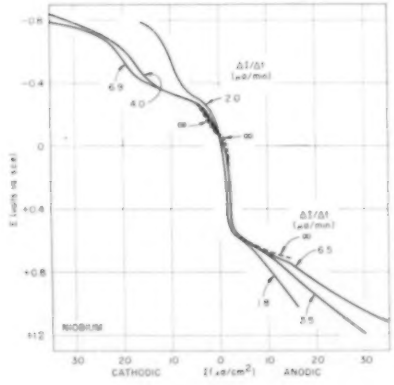

Fig. 2j

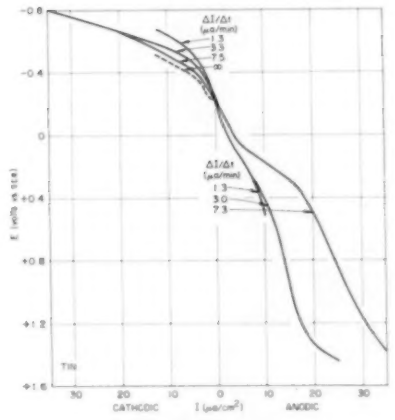

Fig. 2m

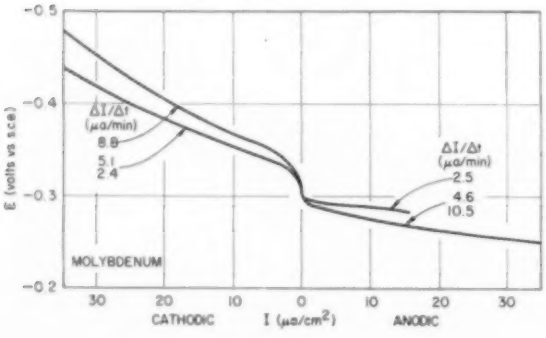

Fig. 2k

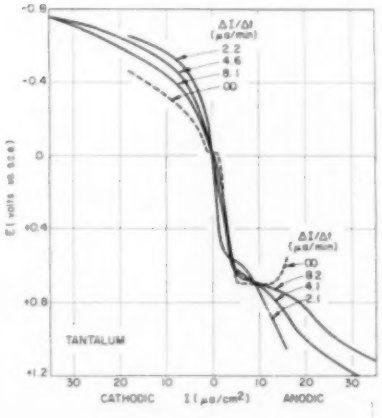

Fig. 2n

anodic (Fig. 3a): Al cathodic and anodic, most Ta anodic, Nb cathodic, Y anodic, Cu cathodic and anodic, a few initial Ni anodic, Co anodic, V cathodic and anodic, and most of the Ti anodic curves. The remainder of the extrapolations are from E *vs.* Q curves similar to those of Fig. 3b. Where no $Q = 0$ curve is shown in Fig. 2, either there is no necessity because there is no dependence on $\Delta I/\Delta t$, or the extrapolation of the E *vs.* Q curve has been considered too uncertain, as for example the cathodic cobalt curve.

In addition to the metals indicated in Fig. 2, four others have been studied but not reported. Zinc and cadmium showed very poor reproducibility in polarization behavior so that no representative families of curves could be drawn. Magnesium corroded in an irregular manner, pitting near the gasket; polarization studies seemed of doubtful applicability. Zirconium showed quite steep polarization curves. It has not been investigated in any detail simply because of the inconvenience associated with the modification of the apparatus which would have been necessary.

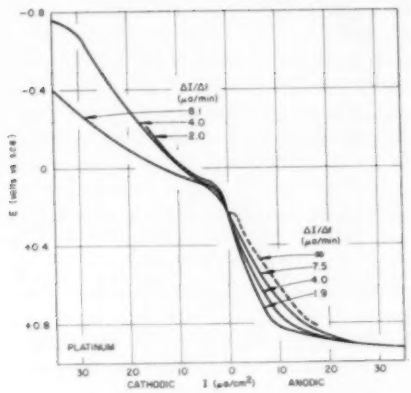

Fig. 2o

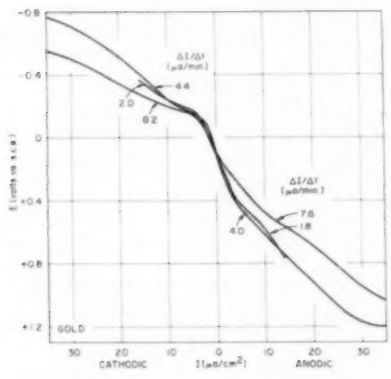

Fig. 2p

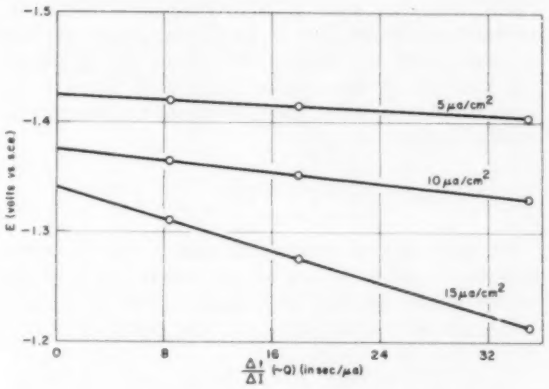

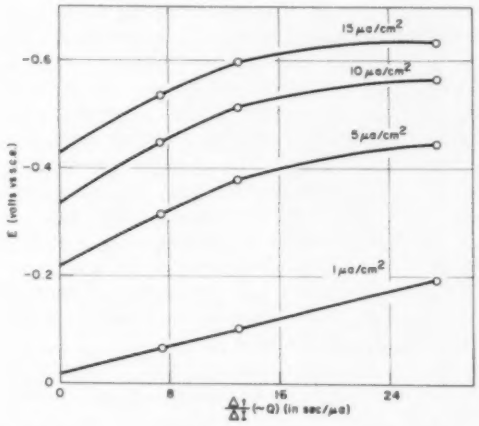

Fig. 3. Two examples of E vs. q curves used to determine the $\Delta T/\Delta t = \infty$ curves of Fig. 2. Fig. 3a (top). Anodic polarization of Al; Fig. 3b (bottom), cathodic polarization of Ta.

Discussion

The primary purpose of this effort is to present polarization behavior of metals in boiling, distilled water, and little detailed analysis will be attempted. Part of the reason for this is the indication during the work that more detailed study (and data) of any one system will be required before it will be possible to analyze it successfully. Such a detailed study is intended to be the next phase of this investigation.

However, it is deemed fruitful to point out a few things about the present results. For most cathodic and anodic curves, increasing the rate of application of the current (and hence decreasing Q at a given current) decreased the polarization. This suggests that changes induced by applied current increased the polarization voltages observed. During anodic polarization of film formers the effect very likely accompanied some anodization. In the other cases, the various corrosion phenomena mentioned in the first paragraphs of this paper (or perhaps impurities in the solution) might have been involved. The contribution of the non-faradaic current to this effect is apparently minor, as will be seen later.

No results are reported as to the effect of exposure time on polarization characteristics. It is to be borne in mind that, for many of the metals, corrosion rates were changing as a function of time and similar changes in polarization behavior as a function of time are to be expected. The observed variations in polarization may also have been a result of variation in the corrosion behavior.

As anticipated, there is a general relation between the slope of the polarization curves, or the over-all retardance, and the corrosion rates. Data are not considered accurate enough to compare "polarization resistances" or retardances at zero applied current with corrosion rates.

Iron, cobalt, and yttrium showed a reversal in anodic polarization curves, sometimes accompanied by irregular oscillatory changes in potential. Because reproducibility was poor, dotted lines are used for the averaged curves shown. This behavior is reminiscent of that of some metals on the verge of passivity.

The basic method of obtaining polarization curves by the method chosen, and extrapolation to $Q = 0$, is subject to criticism. It was chosen because it appeared to offer more promise than alternatives in deriving the most instructive information.

For the continuously changing current method, there is a time lag involved in developing polarized potentials. If the corroding surface is approximated by a resistor (R) and capacitor (C) in parallel, it is clear that at any time the polarization voltage across the resistor is made smaller because some current is used in charging the capacitor (non-fa-

radaic current). For the procedure used in this investigation, where $I = at$ (a is a constant, the rate of application of current), the error, ΔE, in assuming that all of the current is flowing through the resistor R, and thus that all charge transfer is faradaic, is given by

$$\Delta E = aCR^2\left[1 - \exp\left(\frac{-I}{aCR}\right)\right]$$

Another way of expressing this is that an additional time, Δt, will have to pass before the potential which one would want to have been reached at time t has actually been attained. The relation is that $\Delta t = CR$ or $\Delta I = aCR$.

In the actual case, R can be assumed to be approximately equal to the slope of the measured polarization curve. It is seen that the error is greatest at the highest values of C, R, and a. If C is assumed to be $10\mu F/cm^2$ or less (7-9), the error at the maximum R (in Fig. 2n) of about 2×10^5 ohms (at $3\mu a$), for $a = 8$ μa/min is 0.053 v, or 0.3 μa. Such errors seem substantial, but average deviations in the results (Table I) are observed to be greatest where polarizations are greatest, and the calculated errors are almost within experimental error. Also, most of the curves have considerably lower slopes and there the errors estimated in this way are insignificant. Thus the non-faradaic, or capacitance charging, part of the current does not seem significant in these measurements.

It is clear that this type of error limits the rate at which the current can be increased and, hence, the reliability with which the extrapolation of polarization to $Q = 0$ can be made. In addition, the three rates of current increase provide only three points on the extrapolation curves. The extrapolation is thus subject to more error than is desirable. Within the limits of accuracy indicated by the degree of reproducibility of the data, however, the curves given seem correct.

A number of polarization diagrams (*e.g.*, Ta) show low retardances at $I = 0$ for the infinitely fast (extrapolated) curves. The error analysis above does not seem to provide an adequate explanation, although the per cent error does become large at very short times. Correction for the capacity error somewhat increases the slope of such $Q = 0$ curves at no applied current. This aspect of the polarization curve shapes must be viewed with suspicion, particularly since the metals showing the phenomenon in question have low corrosion rates and would be expected to have rather high retardances at $I = 0$.

Acknowledgment

The authors wish to acknowledge the aid of W. Bettin and the kindness of C. S. Smith and L. F. Yntema who supplied some of the materials.

This work was done under the auspices of the U.S. Atomic Energy Commission.

Manuscript received Dec. 8, 1960; revised manuscript received March 5, 1961.

Any discussion of this paper will appear in a Discussion Section to be published in the June 1962 JOURNAL.

REFERENCES

1. For example see (*a*) U. R. Evans, "The Corrosion and Oxidation of Metals," Edward Arnold (Publishers) Ltd. London (1960); (*b*) AEC—Euratom Conference on Aqueous Corrosion of Reactor Materials, Oct. 14-17, 1959, TID-7587; and (*c*) "High Purity Water Corrosion of Metals," N. E. Hamner, editor, National Association of Corrosion Engineers, Houston, Texas (1960).
2. J. E. Draley, W. E. Ruther, F. E. DeBoer, and C. A. Youngdahl, *This Journal*, **106**, 490 (1959).
3. N. D. Tomashov and Ya. N. Mikhailovskii, *Doklady Akad. Nauk S.S.S.R.*, **110**, 1026 (1956).
4. J. E. Draley and W. E. Ruther, Experiments on Corrosion Mechanism: Aluminum at High Temperature, ANL-5658, April 1957.
5. J. O'M. Bockris, I. A. Ammer, and A. K. M. S. Huq, *J. Phys. Chem.*, **61**, 879 (1957).
6. L. P. Bicelli and A. LaVecchia, Researches on Hydrogen Overvoltage on Metallic Single Crystals: Tin, WADD-TN-60-115, July 1960.
7. J. J. McMullen and N. Hackerman, *This Journal*, **106**, 341 (1959).
8. R. J. Brodd and N. Hackerman, *ibid.*, **104**, 704 (1957).
9. R. D. Misch, Characteristics of Anodic and Corrosion Films on Zirconium, ANL-6149, May 1960.

Hydrated Oxide Films on Aluminum

Their Growth and Their Importance in Electrolytic Capacitors

D. Altenpohl[1] and W. Post

Aluminium-Walzwerke Singen, G.m.b.H., Singen-Hohentwiel, West Germany

ABSTRACT

The composition and growth of hydrated aluminum oxide films and their dependence on water temperature, reaction time, SiO_2 content, and *p*H are discussed, with special reference to their influence on etched aluminum foils used in electrolytic capacitors.

The nature of the oxide films present on aluminum exposed to humid air or water of various temperatures is not always clearly understood. Metallic aluminum reacts with atmospheric humidity, producing a hydrated oxide film.[2] The annealing of unetched foil, such as the cathode foil used in

[1] Present address: Aluminium-Industrie A.G., Zurich, Switzerland.

[2] The term "hydrated oxide," as commonly used in the literature, also is applied here, although most of the water present forms a true hydroxide bond with aluminum, leaving only a small part that can be described as H_2O molecules. It would therefore be more accurate to refer to aluminum hydroxides or mixtures of oxides and hydroxides.

electrolytic capacitors, generally results in an increase of this oxide formation. Etched aluminum foils also are usually equipped with a hydrated aluminum oxide layer, produced in deionized water of the greatest possible purity.

All these oxide films are capable of exerting a decisive influence on the capacitor, either improving or worsening the formation process, or affecting shelf life, capacity, and power factor. For this reason a close examination of these oxides is vital.

Theory Concerning the Growth of Hydrated Oxide Films

The presence of a hydrated oxide layer, produced under carefully controlled conditions in double-distilled or deionized water, can be extremely beneficial. One of its principal advantages is protection against corrosion during storage. Its growth critically depends on the water temperature used. Temperatures below about 75°C result in relatively thin layers consisting of bayerite ($Al_2O_3 \cdot 3H_2O$) and other, undefined, aluminum hydroxides. The water content of these layers depends largely on drying conditions; it generally ranges between 35 and 70%. (Bayerite has a theoretical water content of 35%.)

Above 75°C, x-ray or electron-diffraction photographs reveal the presence of boehmite ($Al_2O_3 \cdot 1H_2O$).

Both the film thickness and the percentage content of boehmite increase with increasing temperature and longer reaction time. Between 75° and 120°C the oxide layer gradually reaches, after several minutes of exposure, a thickness between 600 and 3000Å. Figure 1 shows x-ray diffraction patterns of (top) bayerite, (middle) boehmite, and (bottom) a boehmite-containing hydrated aluminum oxide layer generated on high-purity foil at about 90°C. The presence of boehmite can be seen clearly, but there are amorphous hydrated oxides present, which cannot be detected by x-ray diffraction.

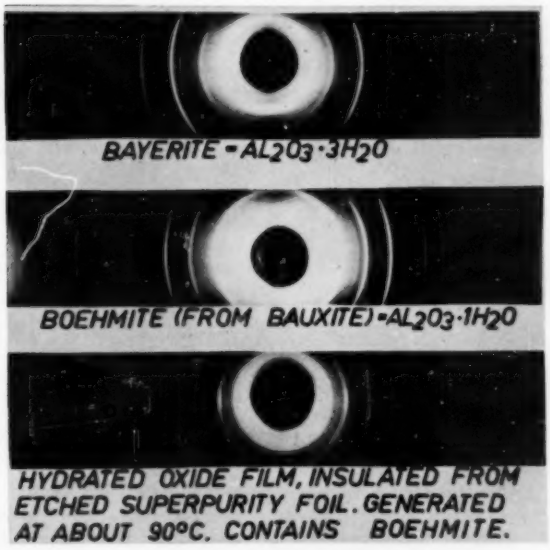
BAYERITE - AL2O3·3H2O
BOEHMITE (FROM BAUXITE) - AL2O3·1H2O
HYDRATED OXIDE FILM, INSULATED FROM ETCHED SUPERPURITY FOIL. GENERATED AT ABOUT 90°C. CONTAINS BOEHMITE.

Fig. 1. X-ray diffraction of three different hydrated aluminum oxides.

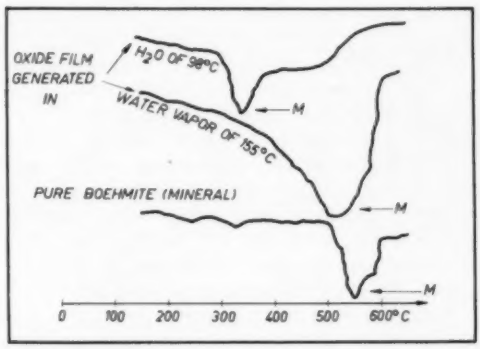

Fig. 2. Differential thermoanalysis (M = maximum of water desorption).

Infrared spectral analysis and differential thermoanalysis (D.T.A.)[3] also have proven to be powerful tools in the investigation of hydrated aluminum oxides. Both revealed the possible presence of trihydrates in films in which x-ray diffraction photos indicated only the presence of boehmite.

Figure 2 shows a comparison of oxide layers produced at (top curve) 98° and (middle curve) 155° with mineral boehmite (bottom curve), where *M* stands for the maximum water evaporation, arrived at by D.T.A. It will be noted that in mineral boehmite the maximum lies near 550°, whereas in a film containing a good deal of bayerite it is near 350°C. This shows that the layer produced in 155° water vapor contains the greatest percentage of boehmite, whereas the 98° film, having its maximum around 350°, is within the realm of the trihydrates. It seems that the bayerite content of the films decreases and the boehmite content increases with increasing reaction temperature. Certain undefined hydroxides also are present in the film, shown by D.T.A. or infrared as probably consisting of trihydrates.

Even minute contaminations in the water used for generating the hydrated oxide can exert a powerful influence of film formation. The principal disturbing contaminants are chloride ions and silicon dioxide. The danger of chloride contamination is common knowledge; we will therefore confine ourselves to recent developments concerning the silicon dioxide influence.

Films created in SiO_2-containing water were found to be more readily soluble in acids than those made in SiO_2-free water. Figure 3 shows that, with equal conditions of temperature and reaction time, layers produced in deionized water without SiO_2 additive are considerably thicker than when SiO_2 is present. Even the presence of only 1 ppm of SiO_2 can reduce film thickness by as much as 50%. It was found also that films produced in water containing 1 or 2 ppm SiO_2 result in instability of the forming films in the capacitor. The reasons for this are not yet fully understood. The presence of SiO_2 in any measurable concentration (above approximately 1 ppm) seems to promote the growth of a hydrated oxide film of unfavorable structure, which subse-

[3] In differential thermoanalysis two containers are heated simultaneously and their temperature differential plotted by means of thermocouples. Container A holds anhydrous (calcined) aluminum oxide, while container B holds the test sample for which the thermal behavior is to be determined.

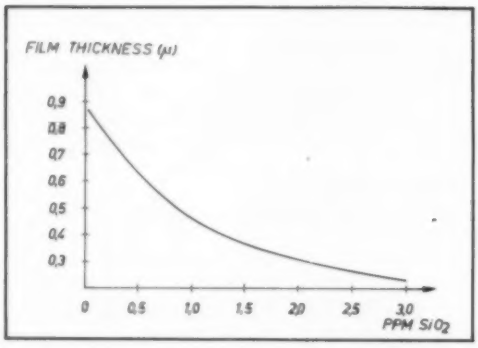

Fig. 3. Influence of SiO_2 content of boiling deionized water on thickness of hydrated oxide film.

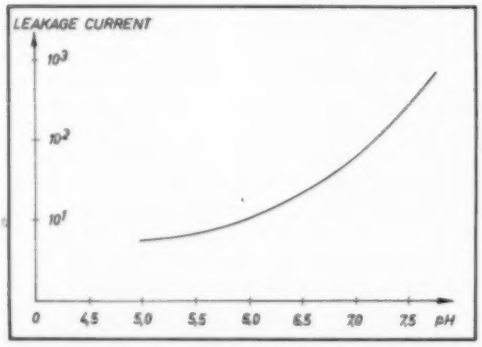

Fig. 4. Influence of pH of water on leakage current of foil

quently has a deleterious effect on the growth of the forming layer.

In any event, the initial oxidation step has very critical effects on subsequent oxidation. It is therefore of utmost importance to avoid any possibility of silicon dioxide contamination in the deionized water used or in the equipment. In order to be certain that all silicon dioxide is removed effectively, only strongly basic and highly effective ion exchangers must be employed in the deionization process.

Another very critical factor is the pH of the water. Our investigations along these lines have been reported in U.S. Patent No. 553 205, in which it was shown that the fully deionized water used for applying the oxide layer should have a pH < 7. pH values between 5 and 6 result in films which have a beneficial effect on the capacitor. If necessary, the pH has to be maintained by the addition of chloride-free acid substances. Figure 4 shows that the leakage currents of formed foils increase as the pH in the water increases.

Excessive variations in storage temperature, as well as high atmospheric humidity, cause hydrated aluminum oxide layers to continue growing. For this reason, packing and storage must be handled carefully. This is especially important for oxide films of less than 500Å thickness.

Effects of Hydrated Oxide Layers on Electrolytic Capacitor Foils

The application of a hydrated oxide layer after etching becomes necessary because at this stage the foil is not protected against corrosion by its natural oxide film.

The type of hydrated oxide to be used depends entirely on the final use of the capacitor. When aluminum foils with hydrated oxide layers are formed, the dielectric grows *underneath* the hydrated oxide film. Figure 5 shows how the latter is actually lifted by the forming layer and is partly consumed by it. In an electrolytic capacitor the hydrated oxide layer is penetrated only partly by the electrolyte, the remainder acting as a dielectric.

Thick hydrated oxide layers are particularly desirable on anodes for high- and medium-voltage electrolytic capacitors for d.c. (above about 100 v), because they greatly reduce the forming-current consumption. As pointed out before, it is advisable to build up such layers only immediately prior to formation. If there is too much of a delay, an unfavorable aging process takes place, which has up to now defied analysis. No difference of thickness or composition could be detected between fresh and aged films developed, but examination after forming revealed a very definite difference (Fig. 6). Although the hydrated oxide films may have identical thicknesses prior to forming, a smaller percentage of readily soluble oxide was found in layers that had been applied immediately before forming than in those that had been stored for two weeks between application and forming. Figure 6 shows the

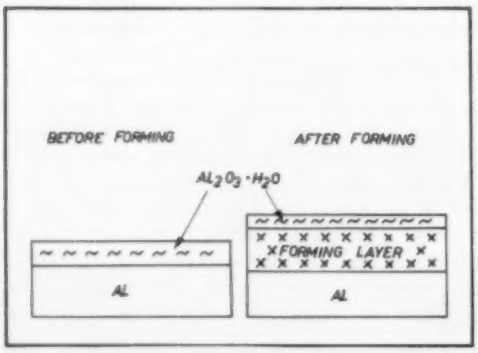

Fig. 5. Formation in presence of hydrated oxide film. Growth of the dielectric underneath a hydrated film.

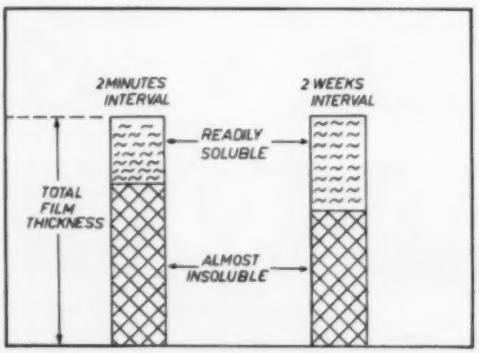

Fig. 6. Composition of the forming layer after different storage intervals between gassing and formation.

approximate composition of two layers after formation, determined by dissolving the soluble part in a phosphoric-chromic acid mixture (1). Thus a freshly made hydrated oxide layer results in a larger percentage being transformed into a dielectric than is the case with an oxide layer that has been stored.

The favorable effect of immediate formation is further confirmed in motor-starter capacitors which, when made with aged hydrated oxide films, heat up quickly and show other untoward attributes, while those made with fresh films show none of these difficulties. This is undoubtedly due to the smaller dielectric loss in the latter film.

The unfavorable influence on dielectric loss can be explained by the fact that any water molecules or hydroxide structures present in the dielectric increase the dielectric loss because they oscillate in the a-c field and thereby absorb energy, thus increasing the power factor. From this it can be concluded indirectly that in the case of freshly hydrated oxide films water is eliminated from the consumed portion of the film whenever this portion crystallizes into γ-aluminum oxide under the influence of a high electric field. On the other hand, when an aged film is partly consumed by the dielectric film, the change from hydrated to water-free aluminum oxide is less complete, and residual water remains in the dielectric.

Another possible explanation of this phenomenon is that the aged film is not penetrated as deeply by the electrolyte and that therefore a larger part of the hydrated oxide layer acts as a dielectric. In other words, Fig. 6 does not give the whole story, since it ought also to indicate the extent to which the dielectric penetrates the hydrated top layer. In any event, there is no sharp border line between the penetrated top layer and the dielectric, but rather a zone of continuous transition.

For low-voltage electrolytic capacitors, especially for very low voltages, the hydrated oxide films should be kept as thin as possible. Of course, it is virtually impossible to have an oxide layer of less than 100Å after etching and washing. Approximately 10-30Å constitutes the so-called barrier layer, a nonporous oxide layer that acts as a dielectric at the bottom of the film. The electric field strength in this barrier layer amounts to about 14Å/v; therefore the barrier layer, the thickness of which is more or less constant irrespective of the hydrated layer above it, alone accounts for a drop of 1 or 2 v. The capacitance of unformed aluminum foils drops as the hydrated oxide film gets thicker because layers are penetrated only partly by the electrolyte. The same is true for unetched cathode foil which, after storage in humid air, can have hydrated oxide films of as much as 100-500Å. Since the capacity of an electrolytic capacitor depends on the oxide films of both electrodes, this can seriously influence capacitor efficiency, especially for low forming voltages.

Summary

In conclusion, it may be observed that our knowledge concerning the growth of hydrated aluminum oxide films and their influence on the dielectric characteristics of electrolytic capacitors is still very limited. Empirical studies made with data gained from finished capacitors are useful to some extent in determining factors that influence the growth and structure of hydrated oxide films, but more systematic studies are needed to increase our fundamental knowledge in this field. High-purity aluminum foil now is used extensively to increase the shelf life of the capacitors, but more attention should be paid to the hydrated oxide films present prior to formation because, as has been shown, they have a very decisive influence on the quality of the capacitors. In some cases, as in motor-starter or low-voltage capacitors, the nature of the hydrated oxide film may be fully as important as the metal purity.

Acknowledgment

The authors wish to thank Miss B. Eytel for valuable assistance in preparing this work.

Manuscript received Sept. 23, 1960. This paper was prepared for delivery before the Chicago Meeting, May 1-5, 1960.

Any discussion of this paper will appear in a Discussion Section to be published in the June 1962 JOURNAL.

REFERENCE

1. D. Altenpohl, IRE Convention Record, Pt. 3, p. 35 (1954).

Immersion Plating of the Platinum Group Metals

R. W. Johnson

The International Nickel Company (Mond) Limited, London, England

ABSTRACT

Satisfactory immersion plating processes have been developed for the deposition of palladium, rhodium, ruthenium, and platinum up to thicknesses of 50, 30, 100, and 65 μ in., respectively. These coatings may be sealed by various means, including immersion in boiling water, in ammonium hydroxide, or in a replacement gold solution. Adherent coatings which provide useful wear-resistance in addition to protection against tarnish and corrosion have been deposited on copper and certain copper alloys.

Platinum group metals are characterized by high corrosion and tarnish resistance and, in the electrodeposited condition, by high hardness. This combination of properties has led to the widespread use of plated coatings, notably of rhodium and palladium, as finishes for a variety of electrical contacts, where low and stable contact resistance coupled with resistance to mechanical wear is essential to effective operation.

Satisfactory solutions for the application of coatings of rhodium, palladium, and platinum by electrodeposition have existed for many years, but more recently the growth of printed circuitry has stimulated interest in the possibilities of nonelectrolytic deposition, especially in view of the difficulty in many cases of making electrical connection to isolated areas of copper. Such a process is also clearly of advantage in the plating of large numbers of small components, *e.g.*, contact tags, etc.

Nonelectrolytic processes are of two main types: (*a*) chemical reduction and (*b*) replacement. The advantages of the first type are that a wide variety of basis metals can usually be plated and that relatively thick deposits are obtainable. A disadvantage, however, is that, even when the process is of the autocatalytic type, metal tends to deposit, at least to some extent, on nonconducting areas. Electroless nickel plating is a well-known example of this type of process, and there has recently been described a procedure for the electroless deposition of palladium based on autocatalytic reduction of the metal from a solution of palladous chloride in ammonia which is stabilized by ethylene-diamine-tetra-acetic acid (1).

Replacement processes eliminate the main disadvantage of chemical reduction processes in relation to the plating of printed circuits in that the replacement deposit discriminates completely between metallic and nonmetallic areas, but in this case the general disadvantage is that the deposit is normally extremely thin due to the self-sealing effect of the deposited metal.

Although it has been claimed that replacement coatings of rhodium only a few molecules thick exert considerable protective value on copper (2), it is unlikely that such extremely thin coatings would confer any useful degree of wear-resistance to the surface.

The aim of the present work, which relates to immersion coatings of palladium, rhodium, platinum, and ruthenium, was to develop a satisfactory procedure for the production of adherent coatings on copper and certain copper alloys of sufficient thickness to provide useful wear-resistance in addition to protection against tarnish and corrosion.[1]

Experimental

Deposition of palladium.—Attention was initially directed to palladium since this metal is already of considerable interest as an alternative to gold in the finishing of printed circuit end connectors in view of its good contact properties, high hardness (ca. 350 D.P.N), excellent solderability, and relative cheapness. It is evident that increase in thickness of a replacement deposit can be achieved only at the expense of encouraging some porosity of the deposited metal to permit the replacement reaction to continue, and it seemed likely that suitable conditions might be established by carrying out the replacement process in a solution which would be fairly corrosive to the basis metal to give some attack of the latter without replacement. In the case of palladium, and indeed of the other platinum group metals, acid chloride solutions were an obvious first choice for experiment.

In the first instance a stock solution of palladous chloride was prepared in the conventional way by dissolving palladium sponge in aqua regia and evaporating the solution several times to near dryness, with the addition of hydrochloric acid. The essential product is chloropalladous acid, and it was later confirmed, as might be expected, that similar results to those described below, could be achieved using sodium or ammonium chloropalladite or solid palladium chloride as starting material.

Exploratory tests were made to evaluate the effect of variables such as palladium concentration, hydrochloric acid content, and temperature of deposition on the characteristics of the coatings. Polished copper specimens were used, cleaning of

[1] The processes described in this paper are the subject of British Provisional Patent Applications No. 44424/59 and 5331/60.

which was carried out by wiping with acetone followed by soaking in a hot detergent solution, in order to conform with the essential nonelectrolytic nature of the process.

With an initial palladium concentration of 5 g/l of metal, bright replacement deposits were obtained on copper over a fairly wide range of acid concentration. The thickness of deposits was, however, limited by the occurrence of exfoliation, and in this respect the concentration of hydrochloric acid was found to be extremely critical, the optimum concentration being 250 ml/l of concentrated (32%) acid. Variations of 5% of either side of this figure resulted in a significant decrease in the maximum thickness of deposit obtainable prior to exfoliation. Under the optimum conditions adherent deposits up to 70 μ in. thick were obtained consistently in an immersion time of 12 min at room temperature (25°C). In view of the nonstoichiometric nature of the process it was not possible to calculate deposit thickness by simple weight change of specimens; thicknesses were determined by the examination of carefully prepared microsections at a magnification of 2000, using a Vickers projection microscope.

With the optimum concentration of hydrochloric acid, variations in the metal content of the solution in the range from 1 to 10 g/l had no significant effect on the maximum thickness of deposits obtainable. The initial content of 5 g/l was therefore retained for further studies.

The effect of plating temperature was to increase the rate of deposition as shown in Fig. 1, but without improvement in the thickness of deposits. Room temperature operation is thus clearly to be preferred as permitting closer control of deposit thickness as well as being more generally convenient. At a temperature of 25°C the rate of deposition was approximately constant up to the limiting time set by the onset of exfoliation.

These exploratory experiments established that, allowing an adequate margin of safety in respect to the exfoliation factor, bright adherent replacement deposits of palladium at least 50 μ in. thick could be produced consistently on pure copper at room temperature from a solution containing 5 g/l of metal and 250 ml/l of hydrochloric acid. However, the brightness and good color of "as-plated" coatings was fairly quickly lost by tarnishing on exposure to the laboratory atmosphere, confirming the essentially porous nature of the coatings and indicating the need for some form of "sealing" treatment.

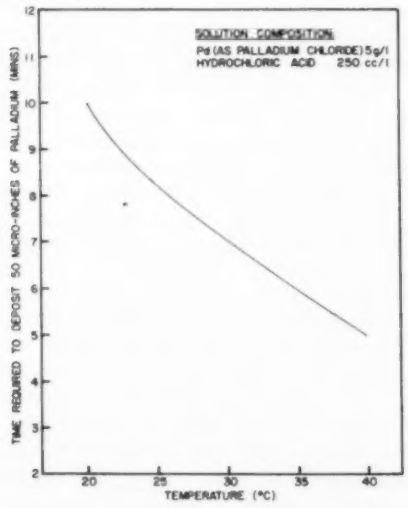

Fig. 1. Effect of temperature on the rate of deposition of palladium on copper.

A number of treatments were tried to this end, based on the approach of attempting to develop insoluble products in the pores of the coating by reaction of residual solution with a suitable reagent, *e.g.*, potassium iodide, hydrazine, ammonia, and two most effective procedures were found to be: (*a*) immersion of the coating in boiling distilled water for 15 min; and (*b*) immersion in ammonia solution (1 part 0.880 ammonia to 2 parts water) for 5 min at room temperature. The boiling water treatment probably functioned by the leaching out of residual acid and the hydrolysis of residual salts, while in the case of the ammonia treatment there was the additional possibility of forming insoluble palladosammine chloride in the pores of the deposit.

In view of the excellent properties of gold as a sliding contact surface, experiments were then made on the sealing of deposits by an immersion gold deposit, using a solution of the following composition: potassium gold cyanide, 5 g/l; ammonium citrate, 20 g/l; urea, 25 g/l; temperature, 95°C; ammonium hydroxide (0.880 sg.), 1 ml/l added every 4 hr at plating temperature. Specimens which were immersed in this solution for 5 min following a quick water rinse after palladium plating, acquired a uniform gold color over the whole of their surface, and the composite coatings resisted tarnish for periods of up to six months of normal chemical laboratory exposure.

All of the plating tests so far described were made in still solutions. It was noted that disturbance of the solution either by mechanical agitation or by movement of the specimen caused very early exfoliation of the deposit. This ruled out the use of this type of procedure as a conventional barrelling process for the treatment of large numbers of small components, but it was found that a modified procedure in which rotation of an inclined barrel (in the present case a glass beaker of 500 ml capacity) was restricted to 5-sec periods at 2 min intervals during a total plating time of 8 min could be used successfully to plate small contacts of the telephone selector bank type. It is to be noted that, in a process of the replacement type, masking of items by one another during the "rest" periods is less of a disadvantage than would be the case in barrel electroplating since, provided that the components are wetted by a film of solution, the replacement reaction can proceed to a reasonable extent.

Deposition of other platinum metals.—Following the experiments on palladium, similar tests were made on the deposition of rhodium, platinum, and ruthenium. Rhodium gave bright replacement deposits up to 30 μ in. thick at room temperature from a chloride solution containing 5 g/l of rhodium and 250 ml/l of hydrochloric acid. Platinum could not

Table I. Optimum conditions for the production of replacement deposits on copper from acid chloride solutions

Metal	Temp, °C	Time, min	Deposit thickness, μin.
Rhodium	25	10	30
Ruthenium	95	30	100
Platinum	65	8	65
Palladium	25	8	50

be deposited satisfactorily from chloride solutions with similar metal and acid concentrations at room temperature, but deposits up to 65 μ in. thick were readily obtained at a temperature of 65°C. No satisfactory deposits were obtained from acid-ruthenium chloride solutions, but excellent deposits up to 0.0001 in. thick were produced from solutions based on ammonium nitroso ruthenium chloride or ruthenium sulfamate, containing 5 g/l of metal and again 250 ml/l of hydrochloric acid. In each case, however, a high operating temperature was required. The results of these experiments in terms of the time and temperature required to produce the optimum thickness of deposit are summarized in Table I, together with the corresponding conditions for palladium.

Deposits of rhodium, ruthenium, and platinum were equally amenable to sealing by the treatments described for palladium, with the gold sealing process again preferred. Deposition rates for platinum and rhodium appeared to be reasonably constant up to the maximum plating time permitted, but in the case of ruthenium there was a gradual falling off in deposition rate with increase of thickness above 50 μ in. (Fig. 2).

Life of plating solutions.—Tests on rhodium and palladium solutions show that at least 80% of the initial metal content could be utilized without deterioration in the rate of deposition or in the general quality and appearance of the coatings, other than an occasional loss of full brightness, which however could readily be restored by filtration of the solution. This corresponds to a coverage of at least 1000 in.[2] of copper with 50 μ in. of deposit from 1 liter of plating solution.

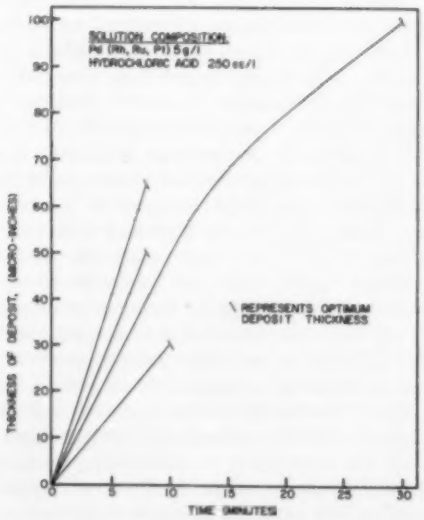

Fig. 2. Variation of thickness with time of immersion for deposits of palladium, rhodium, platinum, and ruthenium.

Application of replacement deposits to other basis metals.—At present the application of the replacement plating procedure to basis metals other than pure copper has been studied mainly for palladium. Satisfactory deposits can be applied to brass, beryllium-copper, phosphor-bronze and nickel-silver, and there are indications that deposits may be obtained on nickel and silver, but reactive metals such as iron, steel, zinc, magnesium, aluminum, and titanium cannot be treated successfully by the process in its present form.

Properties of Deposits

Adhesion.—Up to the optimum thicknesses quoted in Table I the adhesion of deposits was consistently good on properly cleaned copper specimens. Attempts to increase the thickness by prolonged immersion resulted in obvious exfoliation of the deposits due to excessive attack of the basis metal. Adhesion was assessed by scraping deposits with a sharp blade while observing the surfaces under a binocular microscope, and by examination of a large number of microsections. A more graphic demonstration was provided by the results of a test in which a palladium deposit on the end connectors of a printed copper test pattern was subjected to 400 insertions and withdrawals in a standard socket connector without removal of the palladium layer. Under similar conditions there was observed severe "spreading" of unprotected copper connectors, severe fragmentation of an electrodeposited coating of rhodium 0.0001 in. thick. This result suggests equally that the immersion coatings possess a surprisingly good level of wear resistance, a factor which otherwise awaits more systematic assessment.

Tarnish and corrosion resistance.—As already stated, the tarnish resistance of the platinum metal immersion coatings is low in the absence of some type of sealing procedure, the most effective process for this purpose being the immersion gold treatment. Composite platinum metal/gold coatings resist up to several months exposure in a chemical laboratory atmosphere, a result which suggests that they should give an effective protection to copper in the mildly corrosive atmosphere normally encountered in electrical contact applications. In this type of exposure rhodium coatings appeared to be particularly effective.

Preliminary exposure tests have also been carried out on immersion deposits of optimum thickness on copper in a sulfur dioxide cabinet under the conditions of B.S. 1224: 1959.[3] This test is not particularly suitable for electrical contact finishes, but provided a useful relative assessment of deposit and sealing processes after 4 hr of exposure. As anticipated, the gold sealing process was the only sealing technique

[3] British Standard for "Electroplated coatings of Nickel and Chromium" in which plated copper specimens are suspended in a transparent plastic cabinet containing an atmosphere of moist sulfur dioxide.

which conferred any useful protective value on the coatings under the rather severe moist acid test conditions, and the protective power of the various platinum metal finishes with gold sealing appeared to depend on the thickness rather than the nature of the deposit, being greatest in the case of ruthenium (100 μin.)

Qualitative observations during the course of the work indicated that the protective value of replacement coatings depends to a large extent on the surface finish of the basis metal, optimum results being achieved on highly polished surfaces, which are conducive to the formation of deposits of uniform thickness and free from weak spots such as would be encouraged by the presence of surface asperities, particularly in a process involving some solution of the basis metal.

Solderability.—Among the advantages of electrodeposited palladium as a finish for printed circuits is the ready solderability of the deposits. It was of interest, therefore, to check the wettability of the replacement coatings by standard 60-40 lead tin solder. The procedure used was as follows: (*a*) clean surface with acetone; (*b*) dip in a resin-methylated spirit flux; (*c*) immerse in solder bath for 30 sec; and (*d*) examine for completeness of wettability.

Palladium coatings on copper sealed by boiling water treatment or by the immersion gold process were readily wetted, even after several days storage. When the ammonia sealing process was used coatings showed poor wettability unless tested within 1 hr of preparation. Otherwise it was necessary to remove the seal by a dip in hydrochloric acid solution to achieve wetting.

More difficulty was encountered in wetting coatings on brass. Good wettability of gold-sealed coatings was obtained by the above procedure only when the initial surface of the brass was polished to a high finish by buffing. Otherwise it was necessary to use a slightly active flux such as "Tricene."

Discussion

From the nature of the replacement process, the deposit increases in thickness by downward growth. Therefore, the surface of the coating reproduces almost exactly that of the basis metal, both in contour and location. The latter aspect is of significance in the finishing of flush-bonded contact segments in high-speed switches where even minute differences in level between segments and insulator gaps may lead to severe wear on the wiping member.

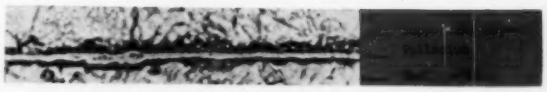

Fig. 3. Microsection of palladium replacement coatings on copper. Magnification 2000X before reduction for publication.

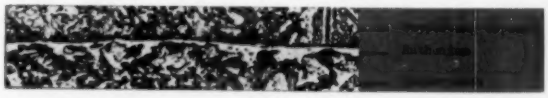

Fig. 4. Microsection of ruthenium replacement coatings on copper. Magnification 1000X before reduction for publication.

In view of the thinness of the coatings it is difficult to resolve any detailed structure in microsections, typical examples of which for palladium and ruthenium deposits are shown in Fig. 3 and 4. It is noteworthy that, whereas the palladium deposit is of fairly uniform thickness, there is, in the case of ruthenium, a tendency for considerably more localized attack of the basis metal, with the formation of characteristic "roots" of the coating into the basis metal. This difference in mode of growth of deposits, which may be related to the difference in temperature of deposition, explains the greater thicknesses of ruthenium coatings attainable without exfoliation.

Acknowledgment

The author's thanks are due to the Mond Nickel Company Ltd., for permission to publish this paper.

Manuscript received Nov. 16, 1960; revised manuscript March 17, 1961. This paper was prepared for delivery before the Houston Meeting, Oct. 9-13, 1960.

Any discussion of this paper will appear in a Discussion Section to be published in the June 1962 JOURNAL.

REFERENCES

1. R. N. Rhoda, *Trans. Inst. Met. Finishing*, **36**, 82 (1959).
2. U.S. Pat. 2,702,252.

Electroluminescence in Zinc Sulfide As Due to Minority Carrier Injection

W. A. Thornton

Research Department, Westinghouse Electric Corporation, Bloomfield, New Jersey

ABSTRACT

Under the proper experimental conditions, which can be fulfilled in conventional electroluminescent ZnS powder dispersions in dielectric material or in luminescent films, the resistive component of the a-c current follows the diode equation (for forward bias) $I = I' [\exp (V/V') - 1]$, where V is the applied rms voltage. The parameter I' is proportional to $\exp (-E/kT)$ and V' is proportional to temperature and phosphor layer thickness. Three independent determinations give the number of active forward-biased junctions per micron of ZnS phosphor as about 15. The forward currents are shown to be directly related to electroluminescence emission and are compared directly to a-c currents in germanium p-n junctions. Irradiation effects on the conductance of a phosphor layer and a Ge photojunction are compared. D-C electroluminescence in ZnS at 2.0 v is also cited against the acceleration-collision theory, and the major arguments in its favor are discounted.

Electroluminescence (1, 2) is, at present, strongest and most efficient in zinc sulfide-type phosphors. The actual excitation mechanism, or the source of the radiated energy, making the major contribution to such electroluminescence may be one of several processes which have been discussed in principle. Destriau (3), Curie (4), and Piper and Williams (5) have proposed the acceleration-collision mechanism, in which all of the ionization energy accumulated by the (majority) carriers is derived from acceleration by the electric field; apparently this is the theory most popularly associated with electroluminescence in zinc sulfide. However, minority carrier injection is thought to be primarily responsible for electroluminescence in a number of other materials, such as Si (6), Ge (6-9), SiC (10-12), GaP (13-16), and CdS (17-21) at least under certain experimental conditions. Theories, of other possible mechanisms, which have been treated less completely in the literature include the "hot electron" model (22, 23), field ionization (24) or Zener effect, and, most recently, the idea of electroluminescence due to minority carrier accumulation (25).

The purpose of this paper is to present experimental evidence in support of the proposition that the well-known electroluminescence in zinc sulfide is actually due to minority carrier injection, rather than to acceleration and collision of majority carriers. There is much recent interest (11-15, 26-28) in electroluminescence in materials which are good well-behaved semiconductors but, in a sense, poor phosphors. Conversely, evidence such as presented in this paper of normal semiconductor behavior in materials such as zinc sulfide and related compounds, which are good phosphors but in many ways poor semiconductors, may shed light on their luminescence properties. The wealth of semiconductor knowledge, if brought to bear on phosphor materials, should lead to great progress in luminescence.

Experimental Results

Current-voltage relationships in electroluminescent materials.—The relations among brightness, voltage, power absorption, and efficiency of electroluminescent phosphors are measured and studied regularly (2, 3, 29). One important relation which has been neglected is the dependence of (resistive) current in the phosphor on the applied voltage. It is an important characteristic for two reasons: (*a*) the current flowing (not including the capacitive current, which in all cases has been eliminated in this paper) may be simply related to the electroluminescence emission, and (*b*) this current is responsible for power absorption in the phosphor and therefore determines the efficiency of light emission. The current-voltage relationship in conventional electroluminescent phosphors is, under the proper conditions, a particularly simple exponential dependence given by Eq. [1], where I' and V' are parameters independent of voltage.

$$I = I' (e^{V/V'} - 1) \qquad [1]$$

For example, the total alternating current was determined in a "Rayescent"[1] Safety Light by measuring the rms voltage across a series resistor. This lamp comprised green-emitting ZnS:Cu,Cl phosphor in a plastic dielectric (PVCA) and was measured at 1000 cps. The capacitance was calculated from the current at low voltage, and the capacitive current subtracted from the total current at each voltage. Results are shown in A of Fig. 1. The solid curve is calculated from Eq. [1]. The good fit is obtained even though the capacitance is actually not constant but in general increases with voltage (30, 31) by a factor of the order of 10-20%. All alter-

[1] Trademark, Westinghouse Electric Corporation.

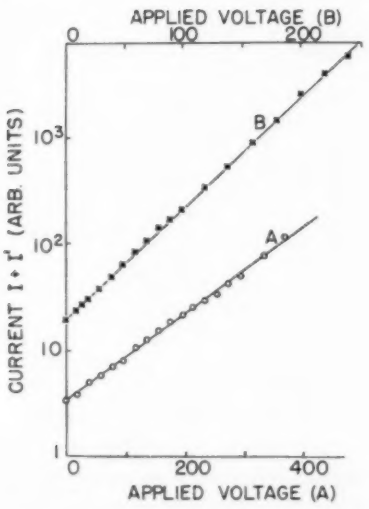

Fig. 1. Current-voltage characteristics of two conventional sprayed green-emitting ZnS:Cu,Cl powder-in-dielectric lamps. I is the resistive (rms) current component at 1000 cps and I' is a constant. Solid curves follow Eq. [1].

nating current data in this paper (with the exception of curve 1-A) were obtained with the use of a high-voltage bridge[2] in which capacitance and conductance of the lamp are measured, correcting for stray capacitance and conductance of the bridge. Light emission in foot-lamberts was measured simultaneously. The rms current is calculated from the lamp conductance; no use is made of the capacitance measurement. Curve B of Fig. 1 represents a similar phosphor layer with, however, a higher weight ratio of phosphor to dielectric so that most of the applied voltage appears across the phosphor; these are bridge measurements at a frequency of 1000 cps.[3] The solid curve was calculated from Eq. [1].

The current, as described by Eq. [1], depends only on the field strength applied to the phosphor. This was determined by varying the phosphor layer thickness "d" (Fig. 2). The upper curves (A) are Eq. [1] fitted to data on sprayed phosphor powder layers of blue-emitting ZnS:Cu,Cl with thicknesses in the ratio 1:2:3. The lower curves (B) represent yellow-emitting ZnS:Cu,Mn,Cl phosphor layers with thicknesses in the ratio 1:2:4. The straight plots are log $(I + I')$ *vs.* V/d. The point at highest voltage for each thickness is in the region of breakdown.

In Eq. [1], V should represent the potential difference actually appearing across the phosphor, rather than that across the phosphor layer including dielectric material. If the volume fraction of phosphor is appreciably less than unity this will not be the case and, furthermore, the voltage fraction appearing across the phosphor will vary with the

[2] Since the phosphor layer has a nonlinear current-voltage characteristic, a minimum rms signal is not sufficient to determine bridge balance. Instead, an oscilloscope was used as detector and balance taken as the point of zero phase difference and zero slope at the origin.

[3] H. F. Ivey points out that the small periodic deviations in Fig. 1 are reminiscent of similar deviations in the characteristics of thermionic cathodes; see also W. A. Thornton, *Phys. Rev.*, **102**, 38 (1956), Fig. 10.

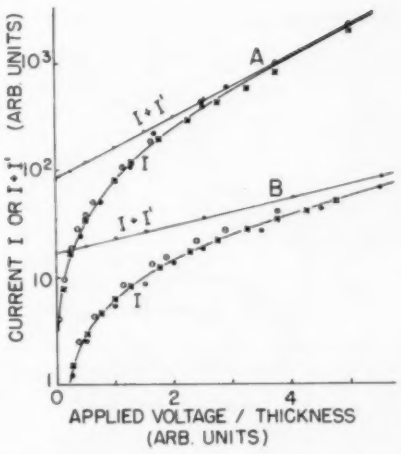

Fig. 2. Dependence of rms current on electric field strength, in phosphor-plastic layers with varying thickness of blue-emitting ZnS:Cu,Cl (A) or yellow-emitting ZnS:Cu,Mn,Cl (B) at 400 cps. Solid curves follow Eq. [1].

magnitude of the applied voltage (30, 31). Therefore the behavior of parameters I' and V' of Eq. [1] with variation in phosphor volume fraction is not strictly meaningful, and large departures from Eq. [1] occur when much dielectric material is present either as the material in which powder phosphor is embedded, or as an additional nonluminescent layer. Series impedance of course causes semiconductor diodes to deviate from Eq. [1] under all but the most ideal conditions also. Figure 3 shows the current-voltage characteristic of a bare ZnS:Cu,Cl film (32) (curve A) where the solid curve is Eq. [1], and also a characteristic of the same film with an insulating plastic coating (curve B). The data were normalized at low voltage and show the deviations at high voltage from Eq. [1] where the dielectric material is present. At low voltages the capacitive reactance of both electroluminescent films and powder layers is normally about ten times

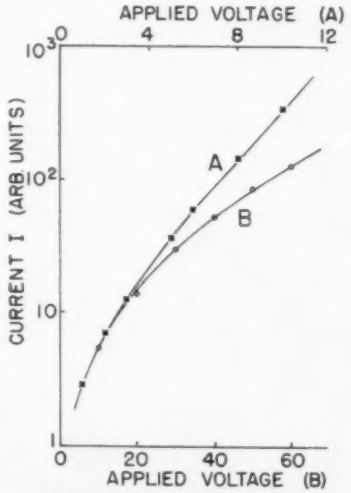

Fig. 3. Current-voltage characteristic of a blue-emitting ZnS:Cu,Cl film, bare (A) and coated (B) with an insulating plastic layer, 400 cps. Curve A follows Eq. [1].

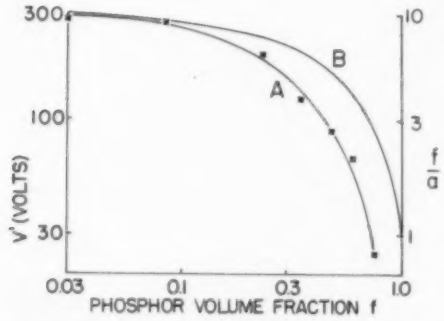

Fig. 4. Dependence of V' (see Eq. [1]) on the volume fraction f of phosphor powder (ZnS:Cu,Cl) in a conventional sprayed phosphor-plastic layer (Curve A), and the calculated dependence (Curve B) of f/a on f, where a is the voltage fraction on the phosphor proper.

less than the resistance, and the resistance is not strongly voltage dependent. Therefore, at low voltage, the voltage fraction a on the phosphor of a phosphor-dielectric mixture can be assumed constant and due to capacitive division; under this restriction, V' in Eq. [1] was determined as a function of the volume fraction f of powder phosphor (ZnS:Cu,Cl) in the phosphor-plastic layer, letting V represent the total applied voltage as before. Figure 4 shows a plot of V' *vs.* f and also, for reasons discussed later, a calculated plot of f/a *vs.* f, where $f/a = f + x\ (1-f)$ and $x = 10$ is the assumed ratio of permittivities of phosphor and dielectric material. Insofar as the shapes of the curves are similar, parameter V' is roughly proportional to f/a. The highest experimental value of f in Fig. 4 is 0.75. This corresponds roughly to the volume fraction of close-packed (identical) spheres, and at this value the phosphor particles are likely to be in contact. This means that the effective experimental value of f, as far as voltage division is concerned, is unity, and the curves of Fig. 4 would roughly coincide.

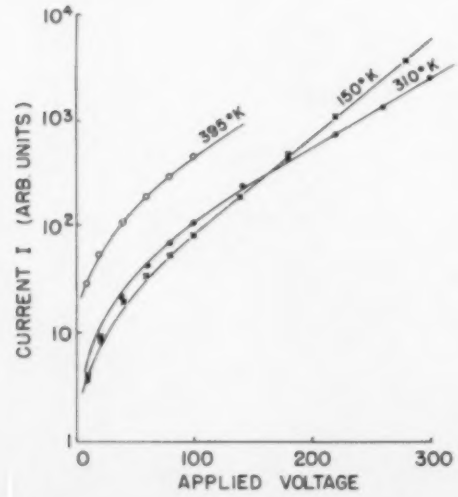

Fig. 5. Current-voltage characteristics of a ZnS:Cu,Cl powder phosphor at three representative temperatures; 400 cps. Solid curves follow Eq. [1].

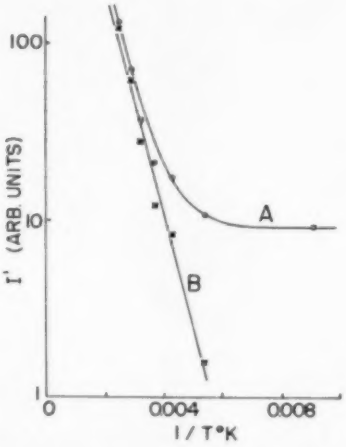

Fig. 6. Dependence of the parameter I' (see Eq. [1]) on temperature before (A) and after (B) subtraction of a "leakage" component independent of temperature. ZnS:Cu,Cl, 400 cps.

The temperature dependence of parameters I' and V' was determined for a green-emitting ZnS:Cu,Cl phosphor powder in PVCA, between 100° and 400°K, at 400 cps. Representative current-voltage plots are shown in Fig. 5. The plotted point at highest voltage is near breakdown in each case, and the curves are calculated from Eq. [1]. The dependence of parameter I' on temperature is shown in Fig. 6 both before and after subtraction of a "leakage" component I'_0 independent of temperature; the corrected point at the lowest temperature cannot be determined accurately of course and is not shown. The dependence of parameter V' on temperature is shown in Fig. 7 both before and after correction as follows: $I = I'$ when $V = V' \ln 2$. The leakage conductance $I'_0/(V' \ln 2)$ was subtracted from the experimental conductance values and new values of V' obtained. The plots at high temperature (Fig. 5) allow a rough determination of intercept I' but are

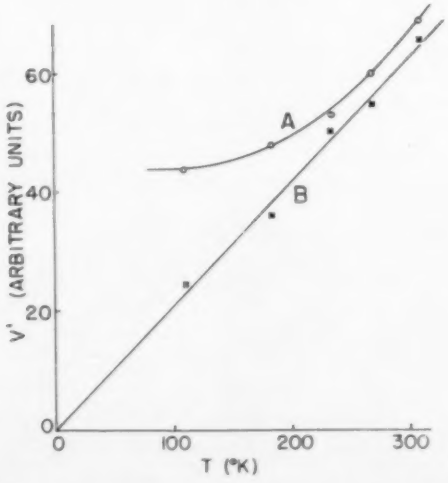

Fig. 7. Dependence of the parameter V' (see Eq. [1]) on temperature, before (A) and after (B) correction as in Fig. 6. ZnS:Cu,Cl, 400 cps.

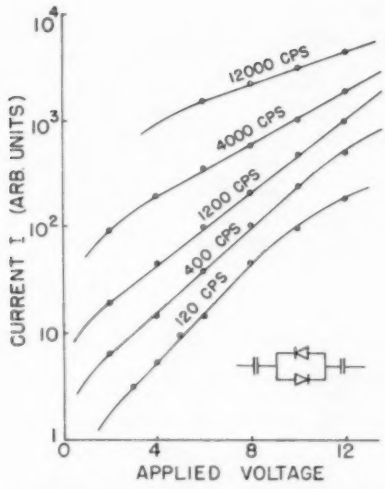

Fig. 8. Dependence of the current-voltage characteristics of a ZnS:Cu,Cl film on frequency and a suggested equivalent circuit with similar properties.

too short, due to breakdown, to allow the slope parameter V' to be determined with any accuracy, and these are omitted in Fig. 7.

The frequency dependence of the current-voltage characteristic was determined for a ZnS:Cu,Cl powder phosphor layer (in PVCA) and for a ZnS:Cu,Cl film; the latter results are shown in Fig. 8, and the behavior of the powder phosphor is similar. With increasing frequency, I' increases very rapidly and V' changes much less rapidly, for both phosphor powder and film; that is, the impedance of the layer decreases rapidly with increase in frequency, and changes from an exponential toward a linear characteristic. Similar behavior is shown by the diode-capacitor circuit also shown in Fig. 8, in that current at constant voltage increases rapidly with increase in frequency, and yet much of the exponential current-voltage behavior is retained if the capacitance values are properly related to the diodes.

Since the radiant efficiency of electroluminescence is quite low, it is not obvious that the measured currents are directly related to light emission. Such a relation can be established in an indirect manner by means of the following experiment. The current-voltage characteristics of a series of forty-nine ZnS:Cu,Cl phosphor,[4] varying only in the additions of copper and chlorine, were measured and fitted by Eq. [1] and the parameters I' and V' determined. Contours of equal I' or V' are shown in Fig. 9, where the axes are gram atom per mole of copper or chlorine added before firing. Also shown in Fig. 9 are contours of equal radiance, measured for each phosphor at constant field strength and frequency. Maximum emission occurs in the region of extremal values of I' and V', and the configurations of the families of contours are quite similar. The indication is, therefore, that the measured currents are directly related to the photon emission of the phosphor.

[4] Kindly supplied by W. Lehmann.

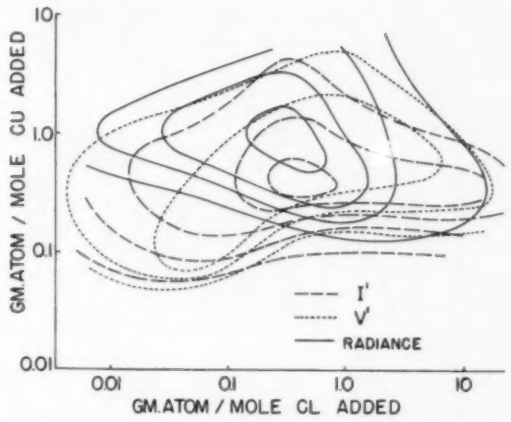

Fig. 9. Equal-value contours of the parameters I', V' (see Eq. [1]), and radiance (emitted watts/cm^2) of a series of ZnS:Cu,Cl phosphors varying in amount of copper and chlorine added.

The currents flowing in a strongly electroluminescent phosphor and in an otherwise similar but unactivated material were compared; the unactivated ZnS was fired and subsequently treated in exactly the same manner as the luminescent material except that the copper and chlorine were omitted. The conductance of the unactivated material was very small and independent of voltage. The current flowing in the electroluminescent material followed the exponential relation [1] and exceeded that in the unactivated material by a factor of 1000 at high voltage.

The type of dielectric medium apparently has little effect on the alternating currents flowing in the phosphor. Figure 10 shows the exponential cur-

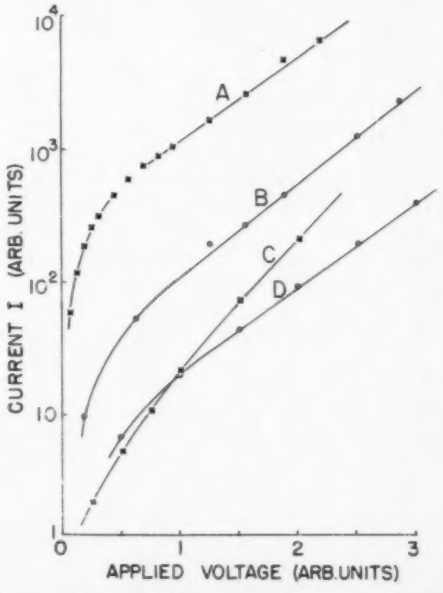

Fig. 10. Current-voltage characteristics of (A) ZnS:Cu,Cl powder phosphor in ceramic dielectric, (B) the same phosphor in air dielectric (dry powder layer), (C) a ZnS:Cu,Mn,Cl film with electrodes in direct contact with the film, and (D) a similar ZnS:Cu,Cl film; 400 cps.

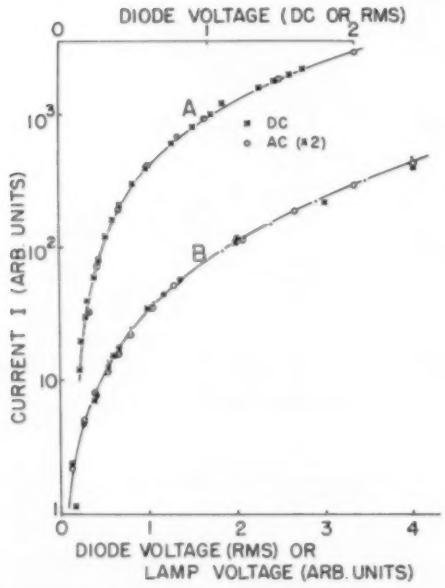

Fig. 11. Curve A: current-voltage characteristics of a 1N34 germanium diode under d-c or 400 cps a-c excitation; top voltage scale; Curve B: comparison of current-voltage characteristics of the 1N34 diode at 400 cps (crosses), a ZnS:Cu,Cl phosphor powder in oil dielectric at 400 cps (open circles), a similar phosphor in plastic at 4000 cps (dots), and a ZnS:Cu,Mn,Cl phosphor powder in plastic at 400 cps (closed circles); bottom voltage scale.

rent-voltage characteristics observed on phosphor powder layers (A) with glass dielectric, (B) with no dielectric other than air, and on two films (with no dielectric layer) of ZnS:Cu,Mn,Cl (C) and ZnS:Cu,Cl (D). Similar characteristics have been observed with a variety of plastic dielectric materials, and with electroluminescent Zn(S,Se):Cu,Cl, ZnSe:Cu,Cl, (Zn,Hg)S:Cu (33) and CaS:Cu,Eu (34) phosphors as well.

Comparison to diode characteristics.—The similarity between current-voltage characteristics of diodes and electroluminescent phosphors is illustrated in Fig. 11. Curve A represents data on a 1N34 germanium diode with d-c or 400 cps a-c voltage (rms); note that the behavior is the same. Curve B represents data on the same diode at 400 cps (crosses) up to higher forward voltages, and also measured (and normalized) currents in ZnS:Cu,Cl powder phosphor in oil dielectric at 400 cps (open circles), the same powder phosphor in plastic at 4000 cps (dots), and ZnS:Cu,Mn,Cl powder phosphor in plastic at 400 cps (closed circles).

There is also similarity between the behavior of the usual phosphor powder-dielectric layer and a germanium p-n junction under illumination. The a-c conductance at 400 cps of a sprayed lamp of green-emitting ZnS:Cu,Cl in PVCA at 50 v rms (A) and that of an RCA 7467 photojunction cell (germanium p-n junction) at 0.1 v rms (B) are shown in Fig. 12 as functions of the intensity of illumination from an unfiltered Osram HBO107 high-pressure mercury-vapor lamp. Roberts (35) obtained results similar to curve A of Fig. 12 on the same type of phosphor-dielectric layer, and Ince

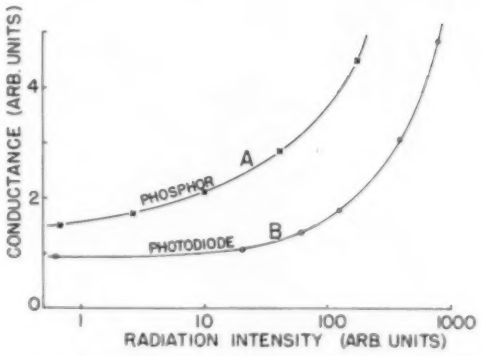

Fig. 12. Dependence of a-c conductance on irradiation of (A) a ZnS:Cu,Cl powder phosphor in plastic at 50 v rms, and (B) an RCA 7467 photo-junction cell (germanium p-n junction) at 0.1 v rms; 400 cps.

and Oatley (36) mention the same effect. In Fig. 13 the differences between conductance in the dark and with illumination are plotted as functions of the radiation intensity.

Light emission vs. current and low-voltage characteristics.—The variation of electroluminescence emission under a-c and d-c excitation for a powder phosphor (crosses) and for a film (open circles) is shown in Fig. 14 as a function of current; the plots have been shifted arbitrarily for comparison. Light emission increases as the square of the current, with d-c excitation of both powder[5] and film, apparently without limit (the brightness at the uppermost point in the film plot is about 600 ft-L). With a-c excitation, the light emission first increases even more rapidly and then apparently approaches a limit at high currents. While the electroluminescence efficiency (photons per watt or photons per ampere) increases rapidly and continuously with d-c excitation, the efficiency with a-c excitation (29) peaks and falls rapidly with increase in power

[5] Electroluminescent powder phosphors are generally strongly responsive to d-c excitation, and no appreciable differences in d-c behavior between powder phosphors and films have been noted; the difficulty in the case of the powders is, of course, to establish large area electrodes in good contact with the particles, and also particle-to-particle contact to enable current flow. See, for example, W. A. Thornton, *Bull. Amer. Phys. Soc. II*, 3, 233 (1958).

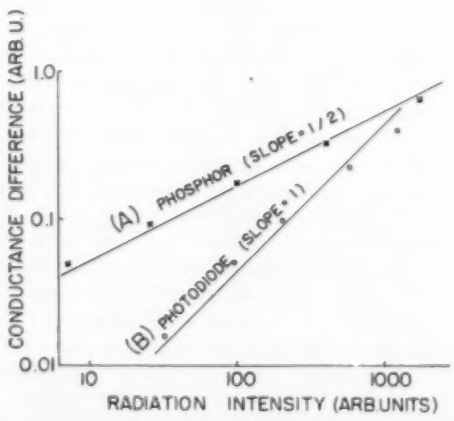

Fig. 13. Difference in a-c conductance (light minus dark) as a function of radiation intensity for the cells and operating conditions of Fig. 12 but with the positions of the curve shifted arbitrarily for convenience.

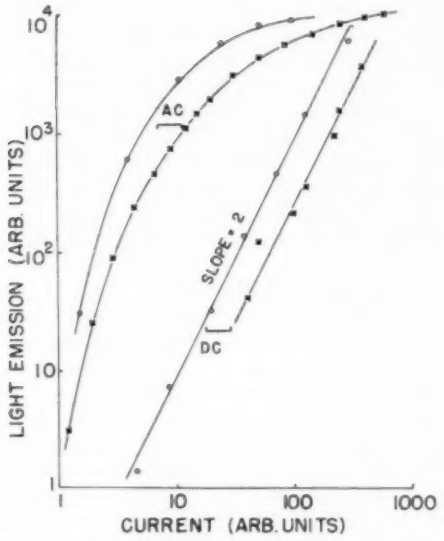

Fig. 14. Electroluminescence light emission as a function of current for ZnS:Cu,Cl powder (crosses) and film (open circles) for both d-c excitation (straight plots) and a-c excitation at 400 cps (curves).

or current. To date, however peak a-c efficiencies greatly exceed maximum d-c efficiencies.

Electroluminescence of ZnS films with a-c excitation has been observed (37) down to 1.5 v rms (2.2 v peak) which is less than the band gap of zinc sulfide or the (blue) photon energy equivalent. Electroluminescence of ZnS phosphor powder layers has been observed at 2.0 v rms. More recent measurements (38) with d-c excitation of films show emission to 2.0 v d-c with no indication of a threshold (Fig. 15); light emission could not be differentiated from noise at lower voltage. With d-c emission, also, an exponential increase of current with voltage is observed (Fig. 16); therefore, forward bias conditions exist and any contact potentials present will reduce, rather than augment, the total applied potential difference. Hence the data of Fig. 15 indicate that electroluminescence occurs at total effective voltages far less than the band gap of the luminescent crystal and less than the mean energy of the photons emitted.

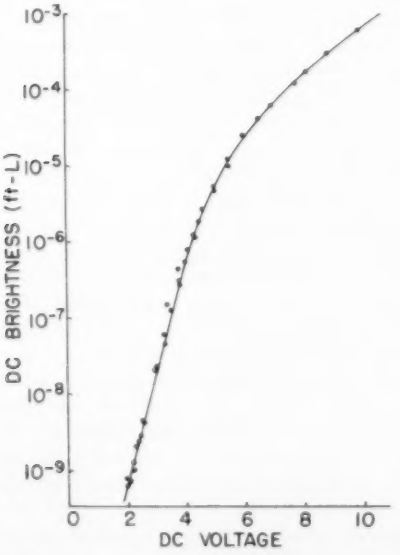

Fig. 15. The d-c emission at low voltages of a thin film of ZnS:Cu,Mn,Cl.

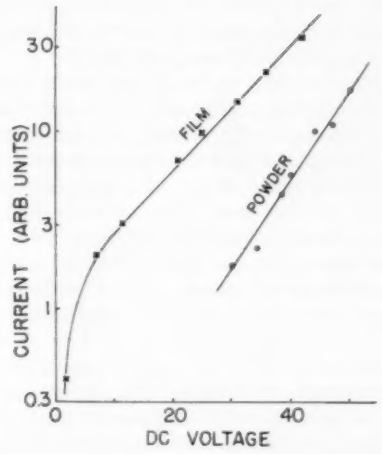

Fig. 16. Current-voltage characteristics of an electroluminescent ZnS:Cu,Mn,Cl film and a ZnS:Cu,Cl powder with d-c excitation.

Discussion

Interpretation on the basis of forward-biased junctions.—The current-voltage characteristics of electroluminescent ZnS phosphors given in this paper suggest that the controlling elements in the phosphor are forward-biased metal-semiconductor junctions or p-n junctions behaving in the usual manner, as typified by Eq. [1]. In a typical phosphor layer, a large number of such junctions probably lie in series, since Fig. 2 shows that the current depends only on the average electric field and not on the amount of phosphor (number of junctions) in series in the phosphor layer; the conversion to orange emission by the manganese in ZnS:Cu,Mn, Cl phosphors does not appear to alter the characteristics of the ZnS:Cu,Cl phosphor, in which the junctions probably depend primarily on the copper. The junctions may occur, for example, at metal or semiconducting inclusions (39, 40) (Cu_xS?) in the phosphor crystal, at dislocations, at interfaces between cubic and hexagonal phases of ZnS or in other minute regions of disorder (41-45). The junctions may occur at random or in regular arrays in the crystal so long as they are interconnected by some material acting like the metal contacts (m) linking a series string of ordinary diodes. This interconnection must be such that current can flow in the order n-p-m-n-p-m-n-p-m, for example, so that all junctions along that current path are forward biased; probably each crystal (not each junction) must have a similar but oppositely oriented return path in parallel which carries forward current during the voltage reversal. Regarding the possibility that the junctions in series are not effectively identical,

Note added in proof: V. E. Oranovskii and B. A. Khmelinin, *Optics and Spectroscopy*, 7, 336 (1959), suggest n- and p-type regions in electroluminescent zinc sulfide, as does Ballentyne (44), and that a field of 10^4 v/cm is sufficient to maintain electroluminescence.

it can be shown that the current-voltage relation for two series junctions differing only in V' will follow Eq. [1] with an intermediate value of V', while that for two series junctions differing only in I' will follow Eq. [1] with an intermediate value of I'. It seems likely, therefore, that the experimental values of I' and V' represent statistically all the junctions along series and parallel paths. The resistivity of the host material between junctions and the capacitive coupling between active regions of the phosphor crystal (Inset, Fig. 8) undoubtedly contribute to deviations by phosphors from Eq. [1] as they do in the best of germanium diodes, for example.

The loss of part of the applied voltage to regions of the phosphor layer other than the phosphor itself may be informative by the following interpretation of the data of Fig. 4. The calculated and experimental curves of Fig. 4 are very similar; they may be taken essentially identical if it is assumed that the highest phosphor volume fraction $f = 0.75$ leads to particle contact and that therefore the effective value of f in that layer is unity. Figure 4 shows then that parameter V' is about proportional to f/a. This proportionality can also be calculated, by recognizing that for equal current in many junctions in series the exponent in Eq. [1]

$$\frac{V}{V'} = \frac{ev}{kT}$$

where V is the total potential difference across the phosphor-dielectric layer, v is the voltage across a single junction, e is the electronic charge, k is Boltzmann's constant, and T is the absolute temperature. If N is the number of junctions per micron of phosphor crystal, d is the over-all thickness of the phosphor-dielectric layer, and a is the voltage fraction across the phosphor proper, then

$$V' = \left(\frac{kT}{e} Nd\right) \frac{f}{a} \qquad [2]$$

From Fig. 4, the factor in parentheses is experimentally equal to 30, and for a 3-mil phosphor (powder) layer at room temperature, N is about sixteen junctions per micron; the same result is obtained from the slope of the plot in Fig. 16 for a two-micron film. For comparison, Esaki (46) gives 150Å as the probable width of some of his junctions, so the indicated 600Å spacing of the junctions in electroluminescent ZnS may not be unreasonable. The parameter V' is proportional to phosphor layer thickness, as shown by Fig. 2, and this is consistent with Eq. [2].

The temperature dependence of the current-voltage characteristics (Fig. 5-7) suggests that Eq. [1] can be rewritten as

$$I = C_1 e^{-E/kT} \left(e^{V/C_2 T} - 1\right) \qquad [3]$$

where C_1, E, and C_2 are independent of temperature; this is, of course, the usual form of temperature dependence of the forward current through semiconductor junctions. The activation energy E determined from curve B of Fig. 6 is about 0.12 ev. A third determination of the number of junctions per micron can be obtained from the slope of curve B of Fig. 7 and Eq. [2]; in this case, f/a is about 2, d is about 3 mils, and N again is calculated to be about 15 junctions per micron. Note that the three determinations of N are independent: the first evolved from an experimental variation of phosphor powder volume fraction f, the second was taken from the d-c current-voltage characteristic of an electroluminescent film, and the third from the temperature dependence of V' in powder-dielectric layers.

It is interesting that Merz, in a study (42) of high photovoltages on ZnS single crystals, speaks of alternating layers of cubic and hexagonal material each of which leads to a rectifying barrier in the same direction; the observed photovoltages are such that several thousand of these barriers must be aligned in series, each barrier generating a photovoltage of 0.15 ev, according to Merz. Numerous junctions in series, and in the same sense, are suggested by the current-voltage data of the present paper. The value of $E = 0.12$ ev obtained from Fig. 6 can be interpreted as the diffusion potential or barrier height obtained by Merz.

The frequency dependence of the current-voltage characteristic (Fig. 8) is at present thought to be a somewhat extraneous consequence of capacitive coupling both of active regions within the phosphor crystal and, in the case of powder-dielectric layers, between phosphor particles, also. Retention of the steeply rising current-voltage characteristic, but with increased current at higher frequencies, can be obtained with the circuit of Fig. 8, for example with 1 μf capacitors and 1N34 diodes. In addition, there is independent evidence (31, 47) that in electroluminescent phosphors increasing frequency leads to reduction in the dimensions of the active regions and to a higher maximum field strength; thus, the junction resistance may fall rapidly with increasing frequency and the ohmic character of the series capacitors lead to the shallow slope at high frequency in Fig. 8.

The contours of Fig. 9 center around the same activator and coactivator properties in the ZnS:Cu,Cl phosphor. Therefore, the currents which show forward-bias characteristics are closely related to the electroluminescence radiance of the phosphor. Another main feature of the contours of I' and V' of Fig. 9 is the steep gradient at minimum copper addition, as if there were a threshold copper content necessary to evolve the currents (junctions) associated with electroluminescence. The configuration of the contours is similar in all regions except that representing low copper and chlorine additions. Here, the indication is that the additions are sufficient for current flow but not enough for efficient recombination and luminescence. That the conditions for junction formation and for luminescence in semiconductors are in general different, and sometimes mutually exclusive so that separate crystal regions must perform the two functions, is already well understood (12).

The change in conductance, under a-c excitation, with variation in radiation intensity is somewhat similar for a germanium p-n junction (RCA 7467)

and a phosphor plastic layer (Fig. 12). In the case of the diode, the increased conductance with irradiation results entirely from the addition of reverse current (leading to an increase in the rms current measured) to the forward current which flows in the dark; the integrated value of the forward current is actually somewhat reduced by the radiation, as shown by oscilloscope. It is suggested here that the increased conductance of the phosphor layer with irradiation is also due to the increase of reverse current in the junctions present in the phosphor crystal. The different dependence on radiation intensity (Fig. 13) may be due to trapping effects (48) in the phosphor which are absent in the germanium diode.

That the electroluminescence emission is due to hole-electron recombination (through activator centers) in the junction region in ZnS phosphors is suggested by the dependence of d-c light emission on the square of the current for both film and powder phosphors (Fig. 14). The a-c light emission bears a more complicated relation to the rms current.

The breakdown field for thin electroluminescent ZnS films is often observed to be 20-30 v/μ, although this may not be so much characteristic of the material as of weak spots and nonuniformities. Assuming the value of 15 junctions per micron, the maximum voltage per junction during electroluminescence may be about 2 v, or about half the band gap equivalent of zinc sulfide. Such a forward voltage is not excessive, since a germanium diode can be operated at a forward voltage several times the band gap equivalent (Fig. 11) and silicon junctions have been operated at forward voltages as much as fifteen times the band gap equivalent (49).

Strong deterioration of electroluminescence by continued operation for long periods results in an increase in V' and little change in I'. Interpreted on the basis of Eq. [2], this suggests that the number N of active junctions per micron in the phosphor increases with time, perhaps due to some gradual forming process, and the exciting voltage, current, and light emission associated with individual junctions is thereby reduced. There is evidence that the maintenance of electroluminescence is adversely affected by oxygen (50) and water (31); transistor characteristics are also affected by these (51). This interpretation is consistent with the facts that deterioration is minimized (31) at higher copper and chlorine additions (larger N) and that light emission at constant field strength falls off (31) at high copper and chlorine additions (larger N, smaller voltage per junction).

These new results all suggest minority carrier injection, or at least currents in forward-biased junctions, as the basic mechanism of ordinary electroluminescence in zinc sulfide. Some other experimental results, consistent with this proposition, are:

1. Numerous barriers or junctions are present, as suggested by the configuration of emitting regions in lines or sheets parallel to the field in GaP (14) and ZnS (39, 52, 53), and the correlation of disorder to electroluminescence in SiC (53) and ZnS (41, 43, 44, 53).

2. These barriers have the character of typical p-n junctions in series, as suggested by large photovoltages in CdTe (54, 55) and ZnS (56-58).

3. Minority carrier injection occurs, as suggested by electroluminescence edge emission in CdS (19, 21), diamond (59), and ZnS (20), by uniform electroluminescence emission in the crystal bulk in CdS (17, 21) and ZnS (20), by bimolecular (band to band) recombination in GaP (15) and ZnS (Fig. 14), and by electroluminescence emission preferentially at the anode in CdS (18, 19).

4. Exponential current-voltage characteristics associated with light emission have also been observed in CdS (18), GaP (13), and in ZnS single crystals (60).

It is believed, in addition, that the arguments for acceleration-collision ionization in electroluminescence in zinc sulfide are easily discounted; this is discussed in the next section.

Evidence for the acceleration-collision process discounted.— In the theory of injection electroluminescence the important action is the introduction of minority carriers in such a way that much of the ultimate transition energy necessary is derived by the minority carriers themselves from thermal energy. Usually the energy gained by the minority carriers from the applied field is a small fraction of the total, *i.e.*, the applied potential difference (Fermi level displacement) is usually small compared to the equivalent band-gap of the material. No threshold voltage exists for injection electroluminescence since a very small voltage in the forward direction is sufficient to upset the equilibrium of the diffusion currents and cause minority carrier injection. The minority carriers may be captured by impurity centers followed by a radiative transition by a majority carrier to the center, or direct electron-hole recombination may occur. In the theory of acceleration electroluminescence (4, 5) a majority carrier is accelerated by the field to energies sufficient to excite or ionize a bound carrier of the same kind, either from an impurity center or from the lattice. All of the excitation energy is derived from the electric field. The probability of acceleration of the carrier to excitation energies is small (even if collision is with an impurity center) but increases with increasing electric field. For these reasons the potential difference where acceleration occurs must be at least as large as the equivalent excitation energy (a threshold exists) and probably in practice would have to be much larger. Radiative recombination then occurs as in the previous example.

The evidence usually cited in favor of the acceleration mechanism is rather readily shown to be inconclusive. Strong magnetic fields do not quench electroluminescence in ZnS detectably (61). This is usually interpreted to mean that the applied potential difference is concentrated in a barrier with a very high local field; otherwise, the maximum energy attainable by the carrier in a free path would be limited by the magnetic field. However, if the electroluminescence is due to the injection mechanism, or other processes not depending on the acceleration of carriers (22-25), it would not be

expected to be quenched by a magnetic field. Therefore, while strong magnetic field quenching would have supported the acceleration theory, its absence is inconclusive.

The observation that electroluminescence in ZnS is often confined to discrete spots or lines has been interpreted to indicate regions of very high local field[6] in which the acceleration process could be active. However, the same phenomena have been observed in GaP (14) in which material it is shown that the emission is at grain boundaries and is due to carrier injection with forward bias. Diemer (39) observed long lines of emitting spots and Short, Steward, and Tomlinson (53) saw sheets of luminescence, in zinc sulfide, which show maximum emission intensity when the electric field is parallel to the lines of spots or sheets. Bontinck and Dekeyser (52) have made similar observations of five or six emitting spots per micron. These observations, together with the admission that there may be numerous nonemitting junctions across which an appreciable potential difference exists, suggest that the spots are not necessarily associated with a particularly high local field.

The probability of a carrier attaining excitation energies has been calculated (3, 4, 62) to be proportional to exp $(-a/E)$, where a is a constant and E is the electric field. Experimentally, the electroluminescence emission is often found (29) to be proportional to exp $(-b/V^{1/2})$, where b is another constant and V is the applied voltage. The correlation is suggested by citing the theoretical result (5) that the maximum electric field in a Mott-Schottky type barrier is proportional to $V^{1/2}$. However, there is apparently no evidence that simple barriers of this type ever occur in phosphors; it has also been shown that, more accurately, electroluminescence emission is experimentally proportional to exp $(-b/V^n)$ where n can be near unity (29) or substantially less than one-half in, for example, ZnS:Cu,Mn,Cl powders. Hence the experimental relation between light emission and the applied voltage is far from simple and, in view of the current-voltage and light-current relationships demonstrated in this paper, is not expected to be either fundamental nor informative.

The acceleration theory is said to be favored by the fact that electroluminescent phosphor crystals emit strongly when embedded in an insulating dielectric material and not in contact with the electrodes to which voltage is applied. However, at least a transient current must flow in both the acceleration and injection mechanisms, and internal discontinuities can serve as appropriate barriers or junctions in either case.

Evidence has also been cited specifically in the past as tending to rule out injection electroluminescence in zinc sulfide. These arguments are no longer valid. Piper and Williams (5), for example, list three reasons why injection electroluminescence seems not to apply to ZnS: (a) threshold voltage of the order of 100 v, (b) luminescence not concentrated at the anode, and (c) no evidence of minority carrier injecting discontinuities in ZnS. It has since been shown that (a) electroluminescence is observed in ZnS at 1.5 v rms (a-c) (37) and 2.0 v (d-c) (38) with no evidence of a threshold in either case; (b) multiple internal discontinuities at which light is emitted do not depend on the (external) anode; and (c) ZnS and related materials show large photovoltages (54-58), electroluminescence edge emission (19-21), and uniform electroluminescence in the crystal bulk (16, 17, 20, 21). The exponential (forward bias) dependence of current on voltage is also strong evidence for typical semiconductor junctions and minority carrier injection in zinc sulfide phosphors.

[6] The following reasoning sequence also appears in the literature: (a) assume the acceleration mechanism, (b) calculate the field necessary for the effect to be appreciable, (c) conclude since the experimental average field is too low that there must exist barrier regions of very high local field. The "evidence" for barriers thereby depends on the initial assumption.

Acknowledgment

It is a pleasure to acknowledge the experimental assistance of G. Grasso and R. M. Potemski, helpful comment by W. Lehmann, L. Patrick, and E. A. Sack, and continued encouragement and discussion by H. F. Ivey.

Manuscript received Jan. 18, 1961; revised manuscript received March 1, 1961. This paper was prepared for delivery before the Indianapolis Meeting, April 30-May 3, 1961.

Any discussion of this paper will appear in a Discussion Section to be published in the June 1962 JOURNAL.

REFERENCES

1. H. F. Ivey, Complete Bibliography in *IRE Trans. Electron Devices*, Vol. ED-6, p. 203 (April 1959) (Part I) and *This Journal*, **108**, 590 (1961) (Part II).
2. G. Destriau and H. F. Ivey, *Proc. IRE*, **43**, 1911 (December 1955) (Review Paper).
3. G. Destriau, *Phil. Mag.*, **38**, 700, 774, 800, 885 (1947); *Trans. Faraday Soc.*, **35**, 227 (1939).
4. D. Curie, *J. Phys. radium*, **13**, 317 (1952); **14**, 135 (1953); **14**, 510 (1953).
5. W. W. Piper and F. E. Williams, *Phys. Rev.*, **87**, 151 (1952); **98**, 1809 (1955); *Brit. J. Appl. Phys.*, Supp. #4, 39 (1955).
6. J. R. Haynes and H. B. Briggs, *Phys. Rev.*, **86**, 647 (1952).
7. R. Newman, *ibid.*, **91**, 1313 (1953).
8. P. Aigrain, *Physica*, **20**, 1010 (1954).
9. J. R. Haynes, *Phys. Rev.*, **98**, 1866 (1955).
10. O. W. Lossew, *Phil. Mag.*, **6**, 1024 (1928).
11. K. Lehovec, C. A. Accardo, and E. Jamgochian, *Phys. Rev.*, **83**, 603 (1951); **89**, 20 (1953).
12. L. Patrick, *J. Appl. Phys.*, **28**, 765 (1957); L. Patrick and W. J. Choyke, *ibid.*, **30**, 236 (1959).
13. G. A. Wolff, R. A. Hebert, and J. D. Broder, *Phys. Rev.*, **100**, 1144 (1955).
14. D. A. Holt, G. F. Alfrey, and C. S. Wiggins, *Nature*, **181**, 109 (1958); G. F. Alfrey and C. S. Wiggins, "Solid State Physics in Electronics and Telecommunications," Vol. 2, p. 747, Academic Press, New York (1960).
15. E. E. Loebner and E. W. Poor, Jr., Phys. Rev. Lett., **3**, 23 (1959).
16. H. G. Grimmeiss and H. Koelmans, *Philips Research Repts.*, **15**, 290 (1960).
17. K. W. Böer, U. Kümmel, and R. Rompe, *Z. Phys. Chem.*, **200**, 180 (1952).
18. G. Diemer, *Philips Research Repts.*, **9**, 109 (1954).
19. R. W. Smith, *Phys. Rev.*, **93**, 347 (1954).
20. R. W. Smith, *ibid.*, **100**, 760 (1955).
21. R. W. Smith, RCA Rep. RB-78 (1956).
22. R. Goffaux, *Bull. Acad. Roy. Belg.*, Cl. Sci., **40**, 508 (1954); *J. Phys. radium*, **17**, 763 (1956); **18**, 1 (1957).

23. E. Nagy, *J. Phys. radium*, **17**, 773 (1956); *Acta Phys. Sci. Hung.*, **6**, 153 (1956).
24. M. Ueta, *J. Phys. Soc. Japan*, **8**, 429 (1953).
25. H. K. Henisch and B. R. Marathe, *Proc. Phys. Soc. (London)*, **76**, 782 (1960).
26. T. S. Moss, "Optical Properties of Semiconductors," p. 91, Academic Press, New York (1959).
27. J. Tauc, *Czech. J. Phys.*, **7**, 275 (1957).
28. M. A. Weinstein, *J. Opt. Soc. Amer.*, **50**, 597 (1960).
29. W. Lehmann, *Illum. Eng.*, **51**, 684 (1956); *This Journal*, **103**, 667 (1956); **105**, 585 (1958).
30. W. Lehmann, *This Journal*, **103**, 24 (1956).
31. W. A. Thornton, *ibid.*, **107**, 895 (1960).
32. W. A. Thornton, *J. Appl. Phys.*, **30**, 123 (1959).
33. A. Wachtel, *This Journal*, **107**, 682 (1960).
34. A. Wachtel, *ibid.*, **107**, 199 (1960).
35. S. Roberts, *J. Opt. Soc. Amer.*, **43**, 590 (1953).
36. A. N. Ince and C. W. Oatley, *Phil Mag.*, **46**, 1081 (1955).
37. W. A. Thornton, *Phys. Rev.*, **116**, 893 (1959).
38. W. A. Thornton, *ibid.*, **122**, 58 (1961).
39. G. Diemer, *Philips Research Repts.*, **10**, 194 (1955).
40. W. Lehmann, *This Journal*, **104**, 45 (1957); **107**, 20 (1960); **107**, 657 (1960).
41. A. H. McKeag and E. G. Steward, *ibid.*, **104**, 41 (1957).
42. W. J. Merz, *Helv. Phys. Acta*, **31**, 6 (1958).
43. L. W. Strock, *Illum. Eng.*, **55**, 24 (1960).
44. D. W. G. Ballentyne, *Phys. Chem. Solids*, **10**, 242 (1959); *This Journal*, **107**, 807 (1960).
45. M. Aven and J. A. Parodi, *J. Phys. Chem. Solids*, **13**, 56 (1960).
46. L. Esaki, *Phys. Rev.*, **109**, 603 (1958).
47. G. F. Alfrey, I. Cooke, and K. N. R. Taylor, "Solid State Physics in Electronics and Telecommunications," Vol. 2, p. 816, Academic Press, New York (1960); G. F. Alfrey and K. N. R. Taylor, *J. Electronics and Control*, **4**, 417 (1958).
48. R. H. Bube, "Photoconductivity of Solids," p. 342, John Wiley & Sons, Inc., New York (1960).
49. L. W. Davies, *Phys. Rev. Letters*, **4**, 11 (1960).
50. W. A. Thornton, "Solid State Physics in Electronics and Telecommunications," Vol. 4, p. 658, Academic Press, New York (1960).
51. A. J. Wahl and J. J. Kleimack, *Proc. IRE*, **44**, 494 (1956).
52. W. Bontinck and W. Dekeyser, *Physica*, **22**, 607 (1956).
53. M. A. Short, E. G. Steward, and T. B. Tomlinson, *Nature*, **177**, 240 (1956).
54. L. Pensak, *Phys. Rev.*, **109**, 601 (1958).
55. B. Goldstein, *ibid.*, **109**, 601 (1958).
56. S. G. Ellis, F. Herman, E. E. Loebner, W. J. Merz, C. W. Struck, and J. G. White, *ibid.*, **109**, 1860 (1958).
57. G. Cheroff and S. P. Keller, *ibid.*, **111**, 98 (1958).
58. A. Lempicki, *ibid.*, **113**, 1204 (1959).
59. J. C. Male and J. R. Prior, *Nature*, **186**, 1037 (1960).
60. D. R. Frankl, Paper No. 32 presented at Electrochemical Society Meeting, Cincinnati, May 1955.
61. A. N. Ince, *Proc. Phys. Soc. (London)*, **B67**, 870 (1954).
62. F. Seitz, *Phys. Rev.*, **76**, 1376 (1949).

Characteristics of the {111} Surfaces of the III-V Intermetallic Compounds

II. Surface Damage

H. C. Gatos, M. C. Lavine, and E. P. Warekois

Lincoln Laboratory,[1] Massachusetts Institute of Technology, Lexington, Massachusetts

ABSTRACT

The dissolution rate technique has been applied in determining the depth of surface damage resulting from cold working (abrasion). The following III-V compounds were employed: GaAs, GaSb, InAs, and InSb. It was shown that the dissolution rates are a function of the actual surface area which in turn depends on the amount of cold work present rather than on the original roughening of the surface. The results obtained by this method were found to be in excellent agreement with results obtained by etching (etch figures) and x-ray diffraction techniques. For the same cold-working treatment the depth of damage in InSb was found to vary for the various orientations as follows: {100} > B{111} > {110} ≥ A{111}, A and B designating the {111} surfaces terminating with In and Sb atoms, respectively. It was further found that for the same cold-working treatment of the A{111} or B{111} surfaces of the four compounds studied, the depth of damage varied as follows: InSb > InAs > GaSb > GaAs, *i.e.*, the depth of damage decreased with increasing energy gap.

It was shown in previous communications (1, 2) that the same cold-work treatment leads to a greater depth of damage in the {111} surfaces of the III-V compounds terminating with group V atoms (B surfaces) than in the surfaces terminating with group III atoms (A surfaces). This behavior is another consequence of the polarity of these compounds (zinc blende structure) along the <111> directions. The depth-of-damage determinations were based on an earlier observation (3) that the characteristic etch figures developed on the {111} surfaces as well as those developed on the {110} and {100} surfaces of the III-V compounds are altered significantly in the presence of cold work (abrasion). Determinations of the depth of damage were also made by employing x-ray diffraction techniques.

In the case of elemental semiconductors the depth of surface damage has been determined by following the dissolution rate which decreases, as the

[1] Operated with support from the U. S. Army, Navy, and Air Force.

damaged layers are being removed, to a limiting value obtained on complete removal of the damaged material (4, 5). In the present investigation, this dissolution method was compared with the etch figure and x-ray techniques and applied to GaAs, GaSb, InAs, and InSb. An empirical relationship was established for these compounds between the energy gap and the depth of surface damage (resulting from the same surface treatment).

Experimental

All samples employed (GaAs, GaSb, InAs, and InSb) were single crystals of high purity, bounded by only one type of low index crystallographic planes cut and ground to the proper orientations as determined by x-ray diffraction. The samples bounded by A{111} and B{111} planes were tetrahedrons. Those bounded by {100} and {110} were cubes and parallelepipeds, respectively.

Cold work was introduced in the samples by abrading on a glass plate with a water slurry abrasive having the desired particle size. Although this operation was performed manually, the results were quite reproducible and independent of the individual manipulator. Actually it was found that the pressure (within reasonable limits) applied during abrasion is not critical with regard to the resulting depth of damage. The abrasives employed were: silicon carbide powder (20μ particle size) garnet powder (10μ particle size) and diamond paste (3μ particle size). Before testing, the samples were freed from loose particles, degreased, and thoroughly rinsed with distilled water.

Dissolution rates were determined by weight loss measurements. In determining the dissolution rates as a function of time the samples were removed from the etching solution, rinsed immediately with distilled water, dried, weighed, and reimmersed in the solution until a steady-state rate was achieved. The results are presented in terms of dissolution rate as a function of distance from the surface. This distance was calculated from the weight loss data and the density of the particular material.

The dissolution of the samples took place very uniformly over the surface. In fact, the geometric shape of the samples was not altered even after their linear dimensions were decreased by a factor of three. No mechanical stirring was associated with the dissolution experiments.

Results

InSb.—The results obtained with B{111}tetrahedrons of InSb in 1 part (by volume) 30% H_2O_2 + 1 48% HF + 8H_2O are shown in Fig. 1. Four surface treatments prior to testing are indicated: abrasion with 3, 10, and 20μ particle size abrasive and chemical polishing. No change in dissolution rate was observed as a function of time when the original surface was chemically polished. However, in the case of the 10μ and 20μ treatment the rate decreased with time (or distance from the surface) and reached a well-defined limiting value. In contrast, when the surface was pretreated with a 3μ abrasive the dissolution rate increased before it reached a limiting value.

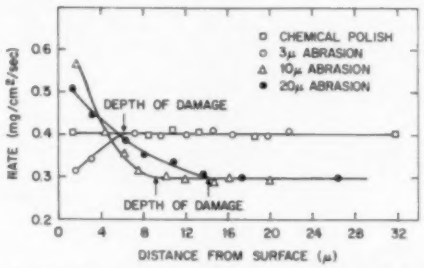

Fig. 1. Dissolution rate of B{111} surfaces of InSb (1 part by volume 30% H_2O_2 + 1 48% HF + 8H_2O at room temperature) as a function of distance from the surface for various surface pretreatment as indicated. Depth of damage is also shown. (Apparent activation energy for the reaction about 6 kcal/mole.)

In all three cases where the surfaces were cold worked the limiting rate was reached at a distance from the surface corresponding to the depth of damage caused by abrasion. These values of depth of damage, 6μ, 9μ, and 14μ of Fig. 1 are in excellent agreement with those obtained for the same abrasive treatments by etch figure and x-ray diffraction techniques (2). The reproducibility of the depth of damage attainable by the present dissolution rate technique is $\pm$ 1μ. Determinations of the depth of damage in A{111} InSb surfaces by dissolution rates were also found in excellent agreement with the etch-figure and x-ray diffraction techniques (2).

The dependence of the dissolution rates on temperature was determined both in the region of the damaged layers and after removal of the surface damage. The apparent activation energies were found to be the same in both cases and equal to about 6 kcal/mole. This value is indicative of reactions controlled by mass transport to the solid liquid interface. It is of interest to note, however, that the depth of damage can also be determined conveniently if the reactions employed are under activation control. For example the reaction of A{111} surfaces of InSb in 2 parts conc. HNO_3 + 1 48% HF + 1 glacial CH_3COOH is under activation control below room temperature (apparent activation energy 25 kcal/mole). Under these experimental conditions the depth of damage of A{111} surfaces of InSb abraded with 20μ particle size abrasive was found to be approximately 9μ (Fig. 2) in

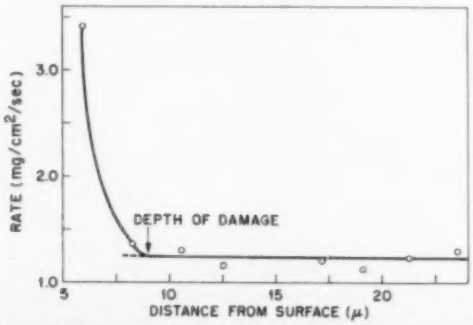

Fig. 2. Dissolution rate of A{111} surfaces of InSb in 2 parts conc. HNO_3 + 1 48% HF + 1 glacial CH_3COOH at 6°C as a function of distance from the surface (apparent activation energy for the reaction about 25 kcal/mole) cold worked with 20μ particle size abrasive.

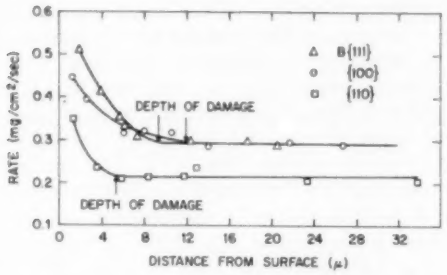

Fig. 3. Effect of orientation on the depth of surface damage in InSb. Surfaces cold worked with 10μ particle size abrasive. Electrolyte composition: 1 part 30% H_2O_2 + 1 48% HF + $8H_2O$. Room temperature.

good agreement with the values obtained by dissolution rates under diffusion control and by other methods (2).

The depth of damage in the other low index surfaces of InSb resulting from a treatment with 10μ abrasive is shown in Fig. 3 together with the corresponding depth of damage in the B{111} surfaces. It is seen that for the same surface treatment the depth of damage in the B{111} surfaces is smaller than that found in the {100} surfaces, and somewhat greater than the corresponding depth of damage in the {110} surfaces. It should also be noted that the limiting dissolution rate of the {110} surfaces is somewhat smaller than the limiting rates of the {100} and B{111} surfaces.

Other III-V compounds.—A behavior similar to that described for InSb was observed for other III-V compounds. Typical results for GaAs are shown in Fig. 4. Here, B{111} surfaces of GaAs cold worked with 20μ particle size abrasive were submitted to two different oxidizing solutions. Although the dissolution rates are appreciably different in the two solutions, the observed depth of damage has the same value within experimental error. The dissolution reaction is under diffusion control in case I and under activation control in case II.

The values of depth of damage resulting from cold working with 20μ particle size abrasive in the A{111} and B{111} surfaces of four III-V compounds are summarized in Fig. 5. It is seen that in all cases, for the same treatment, the depth of damage is greater in the B{111} than in the A{111} surfaces. It should also be noted that there is a distinct relationship between the energy gap of the III-V compounds and the depth of damage resulting from cold working by abrasion.

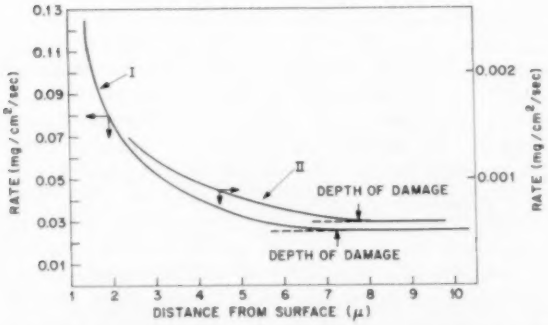

Fig. 4. Depth of damage in B{111} surface of GaAs cold worked with 20μ particle size abrasive. Electrolyte compositions: I, 1part 30% H_2O_2 + 1 48% HF + $2H_2O$. II, 2 conc. HCl + 1 conc. HNO_3 + $2H_2O$. Room temperature.

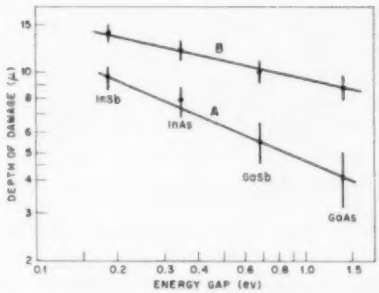

Fig. 5. Depth of damage in the A{111} and B{111} surfaces of III-V compounds as a function of energy gap. Surfaces cold worked with 20μ particle size abrasive. Reproducibility of the depth of damage determinations is within $\pm$ 1μ indicated by the vertical bars.

Discussion

Dissolution process.—The increase in the dissolution rates of solids resulting from the presence of cold work has been attributed to the increased energy associated with cold work which leads to an increase in reactivity of the surface atoms (6, 7). In some instances this increase in rate has been attributed to the increase in the original surface area, resulting from cold working by abrasion (4, 5). Obviously, however, an increase in surface reactivity cannot be considered as a controlling factor in dissolution reactions under mass transport control as in the present cases. Similarly, the *original* surface area alone does not control the over-all dissolution behavior and in particular the dependence of the dissolution rate on time as is apparent from the present data (see Fig. 1). Assuming for example that the dissolution rate is proportional to the surface area, it is seen from Fig. 1 that the original surface area is not related in any obvious way to the subsequent changes in surface area. It is believed that the magnitude of dissolution rate at a given time reflects the actual surface area of the material at that time and that the surface area after the onset of dissolution is not necessarily a direct function of the original surface area as discussed below.

For diffusion controlled processes the dissolution rate, dm/dt, is equal to (8)

$$dm/dt = DAC/\delta \qquad [1]$$

where D is the diffusion coefficient of the diffusing species, A the area, C the concentration of the reacting species (the oxidizing agent in this case), and δ the effective thickness of the boundary (Nernst) layer. A represents the projected area if the roughness is small, *i.e.*, if the surface irregularities are small compared to δ. For systems such as those employed in the present case where there is no mechanical stirring, except of course stirring by convection, δ can be assumed to be approximately 50μ.

Consequently, the surface roughness should have no appreciable effect on the dissolution rates.

However, gas evolution during dissolution may indeed provide vigorous stirring and lead to a pronounced decrease in effective δ. It was determined recently, for example, that for a rate of gas evolution of 10 cm^3/cm^2-min δ has an apparent value of approximately 3μ (9). Such a small value of δ is difficult to attain by mechanical stirring. Thus, in experiments with cylindrical electrodes a value of δ equal to 6μ was attained at a rotation speed of 1360 rpm corresponding to a tangential velocity of 420 cm/sec (10).

In the systems employed in this study there is a vigorous gas evolution during dissolution. No attempt was made to determine experimentally the gas evolution rate or the actual chemical reactions involved in these complex systems. However, it is reasonable to assume that there is a mole of gas evolved per mole of the compound dissolved. In such a case, and for the limiting rates of Fig. 1 and 3 a gas evolution rate of approximately 3 cm^3/cm^2-min is associated with the dissolution process. On the basis of the work of Ibl and Venczel (9) the effective value of δ should then be approximately 10μ. Under such conditions it is expected that the roughness factor should be reflected in the dissolution rates.

Microscopic examination of the surfaces before, during, and after testing indicated that at least qualitatively the dissolution rates are a function of the surface roughness. Typical results are shown in Fig. 6. Although resolution is impaired in the reproduction shown here, it can be seen that the roughness of the sample abraded with a 3μ particle size abrasive (Fig. 6-III) is less than in the chemically polished sample (Fig. 6-I). The surface corresponding to the limiting dissolution rates of cases 6-I and 6-III is typically represented by Fig. 6-V. It is seen further that the original surfaces abraded by 10μ and 20μ abrasives (Fig. 6-II and IV, respectively) exhibit a greater roughness than after they reach their limiting rates (Fig. 6-VI). It is of interest to note that the initial roughness of the sample treated with the 10μ abrasive is greater than that of the sample treated with the 20μ abrasive. This result is not surprising in view of the brittle nature of InSb. The difference in roughness between the cases of Fig. 6-V and Fig. 6-VI and the corresponding difference in rates (Fig. 1) is quite apparent.

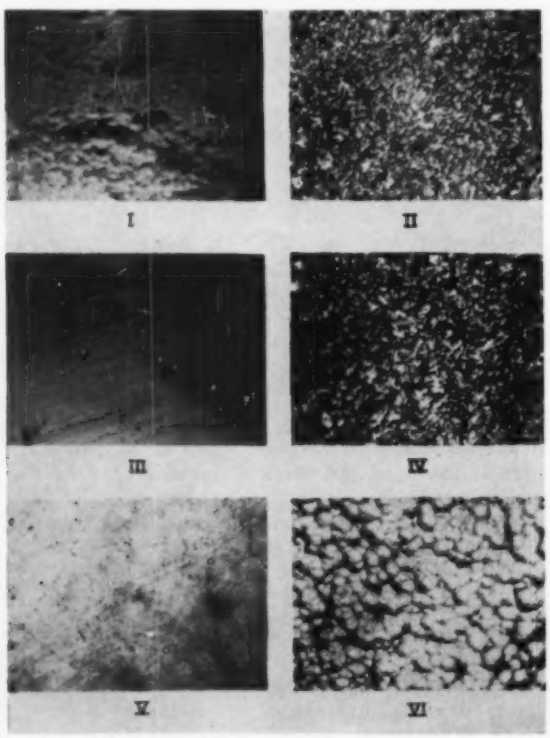

Fig. 6. I-IV. Original surfaces after the following treatments: I, Chemical polish; II, 10μ abrasive; III, 3μ abrasive; IV, 20μ abrasive; V, surface corresponding to limiting rate of surfaces I and III; VI, surface corresponding to limiting rate of surfaces II and IV. Magnification 300X before reduction for publication.

Regarding the dissolution reactions under activation control (Fig. 2) which also lead to results similar to those obtained with reactions under diffusion control, their rates are also a function of the surface A as follows (8)

$$dm/dt = kAC \qquad [2]$$

where k is the reaction constant and C the concentration.

Surface roughness.—It is apparent from the results of Fig. 1 that the initial surface roughness alone as created by the mechanical action of the abrasive does not determine the subsequent behavior of the material. The extent and nature of cold work plays an important role. It can be seen from Fig. 1, for example, that the sample cold worked with the 20μ abrasive reacts slower at first than the sample treated with the 10μ abrasive. Subsequently, the dissolution rates (and therefore the relative magnitudes of surface roughness) are reversed, and the sample treated with the 20μ abrasive continues to exhibit a higher dissolution rate even after the sample treated with the 10μ abrasive has reached the limited rate.

It is believed that after the onset of dissolution the surface roughness is controlled by the pronounced surface energy heterogeneities introduced by cold work. The most distorted parts of the surface serve as effective anodic areas and thus are preferentially attacked leading to surface irregularities. It is reasonable to expect that the more the cold work (the larger the particle size of the abrasive) the greater the surface irregularities and of course the greater the depth of damage. However, even on removal of the cold-worked layers, the roughness of the surface persists. This "hysteresis" in the surface roughness is probably responsible for the differences observed in the apparent limiting rates of Fig. 1. The lower over-all roughness in the case of the {110} surfaces (Fig. 3) could be due to the fact that the principle cleavage planes of the III-V compounds are also the {110} planes. Thus, on these surfaces the microcleavage planes are parallel to the gross surface, and the re-

sulting roughness is expected to be less than in the other surfaces.

Depth of surface damage.—From Fig. 1, 2, and 5 it is seen that for the same material and cold-working treatment the depth of damage for the various orientations is as follows

$$\{100\} > B\{111\} > \{110\} > A\{111\}$$

The observed differences between the A{111} and B{111} surfaces have been attributed to the strain present in the A surfaces owing to the deviation of the A surface atoms from the tetrahedral coordination as discussed elsewhere (1). The depth of damage for the various orientations (excluding the A{111} surfaces) increases with increasing atomic density (atoms/cm^2) of the corresponding crystallographic planes. Thus, for the same treatment and the same material the atomic density of the crystallographic planes may control the differences in the depth of damage. It is possible that the slip characteristics of these compounds play a role in the present experiments. However, a further discussion of this matter must await a better understanding of the actual nature of the damaged surface layer.

The results of Fig. 5 represent an empirical relationship between the depth of damage (in a given orientation) and the energy gap (E_g):

$$\log P = K' - K'' \log E_g \qquad [3]$$

where K' and K'' are constants which appear to depend on the perfection of the surface and probably on orientation.

According to Eq. [3] the depth of damage increases with increasing interatomic distance since the energy gap decreases with increasing interatomic distance. Equation [3] is thus consistent with Goldschmidt's relationship between hardness, H, and interatomic distance, r:

$$\log H = K_1 - K_2 \log r \qquad [4]$$

where K_1 and K_2 are constants. This relationship has been shown to apply in the case of the III-V compounds (11).

From the data of Fig. 5 and the hardness data[2] of ref. (11) (Knoop microhardness on the {111} planes: GaAs = 750 ± 42; GaSb = 448 ± 27; InAs = 381 ± 26; InSb = 223 ± 20) it is found that within the accuracy of the data the depth of damage decreases linearly with increasing hardness.

Acknowledgment

The authors are indebted to Mrs. M. J. Button for performing some of the experiments and to Mr. P. L. Moody for growing the single crystal compounds.

Manuscript received Dec. 16, 1960. This paper was prepared for delivery before the Houston Meeting, Oct. 9-13, 1960.

Any discussion of this paper will appear in a Discussion Section to be published in the June 1962 JOURNAL.

REFERENCES

1. E. P. Warekois, M. C. Lavine, and H. C. Gatos, *J. Appl. Phys.*, **31**, 1302 (1960).
2. H. C. Gatos, M. C. Lavine, and E. P. Warekois, *International Conference on Semiconductors*, Prague, 1960, in press.
3. H. C. Gatos and M. C. Lavine, *This Journal*, **107**, 427 (1960); *ibid.*, **107**, 433 (1960).
4. P. R. Camp, *ibid.*, **102**, 586 (1955).
5. J. W. Faust, Jr., *Am. Soc. Testing Materials*, Symposium on Cleaning of Electronic Device Components and Materials, *Special Tech. Publ. 246*.
6. U. R. Evans, "The Corrosion and Oxidation of Metals," p. 386, St. Martin's Press, Inc., (1960).
7. J. W. Faust, Jr., quoted by T. M. Buck in "The Surface Chemistry of Metals and Semiconductors," H. C. Gatos, Editor, p. 107, John Wiley & Sons, Inc., New York (1960).
8. C. V. King in "The Surface Chemistry of Metals and Semiconductors," H. C. Gatos, Editor, p. 357, John Wiley & Sons, Inc., New York (1960).
9. N. Ibl and J. Venczel, *Electrochimica Acta*, in press.
10. M. Eisenberg, C. W. Tobias, and C. R. Wilke, *This Journal*, **101**, 306 (1954).
11. G. A. Wolff, L. Toman, Jr., N. J. Field, and J. C. Clark, in "Semiconductors and Phosphors," M. Schön and H. Welker, Editors, p. 463, Interscience Publishers, New York (1958).

[2] No difference in hardness is reported in ref. (11) between the A and B{111} surfaces.

Epitaxial Silicon Films by the Hydrogen Reduction of $SiCl_4$

H. C. Theuerer

Bell Telephone Laboratories, Incorporated, Murray Hill, New Jersey

ABSTRACT

Epitaxial films of silicon with controlled thickness and resistivity either n- or p-type may be grown using the hydrogen reduction of silicon tetrachloride appropriately doped with PCl_3 or BBr_3. The basic chemistry and reaction kinetics pertinent to the growth of these films are discussed in detail in this paper.

The new epitaxial mesa transistors (1) and other semiconductor devices utilize silicon single crystal films grown on low resistivity silicon substrates. The hydrogen reduction of silicon tetrachloride is well suited to the preparation of these films since this reaction is surface catalyzed and has a readily controllable rate. For epitaxial growth, n- or p-type substrates having a <111> orientation with resistivities between 0.01 and 0.001 ohm-cm are normally used. The reduction of undoped silicon tetra-

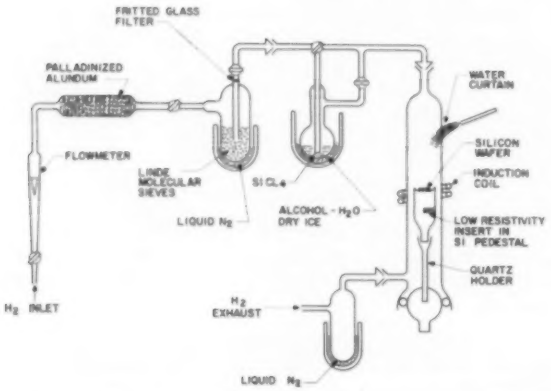

Fig. 1. Apparatus for silicon film preparation by the H_2 reduction of $SiCl_4$.

chloride purified by adsorption techniques (2) results in n-type films with resistivities between 20 and 100 ohm-cm. As required, the film thickness, resistivity, and conductivity type can be controlled by variations in the basic procedures. N- or p-type films with desired resistivities are obtained by doping the silicon tetrachloride with appropriate amounts of phosphorus trichloride or boron tribromide, respectively.

The reaction kinetics and basic chemistry pertinent to the growth of epitaxial films are discussed in detail in this paper.

Experimental Requirements for Film Deposition

The apparatus used to prepare epitaxial films by the hydrogen reduction of silicon tetrachloride is shown schematically in Fig. 1. Essentially, it consists of a source of pure hydrogen, a halide saturating system, the reduction chamber, and a radio-frequency generator for external heating. To purify the hydrogen, tank gas is passed through a trap containing palladinized alundum pellets to remove oxygen. The gas is then passed through a second trap containing No. 5A Molecular Sieves[1] refrigerated with liquid nitrogen for the purpose of removing water and other condensable gases from the hydrogen. The purified gas may then be passed into the reduction chamber either directly or first through the $SiCl_4$ saturator by manipulation of the stopcocks. Control of the $SiCl_4$-H_2 ratio is obtained by refrigerating the saturator with alcohol-water-dry ice mixtures.

The reduction is carried out in a water-cooled quartz tube 1-in. OD x 12-in. long within which the wafer to be treated is supported in a silicon pedestal for heating. The pedestal is mounted in a quartz holder from a nickel end closure. The heating pedestal is made from a high-purity silicon rod ½ in. diameter x 1½ in. long dished out at the top for a depth of 1/16 in. For rf coupling, a low resistivity insert is fused into the silicon ⅝ in. from the top of the pedestal.

The silicon substrates used for epitaxial growth, consist of 6 mil wafers 0.310 in. square with <111> faces. The wafers are ground flat with 1800 alundum and are given a bright etch to expose an undamaged crystal surface. A 5-min etch in a mixture of 30 ml HNO_3, 5 ml HF, and 10 ml acetic acid, followed by washing with deionized water and drying at 110°C was the usual procedure in this work. Prior to film deposition, the silicon wafer is treated in dry hydrogen at 1295°C for ½ hr to remove residual surface oxide. In this treatment the silicon reacts with SiO_2 to form SiO which evaporates and condenses on the tube walls. Following this treatment, the wafer is brought to deposition temperature, and the $SiCl_4$-H_2 mixture is introduced for prescribed times. The variables controlling the deposition rate are temperature, $SiCl_4$-H_2 ratio, flow rate, and time of treatment.

[1] This material may be obtained from the Linde Air Products Co.

Film Evaluation Methods

In this work conductivity type was determined by the hot probe method (3). The resistivity was determined from the film thickness and the sheet resistance obtained using the four point probe method (4). With this method it is necessary that the substrate wafer be of opposite conductivity type to that of the film being measured. In cases where the films are prepared on substrates of the same conductivity type, it is possible to determine resistivity and film thickness from measurements of capacitance as a function of voltage. Film thickness (5) was normally measured by polishing a 2° or 5° bevel on the coated surface of the wafer. The bevel was then stained with HF-HNO_3 100:1 which delineated the film region at the top of the bevel. The thickness can then be determined by counting interference fringes produced along the beveled film using an optical flat and sodium light for illumination. The weight gain of the wafers was also used as an index of thickness. Results by this method are semiquantitative, however, since it has been found that the underside of the wafers are also coated. In general, it has been found that the weight gains are somewhat larger than would be expected for a double film of uniform thickness. The film at the underside of the wafer is produced by transfer from the pedestal silicon by a process not directly related to the hydrogen reduction process under discussion herein.

Effect of Various Reaction Variables on Film Growth

Using a $SiCl_4$-H_2 mole fraction of 0.02 achieved by refrigerating the saturator at −30°C and treating the silicon wafer for 5 min at 1270°C with a hydrogen flow of 1 l/min results in a film 8μ thick. The thickness obtained can be controlled over a wide range by variations in the operating parameters. Most conveniently with other variables fixed, the film thickness may be varied linearly with time of treatment. As shown in Fig. 2, the thickness may also be varied by changes in flow rate for low hydrogen flows but at rates much above 1 l/min a further increase in deposition rate is not observed. Figure 3 gives the dependence of deposition rate on temperature. The data indicate an activation energy for the over-all reaction of 37 kcal, and for the temperature range of interest the deposition rate doubles with an 80°C rise in temperature. Figure 4

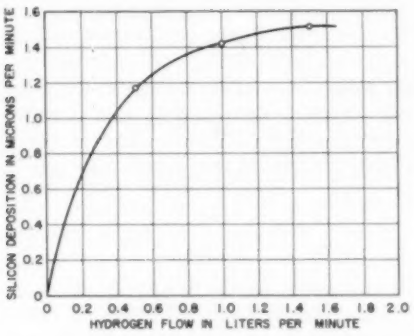

Fig. 2. Effect of gas flow rate on silicon deposition

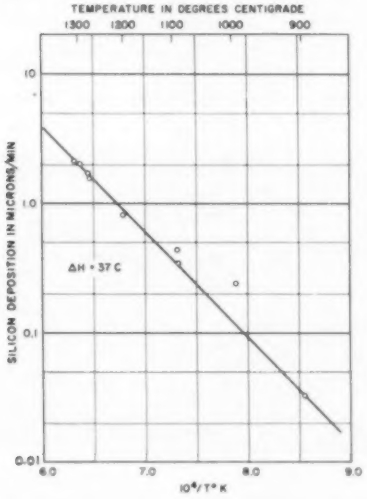

Fig. 3. Temperature dependence of silicon deposition

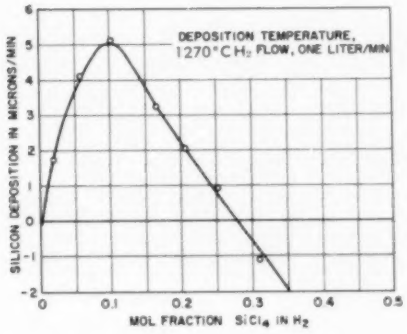

Fig. 4. Effect of $SiCl_4$-H_2 ratio on silicon deposition

shows the effect of variations in the mole fraction of $SiCl_4$ on deposition rate at the normal reduction temperature of 1270°C. It will be seen that the rate of deposition initially increases with increasing $SiCl_4$ concentration, peaks at a mole fraction of 0.10, and then diminished for further increases in $SiCl_4$. Above a mole fraction of 0.28, etching of the silicon substrate occurs.

Reaction Mechanism

The hydrogen reduction of silicon tetrachloride is a more complex reaction than is indicated by the basic equation

$$SiCl_4 + 2H_2 \leftrightharpoons Si + 4HCl$$

This equation does not predict the observed 20% yield of $SiHCl_3$ for a corresponding silicon yield of 10%, or the smaller amounts ($< 1\%$) of high molecular weight polymers, typically (6) $Si_{10}Cl_{20}H_2$, found as a condensate on the reaction tube walls. The reduction mechanism, although not completely understood, undoubtedly occurs by way of intermediate reactions involving subchlorides, possibly the free radical $SiCl_3$. The relatively high activation energy of 37 kcal and the reduction in silicon yield with increasing $SiCl_4$-H_2 ratio suggest that the reaction involves activated adsorption and diffusion mechanisms. One can postulate that $SiCl_2$ is adsorbed on the substrate with the loss of chlorine by reaction with hydrogen which results in the formation of silicon This is followed by diffusion of the HCl from the substrate. At the same time $SiCl_2$ reacting in the gas phase with hydrogen results in the formation of $SiHCl_3$.

Control of Resistivity and Conductivity Type

Using silicon tetrachloride purified by adsorption techniques (2) epitaxial films are n-type with resistivities between 20 and 100 ohm-cm. This silicon tetrachloride is probably capable of producing silicon of much higher resistivity. However, using the described etching techniques an upper limit of about 100 ohm-cm is imposed on the process due to the incomplete removal of impurities from the surface. After etching, residual amounts of a fast diffusing donor impurity (7) to the extent of 0.005 monolayers are found on the surface. During the heat treatment and film deposition, this donor diffuses through the substrate and film resulting in a donor concentration of 5×10^{13} atom/cm^3 $\sim$ 100 ohm-cm.

The resistivity obtained with pure $SiCl_4$ is adequate for most semiconductor requirements. Where lower resistivity films are desired, these can be obtained by appropriate doping using either BBr_3 or PCl_3 for p- and n-type films, respectively. These dopants have been chosen because they are liquids with similar vapor pressures to $SiCl_4$ as shown in Fig. 5. In the case of phosphorus doping, for a saturation temperature of −30°C it has been found that

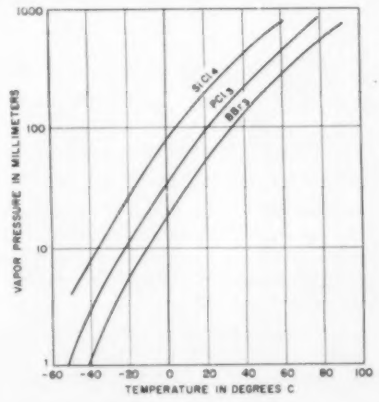

Fig. 5. Vapor pressure curves for various reactants

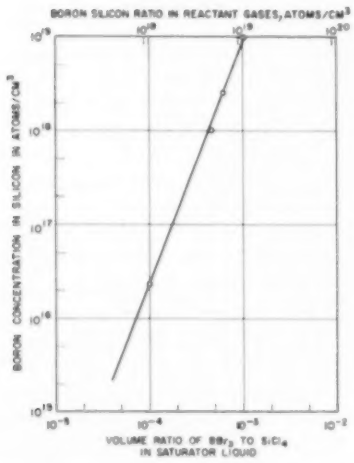
BORON SILICON RATIO IN REACTANT GASES, ATOMS/CM³
BORON CONCENTRATION IN SILICON IN ATOMS/CM³
VOLUME RATIO OF BBr₃ TO SiCl₄ IN SATURATOR LIQUID

Fig. 6. BBr_3 concentration required in $SiCl_4$ for various doping levels in silicon.

good results are obtained using the following equation

$$\frac{V_{PCl_3}}{V_{SiCl_4}} = 3.9 \times 10^{-23} \times N_D$$

where V is the volume in ml and N_D is the concentration of donors in atoms/cm³ of Si. In the derivation of the above equation Raoult's law was used, and it was assumed that the mole ratio of dopant to silicon in the $SiCl_4$ vapor is equal to that obtained in the reduced material. In the case of boron doping, as shown in Fig. 6, it has been found that more BBr_3 is required at concentration below 10^{19} atoms/cm³ than that calculated by the above method. Also, observed with heavy boron doping is a considerable increase in the deposition rate of silicon from the normal 8μ to 18μ, for a 5-min treatment at 1270°C. These findings indicate a marked change in the reduction kinetics, probably involving the oxidation of boron by $SiCl_4$ through the reaction

$$4B + 3SiCl_4 \rightarrow 4BCl_3 + Si$$

In using the above method of doping, since the composition of the gas phase differs from that in the solution, it is obvious that the concentration of the dopants will change as the silicon tetrachloride solution is evaporated. In theory, the change in concentration of the doped solution will vary as follows:

$$C_s = C_o k (1 - x)^{k-1}$$

C_s is the mole fraction of dopant in $SiCl_4$ vapor, C_o the mole fraction of dopant in initial $SiCl_4$ liquid, k the distribution coefficient, and x the fraction evaporated. In the above expression for an ideal solution

$$k = \frac{p_{dopant}}{p_{SiCl_4}}$$

where p is vapor pressure of pure constituents. Figure 7 shows the curves for BBr_3 and PCl_3 when evaporated from $SiCl_4$. It will be seen that in the case of BBr_3 the change in concentration is negligible for the first 50% evaporated. In the case of PCl_3, a variation in concentration from 0.37 to 0.6 would be anticipated for 50% evaporation of the $SiCl_4$

[2] The derivation of this equation is similar to that for normal freezing of a liquid (8).

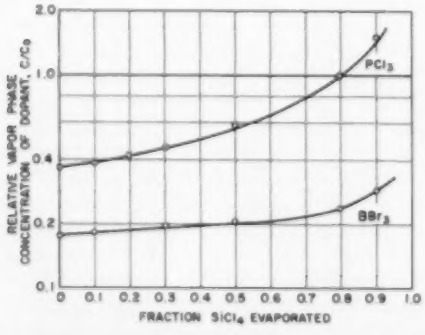

Fig. 7. Change in concentration of dopants as a function of $SiCl_4$ evaporation.

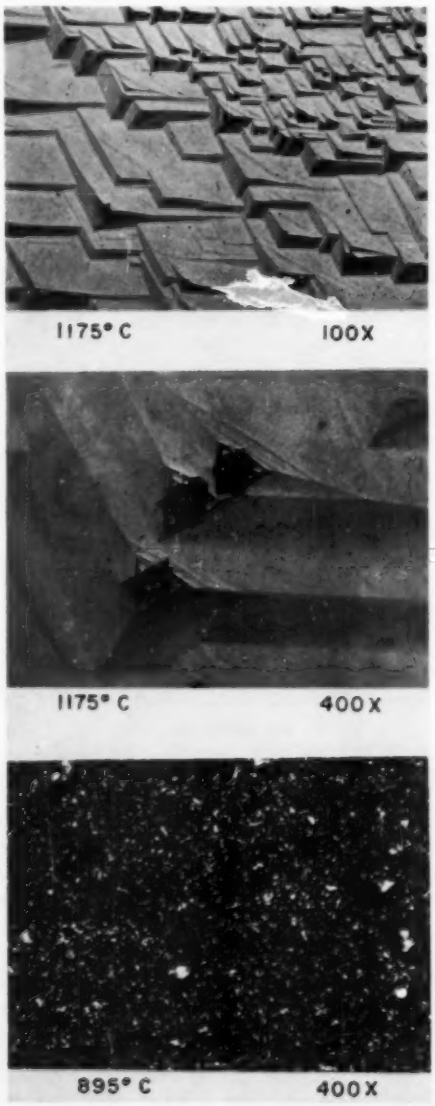

Fig. 8. Effect of deposition temperature on film perfection

solution. These variations can be tolerated for most applications, but where closer control is required, metered aspiration of the doped silicon tetrachloride into the hydrogen stream would be desirable.

Film Perfection

Epitaxially grown films prepared by deposition at 1270°C show specular reflection and replicate the contours of the etched substrate surface. Electron diffraction patterns of such films have the orientation of the <111> substrates and show Kikuchi lines indicating a high order of perfection. At lower deposition temperatures, the films are less perfect. Deposition at 1175°C results in films with the terraced structure shown in Fig. 8.

These films are basically single crystals with the <111> orientation of the substrate. However, triangular <111> faces appear at the corners of the terraces and with continued growth these faces twin and become grossly polycrystalline. At a deposition temperature of 895°C gray films are deposited characteristic of polycrystalline silicon. These results suggest that, during deposition, the high mobility of silicon atoms attained at temperatures above 1175°C is essential for good film perfection. It is probable that high surface mobility is the controlling factor in the deposition of single crystal films irrespective of the reaction used as a source of silicon.

Acknowledgments

The author gratefully acknowledges the aid obtained from his colleagues in much of this work. These include: H. H. Loar, J. J. Kleimack, A. D. Lopez for film evaluation, R. D. Heidenreich and Mrs. M. A. Read for electron diffraction studies, E. E. Thomas for the microscopic photographs, and D. D. Bacon for assistance in film preparation.

Manuscript received Jan. 30, 1961; revised manuscript received March 13, 1961. This paper was prepared for delivery before the Houston Meeting, Oct. 9-13, 1960.

Any discussion of this paper will appear in a Discussion Section to be published in the June 1962 JOURNAL.

REFERENCES

1. H. Theuerer, H. Loar, J. Kleimack, and H. Christensen, *Proc. IRE*, **48**, 1642 (1960).
2. H. Theuerer, *This Journal*, **107**, 29 (1960).
3. G. Pearson, *Trans. AIEE*, **60**, 209 (1947).
4. F. Smits, *Bell System Tech. J.*, **37**, 711 (1958).
5. W. Bond and F. Smits, *ibid.*, **35**, 1209 (1956).
6. R. Schwarz and R. Thiel, *Z. anorg. u. allgem. Chem.*, **235**, 247 (1938).
7. H. Theuerer, J. Whelan, H. Bridgers, and E. Buehler, *This Journal*, **104**, 721 (1957).
8. W. G. Pfann, *Trans. AIME*, **194**, 747 (1952).

The Preparation and Properties of Some II-V Semiconducting Compounds

G. A. Silvey, V. J. Lyons, and V. J. Silvestri

International Business Machines Corporation, Poughkeepsie, New York

ABSTRACT

The methods of purification and single crystal growth of six II-V semiconducting compounds are discussed and crystallographic data are presented. The six compounds, representing three stoichiometries, are Cd_3As_2, $CdAs_2$, CdSb, Zn_3As_2, $ZnAs_2$, and ZnSb. The compounds are thermally dissociated in the vapor phase, and the solid-vapor equilibria of four of the compounds has been measured. Because of the thermal instability, crystal pulling was carried out in sealed quartz tubes employing magnetic suspension of the seed. Through purification of the elements and single crystal growth, high purity was attained in most of the compounds. The highest purity is represented in $CdAs_2$ with an electron carrier concentration of 5×10^{14} cm^{-3}.

The II-V semiconducting compounds may be divided into two general classes according to valence rule considerations. Table I illustrates the division and shows compounds of three different stoichiometries which were prepared. The principal objective of this work was the preparation of high-purity single crystals for subsequent characterization as a group of anisotropic semiconductors. A detailed study of the physics of the materials is the subject of a separate paper by Turner, Fischler, and Reese (1).

Table I. Division and compounds of three stoichiometries

Class I	Class II	
$A_3^{II}B_2^{V}$	$A^{II}B_2^{V}$	$A^{II}B^{V}$
Zn_3As_2	$ZnAs_2$	ZnSb
Cd_3As_2	$CdAs_2$	CdSb

A generic property of the Class I compounds is the occurrence of a crystallographic phase transition well below the compound melting point. This property requires that special thermal treatment be given to single crystals, after growth from stoichiometric melts, in order to avoid excessive strain and cracking of the crystals. The compound Cd_3As_2 has the distinguishing property, in this class, of having an electron mobility higher than that observed for any binary semiconductor having a comparable carrier concentration (1, 2).

The second class of compounds is of particular interest because of the properties of relatively high optical transmission over a broad wavelength range, electrical and optical anisotropy, and the observation of cyclotron resonance in three of the compounds. A greater effort was directed toward the Class II compounds because of these properties. Since the compounds exhibit thermal dissociation, crystal pulling was carried out in sealed quartz tubes under a pressure of the more volatile dissociation product. As in the Class I compounds, emphasis was placed on purification and single crystal growth. It was observed that all of the compounds in this class could be supercooled to temperatures greater than 20°C below their freezing points. Thus, in addition to normal crystal pulling, it was possible to obtain dendrites of the materials by seeding the supercooled melts

Purification of Elements

The techniques of distillation, sublimation, and zone refining were applied in the purification of the elements prior to compound synthesis. In some cases, such as in the preparation of ZnSb, it was felt that the purity of the elements as obtained from a vendor was sufficient to permit a preliminary characterization of the semiconductor properties of the compound. Of course, a degree of purification is generally achieved through crystal pulling of a compound. The lowest net carrier concentration obtained in the purified compounds was 5×10^{14} cm^{-3} in $CdAs_2$.

Purification of Arsenic.—Arsenic of 99.999 +% purity obtained from the American Smelting and Refining Company was found to contain sulfur as an impurity. The sulfur was detected through the formation of carbonyl sulfide when the arsenic was sublimed in sealed quartz tubes containing carbon monoxide. Identification and detection of the carbonyl sulfide were established through its characteristic odor and through microwave spectrographic analysis.[1] Since the sulfur was present probably as an arsenic sulfide, purification was attempted through reduction of the sulfide with hydrogen at an elevated temperature. Purified hydrogen was passed over arsenic at a temperature of 300°C and this vapor stream was then heated to 950°C in a tube furnace. The recrystallized arsenic was tested for the presence of sulfur by subliming in a carbon monoxide atmosphere with the result that no carbonyl sulfide was detected, thereby indicating a significant reduction in the sulfur concentration. During sublimation of the arsenic in H_2 at 300°C, it was observed that a fibrous black residue remained. Spectroscopic analysis of this residue revealed the presence of a large number of impurity elements. The impurities in the recrystallized arsenic were below the limits of detection by emission spectroscopy.

Purification of cadmium.—Two methods were explored in attempts to further purify 99.99% cadmium obtained from the American Smelting and Refining Company: (*a*) zone-refining, and (*b*) vacuum distillation with refluxing. Zone refining was ineffective in removing trace impurities. However, vacuum fractional distillation with refluxing carried out in sealed quartz tubes at 500°C significantly reduced the impurity concentrations. After three distillations, in which about 20% of the cadmium was removed as the purified distillate, the impurity concentrations were reduced to levels below the limits of spectroscopic detection thus showing reductions in the quantities of Fe, Pb, Cu, and Bi. Recently, cadmium of 99.9999% purity has been obtained from the Consolidated Mining and Smelting Company. Because the impurities in this material are on the borderline of detectability by spectroscopic analysis, the effect of purification by distillation was observed through galvanomagnetic and cyclotron resonance measurements made on crystals of $CdAs_2$. The cyclotron resonance measurements indicated a fewer number of imperfections in the $CdAs_2$ prepared from the triply distilled cadmium.

Purification of zinc.—Zone refining of 99.999% zinc (American Smelting and Refining Company) was carried out in evacuated sealed quartz tubes wherein the ingot was maintained at a temperature of about 400°C. The molten zone was controlled through the use of a radiant energy heater employing an ellipsoidal reflector (3). After an average of twenty zone passes, spectroscopic analysis revealed that, while the concentrations of Pb and Fe were reduced, the Cu concentration remained unchanged along the ingot. It was subsequently determined that the zinc used in the preparation of the zinc arsenides could be highly purified through fractional sublimation of the compound Zn_3As_2.

Preparation and Properties of the Compounds

Class I.—Zn_3As_2: The semiconducting properties of Zn_3As_2 were first observed by Braithwaite who found thin films to be photoconductive with an energy gap of 1.1 ev (4). A further investigation of the material was carried out at this laboratory. β-Zn_3As_2 melts at 1015°C under pressure (5) and the compound undergoes a phase transition at 659° ± 3°C (6). The crystal structure of β-Zn_3As_2 is unknown. The α-phase is pseudocubic, being tetragonal with $c/a = 2.007$ (7). The structure had been previously reported as cubic (8) and tetragonal with $c/a = \sqrt{2}$ (9).

The method of preparing Zn_3As_2 from zone-refined $ZnAs_2$ and zinc, which has been described earlier (6), was subsequently discarded in favor of a more direct method requiring less handling of the material and resulting ultimately in higher purity Zn_3As_2. Stoichiometric quantities of high-purity zinc and arsenic were sealed in quartz tubes containing hydrogen and then heated to effect synthesis of the compound. The Zn_3As_2 was purified by slow sublimation in a stream of hydrogen at 800°C. Impurity concentrations in the material thus obtained were below the limits of spectroscopic detection.

Single crystals of Zn_3As_2 were grown by horizontal directional freezing in a temperature gradient, and by the Bridgman technique. In both cases the freezing rate was about 2°C/hr. Due to the

[1] The microwave analysis was carried out at Columbia University by M. J. Stevenson.

solid-solid phase transition it was necessary to cool the ingots very slowly through the transition region in order to minimize cracking of the material. In all cases the horizontally grown crystals were oriented in the crystallographic c-direction within about 10° although seeding of the melts was not attempted. All of the Zn_3As_2 reactions were carried out in quartz which had been carbon-coated through the cracking of propane at 1000°C.

Only p-type conductivity has been observed in Zn_3As_2 although some samples were prepared using slight excesses of zinc or arsenic. The addition of selenium introduced a deep impurity level within the band (1). Resistivity measurements over the range 78°-750°K gave a value for ΔE_0 of 1.1 ev. Optical absorption curves taken at room temperature gave a short wavelength cut-off corresponding to 0.93 ev which is considerably higher than the value of 0.51 ev obtained by Harbeke and Lautz (10). The lowest net carrier concentration obtained was approximately 1×10^{18} cm^{-3}.

Cd_3As_2: Relatively little study has been made of the semiconductor properties of this compound. From electrical measurements on thin films of Cd_3As_2, Moss determined a value of 0.14 ev for the energy gap (11.) From optical absorption measurements Turner *et al.* report a value of 0.13 ev for the energy gap at 300°K. The compound is of considerable interest because of its relatively high electron mobility (1, 2). The crystal structure type is tetragonal, being pseudocubic with a = 12.652Å and c = 12.720Å (12). The crystal structure has been previously reported both as cubic (8) and tetragonal with $c/a = \sqrt{2}$ (9).

The preparation of Cd_3As_2, which has a melting point of 721°C (13), was complicated by the existence of an allotropic phase transition at 578°C. Thus, the procedures used in preparing crystals from stoichiometric melts and subsequently cooling the crystals were the same as those described for Zn_3As_2. In addition, crystal growth was carried out by pulling in the apparatus described in the section under $ZnAs_2$. Some differences in the properties were observed as a function of the method of crystal growth (1).

In an attempt to circumvent the problem of fracture which results from the material experiencing the phase transition, crystals were grown from the vapor phase below the transition temperature. This was accomplished by subliming Cd_3As_2 in a stream of H_2 at 550°C and then recondensing at about 470°C. The crystals grew in the form of thin needles which were roughly square in cross section. The largest was about 2 cm long with an average diameter of 1 mm. Although the impurity concentrations in the crystals were below the limits of spectroscopic detection, the measured room temperature electron concentration remained at approximately 3×10^{18} cm^{-3}, the same as observed in material grown from melts.

The vapor pressure of Cd_3As_2 was measured over the range 434°-695°C using two methods selected for the purpose of determining the nature of the gaseous species (14). Previous vapor pressure measurements were made in the range 238°-375°C by the Knudsen effusion method (15). The solid-vapor equilibria may be represented by the equation

$$Cd_3As_2(s) \rightleftharpoons 3Cd\ (g) + \frac{1}{2}As_4(g) \qquad [1]$$

The equilibrium constant for the dissociation represented by the above equation is

$$Kp = \left(\frac{3.0}{3.5}P\right)^3 \left(\frac{0.5}{3.5}P\right)^{1/2} = 0.24\ P^{3.5} \qquad [2]$$

The vapor pressure data may be represented by the equation

$$\log P_{mm} = -\frac{6600}{T°K} + 9 \qquad [3]$$

Class II.—$ZnAs_2$: The compound was shown by Heike (16) in 1921 to possess rectification properties, and its semiconductor behavior was further investigated by Fritzsche (17) in 1955. More recently, Turner *et al.* (1, 18) and Fox (19) have reported a study of the electrical and optical properties of monocrystalline $ZnAs_2$ prepared at this laboratory. The structure type of $ZnAs_2$ determined by Senko (20) and co-workers at this laboratory is monoclinic with the unit cell dimensions, a = 9.28, b = 7.68, c = 8.03Å and $\beta = 102°19'$. The structure was previously reported by Stackelberg and Paulus (21) to be orthorhombic. $ZnAs_2$ melts at 768° ± 1°C under an arsenic pressure of 3.3 atm (22).

Stoichiometric $ZnAs_2$ may be prepared by crystallization from melts containing in excess of 63 at. % arsenic. Synthesis of the material was initially carried out by heating stoichiometric quantities of zinc and arsenic to 780°C in sealed quartz tubes containing argon at a pressure of 550 mm (STP). The material was contained in a quartz boat which had been carbon-coated by heating at 1000°C in a stream of high-purity propane. Zone-refining was then carried out in a multiple zone resistance furnace using a method applicable to decomposing solids (23). The zone refining was complicated by supercooling of the melt to about 65°C below its freezing point. Therefore, the molten zone was started at a position of 0.5-1 cm away from the tip of the ingot thus using the tip as a seed. After zone-refining, one-half of the ingot (tip-section) was removed and then sealed in another quartz tube for crystal growth by the technique of directional freezing in a temperature gradient. The characteristics of this material have been reported earlier (18, 24).

The quality of the $ZnAs_2$ was considerably improved by changes in the techniques used for purification and crystal growth. High-purity arsenic was further purified by sublimation in hydrogen in the manner described above. The arsenic was then combined with 99.999% zinc in the stoichiometry 3Zn:2As and heated in evacuated sealed quartz tubes at 1020°C to accomplish synthesis of the compound Zn_3As_2. The Zn_3As_2 was purified by sublimation in a stream of hydrogen at 800°C. Impurity concentrations in the Zn_3As_2 were thus reduced to a level below the limits of spectroscopic detection. $ZnAs_2$ was obtained by reacting arsenic

with Zn_3As_2. An extrapolation of the dissociation pressure curve of $ZnAs_2$ obtained from dew-point measurements indicates that the pressure of arsenic in equilibrium with $ZnAs_2$ at the compound melting point was approximately 2 atm. Therefore, an excess of arsenic over stoichiometric proportion was added to the reaction tube in order to provide an arsenic pressure of 2 atm. Zn_3As_2, contained in a quartz boat, and arsenic were sealed in a quartz tube containing He at a pressure of 550 mm (STP). The tube was placed in a two-zone furnace which maintained the Zn_3As_2 at 770°C and the arsenic at 640°C. Under these conditions the time required to complete the synthesis of 50 g of $ZnAs_2$ was about 3 hr.

Crystal pulling was carried out in sealed quartz tubes employing magnetic suspension of the seed and crystal (25). Seeds were cut parallel to the crystallographic b-direction from crystals grown by directional freezing. A quantity of arsenic was added to the reaction tubes in order to provide an arsenic pressure of 2 atm during crystal growth. Helium at a pressure of 550 mm (STP) was used as an ambient. Single crystals of both n- and p-type $ZnAs_2$ were pulled under these conditions. All of the undoped crystals grown were p-type. The impurity levels in these crystals were below the limits of detection by emission spectroscopy. Indium was added to the melts to produce crystals of n-type conductivity. Figure 1 shows a photograph of a typical pulled $ZnAs_2$ crystal.

The vapor pressure of $ZnAs_2$ was first measured by Nesmeyanov *et al.* in the range 279°-410°C by the Knudsen effusion method (26). The authors assumed that $ZnAs_2$ was not dissociated in the vapor phase. However, experiments at this laboratory have demonstrated that the compound decomposes thermally to arsenic and Zn_3As_2 when heated under nonequilibrium conditions. Two standard methods were employed to measure the dissociation pressure of $ZnAs_2$ in the range 612°-770°C (22). A dew-point method was used from 612° to 759°C and triple point measurements covered the range 756°-770°C. In the temperature range 612°-740°C the data may be represented by the straight line equation

$$\log P_{mm} = -\frac{12300}{T°K} + 15 \qquad [4]$$

The equilibrium constant for the dissociation reaction

$$ZnAs_2(s) \rightleftharpoons \frac{1}{3} Zn_3As_2(s) + \frac{1}{3} As_4(g) \qquad [5]$$

may be expressed as the arsenic pressure only since the vapor pressure of Zn_3As_2 is comparatively negligible. The heat of dissociation calculated from Eq. [4] is 18.8 kcal/mole.

A comparison of the dissociation pressure data with the data presented on crystal growth shows that the $ZnAs_2$ crystals were pulled from nonstoichiometric, zinc-rich melts due to the loss of some arsenic to the vapor phase. Volumetric analysis of the material remaining in the quartz crucible after crystal pulling gave a zinc concentration of 32.5 wt % compared with the value of 30.38 wt % for stoichiometric $ZnAs_2$.[2] This condition presented no special disadvantages since (*a*) it would prove difficult to control the arsenic pressure precisely enough to maintain an exactly stoichiometric melt and (*b*) the quantity of $ZnAs_2$ removed from the melt during crystal pulling was only 30-35% of the total initial charge. Volumetric analysis of the pulled crystals indicated no departure from the $ZnAs_2$ stoichiometry.

The resistivity of $ZnAs_2$ crystals has been measured as a function of temperature and of crystallographic direction between 77° and 300°K (18). The maximum axial resistivity ratio is 10 at room temperature and increases to 1000 at 77°K. Resistivity measurements in the intrinsic region above room temperature are not reproducible because of thermal dissociation. The energy gap width, determined from optical absorption studies, is 0.92 ev at 300°K. Transmission curves for light traveling in different crystallographic directions are similar in shape but differ in magnitude as might be expected from an anisotropic structure. An average value of 3.38 for the index of refraction was determined from multiple reflection peaks in the transmission curve of a thin unoriented sample (1). The lowest net carrier concentration obtained was 1×10^{16} cm^{-3}.

$CdAs_2$: Prior to work carried out at this laboratory, the semiconducting properties of $CdAs_2$ had not been discussed in the literature. The published phase diagram of the Cd-As system shows the compound melting point to be 621°C (27). X-ray diffraction studies made at this laboratory by Senko and co-workers indicate that $CdAs_2$ has a tetragonal unit cell with the dimensions a = 4.65Å and c = 7.93Å (28).

The compound thermally decomposes to give Cd_3As_2 and arsenic. The dissociation pressure of solid $CdAs_2$ has been measured over the temperature range 335°-615°C by the dew-point method and by a direct method employing a quartz Bourdon gauge (14). The data can be fitted to the equation

Fig. 1. Typical $ZnAs_2$ crystal pulled from a melt. The crystal is approximately 2 cm long.

[2] The chemical analyses were carried out by E. Morgan, S. L. Phillips, and J. C. Webber of this laboratory.

$$\log P_{mm} = -\frac{7100}{T°K} + 11 \qquad [6]$$

The equilibrium constant for the dissociation reaction

$$CdAs_2(s) \leftrightharpoons \frac{1}{3} Cd_3As_2(s) + \frac{1}{3} As_4(g) \qquad [7]$$

may be expressed in terms of the arsenic pressure only since the pressure contribution from the Cd_3As_2 is negligible. The heat of dissociation for the reaction is 11 kcal/mole.

Crystal pulling of $CdAs_2$ was carried out with an apparatus previously described (25, 29). Prior to crystal pulling, the compound was synthesized in separate sealed quartz tubes by reacting high-purity cadmium and arsenic at 650°C in a hydrogen ambient. An excess of arsenic over stoichiometric proportion was added to the tubes to provide an arsenic pressure of 0.5-0.9 atm. For crystal pulling, additional arsenic was added to the tubes so that this arsenic would provide a pressure of 0.5 atm. Since the dissociation pressure of $CdAs_2$ is greater than 1 atm at the compound melting point, some arsenic was lost by the melt to the vapor phase. However, so long as the arsenic concentration in the melt was maintained greater than 43 wt %, stoichiometric $CdAs_2$ crystals were pulled without difficulty. The stoichiometry was determined by volumetric analysis, and x-ray diffraction examination showed a single phase only. Argon at a pressure of 200 mm (STP) was used as an ambient for most of the crystal pulling. The crystal growth rate varied between 0.5 and 1.0 cm/hr.

While crystals of different carrier concentrations have been produced, all of the material has shown n-type conductivity. Changes in carrier concentrations were observed as a function of the degree of purification applied to the cadmium and arsenic rather than through the addition of impurity elements. The heating of high-purity $CdAs_2$ under the maximum arsenic pressure attainable failed to bring about a conductivity-type change.

The energy gap of $CdAs_2$, determined by optical absorption studies, is 1.0 ev at 300°K (1, 30). The material shows high optical absorption in all crystallographic directions from the absorption edge to about 25μ. Cyclotron resonance has been observed in the higher purity crystals of this compound (31). The lowest net carrier concentration obtained was 5×10^{14} cm^{-3}.

CdSb: Although the semiconducting properties of CdSb have been previously investigated (32-37), the studies were limited to polycrystalline material. The compound is of considerable interest as a potential thermoelectric material (38-41). CdSb is the only stable compound existing in the Cd-Sb system and its melting point is 456°C (42). The compound has an orthorhombic unit cell with a = 6.471Å, b = 8.526Å and c = 8.253Å (43).

During the initial stages in the preparation of the compound it was found that zone-refining would reduce the concentration of impurity elements present in the material. However, this step was subsequently eliminated because (*a*) the cadmium, which introduced the greater concentration of impurities, could be easily purified through distillation and (*b*) the zone-refining, while in itself a method of purification, caused the material to be handled both before and after the process thereby increasing the probability that other impurities would be introduced inadvertently. Thus, the synthesis and crystal pulling were carried out in the following manner. High-purity cadmium and antimony (99.999 + % from United Mineral and Chemical Company used without further purification) were placed in a quartz crucible which was subsequently sealed in a quartz crystal growing tube. An excess of Cd over CdSb stoichiometry was used to provide pressures of 5-20 mm during crystal growth. Hydrogen at a pressure of 300 mm (STP) served as an ambient. After synthesis of the material, crystal pulling was accomplished in the manner previously described. All of the single crystals obtained from this process showed p-type conductivity with a net carrier concentration of 1×10^{16} cm^{-3}. When the melts were doped with indium to a concentration of 5×10^{17} at./cc, the crystal showed n-type conductivity at room temperature. A permanent conversion to p-type conductivity is obtained on heating n-type CdSb to temperatures above 200°C. This is probably due to the creation of cadmium vacancies through thermal dissociation of the compound.

CdSb thermally dissociates according to the reaction

$$CdSb(s) \rightleftharpoons Cd(g) + Sb(s) \qquad [8]$$

The dissociation pressure of the compound has been measured over the range 287°-448°C employing a dew-point technique (44). The data may be represented by the equation

$$\log P_{mm} = -\frac{7200}{T°K} + 10 \qquad [9]$$

From this equation, the heat of dissociation calculated for the reaction is 33 kcal/mole.

The energy gap of CdSb, obtained from room temperature optical absorption studies, is 0.46 ev (1, 18). The transmission is reasonably flat from the short wavelength cut-off to about 25μ and the long wavelength cut-off is 32μ. Cyclotron resonance has been observed in crystals prepared from the highest purity material (45).

ZnSb: The electrical properties of polycrystalline ZnSb have been studied by several investigators (46-48). The compound has shown considerable promise as a thermoelectric material both by itself (49, 50) and in alloys with CdSb (51). ZnSb crystallizes in an orthorhombic unit cell with a = 6.218Å, b = 7.741Å, and c = 8.115Å (46).

ZnSb forms peritectically at a temperature of 546°C (52). Single crystals were pulled, by the technique previously described, from Zn-Sb melts containing 29-31 wt % zinc. The melts were synthesized in a quartz crystal pulling tube from 99.999 + % Zn (Canadian Mining and Smelting Company, Ltd.) and 99.999 + % Sb (United Mineral and Chemical Company) which were not further purified. The crystals were pulled parallel to

the b-axis at rates of 0.5 to 1.0 cm/hr and they all showed p-type conductivity.

Busch, *et al.* (48) reported an energy gap for ZnSb of 0.56 ev determined from resistivity *vs.* temperature measurements. Room temperature optical absorption studies carried out at this laboratory gave an energy gap value of 0.53 ev (1). Cyclotron resonance has been observed in samples of ZnSb obtained from (*a*) a small single crystal section of a polycrystalline ingot, (*b*) a dendrite, and (*c*) a section of a normally pulled single crystal (45).

Acknowledgments

The authors wish to express their thanks to D. P. Cameron for the spectroscopic analyses, to J. S. Hanson for optical orientation of crystals, and to N. R. Stemple for x-ray examination of the crystals.

Manuscript received Jan. 9, 1961; revised manuscript received March 6, 1961. This paper was prepared for delivery before the Columbus Meeting, Oct. 18-22, 1959.

Any discussion of this paper will appear in a Discussion Section to be published in the June 1962 JOURNAL.

REFERENCES

1. W. J. Turner, A. S. Fischler, and W. E. Reese, *Phys. Rev.*, **121**, 759 (1961).
2. A. J. Rosenberg and T. C. Harman, *J. Appl. Phys.*, **30**, 1621 (1959).
3. E. H. Nicollian, G. R. Gunther-Mohr, and L. R. Weisberg, *IBM J. Res. & Dev.*, **1**, 349 (1957).
4. J. G. N. Braithwaite, *Proc. Phys. Soc.*, **B64**, 274 (1951).
5. M. Hansen, "Constitution of Binary Alloys," 2nd ed., pp. 185-187, McGraw-Hill Book Co., Inc., New York (1958).
6. G. A. Silvey, *J. Appl. Phys.*, **29**, 226 (1958).
7. H. Cole, F. Chambers, and H. Dunn, *Acta. Cryst.*, **9**, 685 (1956); *IBM J. Res. and Dev.*, **1**, 90 (1957).
8. G. Natta and L. Passerini, *Gazz Chim. Ital.*, **58**, 541 (1928).
9. M. Von Stackelberg and R. Paulus, *Z. Phys. Chem.*, **22**, 305 (1933).
10. G. Harbeke and G. Lautz, *Phys. Verh.*, **6**, 37 (1956).
11. T. S. Moss, *Proc. Phys. Soc.*, **B63**, 167 (1950).
12. N. R. Stemple, Private communication.
13. M. Hansen, *loc. cit.*, pp. 156-158.
14. V. J. Lyons and V. J. Silvestri, *J. Phys. Chem.*, **64**, 266 (1960).
15. A. N. Nesmeyanov, B. Z. Iofa, A. S. Strel'nikov, and V. G. Fursov, *J. Phys. Chem. USSR*, **30**, 1250 (1956).
16. W. Heike, *Z. anorg. Chem.*, **118**, 264 (1921).
17. C. Fritzsche, *Ann. Physik*, **17**, 94 (1955).
18. W. J. Turner, A. S. Fischler, V. J. Lyons, and W. E. Reese, *Bull. Am. Phys. Soc, Series II*, **3**, 7, 379 (1958).
19. D. Fox, *ibid.*, **3**, 379 (1958).
20. M. E. Senko, H. M. Dunn, J. Weidenborner, and H. Cole, *Acta. Cryst.*, **12**, 76 (1959).
21. M. von Stackelberg and R. Paulus, *Z. Phys. Chem.*, **B28**, 427 (1935).
22. V. J. Lyons, *J. Phys. Chem.*, **63**, 1142 (1959).
23. J. Van Boomgaard, F. A. Kroger, and H. J. Vink, *J. Electronics*, **1**, 212 (1955).
24. G. A. Silvey and V. J. Lyons, *This Journal*, **106**, 61C (1959).
25. R. Gremmelmaier, *Z. Naturforsch.*, **11a**, 511 (1956).
26. A. N. Nesmeyanov, B. Z. Iofa, and A. A. Strel'nikov, *J. Phys. Chem. USSR*, **32**, 955 (1958).
27. M. Hansen, *loc. cit.*, pp. 157.
28. M. E. Senko and N. R. Stemple, Private communication.
29. V. J. Lyons, V. J. Silvestri, and G. A. Silvey, *This Journal*, **106**, 206C (1959).
30. W. J. Turner, A. S. Fischler, and W. E. Reese, *ibid.*, **106**, 206C (1959).
31. M. J. Stevenson, *Phys. Rev. Letters*, **3**, 464 (1959).
32. E. Justi and G. Lautz, *Z. Naturforsch.*, **7a**, 191 (1952).
33. E. Justi and G. Lautz, *ibid.*, 602 (1952).
34. E. Justi and G. Lautz, *Abhandl. braunschweig. wiss. Ges.*, **4**, 107 (1952).
35. I. M. Pilat, *Phys. of Metals and Metallography*, **4**, 31 (1957).
36. G. Kretschmar, R. F. Potter, and P. R. Bradshaw, *Bull. Am. Phys. Soc., Series II*, **4**, 134 (1958).
37. J. Yahia and R. Overstreet, *ibid.*, **4**, 134 (1958).
38. A. Euchen and G. Geldhoff, *Ber. Physik. Ges.*, **14**, 169 (1912).
39. V. A. Iurkov and N. E. Alekseeva, *Soviet Phys. (Tech. Phys.)*, **1**, 898 (1957).
40. H. Hida, *Kanazawa Dargaku Kogakubu Kiyo*, **2**, 6 (1957).
41. A. J. Strauss, *This Journal*, **106**, 206C (1959).
42. M. Hansen, *loc. cit.*, pp. 437-441.
43. K. E. Almin, *Acta. Chem. Scand.*, **2**, 400 (1948).
44. V. J. Silvestri, *J. Phys. Chem.*, **64**, 826 (1960).
45. M. J. Stevenson, *Bull. Am. Phys. Soc.*, Series II, **5**, 177 (1960).
46. I. V. Mochan, *J. Tech. Phys. USSR*, **18**, 1485 (1948).
47. H. Bruns and G. Lautz, *Abhandl. brauschweig. wiss. Ges.*, **6**, 47 (1954).
48. G. Busch, P. Junod, U. Katz, and U. Winkler, *HPA*, **27**, 193 (1959).
49. Maria Telkes, *J. Appl. Phys.*, **18**, 1116 (1947).
50. M. V. Kot, *Uchenge Zapishi Kishinev Univ.*, **24**, 11 (1956).
51. I. M. Pilat, L. D. Chizi, and S. Yu, *Soviet Phys. (Tech. Phys.)*, **3**, 734 (1958).
52. M. Hansen, *loc. cit.*, pp. 1182-1185.

Desensitization of Zirconium Powder, Especially Zirconium Powder Used in Primers

Peter Karlowicz,[1] George Norwitz, and Joseph Cohen

Pitman-Dunn Laboratories, Frankford Arsenal, Philadelphia, Pennsylvania

ABSTRACT

A practical and inexpensive method for desensitization of zirconium powder is proposed by treatment with 1% hydrofluoric acid for 5 min. The electrostatic energy required to set off the powder increased considerably after this treatment, and the usefulness of the zirconium for primers was not impaired. The effect of the desensitization on visual appearance, appearance under the microscope, particle size, and behavior on burning was investigated. The most valid explanation of the desensitization process is that it involves the formation of an adherent layer of zirconium hydride by the reaction of the zirconium and nascent hydrogen generated when the metal is attacked by hydrofluoric acid. Previous investigators not concerned with the problem of desensitization have isolated zirconium hydride films obtained on treating pieces of zirconium metal with dilute hydrofluoric acid. Treatment with nonoxidizing acids produces varying degrees of desensitization, but the use of hydrofluoric acid is preferable. All work on desensitization was performed using zirconium powder intended for use in primers, but the method can also be used for zirconium powder intended for other purposes.

In recent years zirconium powder has become an important constituent of primers because of its sensitivity characteristics, high heat of combustion, stability, and noncorrosive character of the metal itself and its reaction products (1, 2). When used in primers, zirconium powder is mixed with oxidizing agents and primary explosives (1, 2). A drawback to the use of zirconium powder is the hazard involved in handling the material; explosions and fires from zirconium powder have caused deaths and serious injuries (3, 4). In view of these facts, this laboratory undertook an investigation to desensitize zirconium powder so that it would not be subject to premature ignition (by static electricity, heat, or friction), yet still retain its satisfactory characteristics for primers. A considerable advantage in using desensitized zirconium would be that primer compositions could be mixed dry. At the present time they must be mixed wet for reasons of safety.

Factors Influencing the Sensitivity of Zirconium Powder

In order to develop a satisfactory method for desensitizing zirconium powder and evaluate such a method, it was necessary to understand the factors influencing the sensitivity of zirconium powder. These factors are as follows:

Method of manufacture.—The process used for making the powder and variations in the same process will affect the sensitivity. Zirconium sponge made by low-temperature reduction is more pyrophoric than that made by high-temperature reduction (3). When insufficient sodium or magnesium is present in reducing zirconium tetrachloride, the sponge produced is more pyrophoric (3). It can be argued, of course, that these differences are due to the resultant characteristics of the zirconium rather than the process itself.

Physical condition of powder.—The particle size affects the sensitivity; under ordinary conditions, fine material (i.e., material with the greatest surface area) will ignite more readily than coarse material (3-5). Particles below 10μ are especially susceptible to spontaneous combustion (5). It is believed that particle density, apparent density, and geometric shape of the particles affects the sensitivity. The method of grinding used to produce the powder affects all these three properties and is therefore important.

Mass of powder.—Zirconium powder becomes more sensitive as the mass increases (3-5). The explanation of this is that the escape of heat within metal powders must largely take place by radiation through multiple layers of air (in contrast to solid metal in which heat can be transferred internally by the relatively efficient process of direct heat conductivity) and thus the accumulation of heat generated within the metal powder by slow oxidation becomes increasingly probable with increasing size of the powder mass. Andersen and Belz (5) found that the ignition temperature was higher for larger samples of zirconium powder and that the burning frequently took place from the inside of the sample to the outside.

Chemical composition.—Chemical composition has an important bearing on the sensitivity of zirconium powder. Much consideration has been given to the effect of the total oxygen content, but the findings have been inconclusive and contradictory (4-9). Unquestionably, the oxide coating has a profound effect on the sensitivity. When zirconium powder is heated in air (particularly just below the ignition

[1] Present address, 4411 Higbee Street, Philadelphia, Pa.

temperature) it becomes less sensitive because of the thickening of the oxide coating (5). Zirconium sponge metal is passivated for rough handling by treating with air to produce an oxide coating (4, 10). It has been claimed that the longer zirconium powder is exposed to air, the less sensitive it becomes (11). The Bureau of Mines found little significant change in the sensitivity of zirconium powder that had been exposed to the air for 6 weeks (7). If zirconium powder is heated in a vacuum at red heat so that the oxygen from the oxide coating diffuses into the metal, the material becomes more sensitive (5, 12).

The effect of the presence of other metals in the zirconium on the sensitivity is somewhat uncertain because of the difficulty of preparing satisfactory powders of zirconium alloys while keeping other conditions constant. Andersen and Belz (5) prepared a series of powders containing 6% or more of copper, titanium, nickel, iron, and cobalt. The powders containing several per cent of these elements were quite sensitive; the powders containing very large amounts of these elements were less sensitive, but had poor burning characteristics (5). It has been stated that zirconium alloys containing lead (13), or chromium, titanium, and manganese (3) are pyrophoric. A whole series of pyrophoric zirconium alloys containing such metals as titanium, managanese, lead, antimony, and tin has been patented (14). It has been claimed that the presence of even moderate amounts of impurities, such as iron, calcium, and chloride can increase the sensitivity (3).

When zirconium is combined with hydrogen, the sensitivity decreases considerably (5). Andersen and Belz (5) found that the ignition temperature of zirconium hydride was greater than 400°C and that the electrostatic energy was 0.025 joule, but the reaction was not sustained. Hartmann, Nagy, and Jacobson (7) found that the electrostatic energies for two samples of zirconium hydride were 0.320 and 0.064 joules (as contrasted with the electrostatic energies for samples of zirconium powder of 0.0004, 0.0008, 0.0010, 0.0064, and 0.240 joules). The electrostatic energies for two samples of zirconium hydride tested in this laboratory were 0.045 and 0.125 joules. The above figures are cited to illustrate the fact that zirconium hydride is less sensitive than zirconium. This fact is of extreme importance as will be shown later. As far as the authors have been able to ascertain, no serious fires or explosions have resulted from the use of zirconium hydride as such.

Effect of water.—The effect of water on the sensitivity is controversial. Andersen and Belz (5) found that the ignition temperature of zirconium powder increased with increasing amounts of water due in part to slight oxidation of the zirconium by the boiling water. The rate of increase was slight for up to 20% water, but it was rapid for more than 20% water. Herickes and Richardson (15) found that moist zirconium powder was less sensitive to friction than the dry material. The belief persists with the zirconium industry and the Atomic Energy Commission that zirconium powder containing up to about 16% of water is more susceptible to spontaneous combustion than dry zirconium (3). Evidence for this is the fact that a preponderant number of the fires and explosions involving zirconium powder and scrap have taken place when water or moisture were present (3, 4). The Ordnance Department believes that zirconium powder for primers is much safer to transport if it is mixed with water to form a slurry containing at least 25% water by weight (16, 17). Some Atomic Energy establishments recommend that zirconium powder be transported completely dry (3, 8). Wet zirconium, once ignited, will burn more intensely than dry zirconium because at high temperature water actually supports the combustion (3, 6). Also, the capability of water for supporting the combustion makes the presence of oxygen from the air unnecessary. The ability of water to increase the intensity of the combustion of zirconium reaches a maximum when about 5-10% water is present (6).

Effect of the atmosphere.—The susceptibility of zirconium powder to ignition is eliminated if the powder is blanketed with a completely inert atmosphere such as argon or helium (6, 9). Nitrogen has also been used as a protective atmosphere (6), but it is not entirely satisfactory since zirconium can burn in nitrogen and also in carbon dioxide (7, 18).

Methods of Desensitization

Zirconium has been desensitized by coating with copper (7) or by coating with a plastic film produced by applying a solution of polystyrene in benzene (11). Such desensitized zirconium had unsatisfactory burning characteristics.

Another proposed process was treatment with carbon tetrachloride (3). The process seemed to be effective but subsequently was abandoned when a violent explosion took place on treating one batch of powder (3).

Some laboratories have attempted to desensitize zirconium powder by increasing the thickness of the oxide film by exposure to air or oxygen at room temperature. This method has not proved particularly effective.

The sensitivity of zirconium powder has been reduced considerably by eliminating the finer particles by elutriation, but the process is time-consuming, not always reliable, and expensive.

Proposed Method Using Hydrofluoric Acid

After considerable experimental work using different methods of approach, a practical and inexpensive procedure for desensitizing zirconium powder was developed which probably involves the formation of a protective layer of zirconium hydride. In this procedure the powder is treated with 1% HF for 5 min and the zirconium is filtered and washed with water, followed by acetone and ether to remove the water. A patent application has been made for the method (19).

The most desirable concentration of HF is 1%. With lower concentrations of acid the decrease in sensitivity is less; with higher concentrations the reaction is too vigorous. The temperature is regulated between 25° to 55°C by adding crushed ice

(or water at 5°C) when necessary. Above 60°C the reaction becomes vigorous; below 10°C it ceases almost entirely. The loss of metallic zirconium in the method amounts to about 1%. It has not been determined what is the maximum amount of zirconium that can be handled at any one time by the method. The largest amount of zirconium desensitized at any one time in this laboratory was 300 g, which is the amount normally used in making a batch of primers.

Method.—The zirconium is placed in a hard rubber or plastic container resistant to acetone. Enough water is added to just cover the zirconium, and a plastic spatula resistant to acetone is inserted. The container is placed under a hood and 1% HF (1 volume of concentrated HF to 99 volumes of water) is added over a period of 15 sec while stirring. For 20 to 50 g of zirconium, 150 ml of 1% HF is used; for 100 g, 300 ml; for 300 g, 600 ml. After the HF has been added, the time is noted and the reaction is allowed to proceed for 5 min while stirring continuously. The temperature is controlled between 25° and 55°C by adding crushed ice when necessary. The temperature will not rise above 35°C when working with less than 100 g of zirconium. At the end of the 5-min period, sufficient crushed ice is added with stirring so that the temperature drops below 10°C. The zirconium is allowed to settle for a few minutes, and the supernatant liquid is decanted through a coarse filter paper set into a 2½ in. Buchner funnel made of porcelain, hard rubber, or plastic resistant to acetone. The zirconium is washed twice by decantation with distilled or other high-purity water heated to 50°-60°C and then several times with water at room temperature. The volume used for each washing is approximately equal to the volume of 1% HF used for treating the sample. The zirconium is stirred thoroughly and the sides of the container are washed down after each addition of water. After the final washing with water, the zirconium is washed twice with acetone by decantation and once with ethyl ether. In these washings just sufficient acetone and ether are added to cover the zirconium. The zirconium is dried by allowing it to stand overnight in a hood.

Use of Other Reagents in Place of HF

Nitric acid, ammonium hydroxide, and 10% potassium hydroxide did not attack zirconium powder and produced no desensitization. Mixtures of nitric and hydrochloric acids with and without water attacked zirconium (20) but did not desensitize it.

Nonoxidizing acids that attacked zirconium produced desensitization in varying degrees. The nonoxidizing acids that attacked zirconium more readily produced a greater degree of desensitization. Three percent sulfuric acid was fairly effective, but a 30-min reaction period was required, and it was difficult to wash out the sulfuric acid. Hydrochloric acid (1 to 1) produced some desensitization but, a standing period of several days was necessary [at the end of several days the attack of zirconium by hydrochloric acid is quite appreciable (21)]. Phosphoric acid could not be used because insoluble zirconium phosphate precipitated.

Mixtures of nonoxidizing acids that attacked zirconium (H_2SO_4 + HF, HCl + HF, etc.) and mixtures of nonoxidizing acids and fluoride salts could be used. However, these combinations seemed to offer no apparent advantage over the 1% HF.

Comparison of Properties of Untreated and Treated Zirconium

An investigation was made to detect any changes that might have taken place as a result of the hydrofluoric acid treatment. Experimental work for this investigation was carried out on two large lots of zirconium powder. Typical results are given since check results were substantially the same.

Electrostatic energies (16) were as follows:

	Before desensitization	After desensitization
Lot A	<0.000125 joule	0.090 joule
Lot B	0.00125 joule	0.125 joule

The untreated zirconium was charcoal gray in color while the treated material was gray with a slight tinge of gold. The appearance under the microscope of the untreated and treated zirconium was the same with regard to the size and irregularity of the particles, but the treated material seemed somewhat more lustrous. Photomicrographs taken before and after desensitization (300X) seemed identical.

The particle size distribution as determined by the Andreasen pipet (16) showed no significant change. Results obtained were as follows:

Fraction	Lot A		Lot B	
	Before desens.	After desens.	Before desens.	After desens.
10μ or less	1.06	0.99	1.98	2.20
10-20μ	15.97	14.52	15.51	14.93
20-30μ	46.85	45.54	15.84	23.27
30-40μ	32.47	37.29	31.68	24.59
40-50μ	3.19	1.65	28.38	28.54

The behavior of the untreated and treated zirconium powder on ignition with a match was extremely interesting and probably very important. In this test 2 mg of the material was placed on an asbestos pad under a hood and a lighted match applied (in using this test it is essential that all zirconium except the 2 mg sample be removed from the vicinity). The untreated (sensitive) material ignited readily, generally did not give off sparks, and left a brownish colored ash with dark particles that indicated incomplete combustion. The treated material ignited with difficulty, gave off sparks, and left a gray uniform ash that indicated complete combustion.

Treated zirconium was incorporated into a primer mix and used in 3000 rounds of ammunition which were test fired after loading and found to function well ballistically.

Discussion of the Probable Mechanism of Desensitization

It is believed that the desensitization process involves the formation of an adherent layer of zirconium hydride by the reaction of zirconium and nascent hydrogen generated when the metal is attacked by a nonoxidizing acid. James and Straumanis (22),

and Straumanis, James, and Neiman (23) found that a black or gray coating of zirconium hydride was produced on pieces of zirconium metal treated with dilute hydrofluoric acid. They isolated the coating and identified it by x-ray diffraction. Smith found that the zirconium hydride coating was produced by sulfuric acid (24), and Kuhn found that it was produced by hydrochloric acid (after several days) (21). When an oxidizing agent such as nitric acid was present in significant amounts, no film of zirconium hydride could be formed and the zirconium remained bright and shiny (22). None of the above investigators were concerned with the problem of desensitization.

The reactions of zirconium with hydrofluoric, sulfuric, and hydrochloric acids are as follows (20, 21).

$$Zr + 6HF \rightarrow H_2ZrF_6 + 2H_2$$

$$Zr + 3H_2SO_4 + H_2O \rightarrow H_2ZrO(SO_4)_2 + 2H_2$$

$$Zr + 2HCl + H_2O \rightarrow ZrOCl_2 + 2H_2$$

The hydrogen is shown in the above equations as molecular hydrogen as is customary. However, it is well known that when a metal dissolves in a nonoxidizing acid, the hydrogen is released at the surface of the metal in nascent form that is very reactive (12). This is important, since it has been brought out by investigations of the zirconium-hydrogen system that molecular hydrogen does not form a film of zirconium hydride (20, 25).

When nitric acid is present in the dissolving medium, it would be expected that water, ammonium ion, nitrate, and oxides of nitrogen would be produced but no hydrogen (12). The fact that nitric acid can prevent both the formation of a zirconium hydride film and desensitization is a powerful argument in favor of the zirconium hydride theory of desensitization.

How can the coating of zirconium hydride lower the sensitivity of zirconium powder? To answer this, it will be recalled that zirconium hydride is much less sensitive than zirconium, and therefore it would be expected that zirconium powder coated with zirconium hydride would be much less sensitive than the original zirconium powder.

Before deciding on the zirconium hydride theory, it was thought that the mechanism of the method involved the dissolution of the old coating of zirconium oxide and the formation of a new more adherent coating on washing with water ($Zr + 2H_2O \rightarrow ZrO_2 + 2H_2$) (5). The fact that a mixture of nitric and hydrochloric acids did not desensitize zirconium, although it attacked it (20), eliminated this theory as the chief mechanism. However, it is possible that an oxide film is formed over (or conceivably with) the zirconium hydride film. There can be no doubt concerning the fact that a zirconium oxide film forms on zirconium metal and powder exposed to air. Hickman and Gulbransen (26) studied the oxide film on powder and found it to be monoclinic ZrO_2. Meyer (27) removed the old oxide film from pieces of zirconium metal by treating with a mixture of hydrofluoric and nitric acids, followed by heating in a vacuum at 750°C. He then placed the specimens in a sodium sulfate solution and observed the growth of the oxide film by an electrochemical method.

There are certain other aspects of the desensitization process that should be considered. The process would be expected to dissolve off the sharp edges of the particles somewhat and thus increase, if only slightly, the radius of curvature of the sharp protuberances. As a result the "sensitivity to electricity" would tend to diminish, because the resulting greater contact between particles would lower contact resistance and more energy would be required to cause ignition. Higher values would then be obtained with the electrostatic energy test. Another contributing cause to the effectiveness of the desensitization process would be the elimination of impurities from the surface. As stated previously, the desensitization process does not seem to cause a significant change in the particle size distribution. However, it is probable that particles whose diameter is less than 1μ would be eliminated, and this would contribute to the desensitization. These three effects, namely, the smoothing out of the particles, the elimination of surface impurities, and the elimination of very minute particles, may be important, but none of them could be the prime explanation of the desensitization process. If one of them were the prime explanation, then the hydrochloric-nitric acid medium would desensitize zirconium.

It is not believed that fluoride is a component of any protective film that is formed, since other nonoxidizing acids besides hydrofluoric acid produce desensitization (hydrofluoric acid is more effective because it attacks zirconium more readily). Examination of treated zirconium by available analytical methods showed that only traces of fluoride were present.

It is not believed that the process affects the porosity significantly. Andersen and Belz (5) stated that porosity contributes negligibly to the surface area of zirconium powder but their findings were by no means conclusive.

Application of the Method to Other Materials Besides Zirconium Powder Used for Primers

All work in this laboratory on desensitization was performed with zirconium powder used for primers. However, the method could also be used to desensitize zirconium powder used for special pyrotechnics, rockets, powder metallurgy, gettering, and flashbulbs. The method could also probably be used to desensitize Kroll process residues, and zirconium scrap which ordinarily consists of a mixture of zirconium powder, shavings, drillings, pieces, etc. The safe storage of zirconium scrap is a pressing problem, since many fires and explosions have originated from this source (3, 4).

Since titanium also produces a hydride coating on treatment with hydrofluoric acid (28), it would be expected that the method could desensitize titanium powder. However, since titanium powder is much less sensitive than zirconium powder (5, 7), the application of the method to titanium powder would probably be of lesser importance.

Almost certainly the procedure could be used to desensitize hafnium powder, since the reactions of hafnium are almost identical with those of zirconium (20).

Acknowledgment

The authors are indebted to Samuel Sitelman for his suggestions and John Jackiewicz for his assistance with some of the experimental work. Also they wish to thank A. G. Tomassetti, George Younger, and Allen Frank of Ammunition Engineering Branch of the Industrial Group, and R. H. Ristine and L. Jester of the Manufacturing Branch of the Industrial Group for their helpful cooperation.

Manuscript received Oct. 31, 1960; revised manuscript received March 9, 1961.

Any discussion of this paper will appear in a Discussion Section to be published in the June 1962 JOURNAL.

REFERENCES

1. G. H. Chambers, *Metals and Alloys*, **4**, 199 (1933).
2. D. Hart and W. R. Tomlinson, *Metal Progr.*, **59**, 788 (1951).
3. Safety and Fire Protection Branch, Division of Organization and Personnel, U. S. Atomic Energy Commission, "Zirconium Fire and Explosion Hazard Evaluation," TID-5365, Aug. 1956 (Unclassified).
4. R. B. Smith, *Nucleonics*, **14**, No. 12, 28 (1956).
5. H. C. Andersen and L. H. Belz, *This Journal*, **100**, 240 (1953).
6. G. L. Miller, "Metallurgy of Rarer Metals, Vol. 2, Zirconium," 2nd ed., pp. 482, 488, 489, 490, 491, 493, Academic Press, New York (1957).
7. I. Hartmann, J. Nagy, and M. Jacobson, U.S. Bureau of Mines, Report of Investigations, No. 4835 (1951).
8. W. R. DeHollander, "An Evaluation of the Zirconium Hazard," HW-44989, Aug. 1956 (Unclassified).
9. American Society for Metals, "Zirconium and Zirconium Alloys," Chapter by H. S. Kalish, p. 5, Cleveland, Ohio (1953).
10. R. E. Kirk and D. F. Othmer, "Encyclopedia of Chemical Technology," Vol. 15, p. 282, Interscience Publishers, New York (1956).
11. B. Kopelman and V. B. Compton, *Metal Progr.*, **63**, No. 2, 77 (1953).
12. J. W. Mellor, "Comprehensive Treatise on Inorganic and Theoretical Chemistry," Vol. 1, p. 331, Vol. 7, p. 115, Vol. 8, p. 591, Longmans, Green and Co., London (1922).
13. P. Alexander, U. S. Pat. 2, 611,316, Sept. 1952.
14. O. Smetana, H. Nowatny, and G. Purt, Austrian Pat. 194,621; 194,622; 194,623; *C. A.*, **52**, 3656 (1958).
15. J. A. Herickes and P. A. Richardson, "Zirconium Hazards Research," Progress Report No. 1, U.S. Bureau of Mines, Feb. 1957.
16. Frankford Arsenal Purchase Description FA-PD-MI-2364, Granular Zirconium, Aug. 1959.
17. National Military Establishment Specification JAN-Z-399A, Powdered Zirconium, Aug. 1948.
18. I. Hartmann, *Ind. Eng. Chem.*, **40**, 752 (1948).
19. P. Karlowicz, U.S. Patent application, submitted to Frankford Arsenal Patent Division, June 1959.
20. W. B. Blumenthal, "Chemical Behavior of Zirconium," pp. 4, 29-32, Van Nostrand Co., New York (1958).
21. W. E. Kuhn, *Corrosion*, **15**, 103t (1959).
22. W. J. James and M. E. Straumanis, *This Journal*, **106**, 631 (1959).
23. M. E. Straumanis, W. J. James, and A. S. Neiman, *Corrosion*, **15**, 286t (1959).
24. T. Smith, *This Journal*, **107**, 82 (1960).
25. E. A. Gulbransen and R. F. Andrew, *Trans. AIME*, **185**, 515 (1949).
26. J. W. Hickman and E. A. Gulbransen, *Anal. Chem.*, **20**, 158 (1948).
27. R. E. Meyer, *This Journal*, **106**, 930 (1959).
28. M. E. Straumanis and P. C. Chen, *ibid.*, **98**, 234 (1951).

Anodic Polarization Curves in Molten Carbonate Electrolysis

George J. Janz and Fumihiko Saegusa

Department of Chemistry, Rensselaer Polytechnic Institute, Troy, New York

ABSTRACT

Some anodic polarization curves for platinum, gold, and silver, for molten carbonate electrolysis in the range 500°-900°C and 10^{-6}-10^{-2} amp cm^{-2} are reported. All measurements were made using the ternary mixture, Li,Na,K/CO_3 = 4:3:3 (mp 397°C), respectively, and the steady-state overvoltage technique, the measurements being referred to the "platinum" reference electrode. A theoretical kinetic analysis of various possible processes contributing to anodic oxygen evolution is developed. It appears that in the region of 600°C, the rate-determining process is

$$MO + O^{-2} \rightarrow M + O_2 + 2e^-$$

At the higher temperatures, competing processes such as metal dissolution and reduction of the anodic oxide layer are more important as noted from the nature of the anodic polarization curves.

In the previous paper (1), an investigation of the overvoltage of oxygen evolution at a platinum electrode in a mixture of molten alkali carbonates was reported. The overvoltage-current density relations up to 1000°C and the Tafel plot were examined on basis of the carbonate dissociation and oxide ion scheme. Due to the exploratory nature of the work and the inherent experimental difficulties on the oxygen overvoltage measurement, the results were not sufficiently accurate for the determination of the reaction mechanism. The present communication describes a more detailed study of the anodic polariza-

tion curves. Interpretation of electrode kinetics is discussed relative to possible mechanisms for the oxygen evolution reactions in molten carbonate electrolysis.

Experimental

Materials.—Lithium, potassium, and sodium carbonates (AnalaR, Reagent Grade, Fisher Chemical Company) were dried in a platinum crucible under CO_2 atmosphere and stored over P_2O_5 until required for use. The composition of the ternary mixture employed in the present work was Li_2CO_3:K_2CO_3:Na_2CO_3 = 4:3:3 (mole ratio). Sixty-five grams of the homogeneous mixture was prepared for each run in a Hoskins furnace under CO_2 atmosphere prior to the measurements.

Gases.—Oxygen (Linde Company) was purified by passing through cupric oxide heated at 700°C in a Vycor tube, then a column of soda lime and successive trains of drying agents, *i.e.*, silica gel, $Mg(ClO_4)_2$ and P_2O_5. CO_2 (Matheson Company) was dried by passage through columns of silica gel and P_2O_5.

Apparatus.—The general view of the experimental assembly is shown in Fig. 1. The furnace element consisted of an alundum core, A, 2½ in. ID by 22½ in., which was wound with five separate sections of Kanthal resistance wire. The core was protected by an insertion of replaceable inner sheath, B, of 2 in. ID alundum tubing from any carbonate attack either bubble-splashed or vaporized during the measurement. A gold-palladium crucible, C, containing the melt was placed in an alundum support, D, which was positioned in the uniform heating zone by moving an alundum rod, E, through the furnace bottom. Small adjustment of the crucible position could be made by aid of a lab-jack, F. A Pt-Pt, 10% Rh thermocouple, G, housed in the rod, served the furnace temperature control by means of a controller (L&N Speedomax H). A series of alundum disks, H, above the crucible served as baffles to minimize heat losses and, at the same time, as electrode supports. For protection of the electrical leads, the furnace top was water cooled by a copper spiral, I.

Cell design.—Due to the highly corrosive nature of the carbonates, particular difficulty is met in finding suitable materials for contact with the melts. Exploratory tests in this laboratory showed that gold or gold-palladium alloy (80-20%) seemed most satisfactory for the requirement of the present study, showing little or negligible corrosion after 60 hr in molten carbonates at temperatures up to 950°C. Uniform current distribution over the electrode is required in the direct method of overpotential measurement. Techniques developed for aqueous systems are not adapted readily to the molten system. In the present work, the crucible itself as an opposite electrode with a test electrode placed in the geometrical center of the electrolyte therein contained was the arrangement used.

The cell, shown in detail in Fig. 2, consisted of a gold-palladium (80-20%) crucible, A, of approximately 55 ml capacity, which served as a cathode by an attached wire, B, of the same alloy. An anode, C, approximately trapezoid in shape with an apparent surface area of 3.25 cm^2, was positioned in the center of the melt. The platinum reference electrode, D, was positioned 0.2 cm from the anode. A gold-palladium tube, E, of ⅛ in. diameter was used for CO_2 bubbling. A number of small holes at the sealed end ensured effective gas bubbling. The upper end was sealed to an alundum inlet to which the CO_2-oxygen mixtures were monitored by flowmeters. Temperatures were measured with a Pt-Pt, 10% Rh thermocouple, F. The latter was placed in Vycor tubing sheathed with gold and immersed in the carbonate melt.

All metallic parts exposed above the electrolyte were extended bare for an appreciable distance be-

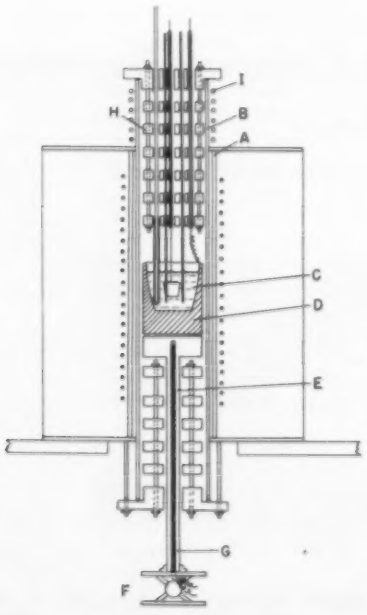

Fig. 1. General view of furnace assembly: A, alundum core, 2½ in. ID; B, inner protective core, 2 in. ID; C, gold-palladium crucible; D, crucible support; E, alundum rod; F, lab-jack; G, Pt-Pt 10% Rh thermocouple; H, alundum baffle; I, copper water-cooled spiral.

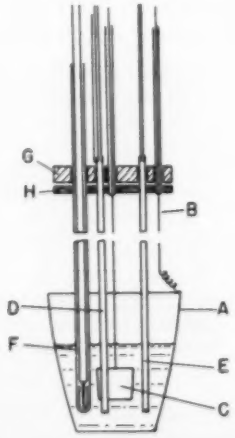

Fig. 2. Cell design: A, gold-palladium crucible; B, cathode wire, gold-palladium; C, anode; D, reference electrode; E, gas bubbling tubing, gold-palladium; F, gold thermocouple sheath; G, alundum baffle; H, protective baffle cover.

fore being encased in the ceramic supports in order to protect against carbonate-ceramic attack by possible splashing. The bottom baffle, G, also was protected by an alundum cover, H, which could be replaced easily.

Electrodes.—Three different kinds of metal sheet, platinum, gold, and silver, were used as anodes, each supported by a thick wire of the same metal. Where the wire was in contact with the electrolyte, a thinner wire was used.

With electrodes for which surface roughness is varied by oxidation during anodic oxygen evolution, "conditioning" of the electrodes to gain a stable surface condition preceding the overpotential measurements is essential. The electrodes used were in solid form and prior to assembly they were subjected to a standard treatment, *i.e.*, degreasing, hot 10*N* HNO_3 bath, and washing with water. For silver, cold dilute acid was used.

If the ratio of the true electrode area to the apparent area is given by q, the Tafel's relation is expressed by

$$\eta = a + b \log i = a + b \log (i'/q) \qquad [1a]$$

or

$$\eta = a' + b \log i' \qquad [1b]$$

where i' is the apparent current density. When the surface roughness of the electrode remains unchanged throughout the measurement, the plot of η against i' gives a correct slope b with an apparent a-value that is $a' = a - b \log q$. On the other hand, if q is changed with the change in current density, the Tafel plot may lead to incorrect a- and b-values. A displacement of the Tafel slope, when determined with ascending and descending current densities, may be attributed, in part, to the latter factor. This criterion was used in all measurements since the results were referred to the apparent areas of the anodes.

Relative to the reference electrode, it has been observed that the "platinum" electrode is reversible to oxygen and oxide ion at elevated temperatures in molten salts such as carbonates (1, 3) borates (4), sulfates (5), and silicates (6). In the present work, the reference electrode consisted of a ⅛ in. diameter platinum tube having a series of small holes for oxygen bubbling pierced in the lower, sealed end. This was welded to a long fine-bore alundum tube support for gas inlet and a platinum lead wire. As procedure for stabilization of the reference electrode, a brief period of oxygen bubbling through the electrode, prior to each series of measurements, was found satisfactory.

Measurements.—Potential measurements were made by the direct method. The electrical circuit was fundamentally the same as that used previously (1), except it was provided with a potential recorder (L&N "Azar"). Polarizing current was supplied from 22.5 v batteries through variable resistors. After the electrolyte had been brought to the desired temperature under continuous CO_2—O_2 bubbling, the electrode was conditioned with maximum current of 30 ma cm^{-2} prior to each measurement. The electrolyte was to be agitated constantly by effective gas-bubbling to minimize the concentration effect.

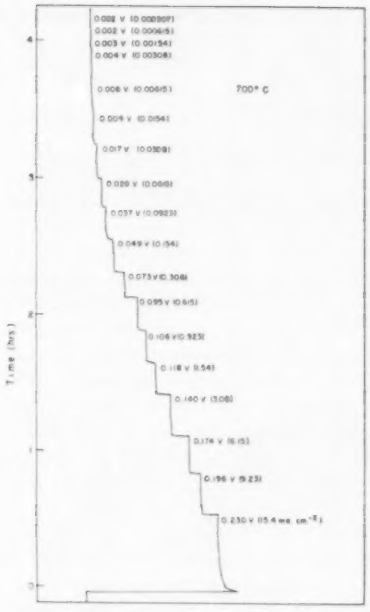

Fig. 3. Typical steady-state potential readings at different current densities.

The use of an arbitrary time as criterion of "a steady value" should be avoided (7), and the use of a potential recorder is most convenient to ascertain when the steady-state overpotential has been attained. The determination of the overvoltage-current density relationship was made by starting at the maximum current density and reducing the current density to zero current. Values obtained by increasing the current density agree within ±2 mv. It was observed that a relatively long period was required for the steady potential to be attained at the starting current density, and that this period decreased with increasing temperature. A typical potential reading on the recorder for measurements at 700°C is shown in Fig. 3. It is readily apparent that the steady-state potential could be observed for relatively long periods of time.

The upper limit to the current density range for accurate measurements is determined either by the *IR* drop in the electrolyte between the electrode surface and the reference electrode or concentration polarization. Knowledge of the electrical conductance is essential to the estimate of the *IR* drop. While no values have been reported for mixtures of carbonates, the specific conductance for the present electrolyte was estimated from the precise conductance data for the three pure carbonates recently reported elsewhere (8), using the simple principle of mole fraction additivity. Evaluation of this estimation method with the data for the pure molten alkali halides and their mixtures (9) shows that the values thus predicted are good first approximations and may be taken as upper limits for these values. The results for the Li_2CO_3—Na_2CO_3—K_2CO_3 mixture (4:3:3) thus obtained, and the limiting current densities thus predicted for $V_{IR} = 1$ mv and a

0.2 cm electrolyte gap between reference and test electrodes, are:

Temp, °C	600	700	800	900
κ (ohm^{-1} cm^{-1})	1.9	2.4	2.9	3.4
i (amp cm^{-2})	0.010	0.012	0.015	0.017

It is apparent that the electrolyte *IR* drop correction is almost negligible in a system of such high electrical conductance. The lower limit to the current density depends on depolarization. No measurements are known for the oxygen electrode with microcurrents. The order of $10^{-5} \sim 10^{-6}$ amp cm^{-2} may be expected to be the lower limit of the current density.

The possible effect of the resistance (*IR*) of corrosion products on the anode, such as oxide films, on the overpotential measurements remains open and must await the extension of more elaborate nonsteady-state techniques to such high temperature systems. The steady-state or direct method offers no insight on this. It was assumed that this *IR* drop in the present range of current density was small enough to be neglected. Some support for this is seen in that the drop in the voltage decay curve as observed by the off-current appeared instantaneous, within the limits of the technique and instruments in this work.

Results

The rate of the mixed gas flow for bubbling was maintained constant, *i.e.*, CO_2: 50 cc/min, and O_2: 42.8 cc/min, throughout the runs. The results thus obtained for the range 600°-900°C are summarized in Table I. For comparison the values were taken from a series of decreasing current. The rather long periods for the attainment of steady-state potentials below 600°C made measurements below this limit impracticable.

Platinum.—The results are illustrated in Fig. 4 where η is graphed as a log function of c.d. for the various temperatures studied. At 600°C and in the low current density range it is apparent that platinum exhibits an overpotential in accord with the Tafel equation. The linear portion decreases with increasing temperatures until it is an almost smooth curve. The platinum surface was grayish in appearance after these measurements.

Table I. Oxygen overpotential at different metal anodes referred to platinum electrode in the same electrolyte

Apparent current density i', $10^{-6}\times$ amp cm^{-2}	Overpotential, mV									
	Platinum				Gold				Silver	
	Temperature, °C				Temperature, °C				Temperature, °C	
	600	700	800	900	600	700	800	900	600	650
15.4	309	230	223	213	356	228	190	183	122	93
9.23	268	196	189	173	314	198	156	150	89	57
6.15	227	174	168	150	289	178	135	129	64	32
3.08	175	140	128	119	255	153	108	99	26	−1
1.54	137	118	102	80	217	129	91	77	−5	−28
0.923	119	106	73	55	191	114	78	64	−20	−39
0.615	108	95	65	38	173	97	69	53	−29	−45
0.308	92	73	37	20	142	75	52	40	−42	−53
0.154	79	49	23	10	118	52	39	32	−48	−57
0.0923	70	37	15	6	102	43	35	29	−50	−59
0.0615	60	28	9	4	90	38	31	27	−53	−60
0.0308	45	17	5	2	72	32	27	25	−54	−62
0.0154	30	9	3	1	55	28	25	24	−55	−63
0.00615	15	6	1	0	42	25	24	23	−55	−63
0.00308	9	4	0		36	25	24	23	−55	−63
0.00154	5	3			33	25	24	23	−56	−63
0.000615	2	2			31	25	24	23	−56	−63
0.000307	1	2			31	25	24	23	−56	−63

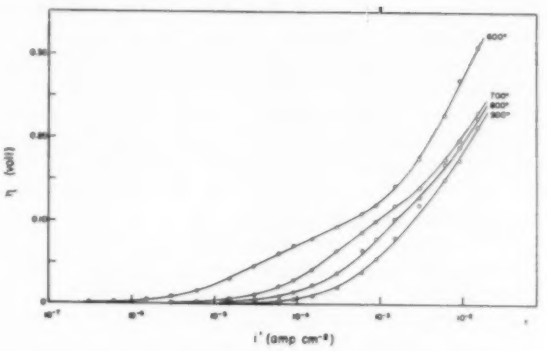

Fig. 4. Oxygen overpotential at platinum plotted against log apparent current density.

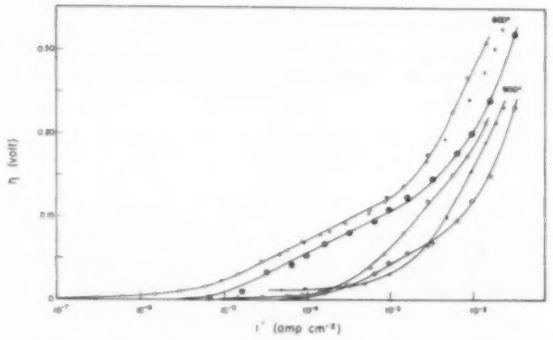

Fig. 5. Effect of cathode materials on the oxygen overpotential at platinum anode at 600° and 900°C. Dotted circle, gold-palladium cathode; encircled circle, open circle, gold; +, platinum [see ref. (1)].

The possible effects of the cathode materials on the anodic polarization measurements were investigated, and the results at the two extreme temperatures are illustrated in Fig. 5. At 600°C and with platinum, gold, and gold-20% palladium alloy as cathodes, the anodic Tafel slopes remain essentially unchanged, but at 900°C, considerable differences were evident. At these higher temperatures the cathode showed evidence of attack, most probably due to alloying reactions with the electrodeposited alkali metal.

The Tafel slopes at the low current densities, by the method of least squares, are 0.050 at 600°C and 0.068 at 700°C.

Gold.—The results are found in Fig. 6 and show the distinct linear relationship at lower temperatures (600°C), with the gradual but definite disappearance of this region with increasing temperatures. In contrast to platinum, two linear portions, of slope 0.062 and then 0.12, are found for the gold anode at 600°C. At 700°C, the observed Tafel slope is 0.070. The anode was clean and bright after the measurements, but the appearance of crystal grains on the gold surface indicated some attack, most probably due to metal dissolution at the higher temperatures.

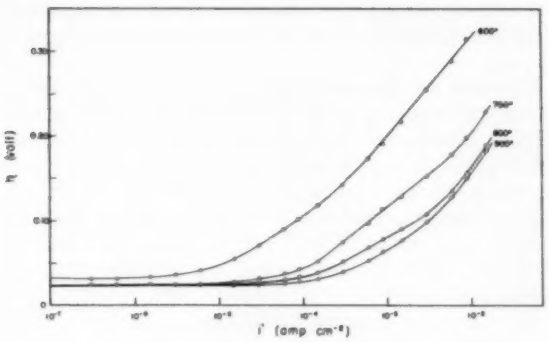

Fig. 6. Oxygen overpotential at gold plotted against log apparent current density.

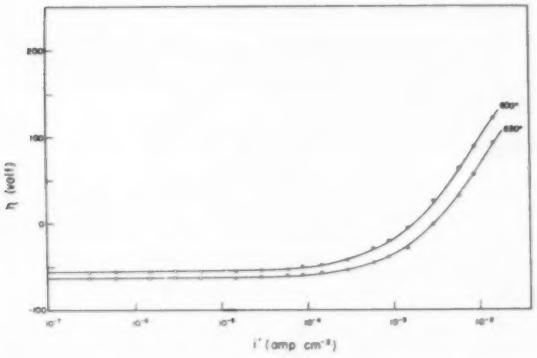

Fig. 7. Oxygen overpotential at silver plotted against log apparent current density.

Silver.—Silver suffered severe anodic dissolution. The attack became considerable with increase of temperature accompanied by a change in electrode shapes. The graph of the experimental values taken at low temperatures is illustrated in Fig. 7. No appreciable polarization is seen until 10^{-4} amp cm^{-2}; this is followed by a gradual smoothed increase as the current density increases. The curves do not exhibit the clear linear relationships noted for platinum and gold for this range of current densities.

Discussion

The process of electrical conductance in molten carbonates is understood (8), in large part, as a Grotthuss-type mechanism in which the "contact-ion" pair $(M^+CO_3^{-2})^-$ is predominant and the rate-determining process is a cooperative jump-rotation. The ions in these melts are predominantly the species M^+ and CO_3^{-2}, with the "contact-ion" pair $(M^+CO_3^{-2})^-$ being statistically a short-lived coulombic complex important in the diffusion and conductance processes. It would be predicted that the activity of the oxide ion, O^{-2}, in these melts is controlled by the equilibrium

$$CO_3^{-2} \rightleftarrows CO_2 + O^{-2} \qquad [2]$$

An estimate of the oxide ion activity can be gained from the recent data on the molar volumes for molten carbonates (8) and the Broers equation (10) for the above equilibrium

Table II. Concentration of oxide and carbonate ions and partial limiting current density

Temp, °C	$a_{O^{-2}}$ mole cm^{-3}	$i^*_{(0.03\ i_o)}$, amp cm^{-2}	C_o (M_2CO_3), mole cm^{-3}	$i^\dagger_{(0.03\ i_o)}$, amp cm^{-2}
600	1.4×10^{-12}	1.2×10^{-11}	1.95×10^{-2}	7.9
700	9.9×10^{-11}	8.6×10^{-10}	1.91×10^{-2}	7.7
800	3.2×10^{-9}	2.8×10^{-8}	1.86×10^{-2}	7.5
900	5.7×10^{-8}	5.0×10^{-7}	1.82×10^{-2}	7.3

* Practical limiting current density referred to $O^{=}$.
† Practical limiting current density referred to $CO_3^{=}$.

$$\log \frac{a_{O^{-2}} P_{CO_2}}{a_{M_2CO_3}} = -\frac{72.7 \times 10^3}{45.7\ T} + 7.80 \qquad [3]$$

The results, at four temperatures, and the calculated limiting current densities, i_o, assuming that oxygen is transported solely by the oxide ions in the bulk of the melt, are given in the 2nd and 3rd columns, respectively, of Table II. The latter were calculated from the well-known relation

$$i_o = nFDC_o/\delta(1 - t) \qquad [4]$$

taking $D = 3 \times 10^{-5}$ cm^2 sec^{-1} for the oxide ion (10), and δ as 10^{-3} cm for a vigorously stirred liquid, and assuming that the term with the transport number was unity as a first estimate. The 3rd and 4th columns in Table II list the results for the case where the oxygen is transported in the solvated state by the jump-rotation mechanism advanced elsewhere (5) in detail. For this calculation, the value of $D = 2.79 \times 10^{-4}$ cm^2 sec^{-1} (894°C) from self-diffusion data (11), and an estimated upper limit (12), for t as 0.8, were used. For both, the value of the practical limiting current density was gained from i_o, taking the value of 3% as an upper limit of the permissible concentration change at the anode (13). It is apparent from these values, and the jump-rotation mechanism of oxygen transport in the melt, that the linear portion of the η-log i relation may be ascribed more properly to an activation-controlled polarization rather than the concentration polarization (oxide-ion buildup) suggested in the previous communication (1).

An analysis of the anodic polarization curves in the light of the possible mechanisms for the oxygen evolution processes in the molten carbonate electrolysis is of interest. The over-all anodic reaction undoubtedly is

$$CO_3^{-2} = CO_2 + \frac{1}{2}O_2 + 2\,e^- \qquad [5]$$

In view of the carbonate ion-oxide ion equilibrium (Eq. [2]), the possible anodic mechanisms may be conceived as:

Mechanism I. The formation of an "oxide" on the anodic surface

$$O^{-2} + M \rightarrow MO + 2\,e^- \qquad [6]$$

with a consecutive "oxide"-oxide ion reaction

$$MO + O^{-2} \rightarrow M + O_2 + 2\,e^- \qquad [7]$$

leading to the oxygen evolution.

Table III. Comparison of Tafel slopes

Temp. °C	Tafel slope predicted, 2.3 $RT/3F$	Tafel slope observed	Apparent c.d. range, amp cm^{-2}
600	0.058	0.050 (Pt)	$10^{-5} \sim 10^{-3}$
		0.062 (Au)	$10^{-5} \sim 10^{-4}$
700	0.064	0.068 (Pt)	$10^{-4} \sim 10^{-3}$
		0.078 (Au)	$10^{-4} \sim 10^{-2}$

Mechanism II. The formation of an "oxide" on the anodic surface

$$O^{-2} + M \rightarrow MO + 2\,e^- \qquad [6]$$

with the consecutive "oxide-oxide" surface reaction

$$MO + MO \rightarrow 2M + O_2 \qquad [8]$$

completing the oxygen evolution process.

The detailed theoretical treatment of the kinetic analysis is given in the Appendix. The predicted Tafel slope is ($RT/\mathbf{F}$) if the "oxide" formation step (Eq. [6]) is rate-determining, or at very high current densities for the metal "oxide"-oxygen ion step (Eq. [7]) as rate-determining. The theoretical Tafel slope will be ($RT/3\mathbf{F}$) at low current densities and low surface coverage if the metal "oxide"-oxygen ion reaction (Eq. [7]) is the slow step. Finally, if the metal-oxide interaction step (Eq. [8]) is rate-determining, the Tafel slope is predicted to be ($RT/4\mathbf{F}$). The observed Tafel slopes at 600° and 700°C for platinum and gold correspond closely to the theoretical value predicted for ($RT/3\mathbf{F}$). The comparison is found in Table III. Support is seen for the "oxide-oxygen ion" reaction (Eq. [7]) as the rate-determining step in the temperature range 600°-700°C at low current densities, and it would appear that oxygen evolution reaction occurs by some such processes as outlined in Mechanism I. That two linear portions are observed experimentally in the η-log i relation (Fig. 4 and 6) corresponds with the prediction in Mechanism I for a change in slope of the Tafel equation from 2.3 $RT/3\mathbf{F}$ to 2.3 $RT/\mathbf{F}$ with increasing current density. In the present work the value of the latter was approached but not completely realized (gold, 600°C: 0.12 observed; 0.17 predicted). Two linear portions in the η-log i relation reported earlier by Flood and Forland (14) are similarly understood in the light of Mechanism I for the oxygen evolution reactions; it is seen (Appendix) that Mechanism II fails to predict two linear Tafel regions for the η-log i relations in molten carbonates.

At the higher temperature (*viz.*, 800°C) the two defined portions in the η-log i curves are no longer observed, and only at the upper limit of c.d. is an approach to linearity apparent. Competing processes relative to the oxygen evolution reaction, such as anodic dissolution (especially silver), and reduction of oxides (15) (favored by the presence of CO), are undoubtedly greatly enhanced at these higher temperatures. It is not improbable that the rate-determining step in the oxygen evolution process becomes the "oxide" formation reaction (Eq. [6]) in view of the noted instability of metal oxides at elevated temperatures. The results are insufficient to resolve this point.

Relative to the anodic processes at the silver electrode, it was clearly apparent that the metal dissolution process is most marked. It would be predicted that under these circumstances the diffusion of dissolving metal ions would contribute; the lower overpotentials, and the displacement from the zero value, are understood in part to cause such effects but the data are insufficient for a more detailed analysis.

Acknowledgments

Helpful discussions with Dr. N. D. Greene are gratefully acknowledged. This work was made possible, in large part, by financial support received from the U.S. Navy, Office of Naval Research, Division of Chemistry, Washington, D.C.

Manuscript received Oct. 21, 1960; revised manuscript received March 13, 1961. This paper was prepared for delivery before the Indianapolis Meeting, Apr. 30-May 1, 1961.

Any discussion of this paper will appear in a Discussion Section to be published in the June 1962 JOURNAL.

APPENDIX

The kinetic analysis of anodic oxygen evolution in aqueous systems has been treated in detail by Bockris (16), the treatment being based on the general theory of consecutive reactions developed by Christiansen (17), and electrode processes postulated for oxygen evolution (18). Its application to a molten salt system is of interest since the number of possible mechanisms may be reduced due to the absence of the aqueous solvent. Two mechanisms for the anodic oxygen evolution processes in molten carbonates may be developed as follows. In the treatment that follows it should be noted that the symmetry factor $\beta = \frac{1}{2}$ is assumed throughout the mathematical development:

Mechanism I. Consider consecutive processes to be

$$O^{-2} + M \underset{k_{-1}}{\overset{k_1}{\rightleftarrows}} MO + 2\,e^- \qquad [6]$$

$$MO + O^{-2} \underset{k_{-2}}{\overset{k_2}{\rightleftarrows}} M + O_2 + 2\,e^- \qquad [7]$$

(i) Assume that the formation of the "metal oxide" layer (reaction [6]) is rate-determining, and that the surface coverage by the MO species is negligible. It can be shown readily (16-18) that the expression for the forward rate, v, for the over-all electrode reaction is

$$v = \frac{k_1 k_2 C^2_{O^{-2}}\, e^{2\Delta\phi\mathbf{F}/RT}}{k_2 C_{O^{-2}}\, e^{\Delta\phi\mathbf{F}/RT} + k_{-1}\, e^{-\Delta\phi\mathbf{F}/RT}} \qquad [9]$$

where the symbols have their conventional significance. As $k_1 \rightarrow k_{-1} \rightarrow 0$, this reduces to

$$v = k_1 C_{O^{-2}}\, e^{\Delta\phi\mathbf{F}/RT} \qquad [10]$$

and

$$i = 2\mathbf{F} k_1 C_{O^{-2}}\, e^{\Delta\phi\mathbf{F}/RT} \qquad [11]$$

from which it follows that the Tafel slope $\dfrac{\partial\Delta\phi}{\partial \ln i} = RT/\mathbf{F}$.

(ii) Assume that the "metal oxide"-oxide in reaction [7] is the rate-determining step and that the surface coverage is given by

$$X_{MO} = k' C_{MO}$$

It then follows (16-18), if $k_2 \rightarrow k_{-2} \rightarrow 0$, that the forward rate, v, may be expressed as

$$v = \frac{k_1 k_2 k' C_{O^{-2}}\, e^{2\Delta\phi\mathbf{F}/RT}}{k_{-1} k' C_{O^{-2}}\, e^{\Delta\phi\mathbf{F}/RT} + k_{-1}\, e^{-\Delta\phi\mathbf{F}/RT}} \qquad [12]$$

Now if $k_{-1}\, e^{-\Delta\phi\mathbf{F}/RT} >> k_1 k' C_{O^{-2}}\, e^{\Delta\phi\mathbf{F}/RT}$, the preceding reduces to

$$v = K_1 k_2 C^2_{O^{-2}}\, e^{3\Delta\phi\mathbf{F}/RT} \qquad [13]$$

and

$$i = 4\,\mathbf{F}\, K_1 k_2 C^2_{O^{-2}}\, e^{3\Delta\phi\mathbf{F}/RT} \qquad [14]$$

It follows that the theoretical Tafel slope is predicted as $RT/3F$. At sufficiently high values of $\Delta\phi$ this would become RT/F.

Mechanism II. Consider the consecutive processes in the oxygen evolution reaction to be

$$O^{-2} + M \underset{k_{-1}}{\overset{k_1}{\rightleftarrows}} MO + 2e^- \quad [6]$$

$$2\,MO \underset{k_{-2}}{\overset{k_2}{\rightleftarrows}} 2\,M + O_2 \quad [8]$$

(i) If the formation of the "metal oxide" layer (reaction [6] is rate-determining), there is no discrimination from Mechanism I (i), and the theoretical Tafel slope is predicted to be RT/F.

(ii) Assume that the "metal oxide" reaction (Eq. [8]) is the rate-determining step, and that $X_{MO} = k'C_{MO}$ as above. The expression for the velocity of the over-all forward reaction can be shown to be

$$v = \frac{k_1 k_2 C_{O^{-2}} C_{MO}\, e^{\Delta\phi F/RT}}{k_1 k' C_{O^{-2}}\, e^{\Delta\phi F/RT} + k_{-1}\, e^{-\Delta\phi F/RT}} \quad [15]$$

If the surface coverage is small, the first step (Eq. [6]) may be taken as equilibrium, so that

$$C_{MO} = C_{O^{-2}} K_1\, e^{2\Delta\phi F/RT} \quad [16]$$

and if

$$k_{-1}\, e^{-\Delta\phi F/RT} >> k_1 k' C_{O^{-2}}\, e^{\Delta\phi F/RT}$$

then the relations for v and i reduce to

$$v = K_1^2 k_2 C^2_{O^{-2}}\, e^{4\Delta\phi F/RT} \quad [17]$$

$$i = 4F K_1^2 k_2 C^2_{O^{-2}}\, e^{4\Delta\phi F/RT} \quad [18]$$

The Tafel slope is thus predicted to be $RT/4F$.

Alternately if $\Delta\phi$ and the surface coverage are both large, the expressions for v and i become

$$v = \frac{k_2}{k'} (C_{MO})_{sat.} \quad [19]$$

$$i = 4F \frac{k_2}{k'} (C_{MO})_{sat.} \quad [20]$$

A possible activation controlled limiting current is thus predicted.

REFERENCES

1. G. J. Janz, F. Colom, and F. Saegusa, *This Journal*, **107**, 581 (1960).
2. O. Kubaschewski, and E. L. Evans, "Metallurgical Thermochemistry," Pergamon Press (1958).
3. E. Bauer and R. Brunner, *Z. Elektrochem.*, **41**, 794 (1935).
4. P. Csaki and A. Dietzel, *Glastech. Ber.*, **18**, 33 (1940).
5. H. Flood, T. Forland, and K. Motzfeldt, *Acta Chem. Scand.*, **6**, 257 (1952).
6. R. Didtschenko and E. G. Rochow, *J. Am. Chem. Soc.*, **76**, 3291 (1954).
7. A. Hickling and S. Hills, *Faraday Soc. Discussions*, **1**, 236 (1949).
8. G. J. Janz and M. R. Lorenz, *This Journal* (1961), submitted.
9. E. R. Van Artsdalen and I. S. Yaffe, *J. Phys. Chem.*, **59**, 118 (1955).
10. G. H. J. Broers, "High Temperature Galvanic Fuel Cells," Ph.D. Thesis, Univ. Amsterdam, 1958.
11. S. Djordjevic and G. J. Hills, *Trans. Faraday Soc.*, **56**, 269 (1960).
12. G. J. Janz, C. Solomons, and H. J. Gardner, *Chem. Rev.*, **58**, 461 (1958).
13. S. Barnartt, *This Journal*, **106**, 991 (1959).
14. H. Flood and T. Forland, *Faraday Soc. Discussions*, **1**, 302 (1949).
15. K. Motzfeldt, *J. Phys. Chem.*, **59**, 139 (1955).
16. J. O'M. Bockris, *J. Chem. Phys.*, **24**, 817 (1956).
17. A. Christiansen, *Z. physik. Chem.*, **B33**, 145 (1936).
18. R. Parsons, *Trans. Faraday Soc.*, **47**, 1332 (1951).

Intermediate Temperature Fuel Cells

G. V. Elmore and H. A. Tanner

Charles F. Kettering Foundation, Yellow Springs, Ohio

ABSTRACT

Gas fuel cells are described which utilize aqueous electrolytes and operate at atmospheric pressure at over 100°C. Under these conditions the product water escapes as vapor, thus avoiding dilution of the electrolyte and flooding of the electrode pores. Both acid and alkaline electrolyte compositions have been employed. The electrolyte contains a solid phase which reduces creep, and the electrodes are made nonwetting by the use of Teflon. Current densities of 50-100 ma/cm² have been realized.

Fuel cells intended for operation on gases are commonly constructed with porous electrodes to maximize the amount of contact between the three phases: gas, electrolyte, and electrode. The electrolyte may be an aqueous solution, fused salt, or ionic membrane (1). Aqueous electrolyte cells generally are operated below 100°C at atmospheric pressure, or at a considerably higher temperature in a closed system under pressure (2). Water produced electrochemically during cell operation on hydrogen fuels becomes a problem because it dilutes the electrolyte and fills the electrode pores causing a severe reduction in current density. This effect has sometimes been overcome by passing a severalfold excess of gas through the cell to carry off the product water.

The aqueous electrolyte, atmospheric pressure hydrogen fuel cell has the inherent advantages of simplicity and long life providing the electrode wetting and electrolyte dilution problems can be overcome. This paper describes experimental cells which can be operated above 100°C at atmospheric pressure, retaining enough water for good electrolytic activity and losing the excess product water as vapor.

Cell Construction

Two types of cells operating from 125° to 200°C were developed, one using an alkaline electrolyte composition and the other an acid electrolyte.

For the alkaline cell, it was found that a eutectic mixture of NaOH and KOH (approximately 50% by weight of NaOH) which melts around 187°C was suitable. In the presence of gases which were saturated with water vapor at room temperature, the mixture at 150°C became molten and yet did not absorb enough water to change volume appreciably. In order to maintain a satisfactory working humidity during cell operation, the influent gases were saturated with water vapor at room temperature.

An additional requirement is that the electrolyte be in the form of a paste which will not migrate into the porous electrodes. It was found that when $Ca(OH)_2$ was added to the eutectic alkali mixture, in amounts of approximately 20% $Ca(OH)_2$, a satisfactory electrolyte paste is formed.

For the electrodes, materials are necessary which have good electronic conductivity, are permeable to the gases, and are impervious to penetration by the electrolyte. In addition, the electrodes must catalytically activate the electrochemical reactions. Palladium foil, 0.0005 in. thick, fulfills all the requirements for a hydrogen electrode. At 150°C, hydrogen diffuses through at a high enough rate to maintain a current density of over 100 ma/cm^2.

In the case of the oxygen electrode, platinum, palladium, or silver can be used as the catalyst. Silver gave the highest open-circuit voltage and is the most economical of the three catalysts, hence it was used in most of the cells. A porous electrode, resistant to penetration by the electrolyte, was made by mixing silver powder[1] with Teflon dispersion, "DuPont Teflon 30," followed by drying and heating to 300°C. The treated silver powder was packed between two silver screens separated by a peripheral Teflon gasket. The hydrogen and oxygen electrodes were spaced apart by a Teflon gasket confining the alkaline electrolyte between them. The outer surfaces of the electrodes were exposed to an atmosphere of hydrogen or oxygen by means of the glass bells shown in the diagram of the cell in Fig. 1. The entire cell was held together with metal clamps and was kept at operating temperature in a constant temperature oven. Larger cells with thermal insulation would be able to maintain temperature from the waste heat when operating at maximum power. In such a cell the exit line, extending out from the insulation, would normally be closed and would only be opened to withdraw condensed water.

[1] Fisher C. P. precipitated.

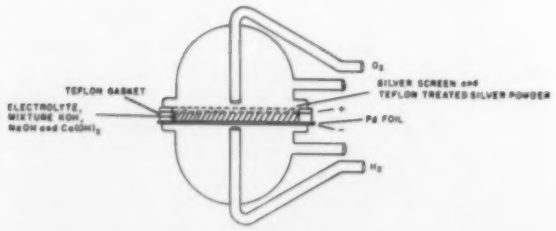

Fig. 1. Diagram of the cell

In constructing an acid cell, it was found that phosphoric acid mixed with silica powder (approximately 65% SiO_2) forms a satisfactory paste electrolyte. Unlike sulfuric, phosphoric acid is not reduced electrochemically under the cell operating conditions. For the electrodes, either platinum or palladium can be used as a catalyst for both the hydrogen and oxygen electrodes. Porous carbon blocks were wet with Teflon dispersion, and a thin coat of platinum or palladium black was then pressed on the top surfaces of the blocks while they were still wet. The blocks were then dried and heated to 300°C. As in the alkaline cell, the electrodes were separated by a Teflon gasket containing the phosphoric acid paste electrolyte. The design of the cell is shown in Fig. 2. In the acid cell, air can be used instead of oxygen with little loss of current density and without the electrolyte being affected by the CO_2 in the air. Almost all of the acid cell experiments were made using air rather than oxygen.

Results and Discussion

The performance of a typical alkaline cell using a silver powder cathode and a palladium foil anode is shown in Fig. 3. The open-circuit voltage with the silver cathode was 1.15 v. When platinum was used as the cathode, the open-circuit voltage was 0.98 v. Palladium gave 0.90 v on open circuit.

The silver powder cathode-palladium foil anode alkaline cell, operating on hydrogen and oxygen,

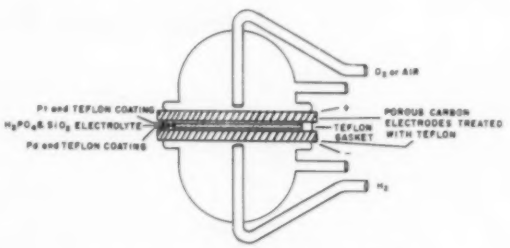

Fig. 2. Construction of acid H_2-O_2 fuel cell

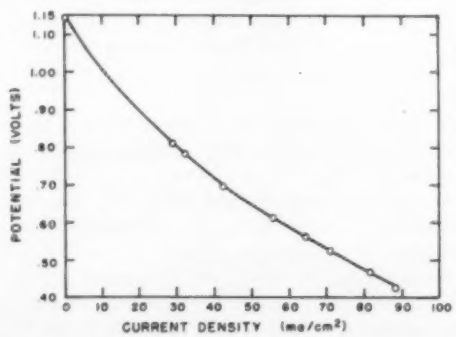

Fig. 3. Potential vs. current density of hydrogen-oxygen fuel cell with 40% NaOH, 40% KOH, 20% $Ca(OH)_2$ electrolyte at 150°C.

gave maximum power at 0.46 v with a current density of about 84 ma/cm². An alkaline cell of this type which was started at a current density of 100 ma/cm² at 0.37 v ran for 19 days, at which time the current density was 60 ma/cm² at 0.59 v. For most of the 19-day period the current density was approximately 75 ma/cm² at 0.50 v. At these high current densities, some penetration of the electrolyte into the silver powder is believed to have caused the current decrease.

The performance, at various temperatures, of a typical acid cell with both electrodes coated with palladium, operating on hydrogen and air, is shown in Fig. 4, 5, and 6. The open-circuit voltage was 0.83 v. At maximum power, the voltage was 0.42 v and the current density was 60 ma/cm² at both 100° and 125°C. At 150°C the current density at maximum power was approximately 75 ma/cm² and the voltage was 0.42 v. An acid cell was operated for six months at a current density of 90 ma/cm² and 0.25 v with no apparent deterioration.

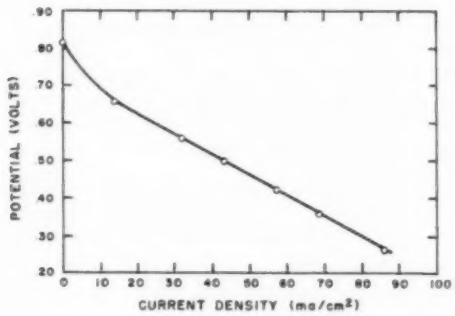

Fig. 4. Potential vs. current density of hydrogen-air fuel cell with 35% H_3PO_4, 65% SiO_2 electrolyte at 100°C.

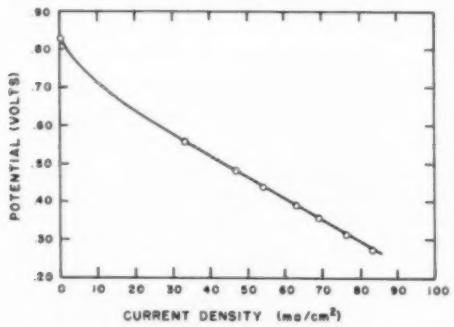

Fig. 5. Potential vs. current density of hydrogen-air fuel cell with 35% H_3PO_4, 65% SiO_2 electrolyte at 125°C.

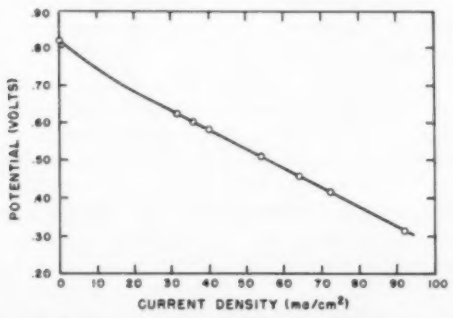

Fig. 6. Potential vs. current density of hydrogen-air fuel cell with 35% H_3PO_4, 65% SiO_2 electrolyte at 150°C.

An acid electrolyte fuel cell will not absorb carbon dioxide as alkaline electrolytes will, and it may therefore in theory be operated on organic fuels. Only a very limited number of organic fuel candidates will actually oxidize in the acid cell, however. Formic acid vapor as a fuel gave a current density about half that obtained with hydrogen. Some of the fuel value was lost due to a side reaction in the presence of H_3PO_4 to form CO and H_2O. Formaldehyde also can be used as an acid cell fuel. In this case CO is formed and is not utilized, representing a loss of fuel value. Again the current density was about half that obtained with hydrogen.

These acid cell results are explainable on the basis of the formation of chemisorbed hydrogen on the anode:

$$H_2 \xrightarrow{Pd} 2Hads \qquad [1]$$

$$HCOOH \xrightarrow{Pd} 2Hads + CO_2 \qquad [2]$$

$$HCHO \xrightarrow{Pd} 2Hads + CO \qquad [3]$$

followed by the electrochemical step

$$2Hads \xrightarrow{Pd} 2H^+ + 2e^- \qquad [4]$$

Alkaline cells can utilize any of the above fuels and also methyl alcohol. The mechanism for the latter must require hydroxyl ion:

$$CH_3OH + 2\,OH^- \xrightarrow{Pd} 6Hads + CO_3^{2-} \qquad [5]$$

The resulting accumulation of carbonate caused increased internal resistance leading to a decrease in power output with time of operation. The current density for an alkaline cell operating on formic acid, formaldehyde, or methyl alcohol was about half the value for hydrogen.

The results on organic fuels are exploratory, and the partial pressure of the fuel vapor at the electrode was not determined but obviously would be well below 1 atm since the vapor was introduced by bubbling nitrogen through a warm aqueous solution. The open-circuit voltages ranged from 0.5 to 0.7 v.

Acknowledgments

The authors are indebted to Mr. Robert Davidson, Mr. Robert Wesley, and Mr. Anthony Stankavich for their assistance in the experimental work of this investigation.

Manuscript received Jan. 9, 1961; revised manuscript received March 15, 1961. This paper was prepared for delivery before the Chicago Meeting, May 1-5, 1960.

Any discussion of this paper will appear in a Discussion Section to be published in the June 1962 JOURNAL.

REFERENCES

1. W. T. Grubb and L. W. Niedrach, *This Journal*, **107**, 131 (1960).
2. F. T. Bacon and J. S. Forrest, *The Engineer*, *July 20*, 93 (1956). See also *Ind. Eng. Chem.*, **52**, 291 (1960).

The Temperature Coefficients of Electrode Potentials

II. The Second Isothermal Temperature Coefficient

G. R. Salvi and A. J. deBethune

Chemistry Department, Boston College, Chestnut Hill, Massachusetts

ABSTRACT

The second isothermal temperature coefficient of the potential of an electrode is equal to $\Delta C_p/n\mathbf{F}T$ where ΔC_p is the heat capacity change of the "SHE/Electrode" cell reaction. The mass-action dependence of the second coefficient is given. Values of the second coefficient are tabulated for 58 standard electrodes, together with the first coefficients. Application of the data to fuel cells, and to emf-temperature relationships, is discussed.

In a previous publication (1), the isothermal temperature coefficient $(dV/dT)_{isoth}$ of electrode potentials[1] was defined as the temperature derivative dE/dT of the emf E of the isothermal cell[2]

$$\text{SHE//Electrolyte/Electrode} \qquad [1]$$

where the left electrode is a standard hydrogen electrode (SHE). If the reversible reaction at the right-hand electrode is written

$$\text{Ox} + ne^- = \text{Red} \qquad [2]$$

the over-all reaction of cell [1] can be written

$$\text{Ox} + (n/2)\text{H}_2(a = 1) = n\text{H}^+ (a = 1) + \text{Red} \qquad [3]$$

for the reversible passage of n faradays of positive electricity through the cell from left to right. The isothermal temperature coefficient of the electrode potential V of this reversible electrode is

$$(dV/dT)_{isoth} = \Delta S/n\mathbf{F}$$
$$= [S(\text{Red}) - S(\text{Ox}) + nS^\circ(\text{H}^+) - (n/2)S^\circ(\text{H}_2)]/n\mathbf{F} \qquad [4]$$

where the S's denote the (partial) molal entropies of the given substances.

Since $dS/dT = C_p/T$, where C_p is the (partial) molal heat capacity, it can be shown that the *second isothermal temperature coefficient* of the electrode potential V, equal to the second temperature derivative d^2E/dT^2 of the emf E of isothermal cell [1], takes the form

$$(d^2V/dT^2)_{isoth} = \Delta C_p/n\mathbf{F}T = [C_p(\text{Red}) - C_p(\text{Ox}) + nC_p^\circ(\text{H}^+) - (n/2)\,C_p^\circ(\text{H}_2)]/n\mathbf{F}T \qquad [5]$$

In Eq. [4] and [5], S° (H^+) and $C_p^\circ(H^+)$ have their conventional values of zero at all temperatures, and S and C_p for other ionic species have values based on this conventional standard.

Mass Action Dependence

For a nonstandard electrode, the electrode potential V is related to the standard electrode potential V° by the Nernst equation

$$V = V^\circ - (RT/n\mathbf{F}) \ln [(\text{Red})/(\text{Ox})] = V^\circ + (RT/n\mathbf{F}) \ln [(\text{Ox})/(\text{Red})] \qquad [6]$$

where (Ox) and (Red) denote the activities or activity products of the electromotively active substances appearing on the left and right hand sides, respectively, of Eq. [2]. Let

$$(\text{Ox}) = m(\text{Ox})\,\gamma(\text{Ox}) \qquad [7]$$

$$(\text{Red}) = m(\text{Red})\,\gamma(\text{Red}) \qquad [8]$$

where the m's denote molalities, (or molality products, as the case may be) and the γ's denote activity coefficients (or activity coefficient products). The first temperature coefficient of the electrode potential V exhibits a mass-action dependence which can be described by the equation

$$(dV/dT)_{isoth} = (dV^\circ/dT)_{isoth} + (R/n\mathbf{F})\ln[m(\text{Ox})\gamma(\text{Ox})/m(\text{Red})\gamma(\text{Red})] + (RT/n\mathbf{F})d\ln[\gamma(\text{Ox})/\gamma(\text{Red})]/dT \qquad [9]$$

The second isothermal temperature coefficient then exhibits a mass-action dependence given by

$$(d^2V/dT^2)_{isoth} = (d^2V^\circ/dT^2)_{isoth} + (2R/n\mathbf{F})d\ln[\gamma(\text{Ox})/\gamma(\text{Red})]/dT + (RT/n\mathbf{F})d^2\ln[\gamma(\text{Ox})/\gamma(\text{Red})]/dT^2 \qquad [10]$$

Molalities do not appear in Eq. [10] and there is no mass-action dependence of the second coefficient if all activity coefficients are temperature invariant, *e.g.*, in ideal solutions.

Since $-RT^2(d\ln\gamma_i/dT) = H_i - H^\circ_i = L_i = H'_i$ is the relative partial molal enthalpy of species i, and $C_{p,i}' = dH'_i/dT$ is the relative partial molal heat capacity of species i, both values relative to the standard state values, the last two expressions for mass-action dependence can be rewritten in the forms

$$(dV/dT)_{isoth} = (dV^\circ/dT)_{isoth} + (R/n\mathbf{F})\ln[(\text{Ox})/(\text{Red})] + \Delta H'/n\mathbf{F}T \qquad [11]$$

[1] The single electrode potential V, following the Gibbs-Stockholm convention (3-5), is positive if the electrode in question is the (+) terminal of a cell whose other electrode is a standard hydrogen electrode (SHE).

[2] Cell emf's, following the Lewis-Stockholm convention (3-7), are positive if positive current tends to flow through the cell as written from left to right.

where $\Delta H' = \Delta H - \Delta H^\circ$ is the enthalpy change of reaction [2] and [3] relative to the standard value, and

$$(d^2V/dT^2)_{\text{isoth}} = (d^2V^\circ/dT^2)_{\text{isoth}} + \Delta C_p'/n\mathbf{F}T \quad [12]$$

where $\Delta C_p' = \Delta C_p - \Delta C_p^\circ$ is the heat capacity change of reaction [2] or [3] relative to the standard value.

Table of Second Temperature Coefficients

Table I lists a number of electrodes, their standard electrode potentials, and the first and second isothermal temperature coefficients. The potentials and the first coefficients are taken from deBethune, Licht, and Swendeman (1). The second coefficients have been computed from Eq. [5] by use of heat capacity data from Circular 500 of the National Bureau of Standards (8). All values refer to 25°C. The values in parentheses are experimental observations, taken from the sources noted. An error of 1 cal/deg (molal reaction unit) in ΔC_p corresponds to an uncertainty of 0.145 μv/deg[2] in the second coefficient for a 1 faraday reaction, and to half as much for a 2 faraday reaction.

Application to Fuel Cells

In the thermodynamic theory of fuel cells (17), it is shown that the desirable thermodynamic properties for a simple fuel cell are

ΔG negative
ΔS zero or positive
ΔC_p zero or positive

where ΔG, ΔS, and ΔC_p are the free enthalpy (Gibbs free energy), entropy and heat capacity, respectively, of the fuel cell reaction. For a regenerative fuel cell, the desirable properties are

ΔG negative
ΔS negative
ΔC_p zero

for the fuel cell reaction at low temperature. These properties can be computed from electrode potentials (1, 7), and their first (1) and second isothermal temperature coefficients, as follows

$$\Delta G = -n\mathbf{F}E = -n\mathbf{F}(V_r - V_l) \quad [13]$$

$$\Delta S = n\mathbf{F}(dE/dT) = n\mathbf{F}[(dV_r/dT)_{\text{isoth}} - (dV_l/dT)_{\text{isoth}}] \quad [14]$$

$$\Delta C_p = n\mathbf{F}T(d^2E/dT^2) = n\mathbf{F}T[(d^2V_r/dT^2)_{\text{isoth}} - (d^2V_l/dT^2)_{\text{isoth}}] \quad [15]$$

where the subscripts r and l refer to the right- and left-hand electrodes, respectively, of the fuel cell as written, and the changes refer to the reaction which transfers n faradays of positive electricity through the cell from left to right.

Thus the tabulation of first and second isothermal temperature coefficients of electrode potentials provides data useful to the thermodynamic screening of fuel cell reactions.

The standard electromotive force of a cell can be computed from the data of Table I, as a function of temperature, by means of Taylor's theorem in the form

$$E^\circ(t) = D[V^\circ] + D[dV^\circ/dT](t-25) + \frac{1}{2}D[d^2V^\circ/dT^2](t-25)^2 \quad [16]$$

where the operator D denotes the algebraic difference of the tabular values for the two electrodes, taken in the order: *right electrode minus left electrode.*[3] For nonstandard emf's, the Nernst equation and its temperature derivatives, Eq. [6], [9], and [10], must be applied, to the two electrodes separately, in the order: *right minus left.*[3]

Acknowledgment

The authors wish to thank the International Nickel Company for a Grant-in-Aid in support of this work.

Manuscript received Sept. 2, 1960; revised manuscript received April 1, 1961. This paper was prepared for delivery before the Indianapolis Meeting, April 30-May 3, 1961.

Any discussion of this paper will appear in a Discussion Section to be published in the June 1962 JOURNAL.

REFERENCES

1. A. J. deBethune, T. S. Licht, and N. Swendeman, *This Journal*, **106**, 616 (1959).
2. J. Willard Gibbs, "Collected Works," Vol. I, pp. 332-349, 429, Longmans Green, New York (1928).
3. J. A. Christiansen, *J. Am. Chem. Soc.*, **82**, 5517 (1960); J. A. Christiansen and M. Pourbaix, *Compt. Rend.*, 17th Conf. I.U.P.A.C., pp. 82-84, Maison de la Chimie, Paris (1954).
4. A. J. deBethune, *This Journal*, **102**, 288C (1955).
5. T. S. Licht and A. J. deBethune, *J. Chem. Education*, **34**, 433 (1957).
6. G. N. Lewis and M. Randall, "Thermodynamics and the Free Energy of Chemical Substances," McGraw Hill Book Co., New York (1923).
7. W. M. Latimer, "Oxidation Potentials—The Oxidation States of the Elements and Their Potentials in Aqueous Solutions," 2nd Ed., Prentice Hall, New York (1952).
8. F. D. Rossini, D. D. Wagman, W. H. Evans, S. Levine, and I. Jaffe, "Selected Values of Chemical Thermodynamic Properties," National Bureau of Standards Circular 500, U.S. Govt. Printing Office, Washington, D. C. (1952).
9. D. A. MacInnes, "The Principles of Electrochemistry," Reinhold Publishing Co., New York (1939).
10. H. S. Harned and B. B. Owen, "The Physical Chemistry of Electrolytic Solutions," 3rd Ed., Reinhold Publishing Co., New York (1958).
11. R. G. Bates, *J. Am. Chem. Soc.*, **60**, 2983 (1938); R. A. Robinson and R. H. Stokes, *Trans. Faraday Soc.*, **36**, 740 (1940).
12. B. B. Owen, *J. Am. Chem. Soc.*, **57**, 1526 (1935).
13. R. G. Bates and V. E. Bower, *J. Research Nat. Bur. Standards*, **53**, 283 (1954).
14. A. K. Grzybowski, *J. Phys. Chem.*, **62**, 550 (1958).
15. R. H. Gerke, *J. Am. Chem. Soc.*, **44**, 1684 (1922).
16. W. J Hamer, *J. Am. Chem. Soc.*, **57**, 9 (1935); H. S. Harned and W. J. Hamer, *ibid.*, **57**, 27 33 (1935).
17. A. J. deBethune, *This Journal*, **107**, 937 (1960).
18. R. S. Greeley, W. T. Smith, M. H. Lietzke, R. W. Stoughton, *J. Phys. Chem.*, **64**, 652, 1445 (1960); M. B. Towns, R. S. Greeley, and M. H. Lietzke, *ibid.*, **64**, 1861 (1960).

[3] For the Cell Tension (Zell Spannung) of C.I.T.C.E. (26), the inverse order should be taken.

Table I. First and second isothermal temperature coefficients of the standard electrode potentials at 25°C

The electrode potential V° is given a positive value if the electrode is the (+) terminal of a cell whose second electrode is the SHE.

Electrode	V°, v	$(dV^\circ/dT)_{isoth}$, mv/deg	$(d^2V^\circ/dT^2)_{isoth}$, μv/deg^2
	(Acid Solutions)		
$HN_3(g) = (3/2)N_2 + H^+ + e^-$	−3.40	−1.193	−0.562
$H(g) = H^+ + e^-$	−2.1065	+0.511	+0.221
$Si + 2H_2O = SiO_2(quartz) + 4H^+ + 4e^-$	−0.857	−0.374	+0.594
$2Ta + 5H_2O = Ta_2O_5 + 10H^+ + 10e^-$	−0.812	−0.377	+0.514
$Zn = Zn^{++} + 2e^-$	−0.7628	+0.091 (+0.166[a])	— (+3.84[a])
$Zn(Hg) = Zn^{++} + Hg + 2e^-$	−0.7627[b,c] −0.7625[b,d]	(+0.100[b,c]) (+0.103[b,d])	(+0.62[b,c]) (+1.6[b,d])
$Cd = Cd^{++} + 2e^-$	−0.4029	−0.093 (−0.053[a])	— (+2.2[a])
$Pb + SO_4^= = PbSO_4 + 2e^-$	−0.3588	−1.015	−1.555
$Cd(Hg) = Cd^{++} + Hg + 2e^-$	−0.3516[a] −0.3515[b] −0.3514[b]	(−0.250[a]) (−0.252[b]) (−0.292[b])	(+1.6[a]) (−0.56[b]) (+0.20[b])
$Pb(Hg) + SO_4^= = PbSO_4 + Hg + 2e^-$	−0.3505	(−0.914[a])	(−1.71[a])
$Tl = Tl^+ + e^-$	−0.3363	−1.327 (−1.314[a])	— (−0.85[a])
$Cu + I^- = CuI + e^-$	−0.1852	−0.200	−6.038
$Ag + I^- = AgI + e^-$	−0.1518	−0.284 (−0.328[e])	−6.016 (−7.2[e])
$W + 3H_2O = WO_3(c) + 6H^+ + 6e^-$	−0.090	−0.400	+0.480
$2Hg + 2I^- = Hg_2I_2 + 2e^-$	−0.0405	+0.019	−5.883
$H_2 = 2H^+ + 2e^-$ (SHE)	±0.0000[f]	±0.000[f]	±0.000[f]
$Ag + Br^- = AgBr + e^-$	+0.0713 (+0.0711[a]) (+0.0713[g]) (+0.0712[p])	−0.508 (−0.488[a]) (−0.499[g]) (−0.526[p])	−5.901 (−5.97[a]) (−6.90[g]) (−4.80[p])
$SiH_4(g) = Si + 4H^+ + 4e^-$	+0.102	−0.197	−0.302
$CH_4(g) = C(graphite) + 4H^+ + 4e^-$	+0.1316	−0.209	−0.266
$Ag + Cl^- = AgCl + e^-$	+0.2222 (+0.2225[a]) (+0.2224[h]) (+0.2224[p]) (+0.2225[q])	−0.658 (−0.638[a]) (−0.646[h]) (−0.656[p]) (−0.645[q]) (−0.65[r])	−5.744 (−6.61[a]) (−5.961[h]) (−4.746[p]) (−6.554[q])
$2Hg + 2Cl^- = Hg_2Cl_2 + 2e^-$	+0.2676 (+0.2681[i]) (+0.2679[r]) (+0.26790[s])	−0.317 (−0.317[i]) (−0.312[r]) (−0.307[s]) (−0.320[j])	−5.664 (−5.986[i]) (−6.74[r]) (−5.961[s])
$Ag + IO_3^- = AgIO_3 + e^-$	+0.354	−0.568	−5.956
$C_2H_6(g) = C_2H_4(g) + 2H^+ + 2e^-$	+0.52	−0.625	−0.343
$Te + 2H_2O = TeO_2(c) + 4H^+ + 4e^-$	+0.529	−0.370	+0.453
$2I^- = I_2(c) + 2e^-$	+0.5355	−0.148	−5.965
$2Hg + SO_4^= = Hg_2SO_4 + 2e^-$	+0.6151 (+0.6151[i]) (+0.6119[k])	−0.826 (−0.803[i])	−1.537 (−0.854[i]) (−1.685[m])

Table I (Continued)

Electrode	V°, v	$(dV^\circ/dT)_{isoth}$, mv/deg	$(d^2V^\circ/dT^2)_{isoth}$, μv/deg²
$2Ag + SO_4^{=} = Ag_2SO_4 + 2e^-$	+0.654	−1.182	−1.608
$C_2H_4(g) = C_2H_2(g) + 2H^+ + 2e^-$	+0.731	−0.580	−0.508
$Ag = Ag^+ + e^-$	+0.7991	−1.000	−0.924
$2Rh + 3H_2O = Rh_2O_3 + 6H^+ + 6e^-$	+0.87	−0.40	+0.50
$2Br^- = Br_2(l) + 2e^-$	+1.0652	−0.629	−6.210[a]
$4Cl^- + C + 4H^+ = CCl_4 + 4H^+ + 4e^-$	+1.18	−0.645	−5.934
$2H_2O(g) = O_2 + 4H^+ + 4e^-$	+1.185	−0.230	−0.173
$\frac{1}{2}I_2 + 3H_2O = IO_3^- + 6H^+ + 5e^-$	+1.195	−0.364	+1.813
$2H_2O(l) = O_2 + 4H^+ + 4e^-$	+1.229	−0.846	+0.552
$2S + 2Cl^- = S_2Cl_2 + 2e^-$	+1.23	−0.64	−6.261
$2Cl^- = Cl_2 + 2e^-$	+1.3595	−1.260 (−1.26[f])	−5.454
$\frac{1}{2}Br_2(l) + 3H_2O = BrO_3^- + 6H^+ + 5e^-$	+1.52	−0.418	+1.871[a]
$PbSO_4 + 2H_2O = PbO_2 + SO_4^{=} + 4H^+ + 2e^-$	+1.685	+0.326 (+0.347[a])	+2.516 (+2.493[a])
$O_2 + H_2O = O_3 + 2H^+ + 2e^-$	+2.07	−0.483	+0.655
$H_2O = O(g) + 2H^+ + 2e^-$	+2.422	−1.148	+0.427
$H_2O = OH + H^+ + e^-$	+2.85	−1.855	+1.078
$2F^- = F_2(g) + 2e^-$	+2.87	−1.830	−5.339
(Basic Solutions)			
$H(g) + OH^- = H_2O + e^-$	−2.9345	−0.323	−7.050
$Mg + 2OH^- = Mg(OH)_2 + 2e^-$	−2.69	−0.945	−6.079
$Zn + 2OH^- = Zn(OH)_2 + 2e^-$	−1.245	−1.002	−5.978
$H_2 + 2OH^- = 2H_2O + 2e^-$	−0.82806	−0.8342	−7.272
$Pb + 2OH^- = PbO(r) + H_2O + 2e^-$	−0.580 (−0.577[a])	−1.163 (−1.188[a])	−6.841[f] (≃ −6.7[a])
$2Bi + 6OH^- = Bi_2O_3 + 3H_2O + 6e^-$	−0.46	−1.214	−6.828
$2Cu + 2OH^- = Cu_2O + H_2O + 2e^-$	−0.358	−1.326	−6.828
$2Rh + 6OH^- = Rh_2O_3 + 3H_2O + 6e^-$	+0.04	−1.23	−6.772
$Hg + 2OH^- = HgO(r) + H_2O + 2e^-$	+0.098 (+0.098[a])	−1.120 (−1.127[a])	−6.775 (−6.749[a])
$I^- + 6OH^- = IO_3^- + 3H_2O + 6e^-$	+0.26	−1.162	−6.755
$2Ag + 2OH^- = Ag_2O + H_2O + 2e^-$	+0.345 (+0.342[w])	−1.337 (−1.325[w])	−6.718 (≃6.7[w])
$4OH^- = O_2 + 2H_2O + 4e^-$	+0.401	−1.680	−6.719
$Br^- + 6OH^- = BrO_3^- + 3H_2O + 6e^-$	+0.61	−1.287	−6.748
$O_2 + 2OH^- = O_3(g) + H_2 + 2e^-$	+1.24	−1.318	−6.617
$OH^- = OH(g) + e^-$	+2.02	−2.689	−6.194

[a] MacInnes (9), p. 201. [b] Harned and Owen (10), p. 741. [c] Bates (11). [d] Robinson and Stokes (11). [e] Owen (12). [f] By definition. [g] Harned and Owen (10), pp. 495-6. [h] Bates and Bower (13). [i] Grzybowski (14). [j] From isothermal cell temperature coefficients of Gerke (15) and the isothermal coefficients of the calomel, silver chloride, silver iodide and lead iodide electrodes as computed by deBethune, Licht, and Swendeman (1) from Latimer's entropies (7). [k] From Latimer's (7) free enthalpies of formation. [l] Harned and Owen (10), Eq. [13-12-1]. [m] Value based on Eq. [13-12-1] above, corrected for the incomplete ionization of HSO_4^- ion by the method of Harned and Owen (10), pp. 570-3. [n] Harned and Owen (10) Eq. [13-9-7]; Harned and Hamer (16). [o] Greeley, Lietzke *et al.* (18). [q] Swinehart (19), Harned and Ehlers (20). [r] Muller and Reuther (21). [s] From Pouradier and Chateau's data (22) for the calomel *vs.* silver chloride cell, and Bates and Bower's data (13) for silver chloride *vs.* SHE. [t] Calculated from heat capacity of yellow-PbO. [u] Calculated from C_{p° (Br_2) (1) = 17.1 cal/deg mole (23). [v] Fried (24); observed for H_2/NaOH/HgO/Hg, E° = +0.9260 v; dE°/dT = −0.2924 mv/deg; d^2E°/dT^2 = +0.523 μv/deg². Observed for Pb/PbO/NaOH/HgO/Hg, E° = +0.675 v; dE°/dT = +0.061 mv/deg; $d^2E^\circ/dT^2 \simeq$ 0.0 μv/deg². Converted to SHE basis by use of tabulated values for standard H_2/OH^- electrode. [w] Fried (24); Hamer and Craig (25); observed for Hg/HgO/NaOH/Ag_2O/Ag, E° = +0.2440 v; dE°/dT = −0.198 mv/deg; $d^2E^\circ/dT^2 \simeq$ 0.0 μv/deg². [x] Uhlig (27).

19. D. F. Swinehart, *J. Am. Chem. Soc.*, **74**, 1100 (1952).
20. H. S. Harned and R. W. Ehlers, *J. Am. Chem. Soc.*, **55**, 2179 (1933).
21. F. Müller and H. Reuther, *Z. Elektrochem.*, **49**, 497 (1943).
22. J. Pouradier and H. Chateau, *Compt. Rend.*, **237**, 711 (1953).
23. Int. Crit. Tables, **5**, 94.
24. F. Fried, *Z. physik Chem.*, **123**, 406 (1926).
25. W. J. Hamer and D. N. Craig, *This Journal*, **104**, 206 (1957).
26. P. Van Rysselberghe, Report of C.I.T.C.E. Commission on Nomenclature and Terminology, tr. E. Lange, *Z. Elektrochem.*, **58**, 530 (1954).
27. H. H. Uhlig, "Corrosion Handbook," p. 1137, John Wiley & Sons, Inc., New York (1948).

Analysis of Galvanostatic Transients and Application to the Iron Electrode Reaction

J. O'M. Bockris and Hideaki Kita

John Harrison Laboratory of Chemistry, The University of Pennsylvania, Philadelphia, Pennsylvania

ABSTRACT

Processes of charging electrodes under galvanostatic conditions are examined for electrodes in which there is a foregoing or simultaneous equilibrium step, $A^+ + e \rightleftarrows A(Ads)$, followed by a rate-determining reaction. The associated pseudocapacity is evaluated. It may amount to a few thousand microfarads over a critical potential range.

The forms of the $\eta_t - t$ relations in decay are also evaluated for the special cases: (i) $A^+ + e \rightleftarrows A(Ads)$, $2A(Ads) \rightarrow X$; (ii) $A^+ + e \rightleftarrows A(Ads)$; $M^+ + e \rightarrow M$; and (iii) $A^+ + e \rightleftarrows A(Ads)$; $A^+ + A(Ads) + e \rightarrow X$. They characterize the process occurring. The coverage of electrodes by adsorbed radicles (H, OH, etc.) at the reversible potential may be estimated, even in systems in which the metal corrodes.

The theory is applied to the complex simultaneous reactions: $Fe^{2+} + 2e_o^- \rightleftarrows Fe$; $2H^+ + 2e_o^- \rightleftarrows H_2$. The coverage of a corroding Fe electrode with H is about 3% at the corrosion potential for pH = 4. Super polarization in anodic charging and potential decay curves after Fe dissolution are interpreted in terms of the temporary build up of nonequilibrium concentrations of H^+ and OH^- on the solution side of the double layer, respectively. The slopes of $\frac{RT}{\mathbf{F}}$ and $\frac{RT}{(1+\beta)\mathbf{F}}$, respectively, obtained when the maximum value and steady-state value of potentials in Fe dissolution are plotted against ln i, follow from the model.

Recently, the kinetics of the iron electrodeposition and dissolution reaction have been studied in detail by the galvanostatic method (1).

From an analysis of the steady state, under the conditions of the experiments, the reaction mechanism has been found to be:

$$Fe^+ + OH^- \rightleftarrows (FeOH)^+ \qquad [1]$$

$$(FeOH)^+ + e \rightarrow (FeOH) \qquad [2]$$

$$(FeOH) + e \rightleftarrows Fe + OH^- \qquad [3]$$

where the rate-determining step is [2].

The galvanostatic transients of the iron electrode reaction differ qualitatively from "normal" transients such as the high c.d. transients of the copper electrode reaction (2). Thus, the rise times are abnormally large and decay rate of the cathodic transients abnormally small; a maximum and minimum occur in the anodic charging and decay transients; the apparent double layer capacity is abnormally high, etc. Typical transients are shown in Fig. 1 and 2.

General Case

Consider the following potential dependent adsorption phenomenon:

$$A^+ + e \rightleftharpoons A(Ads) \qquad [4]$$

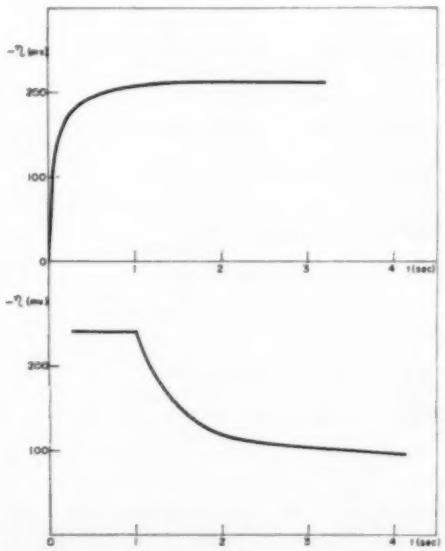

Fig. 1. Cathodic transients: (a) charging curve, $i = 1.85 \times 10^{-3}$ amp/cm², $C_{Fe^{++}} = 0.5$ mole/l, pH = 4.9; (b) decay curve, $i = 1.4 \times 10^{-2}$ amp/cm², $C_{Fe^{++}} = 0.5$ mole/l, pH = 4.0, $i_{cor} = 10^{-5}$ amp/cm², $i_o = 2.4 \times 10^{-6}$ amp/cm², $V_{Fe,\,rev} - V_{cor} = 48$ mv.

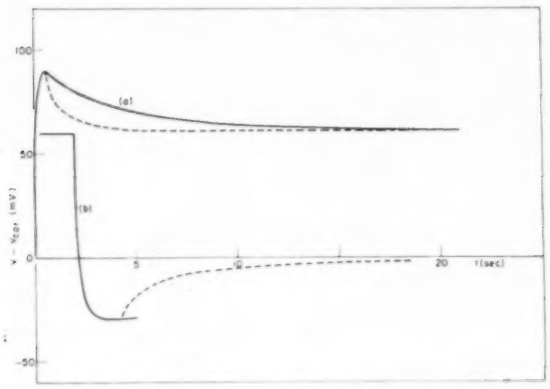

Fig. 2. Anodic transients: (a) anodic charging, $i = 1.1 \times 10^{-3}$ amp/cm², pH = 4.9, — experimental, — — — — calculated; (b) anodic decay, pH = 4.9, — experimental, — — — — calculated.

Reaction [4] is at an equilibrium corresponding to an electrode potential determined by a following or simultaneous rate-determining step. Then,

$$\vec{k}_A(1-\theta_A)[A^+]\,e^{-\frac{\beta F\eta}{RT}} = \overleftarrow{k}_A\theta_A e^{\frac{(1-\beta)F\eta}{RT}} \qquad [5]$$

where $\vec{k}_A$ and $\overleftarrow{k}_A$ are "rate constants" at the reversible potential, θ_A is the coverage of A(Ads) at the potential η, η is the overpotential and β is the symmetry factor.

From Eq. [5]

$$\theta_A = \frac{1}{1+\frac{K_A}{[A^+]}e^{\frac{F\eta}{RT}}} \qquad [6]$$

where K_A is $\overleftarrow{k}_A/\vec{k}_A$ (and is concentration dependent).

When $\frac{K_A}{[A^+]}e^{\frac{F\eta}{RT}} \gg 1$

$$\theta_A = \frac{[A^+]}{K_A}e^{-\frac{F\eta}{RT}} \qquad [7]$$

At $\eta = 0$, Eq. [6] is

$$\frac{K_A}{[A^+]} = \frac{1-\theta_{A,o}}{\theta_{A,o}} \qquad [8]$$

where $\theta_{A,o}$ is the coverage of A(Ads) at $\eta = 0$.

Effect of A(Ads) on the apparent double layer capacity.—Let the differential capacity of the double layer (when the electrode is polarizable) be $C_{D.L.}$, and the differential capacity due to A(Ads) be $(C_{Ads})_\eta$. Then, $C_{D.L.}$ and $(C_{Ads})_\eta$ can be treated as if in parallel, i.e.

$$C = C_{D.L.} + (C_{Ads})_\eta \qquad [9]$$

Also

$$(C_{Ads})_\eta = -FZ\frac{d\theta_A}{d\eta} \qquad [10]$$

where F is the Faraday, and Z is the number of sites (mole cm⁻²). The negative sign indicates that θ_A increases as η becomes more negative (valid for [4]).

From Eq. [6], [8], and [10]

$$(C_{Ads})_\eta = \frac{F^2Z}{RT}\frac{K_A}{[A^+]}\frac{e^{\frac{F\eta}{RT}}}{\left[1+\frac{K_A}{[A^+]}e^{\frac{F\eta}{RT}}\right]^2} \qquad [11]$$

Hence, $(C_{Ads})_{max.}$ occurs at an overpotential

$$\eta_{C_{max.}} = \frac{RT}{F}\ln\frac{[A^+]}{K_A} = \frac{RT}{F}\ln\frac{\theta_{A,o}}{1-\theta_{A,o}} \qquad [12]$$

and its maximum value is given by

$$(C_{Ads})_{max.} = \frac{F^2Z}{4RT} \qquad [13]$$

With $Z = \frac{10^{15}}{6.10^{23}}$ cm⁻², (roughness factor assumed unity), $(C_{Ads})_{max.}$ is 1.6×10^3 μF cm⁻². $(C_{Ads})_\eta$ is shown as a function of overpotential in Fig. 3 at given $\theta_{A,o}$ values.

Figure 3 shows that a knowledge of the differential pseudocapacity due to adsorption over a potential range allows determination of $\theta_{A,o}$. As $\theta_{A,o}$ is reduced, it is necessary to practice to find a potential region for which $C_{Ads} > C_{D.L.}$ by using increasingly negative potentials. The limit of potential is that at which the faradaic current (due to reaction) becomes appreciable compared with the charging current.

Figure 3 shows that in a galvanostatic charging curve for which reaction [4] is in equilibrium and is succeeded by some rate determining reaction, there may be a potential region in which the η_t-t slope decreases in value and then again increases [as $(C_{Ads})_\eta$ decreases with increasingly negative potential]. The potential region over which the deviation from the expected value of $d\eta_t/dt$ for *double layer* charging would occur may be seen from Fig. 3 to be about 200 mv: its location with respect to the reversible potential depends on $\theta_{A,o}$.

An observation that the slope of an η_t-t relation deviates from that expected for double layer charging and faradaic transfer over a potential interval of

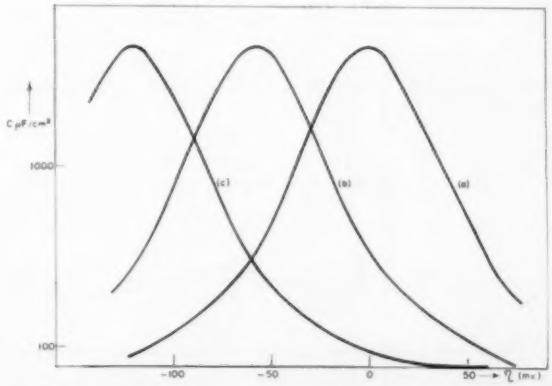

Fig. 3. Calculated $C_{Ads.}$ according to Eq. [11], (a) value of $\theta_{A,o}$ is 0.5, (b) 0.1, (c) 0.01.

200 mv confirms that an inflection may be interpreted as here suggested. If, in an η_t-t curve, no inflection occurs in a potential region corresponding to double layer charging (i.e., one for which $i_{transient}$ is less than, say, one-tenth of the total current density), then, either the mechanism of the reaction is not one in which a reversible reaction precedes the rate determining step, or $\theta_{A,o}$ is such that (cf. Fig. 3) appreciable $(C_{Ads})_\eta$ values occur only at potentials outside the charging region. Deviation of the η_t-t slope from that of double layer charging only, will not occur if the c.d. used for the transient is so high that the preliminary reaction is no longer in pseudoequilibrium. Thus, in practice, $d\eta_t/dt$ should be determined first for a high c.d., for, then, the potential region in which the characteristic potential range for inflection on η_t-t curves may be observed, is maximized. If, however, no inflection is thereby observed, the transients should be examined in steps, starting at the reversible potential and using the lowest c.d. at which an appreciable region of double layer charging can be observed. Thus, the possibility of causing reaction [4] to go out of equilibrium is reduced.

Equation [11] becomes, at $\eta = 0$

$$(C_{Ads})_{\eta=0} = \frac{F^2Z}{RT}\frac{K_A}{[A^+]}\frac{1}{\left(1+\frac{K_A}{[A^+]}\right)^2} = \frac{F^2Z}{RT}\frac{1-\theta_{A,o}}{\theta_{A,o}}\frac{1}{\left(1+\frac{1-\theta_{A,o}}{\theta_{A,o}}\right)^2} \quad [14]$$

From Eq. [14], $\theta_{A,o}$ can be estimated by knowing $(C_{Ads})_{\eta=0}$ experimentally.

Fundamental equation for transients.—In a galvanostatic transient, the total current density, i, is used: (i) in charging of the double layer, $i_{D.L.}$; (ii) in changing the equilibrium concentration of a discharging species, i_{Ads}; and (iii) in an electrode reaction, i_E.

$$i = i_{D.L.} + i_{Ads} + i_E \quad [15]$$

where

$$i_{D.L.} = C_{D.L.}\frac{d\eta_t}{dt};\quad i_{Ads} = (C_{Ads})_\eta\frac{d\eta_t}{dt} \quad [16]$$

$C_{D.L.}$ is constant[1] and $(C_{Ads})_\eta$ is a function of η. With Eq. [16] into Eq. [15]

$$\frac{d\eta_t}{dt} = \frac{i-i_E}{C_{D.L.}+(C_{Ads})_\eta} \quad [17]$$

or

$$\eta_t = \int_o^t \frac{i-i_E}{C_{D.L.}+(C_{Ads})_\eta}dt \quad [18]$$

Equation [18] gives the basic relationship between η_t and t in galvanostatic charging. If reaction [4] is the cause of i_{Ads}, Eq. [17] becomes, using the expression for $(C_{Ads})_\eta$ from Eq. [11]

$$\frac{d\eta_t}{dt} = \frac{i-i_E}{C_{D.L.}+\frac{F^2Z}{RT}\frac{K_A}{[A^+]}\frac{e^{\frac{F\eta_t}{RT}}}{\left(1+\frac{K_A}{[A^+]}e^{\frac{F\eta_t}{RT}}\right)^2}} \quad [19]$$

and Eq. [18] becomes

$$\eta_t = \int_o^t \frac{i-i_E}{C_{D.L.}+\frac{F^2Z}{RT}\frac{K_A}{[A^+]}\frac{e^{\frac{F\eta_t}{RT}}}{\left(1+\frac{K_A}{[A^+]}e^{\frac{F\eta_t}{RT}}\right)^2}}dt \quad [20]$$

$C_{D.L.}$ is neglected in the following because of its small value compared with $(C_{Ads})_\eta$, in potential regions of interest.

Cathodic transients.—Case (i): Suppose the reaction sequence is

$$A^+ + e \rightleftarrows A(Ads) \quad [4]$$

$$2A(Ads) \rightarrow X \quad [21]$$

where X is the final product and the rate-determining step is [21]. As [4] is taken as in equilibrium, it follows that its rate constants will tend to be much greater than those of [21]. Thence, approximately

$$i_E = -\vec{k}_E\theta_A^2 + \overleftarrow{k}_E(1-\theta_A)^2[X] \quad [22]$$

or

$$i_E = i_o\left[-\frac{\theta_A^2}{\theta_{A,o}^2}+\frac{(1-\theta_A)^2}{(1-\theta_{A,o})^2}\right] \quad [23]$$

where $\vec{k}_E$, $\overleftarrow{k}_E$, and i_o are rate constants and exchange current density, respectively.

Equations [6] and [23] give

$$i_E = -\frac{i_o}{\theta_{A,o}^2(1-\theta_{A,o})^2}\left[\frac{1-2\theta_{A,o}}{\left(1+\frac{K_A}{[A^+]}e^{\frac{F\eta_t}{RT}}\right)^2}+\frac{2\theta_{A,o}^2}{\left(1+\frac{K_A}{[A^+]}e^{\frac{F\eta_t}{RT}}\right)}-\theta_{A,o}^2\right] \quad [24]$$

If $\theta_{A,o} << 1$, Eq. [24] becomes

$$i_E = -\frac{i_o}{\theta_{A,o}^2}\frac{1}{\left(1+\frac{K_A}{[A^+]}e^{\frac{F\eta_t}{RT}}\right)^2} \quad [25]$$

[1] The variation of $C_{D.L.}$ with potential is negligible compared with that of $(C_{Ads})_\eta$ in regions of interest.

With Eq. [25] in Eq. [19] (neglecting $C_{D.L.}$)

$$\frac{d\eta_t}{dt} = \frac{-i + \frac{i_o}{\theta_{A,o}^2}\frac{1}{\left(1 + \frac{K_A}{[A^+]}e^{\frac{F\eta_t}{RT}}\right)^2}}{\frac{F^2Z}{RT}\frac{K_A}{[A^+]}\frac{e^{\frac{F\eta_t}{RT}}}{\left(1 + \frac{K_A}{[A^+]}e^{\frac{F\eta_t}{RT}}\right)^2}} \quad [26]$$

This Equation is transformed into

$$\frac{e^{\frac{F\eta_t}{RT}}}{-i\left(1 + \frac{K_A}{[A^+]}e^{\frac{F\eta_t}{RT}}\right) + \frac{i_o}{\theta_{A,o}^2}} d\eta_t = \frac{RT}{F^2Z}\frac{[A^+]}{K_A}dt \quad [27]$$

Integration of Eq. [27] gives

$$t = \frac{2FZ\theta_{A,o}}{(i\,i_o)^{1/2}} \ln \frac{\left[\left(\frac{i_o}{i}\right)^{1/2}\frac{[A^+]}{\theta_{A,o}K_A} + \frac{[A^+]}{K_A} + Y\right]\left[\left(\frac{i_o}{i}\right)^{1/2}\frac{[A^+]}{\theta_{A,o}K_A} - \frac{[A^+]}{K_A} - 1\right]}{\left[\left(\frac{i_o}{i}\right)^{1/2}\frac{[A^+]}{\theta_{A,o}K_A} - \frac{[A^+]}{K_A} - Y\right]\left[\left(\frac{i_o}{i}\right)^{1/2}\frac{[A^+]}{\theta_{A,o}K_A} + \frac{[A^+]}{K_A} + 1\right]} \quad [28]$$

where $Y = e^{\frac{F\eta_t}{RT}}$. Equation [28] can be examined by an independent determination of $\theta_{A,o}$ [$(C_{Ads})_{\eta=0}$ determinations near the reversible potential] and using i_o determined from steady-state conditions. When the denominator of the right-hand side of Eq. [28] approaches zero, $t \to \infty$, a condition corresponding to steady state. Then

$$\left(\frac{i_o}{i}\right)^{1/2}\frac{[A^+]}{\theta_{A,o}K_A} - \frac{[A^+]}{K_A} - Y = 0 \quad [29]$$

and

$$-i = -\frac{i_o}{\theta_{A,o}^2}\frac{1}{\left(1 + \frac{K_A}{[A^+]}Y\right)^2} = -i_o\frac{\theta_A^2}{\theta_{A,o}^2} \quad [30]$$

which is Eq. [23] for $\theta_{A,o} << 1$.

Case (ii): Suppose the reaction sequence is

$$A^+ + e \rightleftarrows A(Ads) \quad [4]$$

$$M^+ + e \rightarrow M \quad [31]$$

A^+ can be, for example, an ionized organic compound (*e.g.*, $PhNH_3^+$) in equilibrium with adsorbed neutral molecules according to reaction [4]. The effect of A_{Ads} is assumed simply to be that of blocking sites available to metal-solution exchange reactions [31]. In reaction [31], the charge transfer is rate determining (*e.g.*, in metal deposition).

Then ,i_g is expressed as

$$i_g = i_o\left(-e^{-\frac{\beta F\eta_t}{RT}} + e^{\frac{(1-\beta)F\eta_t}{RT}}\right)\frac{(1-\theta_A)}{(1-\theta_{A,o})} \quad [32]$$

Hence, Eq. [19] becomes

$$\frac{d\eta_t}{dt} = \frac{-i + i_o\left(e^{-\frac{\beta F\eta_t}{RT}} - e^{\frac{(1-\beta)F\eta_t}{RT}}\right)\frac{(1-\theta_A)}{(1-\theta_{A,o})}}{C_{D.L.} + \frac{F^2Z}{RT}\frac{K_A}{[A^+]}\frac{e^{\frac{F\eta_t}{RT}}}{\left(1 + \frac{K_A}{[A^+]}e^{\frac{F\eta_t}{RT}}\right)^2}} \quad [33]$$

If $C_{D.L.} << C_{Ads}$ and $\theta_{A,o} << 1$, Eq. [33] becomes with Eq. [6] for θ_A

$$\frac{d\eta_t}{dt} = \frac{-i\frac{[A^+]}{K_A}e^{-\frac{F\eta_t}{RT}}\left(1 + \frac{K_A}{[A^+]}e^{\frac{F\eta_t}{RT}}\right) + i_o\left(e^{-\frac{\beta F\eta_t}{RT}} - e^{\frac{(1-\beta)F\eta_t}{RT}}\right)}{\frac{F^2Z}{RT}\frac{1}{\left(1 + \frac{K_A}{[A^+]}e^{\frac{F\eta_t}{RT}}\right)}} \quad [34]$$

If, in the steady state, $1 << \frac{K_A}{[A^+]}e^{\frac{F\eta_s}{RT}}$, Eq. [34] becomes

$$\frac{e^{-\frac{F\eta_t}{RT}}}{-i + i_o\left(e^{-\frac{\beta F\eta_t}{RT}} - e^{\frac{(1-\beta)F\eta_t}{RT}}\right)} d\eta_t = \frac{RT}{F^2Z}\frac{K_A}{[A^+]}dt \quad [35]$$

Integration gives: ($\beta = 0.5$)

$$t = \frac{FZ\,[A^+]}{\beta i_o K_A}\left\{\frac{i}{2i_o}\frac{\beta F\eta_t}{RT} - \frac{1}{Y} - \frac{i}{2i_o}\ln\left(Y^2 + \frac{i}{i_o}Y - 1\right) - \frac{\left(\frac{i^2}{2i_o^2} + 1\right)}{2\left(\frac{i^2}{4i_o^2} + 1\right)}\ln\right.$$

$$\left. \frac{Y + \frac{i}{2i_o} - \left(1 + \left(\frac{i}{2i_o}\right)^2\right)^{1/2}}{Y + \frac{i}{2i_o} + \left(1 + \left(\frac{i}{2i_o}\right)^2\right)^{1/2}} \right| + \text{const.} \quad [36]$$

where $Y = e^{\frac{\beta F \eta_t}{RT}}$

In Eq. [36], for $t \to \infty$

$$Y + \frac{i}{2i_o} - \left(1 + \left(\frac{i}{2i_o}\right)^2\right)^{1/2} = 0 \quad [37]$$

or

$$-i = i_o \left[-e^{-\frac{\beta F \eta_\infty}{RT}} + e^{\frac{\beta F \eta_\infty}{RT}} \right] \quad [38]$$

i.e., Eq. [32] is recovered for the condition $\frac{K_A}{[A^+]} e^{\frac{\beta F \eta_\infty}{RT}} << 1$.

Case (iii): Let the reaction sequence be only reaction [31] and charging up of double layer [*cf.* Roiter *et al.* (3)]. Then Eq. [33] becomes

$$\frac{d\eta_t}{dt} = \frac{-i + i_o \left[-e^{-\frac{\beta F \eta_t}{RT}} - e^{\frac{(1-\beta) F \eta_t}{RT}} \right]}{C_{D.L.}} \quad [39]$$

or, upon integration

$$t = \frac{C_{D.L.}\, RT}{2i_o \beta F \left(1 + \left(\frac{i}{2i_o}\right)^2\right)^{1/2}} \ln \frac{Y + \frac{i}{2i_o} + \left(1 + \left(\frac{i}{2i_o}\right)^2\right)^{1/2}}{Y + \frac{i}{2i_o} - \left(1 + \left(\frac{i}{2i_o}\right)^2\right)^{1/2}} + \text{const} \quad [40]$$

By comparing the $\eta_t - t$ relation arising from Eq. [36] and [40], the effect of adsorption on the charging curves may be examined. In Fig. 4, the calculated results are shown for conditions $i_o = 10^{-4}$ amp cm^{-2} and $\theta_{A,o} = 10^{-2}$.

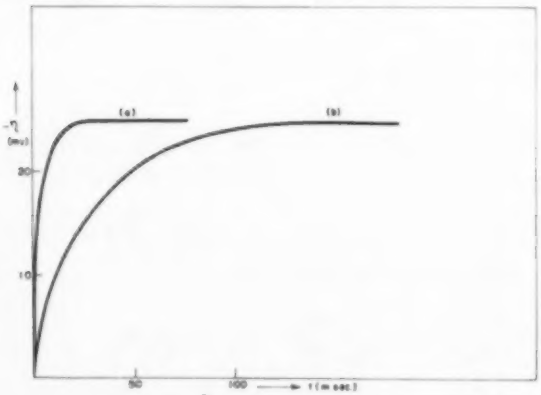

Fig. 4. Comparison of calculated charging curves, (a) no adsorption (according to Eq. [40]), $i_o = 10^{-4}$ amp/cm^2, $i = 10^{-4}$ amp/cm^2; (b) adsorption (according to Eq. [36]), $\theta_{A,o} = 0.01$, $i_o = 10^{-4}$ amp/cm.

Cathodic decay curves.—Here, $i = 0$. Let the cases be as above:

Case (i): Equation [27] becomes[2]

$$e^{\frac{F\eta_t}{RT}} d\eta_t = \frac{RT}{F^2 Z} \frac{i_o [A^+]}{\theta_{A,o}^2 K_A} dt \quad [41]$$

Integrating Eq. [41]

$$t = \frac{FZ\theta_{A,o}^2 K_A}{i_o [A^+]} \left[e^{\frac{F\eta_t}{RT}} - e^{\frac{F\eta_{t=0}}{RT}} \right] \quad [42]$$

or at the condition $e^{F(\eta_t - \eta_{t=0})/RT} >> 1$

$$\eta_t - \eta_{t=0} = \frac{RT}{F} \ln t + \frac{RT}{F} \ln \frac{i_o [A^+] e^{\frac{F\eta_{t=0}}{RT}}}{FZ\theta_{A,o}^2 K_A} \quad [43]$$

Hence, for systems of case (i), $\frac{\partial(\eta_t - \eta_{t=0})}{\partial \ln t} = \frac{RT}{F}$.

Since $\frac{K_A}{[A^+]} = \frac{1 - \theta_{A,o}}{\theta_{A,o}}$, if i_o is known from steady-state determinations, $\theta_{A,o}$ can be approximately obtained from the $(\eta_t - \eta_{t=0}) \sim \ln t$ relation for $t = 1$. Past and Iofa (4) treated the same case but only valid at special conditions.

Case (ii): Equation [34] becomes

$$\frac{d\eta_t}{dt} = \frac{i_o RT}{F^2 Z} \left[e^{-\frac{\beta F \eta_t}{RT}} - e^{\frac{(1-\beta) F \eta_t}{RT}} \right] \left[1 + \frac{K_A}{[A^+]} e^{\frac{F\eta_t}{RT}} \right] \quad [44]$$

At cathodic polarizations such that the reverse reaction of [31] is negligible, and $\frac{K_A}{[A^+]} e^{\frac{F\eta_t}{RT}} << 1$ (i.e., $\theta_A \to 1$), Eq. [44] becomes

$$\frac{d\eta_t}{dt} = \frac{i_o RT}{F^2 Z} e^{-\frac{\beta F \eta_t}{RT}} \quad [45]$$

Integration gives

$$t = \frac{FZ}{i_o \beta} \left[e^{\frac{\beta F \eta_t}{RT}} - e^{\frac{\beta F \eta_{t=0}}{RT}} \right] \quad [46]$$

or at $e^{\frac{\beta F}{RT}(\eta_t - \eta_{t=0})} >> 1$.

$$\eta_t - \eta_{t=0} = \frac{RT}{\beta F} \ln t + \frac{RT}{\beta F} \ln \frac{i_o \beta}{FZ} e^{-\frac{\beta F \eta_{t=0}}{RT}} \quad [47]$$

[2] $K_A = K_{A,o} e^{-\frac{V_H F}{RT}}$, but it is assumed here that the ion, A^+, desorbed due to the shift of potential, diffuses to the bulk of the solution sufficiently rapidly so that the concentration of A^+ at the Helmholtz double layer, and hence V_H, does not change with time.

Equation [47] is applicable only under the limited potential range permitted by the assumption leading to Eq. [45] (exponential dependence of number of nonpoisoned sites on time after switching off). A linear dependence of $(\eta_t - \eta_{t=0})$ against ln t (slope $RT/\beta\mathbf{F}$) would be succeeded by a further line of the same slope displaced along the axis.

Case (iii): When there is no parallel adsorption, putting $i = 0$ in Eq. [39], integration gives

$$t = \frac{RT\,C_{D.L.}}{2\mathbf{F}i_o\beta} \ln \frac{(1+Y)(1-Y_{t=0})}{(1-Y)(1+Y_{t=0})} \qquad [48]$$

where $Y = e^{\frac{\mathbf{F}\eta_t}{RT}}$. Comparison of Eq. [47] and [48] is given in Fig. 5; the poisoned electrode, its capacity much greater than that of the unpoisoned one, decays at a much slower rate.

At the beginning of decay at high cathodic polarization, $Y << 1$ and hence Eq. [48] reduces to

$$t = \frac{RTC_{D.L.}}{\mathbf{F}i_o\beta} Y_{t=0}\left(\frac{Y}{Y_{t=0}} - 1\right) \qquad [49]$$

and for the condition $Y >> Y_{t=0}$, Eq. [49] becomes

$$\eta_t - \eta_{t=0} = \frac{RT}{\beta\mathbf{F}} \ln t - \frac{RT}{\beta\mathbf{F}} \ln \frac{RTC_{D.L.}}{\mathbf{F}i_o\beta} Y_{t=0} \qquad [50]$$

which is that derived by Bockris and Potter (5).

Case (iv): Let us consider the following electrode reaction

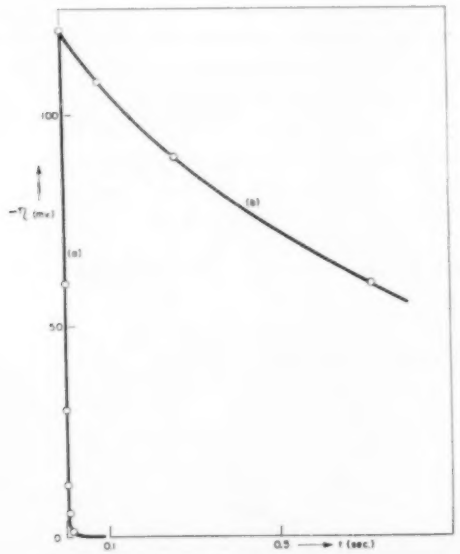

Fig. 5. Comparison of calculated decay curves, (a) no adsorption, according to Eq. [48]; (b) adsorption of $A^+ + e \rightleftharpoons A(Ads.)$ occurs on the electrode, according to Eq. [47]. $\eta_{t=0}$ and i_o were taken as 120 mv and 10^{-4} amp/cm^2.

$$A^+ + e \rightleftarrows A(Ads) \qquad [4]$$

$$A^+ + A(Ads) + e \rightarrow X \qquad [51]$$

The kinetic expression for i_g is

$$i_g = i_o\left[-\frac{\theta_A}{\theta_{A,o}} e^{-\frac{\beta\mathbf{F}\eta_t}{RT}} + \frac{1-\theta_A}{1-\theta_{A,o}} e^{\frac{(1-\beta)\mathbf{F}\eta_t}{RT}}\right] \qquad [52]$$

From Eq. [19] and [52], neglecting $C_{D.L.}$, one finds

$$\frac{d\eta_t}{dt} = \frac{\left[-i + i_o\left[\frac{\theta_A}{\theta_{A,o}} e^{-\frac{\beta\mathbf{F}\eta_t}{RT}} - \frac{(1-\theta_A)}{(1-\theta_{A,o})} e^{\frac{(1-\beta)\mathbf{F}\eta_t}{RT}}\right]\right]\left[1 + \frac{K_A}{[A^+]} e^{\frac{\mathbf{F}\eta_t}{RT}}\right]^a}{\frac{\mathbf{F}^a Z}{RT}\frac{K_A}{[A^+]} e^{\frac{\mathbf{F}\eta_t}{RT}}} \qquad [53]$$

For decay, $i = 0$ and $\frac{\theta_A}{\theta_{A,o}} e^{-\frac{\beta\mathbf{F}\eta_t}{RT}} >> \frac{1-\theta_A}{1-\theta_{A,o}} e^{\frac{(1-\beta)\mathbf{F}\eta_t}{RT}}$ (*i.e.*, the deposition reaction is much greater than the dissolution reaction in the region $-\eta > RT/\mathbf{F}$). Then, with Eq. [6], one obtains

$$\frac{d\eta_t}{dt} = \frac{\frac{i_o}{\theta_{A,o}}\left[1 + \frac{K_A}{[A^+]} e^{\frac{\mathbf{F}\eta_t}{RT}}\right] e^{-\frac{\beta\mathbf{F}\eta_t}{RT}}}{\frac{\mathbf{F}^a Z}{RT}\frac{K_A}{[A^+]} e^{\frac{\mathbf{F}\eta_t}{RT}}} \qquad [54]$$

Before integration of Eq. [54], the case where the cathodic polarization is so high that the coverage is nearly unity may be considered, if $(C_{Ads})_\eta$ is smaller than $C_{D.L.}$. At this condition, neglecting C_{Ads} compared with $C_{D.L.}$, one obtains

$$\frac{d\eta_t}{dt} = \frac{i_o}{C_{D.L.}\,\theta_{A,o}} e^{-\frac{\beta\mathbf{F}\eta_t}{RT}} \qquad [55]$$

Thus, integration of Eq. [55] gives a slope of $RT/\beta\mathbf{F}$ when $(\eta_t - \eta_{t=0})$ is plotted against ln t.

Second, consider the case where $(C_{Ads})_\eta >> C_{D.L.}$, but proportional to exp $(\mathbf{F}\eta_t/RT)$; *i.e.*, $\frac{K_A}{[A^+]} e^{\frac{\mathbf{F}\eta_t}{RT}} << 1$. This case corresponds to the electrochemical mechanism of hydrogen evolution reaction in which the coverage of the electrode with H(Ads) in the steady state is high and the Tafel slope is $RT/\beta\mathbf{F}$. Equation [54] becomes

$$\frac{d\eta_t}{dt} = \frac{RT\,i_o\,[A^+]}{\mathbf{F}^a Z\,\theta_{A,o}\,K_A} e^{-\frac{(1+\beta)\mathbf{F}\eta_t}{RT}} \qquad [56]$$

Integration of Eq. [56] gives

$$t = \frac{\mathbf{F}Z\,\theta_{A,o}\,K_A}{(1+\beta)\,i_o\,[A^+]}\left[e^{\frac{(1+\beta)\mathbf{F}\eta_t}{RT}} - e^{\frac{(1+\beta)\mathbf{F}\eta_{t=0}}{RT}}\right] \qquad [57]$$

When $\exp\ [(1+\beta)\mathbf{F}(\eta_t - \eta_{t=0})/RT] >> 1$, rearrangement gives

$$\eta_t - \eta_{t=0} = \frac{RT}{(1+\beta)\mathbf{F}} \ln t + \frac{RT}{(1+\beta)\mathbf{F}} \ln \frac{(1+\beta)\, i_o\, [A^+]\, e^{-\frac{(1+\beta)\mathbf{F}\eta_{t=0}}{RT}}}{\mathbf{F}Z\,\theta_{A,o}\,K_A} \quad [58]$$

In this case, the value of slope is $\dfrac{RT}{(1+\beta)\mathbf{F}}$.

As a third case, consider the condition that $\dfrac{K_A}{[A^+]} e^{\frac{\beta\mathbf{F}\eta_t}{RT}} >> 1$. This case corresponds to the electrochemical mechanism of hydrogen evolution reaction in which the coverage of the electrode with H(Ads) in steady state is small so that the coverage is proportional to $\exp(-\mathbf{F}\eta_t/RT)$. Equation [54] becomes

$$\frac{d\eta_t}{dt} = \frac{RT\, i_o}{\mathbf{F}^2 Z\,\theta_{A,o}} e^{-\frac{\beta\mathbf{F}\eta_t}{RT}} \quad [59]$$

Integration gives

$$t = \frac{\mathbf{F}Z\,\theta_{A,o}}{\beta i_o} \left[e^{\frac{\beta\mathbf{F}\eta_t}{RT}} - e^{\frac{\beta\mathbf{F}\eta_{t=0}}{RT}} \right] \quad [60]$$

and when $e^{\frac{\beta\mathbf{F}}{RT}(\eta_t - \eta_{t=0})} >> 1$

$$\eta_t - \eta_{t=0} = \frac{RT}{\beta\mathbf{F}} \ln t + \frac{RT}{\beta\mathbf{F}} \ln \frac{\beta i_o}{\mathbf{F}Z\,\theta_{A,o}} e^{-\frac{\beta\mathbf{F}\eta_{t=0}}{RT}} \quad [61]$$

In this case, value of slope is $RT/\beta\mathbf{F}$.

As a fourth case, if the coverage is very small and $C_{Ads.} << C_{D.L.}$, then one obtains from Eq. [17] and [52]

$$\frac{d\eta_t}{dt} = \frac{i_o[A^+]}{C_{D.L.}\,\theta_{A,o}\,K_A} e^{\frac{(1+\beta)\mathbf{F}\eta_t}{RT}} \quad [62]$$

Integration and rearrangement under the condition $e^{\frac{(1+\beta)\mathbf{F}}{RT}(\eta_t - \eta_{t=0})} >> 1$, gives

$$\eta_t - \eta_{t=0} = \frac{RT}{(1+\beta)\mathbf{F}} \ln t + \frac{RT}{(1+\beta)\mathbf{F}} \ln \frac{i_o\,[A^+]\, e^{\frac{(1+\beta)\mathbf{F}\eta_{t=0}}{RT}}}{C_{D.L.}\,\theta_{A,o}\,K_A} \quad [63]$$

These considerations suggest that the decay curve, with the initial condition of high cathodic polarization, such that the coverage is nearly unity, the slope of $(\eta_t - \eta_{t=0})$ against $\ln t$ can change from $RT/\beta\mathbf{F}$ to $RT/(1+\beta)\mathbf{F}$, then to $RT/\beta\mathbf{F}$ and again $RT/(1+\beta)\mathbf{F}$. Such behavior during decay would provide a criterion for the presence of the electrochemical desorption mechanism, under conditions such that the Tafel slopes are the same as those corresponding to a rate-determining proton transfer mechanism.

Anodic transients.—The above discussions for cathodic transients can be applied for anodic transients in the same way (i is then positive).

Iron Electrode Transients

A summary of the experimental facts recorded by Bockris, Drazic, and Despic, is as follows (1). (*A*) The apparent differential double layer capacity is 230 μF/cm^2 near the corrosion potential. (*B*) The initial rate of decay of potential after cathodic polarization is 1/100th-1/1000th of the value calculated from the measured parameters for the dissolution of Fe. (*C*) In galvanostatic anodic charging, a maximum occurs on the $\eta_t - t$ line at low times. (*D*) A plot of overpotential corresponding to this maximum against the logarithm of current density gives the Tafel slope of $RT/\mathbf{F}$ (Tafel slope of steady state: $2RT/3\mathbf{F}$). (*E*) In anodic decay, a minimum is observed on the $\eta_t - t$ relation.

The mechanism suggested by Bockris, Drazic, and Despic is [1], [2], and [3]. Here, the equivalent mechanisms

$$Fe^{++} + H_2O \rightleftarrows (FeOH)^+ + H^+ \quad [64]$$

$$(FeOH)^+ + e \rightarrow (FeOH) \quad [65]$$

$$(FeOH) + H^+ + e \rightleftarrows Fe + H_2O \quad [66]$$

will be assumed.

Apparent Differential Double Layer Capacity

Two kinds of adsorbed species H(Ads) and FeOH(Ads) exist on the electrode surface. If it is assumed that rate-determining electrochemical desorption is that which applies to hydrogen evolution on Fe under conditions of the experimental work, H(Ads) is in equilibrium with H^+. FeOH(Ads) is in equilibrium with OH^-, Fe, and e_o^-.

The coverage of H(Ads), θ_H, increases with increase of cathodic polarization (Eq. [6]); while θ_{FeOH} decreases according to

$$\theta_{FeOH} = \frac{1}{1 + \frac{\overleftarrow{k}}{\vec{k}} [H^+]\, e^{-\frac{\mathbf{F}\eta}{RT}}} \quad [67]$$

where $\vec{k}$ and $\overleftarrow{k}$ are rate constants of the reaction of [66], respectively. For $\frac{\overleftarrow{k}}{\vec{k}} [H^+]\, e^{-\frac{\mathbf{F}\eta}{RT}} >> 1$

$$\theta_{FeOH} = \frac{\vec{k}}{\overleftarrow{k}\,[H^+]} e^{\frac{\mathbf{F}\eta}{RT}} \quad [68]$$

The steady-state kinetics is consistent with [68]. It will be assumed (electrochemical mechanism indicates high concentration of H(Ads) in region of Tafel slope = $2RT/\mathbf{F}$) that $\theta_{H,o} > \theta_{FeOH,o}$.

Applying Eq. [8] and [11] to the transient near to the corrosion potential, it is found that the apparent double layer capacitance of 230 μF/cm^2 is equivalent to $\theta_{H,o} = 0.03$. A similar value may be calculated from cathodic decay.

Cathodic Decay

Analysis of the cathodic decay is complicated for the iron electrode by the fact that in the steady-state deposition of Fe^{2+} the concentration of protons at the Helmholtz double layer, $[H^+]_{D.L.}$, differs from the concentration in the bulk $[H^+]_B$, because (except at very low pH) the limiting current density for the h.e.r. is exceeded (1).

Thus, according to Bockris, Drazic, and Despic (1), $[H^+]_{D.L.}$ can be expressed as

$$[H^+]_{D.L.} = [H^+]_B\, e^{-\frac{\beta F \eta_{C.H.}}{RT}} \qquad [69]$$

$$= [H^+]_B\, e^{-\frac{\beta F}{RT}(V - V_{H,\eta_{C=0}})} \qquad [70]$$

$$\frac{d\eta_t}{dt} = \frac{(i_o)_{Fe}\, e^{-\frac{F\eta_t}{RT}}\left[1 + \frac{Q_H}{[H^+]_B} e^{\frac{\beta F}{RT}(V_{H,\eta_{C=0}} - V_{Fe,rev.})} e^{\frac{\beta F \eta_t}{RT}}\right]^2}{\frac{\beta F^2 Z}{RT}\frac{Q_H}{[H^+]_B} e^{\frac{\beta F}{RT}(V_{H,\eta_{C=0}} - V_{Fe,rev.})} e^{\frac{\beta F \eta_t}{RT}}} \qquad [77]$$

$$= [H^+]_B\, e^{-\frac{\beta F}{RT}[(V - V_{Fe,rev.}) - (V_{H,\eta_{C=0}} - V_{Fe,rev.})]} \qquad [71]$$

$$= [H^+]_B\, e^{-\frac{\beta F \eta}{RT}} e^{\frac{\beta F}{RT}(V_{H,\eta_{C=0}} - V_{Fe,rev.})} \qquad [72]$$

where $V_{H\eta_{C=0}}$ is the potential which the electrode would have if only the hydrogen evolution occurred on it at this given current density and in the absence of concentration overpotential.

Then, the expression for θ_H using Eq. [6] and [72], is

$$\theta_H = \frac{1}{1 + \frac{Q_H}{[H^+]_B} e^{\frac{\beta F}{RT}(V_{H,\eta_{C=0}} - V_{Fe,rev.})} e^{\frac{\beta F \eta}{RT}}} \qquad [73]$$

where

$$Q_H = \frac{\overleftarrow{k}_{H,o}}{\overrightarrow{k}_{H,o}} e^{\frac{FV}{RT}} F_{e,rev.}$$

Hence, for $\eta = 0$

$$\frac{Q_H}{[H^+]_B} = \frac{1 - \theta_{H,o}}{\theta_{H,o}} \qquad [74]$$

By differentiating Eq. [72], an expression for the pseudocapacitance due to the equilibrium of protons and H(Ads) in the mechanism concerned, can be obtained.

$$(C_{Ads})_\eta = \frac{\beta F^2 Z\, Q_H\, e^{\frac{\beta F}{RT}(V_{H,\eta_{C=0}} - V_{Fe,rev.})}}{RT\,[H^+]_B} \frac{e^{\frac{\beta F \eta}{RT}}}{\left[1 + \frac{Q_H}{[H^+]_B} e^{\frac{\beta F}{RT}(V_{H,\eta_{C=0}} - V_{Fe,rev.})} e^{\frac{\beta F \eta}{RT}}\right]^2} \qquad [75]$$

The rate of the cathodic iron electrode reaction, i_{Fe}, is found experimentally (1) to be

$$i_{Fe} = -(i_o)_{Fe}\, e^{-\frac{F\eta}{RT}} \qquad [76]$$

where $(i_o)_{Fe}$ is a constant.

Hence using Eq. [76] and [75], Eq. [19] for the decay at the region of high cathodic polarization, where iron dissolution is negligible, becomes

For the region in which: $\frac{Q_H}{[H^+]_B} e^{\frac{\beta F}{RT}(V_{H,\eta_{C=0}} - V_{Fe,rev.})} e^{\frac{\beta F \eta_t}{RT}} << 1$, Eq. [77] becomes

$$\frac{d\eta_t}{dt} = \frac{RT(i_o)_{Fe}[H^+]_B}{\beta F^2 Z\, Q_H} e^{-\frac{\beta F}{RT}(V_{H,\eta_{C=0}} - V_{Fe,rev.})} e^{-\frac{(1+\beta)F\eta_t}{RT}} \qquad [78]$$

Integration of Eq. [74] gives

$$t = \frac{\beta F Z\, Q_H}{(1+\beta)(i_o)_{Fe}[H^+]_B} e^{\frac{\beta F}{RT}(V_{H,\eta_{C=0}} - V_{Fe,rev.})} \left[e^{\frac{(1+\beta)F\eta_t}{RT}} - e^{\frac{(1+\beta)F\eta_{t=0}}{RT}}\right] \qquad [79]$$

For the condition $e^{\frac{(1+\beta)F}{RT}(\eta_t - \eta_{t=0})} >> 1$, one obtains

$$\eta_t - \eta_{t=0} = \frac{RT}{(1+\beta)F} \ln t - \frac{RT}{(1+\beta)F} \ln \frac{\beta Q_H F Z}{(1+\beta)[H^+]_B (i_o)_{Fe}} e^{\frac{\beta F}{RT}(V_{H,\eta_{C=0}} - V_{Fe,rev.})} e^{-\frac{(1+\beta)F\eta_{t=0}}{RT}} \qquad [80]$$

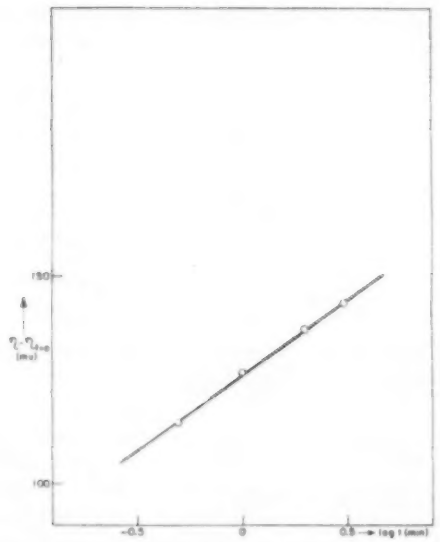

Fig. 6. Linear relationship between log t and η-$\eta_{t=0}$. Decay curve of Fig. 1 was used, slope is 38 mv.

Linearity between $(\eta_t - \eta_{t=0})$ and ln t was examined using observed decay curves (Fig. 6). The experimental slope is 38 mv, in good agreement with Eq. [80]. The value of $\theta_{H,0}$ from the value of $(\eta_t - \eta_{t=0})$ at $t = 1$ and the known value of $(i_o)_{Fe}$ and $(V_{H,eq=0} - V_{Fe,rev.})$ was estimated as 0.3. Then, using Eq. [6] and [8] $\theta_{H,eqr.}$ can be estimated. It is 0.06 in agreement with the value calculated from the apparent differential capacity. This is the first time a value for the coverage of a corroding metal with H(Ads) has been reported.

Anodic Charging

$\theta_{H,eqr.}$ is of the order of 10^{-3}, and decreases with anodic polarization (Eq. [6]). Hence the effect of θ_H on the anodic charging curve can be neglected, whereas θ_{FeOH} increases exponentially with anodic charging (Eq. [61]). Thus, only the effect of θ_{FeOH} will be considered in the following discussion of the anodic transients.

In galvanostatic charging, a large fraction of i may be used to increase θ_{FeOH} at the beginning of the transient (FeOH is *in equilibrium*). This fraction decreases with time (Eq. [15]) and that due to the electrode reaction becomes predominant.

At typical experimental conditions, the concentration of OH^- in the bulk is small. Consider the maximum rate of diffusion of OH^- ions to the electrode surface during anodic charging.

$$(i_{Diff})_{max.} = \mathbf{F}\sqrt{\frac{D_{OH^-}}{\pi t}}\,[OH^-]_b$$

Thus, *e.g.*, at $t = 0.5$ sec, $[OH^-]_b = 10^{-13}$ moles cc^{-1} (pH = 4), $(i_{Diff})_{max.} = 10^{-9}$ amp cm^{-2}. OH^- ions hence do not easily reach the electrode surface sufficiently rapidly to take part in the mechanism. This is the basis of use of the alternative reaction sequence [64]-[66].

Reaction [66] shows that the increase of θ_{FeOH} produces protons which pile up at the Helmholtz double layer and diffuse into the solution. Reaction [66] is in equilibrium, *i.e.*,

$$\Delta\mu^{FeOH} + \Delta\mu^{H^+_{D.L.}} + \Delta\mu^e = 0 \qquad [81]$$

where $\Delta\mu$ is the change of chemical potential during charging from the corrosion potential to a given anodic potential. From [81],

$$\frac{\theta_{FeOH}}{1-\theta_{FeOH}}(H^+)_{D.L.} = \frac{\theta_{FeOH,0}}{1-\theta_{FeOH,0}}(H^+)_{D.L.0}\,e^{\frac{\mathbf{F}\eta_t}{RT}} \qquad [82]$$

where $(H^+)_{D.L.}$ is the concentration of protons in the Helmholtz double layer (mole/cm^3). For the condition $1 >> \theta_{FeOH,0}$

$$\theta_{FeOH}\,(H^+)_{D.L.} = \theta_{FeOH,0}\,(H^+)_{D.L.0}\,e^{\frac{\mathbf{F}\eta_t}{RT}} \qquad [83]$$

Let the proton diffusion be assumed to commence at the maximum of the anodic transient. For pH > 2 the traction of the Helmholtz double layer occupied by H^+ is $< 10^{-4}$, *i.e.*, negligible. Hence, during the anodic transients, according to reaction [66], the decrease of (FeOH) is nearly equal to the increase of protons at the Helmholtz double layer, *i.e.*, $C(H^+)_{D.L.} \simeq Z\,\theta_{FeOH}$.

$$Z\theta_{FeOH} = (H^+)_{D.L.} = [Z\theta_{FeOH,0}\;(H^+)_{D.L.0}]^{1/2}\,e^{\frac{\mathbf{F}\eta_t}{2RT}} \qquad [84]$$

At $\eta = \eta_{max.}$, if $i \simeq i_{Fe}$, *i.e.*, if double layer *charging* is negligible

$$i \simeq i_{Fe} = (i_o)_{Fe}\frac{\theta_{FeOH,\eta_{max.}}}{\theta_{FeOH,0}}\,e^{\frac{\beta\mathbf{F}\eta_{max.}}{RT}} =$$

$$(i_o)_{Fe}\left(\frac{(H^+)_{D.L.0}}{Z\theta_{FeOH,0}}\right)^{1/2}e^{\frac{\mathbf{F}\eta_{max.}}{RT}} \qquad [85]$$

Plotting $\eta_{max.}$ against ln i, one obtains the slope $RT/\mathbf{F}$, as observed experimentally [D].

After the maximum, the concentration of protons in the Helmholtz double layer decreases by diffusion of protons to the bulk.

$$-\frac{d[H^+]}{dt} = D_{H^+}\frac{d^2[H^+]}{dx^2} \qquad [86]$$

where $[H^+]$ is the concentration of protons at a distance, x, from the Helmholtz double layer to the solution. The initial and boundary conditions are

$$[H^+] = [H^+]_b \qquad 0 < x, t = 0$$

$$[H^+] = [H^+]_b \qquad x = \infty, t > 0$$

Solution of Eq. [86] is then (6)

$$[H^+] = [H^+]_b + \frac{\Gamma_{H^+}}{(\pi D_{H^+}t)^{1/2}}\,e^{-\frac{x^2}{4D_{H^+}t}} \qquad [87]$$

where Γ_{H^+} is the surface excess of protons in the double layer at $t = 0$.

At $x = 0$ and $t > 0$,

$$[H^+]_{x=0} = [H^+]_b + \frac{\Gamma_{H^+}}{(\pi D_{H^+} t)^{1/2}} \quad [88]$$

From Eq. [68] and [88]

$$\theta_{FeOH} = \frac{\vec{k}}{\overleftarrow{k}[H^+]_b}\left[1 + \frac{\Gamma_{H^+}}{[H^+]_b(\pi D_{H^+} t)^{1/2}}\right]^{-1} e^{\frac{F\eta_t}{RT}} \quad [89]$$

where $\dfrac{\vec{k}}{\overleftarrow{k}[H^+]_b} = \theta_{FeOH,0}$

Using Eq. [89] in [85]

$$i = (i_o)_{Fe}\left[1 + \frac{\Gamma_{H^+}}{[H^+]_b(\pi D_{H^+} t)^{1/2}}\right]^{-1} e^{\frac{(1+\beta)F\eta_t}{RT}} \quad [90]$$

At $t \to \infty$, Eq. [90] becomes

$$i = (i_o)_{Fe}\, e^{\frac{(1+\beta)F\eta_\infty}{RT}} \quad [91]$$

in agreement with experiment.

From Eq. [90], η_t can be expressed as a function of time, t, as:

$$\eta = \frac{RT}{(1+\beta)F} \ln \frac{i}{(i_o)_{Fe}}\left[1 + \frac{\Gamma_{H^+}}{[H^+]_b(\pi D_{H^+} t)^{1/2}}\right] \quad [92]$$

A maximum limit to the value of Γ_{H^+} which may be assumed in a comparison of [92] with experiment can be arrived at so: The Tafel line in steady state is consistent with $\theta_{FeOH} << 1$, *i.e.*, the maximum value of θ_{FeOH} $Z = 10^{-10}$ mole/cm^2. But, under the conditions $\theta_{FeOH} << 1$, $\theta_{FeOH} = \theta_{FeOH,0}\, e^{F\eta/RT}$. The maximum c.d. for the steady-state results is 10^{-6} amp cm^{-2}. Hence, at 10^{-4} amp cm^{-2}, θ_{FeOH} $Z < 5 \times 10^{-11}$.

Giving numerical values with $D_{H^+} = 10^{-4}$ cm^2/sec and $\Gamma_{H^+} = 5 \times 10^{-11}$ mole/cm^2, η_t was calculated. Results are shown in Fig. 2, curve (a).

Anodic Decay

After switching off the anodic current, the concentration of FeOH on the electrode surface decreases with decreasingly positive overpotential. When FeOH decomposes, it produces OH^- or consumes H^+. On the other hand, the concentration of the adsorbed hydrogen atoms increases with decrease of potential.

It will be assumed that there is negligible diffusion of protons from the bulk of the solution to the interface up to the time corresponding to the minimum in the potential-time curve in the anodic decay minimum point (Fig. 2), *i.e.*, H^+ ions are used up in the double layer (Eq. [66]). And then after the minimum in the potential-time curve, diffusion commences.

The diffusion could be that of H^+ ions from the bulk to the double layer. However, the order of magnitude of the current density due to this diffusion is, for a process occurring over a time interval of about 0.1 sec (Fig. 2): $F\sqrt{\dfrac{D_{H^+}}{\pi}}\dfrac{[H^+]_b}{t^{1/2}} \cong 10^{-4}$ amp/cm^2. This current density is at least two orders of magnitude less than the current density on decay (which is of the order of $(C_{ads})_\eta \dfrac{d\eta}{dt} > 10^{-4}$ amp/cm^2). It is hence unreasonable to involve diffusion of protons in the mechanism of [66]; and more reasonable to suppose that, during decay, [3] occurs. This implies that excess OH^- ions are built up in the double layer and the slow process for the relaxation of the potential then becomes their diffusion into the bulk in a way analogous to the diffusion away of the built up protons on anodic charging. By analogy to this calculation (*cf.* Eq. [86] and [87]):

$$[OH^-]_{x=0} = [OH^-]_b + \frac{\Gamma_{OH^-}}{(\pi D_{OH^-} t)^{1/2}} \quad [93]$$

where Γ_{OH^-} in the surface excess of OH^- at the point of minimum potential. A maximum value of Γ_{OH^-} can be estimated to be about 10^{-11} moles·cm^{-2}, but this value would put the potential minimum for the conditions of Fig. 2 at a value much more negative than that observed. A value of 10^{-14} moles·cm^{-2} is consistent with the observed minimum and the theoretical line in Fig. 2, calculated from

$$(V_{cor})_t = (V_{cor})_{t=\infty} - \frac{RT}{F} \ln \left[1 + \frac{\Gamma_{OH^-}}{[OH^-]_b(\pi D_{OH^-} t)^{1/2}}\right] \quad [94]$$

fits that of experiment well.

Acknowledgment

The authors wish to thank the American Electroplater's Society for financial support of the present work, and the Supervising Committee of Project 16 of the Society for Discussion.

Manuscript received Feb. 2, 1961; revised manuscript received March 3, 1961.

Any discussion of this paper will appear in a Discussion Section to be published in the June 1962 JOURNAL.

REFERENCES

1. J. O'M. Bockris, D. Drazic, and A. R. Despic, *Acta Electrochim.*, In press.
2. M. Enyo, Thesis, University of Pennsylvania (1959); J. O'M. Bockris and M. Enyo, To be published.
3. W. A. Roiter, W. A. Juza, and E. S. Polujans, *Acta Physiochim. U.R.S.S.*, **10**, 389, 845 (1939).
4. V. E. Past and Z. A. Iofa, *J. Phys. Chem., U.S.S.R.*, **33**, 1230 (1959).
5. J. O'M. Bockris and E. C. Potter, *This Journal*, **99**, 169 (1952).
6. J. Crank, "The Mathematics of Diffusion," Oxford University Press (1957).

Characteristic Functions and Parameters in the Theory of Hydrogen Overpotential

III. General Considerations

Gilbert W. Castellan

The Catholic University of America, Washington, D. C.

ABSTRACT

It is shown that the characteristic functions suggested in an earlier paper on the basis of the Langmuir isotherm are useful for any isotherm. The concept of a characteristic function is generalized somewhat in a function $1/\Sigma$. The properties of $1/\Sigma$ are discussed. The effect of the logarithmic isotherm on the position of the curves is described. It is shown that ρ measures the variation of adsorption affinity with η near $\eta = 0$.

In two papers (1, 2), designated I and II, it was shown that if the adsorption of hydrogen on a metal follows a Langmuir isotherm, there are two characteristic parameters, i_o and ρ, and two characteristic functions, g_1 and g_2, which have significance in the kinetic equations for hydrogen evolution. The definitions given in I are:

$$i_o = (di/d\eta)_{\eta=0} \qquad [1]$$

$$\rho = \{d \ \ln[\theta/(1-\theta)]/d\,\eta\}_{\eta=0} \qquad [2]$$

$$g_1 = \{\exp[(\alpha - 1/2)\eta] \sinh \eta/2\}/i \qquad [3]$$

$$g_2 = [\tanh(\eta/2)/i]^{1/2} \qquad [4]$$

In this paper the definition of ρ is generalized to eliminate the restriction to the Langmuir isotherm. It will be shown that the functions g_1 and g_2 are natural functions for expressing the $i - \eta$ relationship. The notation used is the same as in I.

Rate Equations

Only three elementary reactions are considered.

		Rate
Reaction 1:	$H_{ad} \rightleftarrows H^+ + e^- + V$	i_1
Reaction 2:	$H_{2(g)} + V \rightleftarrows H_{ad} + H^+ + e^-$	i_2
Reaction 3:	$H_{2(g)} + 2V \rightleftarrows 2H_{ad}$	i_3

Here V symbolizes a vacant site on the surface. The rate equations are

$$i_1 = i_{10}\, e^{\alpha\eta}\,[(a/a_o) - (a_v/a_{vo})\, e^{-\eta}] \qquad [5]$$

$$i_2 = i_{20}\, e^{\alpha\eta}\,[(a_v/a_{vo}) - (a/a_o)\, e^{-\eta}] \qquad [6]$$

$$i_3 = i_{30}\,[(a_v/a_{vo})^2 - (a/a_o)^2] \qquad [7]$$

In these equations concentration polarization in H^+ and $H_{2(g)}$ has been ignored, and α has been given the same value for reactions 1 and 2. However, a and a_v have been used for the activities of the adsorbed H atoms and the vacancies on the surface. Subscripts zero refer to the value of the quantity at equilibrium.

The parameter i_o, and the functions g_1 and g_2 are defined as before, but ρ is now defined generally:

$$\rho = [d \ \ln (a/a_v)/d\eta]_{\eta=0} \qquad [8]$$

Differentiating Eq. [5], [6], and [7] and reducing to the limit $\eta = 0$ yields

$$(di_1/d\eta)_{\eta=0} = i_{10}\,(1 + \rho) \qquad [9]$$

$$(di_2/d\eta)_{\eta=0} = i_{20}\,(1 - \rho) \qquad [10]$$

$$(di_3/d\eta)_{\eta=0} = -2i_{30}\rho \qquad [11]$$

Equations [9], [10], and [11] are formally the same as the corresponding ones restricted to the Langmuir isotherm, consequently much of the formalism in I is still applicable. For the various two-step mechanisms discussed in I, Eq. [9], [10], and [11] yield values of i_o and ρ in terms of the individual exchange currents which are exactly the same as for the Langmuir case.

Defining:

$$\Sigma = (a/a_o) + (a_v/a_{vo}) \qquad [12]$$

$$\Delta = (a/a_o) - (a_v/a_{vo}) \qquad [13]$$

the rate equations become

$$i_1 = i_{10}\, e^{(\alpha - 1/2)\eta}\,[\Sigma \sinh \eta/2 + \Delta \cosh \eta/2] \qquad [5a]$$

$$i_2 = i_{20}\, e^{(\alpha - 1/2)\eta}\,[\Sigma \sinh \eta/2 - \Delta \cosh \eta/2] \qquad [6a]$$

$$i_3 = -\,i_{30}\Sigma\Delta \qquad [7a]$$

The Electrochemical Mechanism

The electrochemical mechanism, reaction 1 with reaction 2, has the steady-state conditions: $i = i_1 + i_2$ and $i_1 = i_2$. Using [5a] and [6a] these conditions after some rearrangement become

$$\Delta = \rho\,\Sigma t \qquad [14]$$

$$g_1 = (i_o\Sigma)^{-1} \qquad [15]$$

in which $t = \tanh \eta/2$. The function g_1 is proportional to $1/\Sigma$. The two steady-state conditions contain both Σ and Δ; one could equally well have chosen to eliminate Σ and write an analogue of Eq. [15] in terms of Δ. The use of Σ rather than Δ is defensible on the grounds that for the Langmuir isotherm case, $1/\Sigma$ is a simple function of t.

The Combination Mechanism

The combination mechanism, reaction 1 with reaction 3, has the steady-state conditions: $i = i_1$ and $i_1 = i_3$. Using [5a] and [7a] these conditions become

$$\Delta[(1+\rho)\Sigma - 2\rho\, e^{(a-1/2)\eta}\cosh\eta/2] = 2\rho\Sigma\, e^{(a-1/2)\eta}\sinh\eta/2 \quad [16]$$

$$i_0 = [(1+\rho)/g_1\Sigma] - [2\rho/(g_2\Sigma)^2] \quad [17]$$

Two cases of Eq. [17] arise:

Case I: $\rho = 0$, slow discharge.

Equation [17] becomes

$$g_1 = (i_0\Sigma)^{-1} \quad [17a]$$

Also it may be shown that $\Sigma = 2$.

Case II: $\rho = -1$, slow combination.

Equation [17] becomes

$$g_2 = (2/i_0)^{1/2}\,\Sigma^{-1} \quad [17b]$$

Thus, in each of the important cases, the appropriate characteristic function is proportional to $1/\Sigma$; therefore, $1/\Sigma$ is effectively the characteristic function in all cases.

The Properties of $1/\Sigma$

From the form of $\Sigma = (a/a_0) + (a_r/a_{r_0})$, it is clear that Σ is always positive and never zero. Furthermore, since an increase in a is accompanied by a decrease in a_r, Σ and therefore its reciprocal is bounded in its variation. Consequently, $1/\Sigma$ can be developed in positive powers of t which is itself bounded in its variation. Formally we write a Taylor series for $1/\Sigma$ about the equilibrium value.

$$1/\Sigma = (1/\Sigma)_0 + (1/\Sigma)_0' t + (1/\Sigma)_0'' t^2/2 + \ldots \quad [18]$$

From the definition of Σ, $(1/\Sigma)_0 = 1/2$.

The coefficient of the second term is obtained by differentiation:

$$(1/\Sigma)_0' = (d\eta/dt)_0\,[\partial(1/\Sigma)/\partial\eta]_0 = -1/2(\partial\Sigma/\partial\eta)_0$$

$$= -\frac{1}{2}\left[\frac{1}{a_0}\left(\frac{\partial a}{\partial\eta}\right)_0 + \frac{1}{a_{r_0}}\left(\frac{\partial a_r}{\partial\eta}\right)_0\right] \quad [19]$$

It is possible to evaluate the two derivatives on the right of Eq. [19] in terms of ρ and θ_0, the fraction of the surface sites covered by H atoms at equilibrium.

Let N_0 = the number of sites on the surface. Then $n = \theta N_0$ = the number of adsorbed H atoms on the surface, $n_r = (1-\theta)N_0$ = the number of vacant sites on the surface. The Gibbs-Duhem equation, valid at $\eta = 0$, for atoms and vacancies on the surface is

$$n_0\left(\frac{\partial \ln a}{\partial n}\right)_0 + n_{r_0}\left(\frac{\partial \ln a_r}{\partial n}\right)_0 = 0$$

which becomes

$$\frac{\theta_0}{a_0}\left(\frac{\partial a}{\partial\theta}\right)_0 + \frac{1-\theta_0}{a_{r_0}}\left(\frac{\partial a_r}{\partial\theta}\right)_0 = 0 \quad [20]$$

From the definition of ρ:

$$\rho = \frac{1}{a_0}\left(\frac{\partial a}{\partial\eta}\right)_0 - \frac{1}{a_{r_0}}\left(\frac{\partial a_r}{\partial\eta}\right)_0$$

$$= \left[\frac{1}{a_0}\left(\frac{\partial a}{\partial\theta}\right)_0 - \frac{1}{a_{r_0}}\left(\frac{\partial a_r}{\partial\theta}\right)_0\right]\left(\frac{\partial\theta}{\partial\eta}\right)_0 \quad [21]$$

Using [20] in [21]

$$\frac{1}{a_0}\left(\frac{\partial a}{\partial\theta}\right)_0\left(\frac{\partial\theta}{\partial\eta}\right)_0 = \frac{1}{a_0}\left(\frac{\partial a}{\partial\eta}\right)_0 = (1-\theta_0)\rho \quad [22]$$

and

$$\frac{1}{a_{r_0}}\left(\frac{\partial a_r}{\partial\theta}\right)_0\left(\frac{\partial\theta}{\partial\eta}\right)_0 = \frac{1}{a_{r_0}}\left(\frac{\partial a_r}{\partial\eta}\right)_0 = -\theta_0\rho \quad [23]$$

Using [22] and [23] in [19]:

$$(1/\Sigma)_0' = (\theta_0 - 1/2)\rho \quad [24]$$

The expansion of $1/\Sigma$ correct to the first power of t is

$$1/\Sigma = \frac{1}{2} + (\theta_0 - 1/2)\rho t + \ldots \quad [25]$$

The result in Eq. [25] is independent of the mechanism and the form of the isotherm.

The plot of the characteristic function *vs.* t has a slope and intercept determined by the exchange current. The ratio of the initial slope to the intercept is $2(\theta_0 - 1/2)\rho$. If it is possible to decide on the value of ρ, then the value of θ_0 can be gotten from the slope-intercept ratio.

Logarithmic Isotherm

For the Langmuir isotherm, the higher derivatives of $1/\Sigma$ are zero for the limiting cases and Eq. [25] represents the complete dependence of $1/\Sigma$ on t. However, if the isotherm is the logarithmic type used by Temkin (3), then $1/\Sigma$ will not be linear in t. The activities are

$$a = \theta\, e^{x(1-\theta)^2} \quad [26]$$

$$a_r = (1-\theta)\, e^{x\theta^2} \quad [27]$$

where $x = \omega/RT$, ω being the interaction energy. The isotherm has the form

$$[\theta_0/(1-\theta_0)]\, e^{x(1-2\theta_0)} = K^{1/2}\, p_0^{1/2} \quad [28]$$

Rather than present the dependence of $1/\Sigma$ on x in laborious detail, only the general effect of x on $1/\Sigma$ will be determined. By standard methods we obtain

$$\left(\frac{\partial\, 1/\Sigma}{\partial x}\right)_\eta = \left(\frac{\partial\, 1/\Sigma}{\partial x}\right)_\theta + \left(\frac{\partial\, 1/\Sigma}{\partial\theta}\right)_x\left(\frac{\partial\theta}{\partial x}\right)_\eta \quad [29]$$

and a similar equation in $1/\Delta$. Elimination of $(\partial\theta/\partial x)_\eta$ between these two equations, and use of the definitions of Σ and Δ, yields the relation

$$\Sigma^2\left(\frac{\partial\, 1/\Sigma}{\partial x}\right)_\eta\left[\frac{\theta}{\Sigma+\Delta} + \frac{1-\theta}{\Sigma-\Delta}\right] + \Delta^2\left(\frac{\partial\, 1/\Delta}{\partial x}\right)_\eta\left[\frac{\theta}{\Sigma+\Delta} - \frac{1-\theta}{\Sigma-\Delta}\right] = (\theta-\theta_0)^2 \quad [30]$$

The steady-state relation for either mechanism, [14] or [16], can be used to eliminate Δ and $(\partial[1/\Delta]/\partial x)_\eta$ from [30] and yield a value of $[\partial(1/\Sigma)/\partial x]_\eta$.

For the electrochemical case, differentiation of [14] yields

$$\left(\frac{\partial\, 1/\Sigma}{\partial x}\right)_\eta = \rho t\left(\frac{\partial\, 1/\Delta}{\partial x}\right)_\eta$$

Using this and [14] in [30] yields ultimately

$$\left(\frac{\partial\, 1/\Sigma}{\partial x}\right)_\eta = \frac{(\theta - \theta_\circ)^2}{\Sigma} \qquad [31]$$

At any specified value of η, the value of the characteristic function increases with increase in x since the right-hand side of [31] is always positive. In particular this means that if x is positive the curve of $1/\Sigma$ *vs.* t will always lie *above* the straight line corresponding to the Langmuir isotherm, while if x is negative the curve will lie always below that line.

In the two cases of the combination mechanism, using [16] and its derivative with [30]: when $\rho = -1$, the result is the same as in [31] and the same argument about the position of the curve applies. When $\rho = 0$, $\Sigma = 2$; hence $[\partial(1/\Sigma)/\partial x]_\eta = 0$. The curve of $1/\Sigma$ *vs.* t is thus a straight line just as it is for the Langmuir isotherm. This situation prevails because combination is so rapid that the coverage remains at the equilibrium value. The potential is then determined solely by the current density; consequently, the form of the isotherm cannot affect the current-potential relation at a specified pressure. The variation of the parameters with pressure will depend on the form of the isotherm.

The Adsorption Affinity and ρ

The adsorption reaction is written

$$\frac{1}{2}\,H_2 + V \rightleftarrows H_{ad}$$

The affinity, A, is

$$A = A^\circ - RT \ln (a/a_\circ p^{1/2}) \qquad [32]$$

Keeping $p = p_\circ$, differentiation yields

$$\left(\frac{dA}{d\eta}\right)_{\eta=0} = -\rho RT \qquad [33]$$

The parameter ρ is a measure of how the variation in potential affects the affinity of the adsorption reaction near $\eta = 0$.

In the electrochemical mechanism, $\rho = 1$ (slow discharge) corresponds to a decrease in A with increase in η; this occurs because the surface is accumulating H atoms. This increase in concentration of H atoms decreases the affinity. If $\rho = -1$, increase in potential increases the affinity because the surface is being denuded of H atoms.

For the combination mechanism: $\rho = 0$ (slow discharge) the affinity is unaffected by change in potential since the coverage remains at the equilibrium value. If $\rho = -1$ (slow combination) increase in potential denudes the surface and increases the affinity.

Acknowledgment

This research was supported by the Air Force Office of Scientific Research.

Manuscript received Nov. 28, 1960; revised manuscript received March 21, 1961.

Any discussion of this paper will appear in a Discussion Section to be published in the June 1962 JOURNAL.

REFERENCES

1. G. W. Castellan, *This Journal*, **108**, 277 (1961).
2. G. W. Castellan, *ibid.*, **108**, 282 (1961).
3. M. I. Temkin, *Zhur. Fiz. Khim.*, **15**, 296 (1941).

APPENDIX

The coefficient of t^2 in the series of Eq. [18] has the values:

Electrochemical mechanism:

$$\frac{1}{2}\,(1/\Sigma)_\circ'' = 2\rho^2 x\,\theta_\circ^2\,(1-\theta_\circ)^2/[1 - 2x\,\theta_\circ\,(1-\theta_\circ)]$$

Combination mechanism:

$$\frac{1}{2}\,(1/\Sigma)_\circ'' = (1+\rho)\,[2\rho^2(\theta_\circ - \tfrac{1}{2})^2 + 2\rho(\alpha - \tfrac{1}{2})\,(\theta_\circ - \tfrac{1}{2})] + \frac{2\rho^2 x\,\theta_\circ^2\,(1-\theta_\circ)^2}{1 - 2x\,\theta_\circ(1-\theta_\circ)}$$

Reaction 2 with reaction 3:

The coefficient of t^2 has the same form as for the combination mechanism except that the factor $(1+\rho)$ in front of the bracket is replaced by $(1-\rho)$.

The Influence of Ion-Pairs on Reaction Mechanism

The Bromoacetate-Thiosulfate Reaction

G. Corsaro and M. C. Morris

Department of Chemistry, The University of Akron, Akron, Ohio

ABSTRACT

The existence and participation of associated ion-pairs in an ionic reaction mechanism are demonstrated by rate behavior of the bromoacetate-thiosulfate ionic reaction.

Whereas the salts of the reactants are presumed to provide the ion which takes part in reaction, the electrostatic influence of the cations present in solution becomes evident when solvent mixtures other than water are employed. The observed results may be best interpreted by assuming that the thiosulfate ion associated with its cation becomes a part of a critical complex structure. The size and charge of the cation, and the dielectric constant of the reaction medium, can be correlated with the observed bimolecular rate constants. The nature of the ion-pair involved conforms with a species in which the cation and anion are separated sufficiently that they retain their discrete identities. However, the ion-pair may behave as a single entity with an effective net charge which is the algebraic sum of the cation and anion charges. The latter behavior is manifest in the Brönsted primary salt effect concerning the variation of ionic strength on rate constants. A mechanism for the ionic reaction in which ion-pair participation is involved is described.

The study of ionic reactions and their rates provides experimental evidence for the transition state concept. The theoretical correlation of ionic and dielectric environment with the bimolecular rate constants for such reactions has been provided by Brönsted (1), Bjerrum (2), and Scatchard (3).

A number of ionic reactions have been investigated which apparently conform with the expectation of theory (4-6). The bromoacetate-thiosulfate reaction shows serious deviation from theory which cannot be reconciled with the assumption that "free" ions are reactants. Corsaro (7) has summarized the nature and magnitude of these deviations and proposed a mechanism which accounts for them based on the postulate that ion-pairs are participants in reaction.

Davies and Williams (8) developed a two term rate expression for reactions involving bromoacetate and thiosulfate ions which took into account the ion-pair concentration as a reactant and were able to correlate the rate data with a modified Brönsted primary salt effect expression which they derive. They were able to utilize the measured dissociation constants (9-11) of the ion-pair species to calculate an ionic strength function involved in their rate expression. It should be noted that the concentration of ion-pairs involving bromoacetate ion were negligible.

Winstein (12-14), Denny and Monk (9), Righellato and Davies (10), and Jenkins and Monk (11) have provided data concerning the nature of ion-pairs, the techniques which may be employed for the estimation of their dissociation constants, and the modification of electrolytic solution properties which may be expected from their presence in solution. Recent papers by Davies (15) and by Duncan and Kepert (16) call attention to a several ion-pair species which may form in solution including one type in which the constituent ions of the pair may be separated sufficiently to be recognized as discrete entities but which nevertheless often behave as if they had combined to form a third entity.

It is the objective of this paper to demonstrate the presence of ion-pairs in reactions involving thiosulfate and bromoacetate ions, and the contributions these ion-pairs make to the mechanism of the reaction. Previous studies of the bromoacetate-thiosulfate ionic reaction (4, 7, 8, 17-21) usually have concerned themselves with the effect of added salts to sodium reactant mixtures. In this investigation reactant mixtures consisted of sodium, cesium, potassium, and calcium thiosulfate with the corresponding bromoacetate salt. In this way only one cation was present in the reaction mixture. Reactions were carried out in solvent mixtures consisting of 30, 40, 50, and 60% by weight isopropanol and water in order to determine the effect of variation of dielectric constant. Some rate data were obtained for reactions in which ethyl bromoacetate replaced bromoacetate salts.

Experimental

The rate measurements were made by a procedure similar to that used by Davis and LaMer (22). The initial reaction mixture contained quantities of reactant salts which provided equimolar anion concentrations. These consisted of one of the pairs: sodium, potassium, cesium, and calcium thiosulfate with the corresponding bromoacetate salt. All rate measurements were made at 25° ± 0.01°C. The

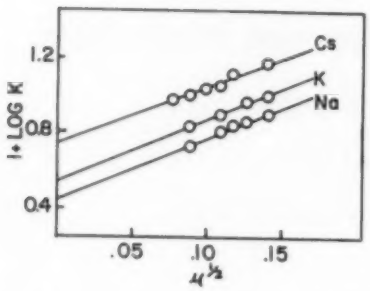

Fig. 1. Log k vs. $\mu^{1/2}$ for alkali reactants in 60% isopropanol-water mixtures.

bromoacetate salts were prepared at the start of each rate run by equilibrating the required amount of bromoacetic acid with the appropriate metal hydroxide.

At $t = 0$, two separate portions of solvent each containing one of the reactants are mixed, and the reacted thiosulfate is determined by analysis of residual thiosulfate concentration by titration. Thiosulfate concentrations are used to calculate the rate constant by the expression

$$k = \frac{X}{at(a-x)} \qquad [1]$$

in which "a" is the initial reactant salt concentration, x, the amount reacted in time t, and k, the bimolecular rate constant. The end points for the titration were determined by adding an excess of 0.01N iodine solution which was then estimated with a photoelectric colorimeter using previously constructed calibration curves. The thiosulfate salt solutions were prepared from analyzed stock solutions. Sodium and potassium thiosulfate were C.P. grades and used as purchased after analysis for impurities. Cesium thiosulfate was prepared by A. D. Mackay Company of New York. Calcium thiosulfate was prepared by reaction of calcium sulfate with barium thiosulfate. The salt was precipitated from acetone-methanol solutions at low temperatures. Bromoacetic acid, ethyl bromoacetate, and isopropanol were Eastman white label products. Bromoacetic acid was purified by vacuum distillation, ethyl bromoacetate by distillation and checked chromatographically for impurities, and isopropanol was dried over CaO, distilled, and redistilled as needed.

The results recorded for rate constants represent duplicate runs and the average of k values calculated by expression [1]. The precision of the data can be checked in several ways: a plot of the concentration-time data should be linear and the extrapolated line at $t = 0$ should agree with the initial thiosulfate concentration found by analysis. The intercept of the time plot was calculated from the data by the method of averages. The slope of the plot calculated by the method of least squares should be within the average of the k values obtained for each individual time run. A typical set of data is recorded in Table I.

Table I. Calculation of and comparison of rate constants for a typical run

	Slope × 10^4	Rate constant	Intercept
Method of least squares	0.8130 ± 0.01	0.400 ± 0.005	0.04995
Method of averages	0.808 ± 0.01	0.404 ± 0.005	0.4998
Graphically	0.812	0.406	0.0500
Analysis	—	—	0.49987

Treatment of Data

To test the observed data for conformity with the Brönsted-Bjerrum (1, 2) rate expression, log k values should be plotted against $\mu^{1/2}$. In this investigation the values for μ were calculated by assuming that thiosulfate salts provide ion-pairs $NaS_2O_3^-$, $KS_2O_3^-$, and $CaS_2O_3^\circ$ in all solvents except water and that association was complete. This assumption may not be valid in solutions containing low concentrations of alcohol and in the absence of dissociation constant data for the ion-pairs presumed to be formed in the reaction mixtures probably is approached in solutions of alcohol of 40% or greater. These species rather than free thiosulfate ion contribute to the ionic strength. A 0.005M solution of equimolar alkali metal salts thus gives an ionic strength, ½ (0.005 x 4) and 0.005M calcium thiosulfate with 0.0025M calcium bromoacetate, ½ (0.005 x 3).

The slopes for log k *vs.* $\mu^{1/2}$ plots, $2A \cdot Z_A \cdot Z_B$, are +1 or zero for alkali and calcium salt reactants, respectively. All of the data are recorded in Tables II through V and will be referred to in this discussion.

To facilitate the description of reactant systems the element symbols Na, K, Cs, and Ca will be used to represent the pair of thiosulfate-bromoacetate salts of the metal indicated. The concentrations of the salts were chosen to provide equimolar mixtures of their respective anions. The solvent media are described by the per cent by weight of the alcohol used with water. The dielectric constant values of the various solvent mixtures are those reported by Akerlof (23) at 25°C. The bimolecular rate constants, k and k_o, are expressed in the usual units of L/moles x sec. The notation I-PrOH will be used to stand for isopropanol.

Discussion of Results

The rate constants obtained for reactions in which ethyl bromoacetate is one of the reactants in place of bromoacetate salt are larger in magnitude than those for the ion-ion reaction. Sodium thiosulfate, with ethyl bromoacetate in water, gives a k value almost sixty times greater than for the sodium salt reaction. Apparently the ion-ester reaction is free from repulsive forces which obtain in the ion-ion reaction. In both reactions the thiosulfate ion is a nucleophile which displaces the bromine atom from the ester or bromoacetate ion.

If ethyl bromoacetate is a reactant with the thiosulfates of sodium, cesium, calcium, or an equimolar mixture of sodium thiosulfate and lanthanum

Table II. Rate constants for alkali metal reactants

Conc (M)	$\mu^{1/2}$	log k + 1 (Na)	log k + 1 (K)	log k + 1 (Cs)
		72% N-PrOH (D = 30)		
0.001	0.0447	0.621*	—	—
0.003	0.0775	0.782*	—	—
0.005	0.1000	0.877*	—	—
		60% I-PrOH (D = 35.3)		
0.003	0.0775	—	—	0.974
0.004	0.0895	0.722	0.831	1.014
0.005	0.1000	—	—	1.048
0.006	0.1097	0.798	0.898	1.058
0.007	0.1183	0.830	—	1.124
0.008	0.1265	0.854	0.958	—
0.010	0.1414	0.895	0.986	1.170
		50% I-PrOH (D = 42.5)		
0.003	0.0775	0.561	—	—
0.004	0.0895	0.617	0.702	0.891
0.006	0.1097	0.667	0.769	0.935
0.008	0.1265	—	0.821	0.987
0.010	0.1414	0.763	0.858	1.033
		40% I-PrOH (D = 49.7)		
0.002	0.0632	0.467	0.532	—
0.004	0.0895	0.549	0.617	—
0.006	0.1097	0.617	0.689	—
0.008	0.1265	0.683	0.748	—
0.010	0.1414	0.704	0.773	—
		30% I-PrOH (D = 56.9)		
0.002	0.0632	0.487	0.527	—
0.004	0.0895	0.565	0.617	—
0.006	0.1097	0.632	0.659	—
0.008	0.1265	0.687	0.704	—
0.010	0.1414	0.684	0.736	—
		H_2O (D = 78.5)		
0.0025*	0.100‡	0.576	—	—
0.004	0.126	0.619	0.601	0.634
0.005†	0.141	0.618	—	—
0.006	0.155	0.648	0.642	0.675
0.008	0.179	0.673	0.678	0.708
0.010	0.200	0.691	0.694	0.734
0.025†	0.316	0.771	—	—
0.033†	0.363	0.813	—	—
0.050	0.436	0.863	—	—

* Data from ref. (19).
† Data from ref. (17).
‡ Ionic strengths calculated by 4M.

Table III. Slopes from log k vs. $\mu^{1/2}$ plots

Reactants	D	Observed slope	$2AZ_AZ_B$
Na	30	4.30	4.31
Na	35.3	3.38	3.36
K	35.3	3.12	3.36
Cs	35.3	3.36	3.36
Na	42.5	3.08	2.56
K	42.5	2.90	2.56
Cs	42.5	2.80	2.56
Na	49.7	3.23	2.02
K	49.7	3.16	2.02
Na	56.9	2.36	1.66
K	56.9	2.44	1.66
Na	78.5	1.40	1.02
K	78.5	1.40	1.02
Cs	78.5	1.40	1.02
Na-La*	30	−4.31	−4.31
Ca	42.5	0.0	0.0

* Equimolar mixtures of $La(NO_3)_3$-$Na_2S_2O_3$-NaBrAc, 1M 72% N-PrOH. Data from ref. (19) but recalculated.

Table IV. Summary of k_o/r and k_oD/r data

r† = 1.69Å (Cs), 1.33Å (K), and 0.95Å (Na)

Reactants	D	k_o	k_o/r	k_oD/r	Dev. from avg
Na	30	0.292	0.308	9.25	−0.46
			(—)		
Na	35.3	0.264	0.278	9.80	+0.09
K	35.3	0.357	0.268	9.49	−0.22
Cs	35.3	0.512	0.306	10.51	+0.86
			(0.224)*		
Na	42.5	0.213	0.224	9.51	−0.20
K	42.5	0.282	0.212	9.00	−0.71
Cs	42.5	0.421	0.249	10.57	+0.86
			(0.226)		
Na	49.7	0.183	0.192	9.55	−0.21
K	49.7	0.251	0.189	9.43	−0.28
			(0.191)	(9.71)*	
Na	56.9	0.197	0.208	11.82	—
K	56.9	0.246	0.185	10.52	—
Na	78.5	0.302	0.318	24.95	—
K	78.5	0.266	0.200	15.70	—
Cs	78.5	0.286	0.169	13.28	—

* Results in parentheses are average of values above them.
† Radii, from crystal lattice ion sizes.

Table V. Rate constants for reactions with ethyl bromoacetate

Reactant SaH	Conc (M)	Solvent	k $\frac{L}{moles \times sec}$
Na	0.008	Water	14.5
Na	0.004	Water	14.5
Na	0.008	50% I-PrOH	20.42
Cs	0.008	50% I-PrOH	20.50
Ca	0.008	50% I-PrOH	12.18
Ca	0.004	50% I-PrOH	10.55
La-Na*	0.008	50% I-PrOH	3.61

* Equimolar $La(NO_3)_3$ – $Na_2S_2O_3$ – Ester.

nitrate, the observed rate constants stand in the decreasing order Na=Cs > Ca > La–Na. Table V records the rate constants obtained for these salt-ester systems in 50% I-PrOH. The values decrease from 20.2 for sodium thiosulfate and ester to 3.61 for the sodium-lanthanum-ester mixture. These results may be accounted for if the ion-pairs, $M^+S_2O_3^=$, $Ca^{++}S_2O_3^=$, and $La^{+++}S_2O_3^=$ are assumed to have been created in the reaction mixtures and the reactivity of the thiosulfate ion is affected to a greater extent by its association with polyvalent cations.

Figure 2 contains some of the k_o results collected and reported by Davis and LaMer (22), and those values obtained in this investigation. They represent the rate constants at zero ionic strength for sodium reactants in a variety of solvent mixtures. The expected linear plots for log k_o *vs.* $1/D$ are confined apparently to that data obtained with solvents for which the dielectric constants are greater than 80. In the range D = 50 to 80, the observed k_o values appear scattered along a flat minimum of the curve, and the remainder of the plot with a positive slope contains rate constants obtained with solvents con-

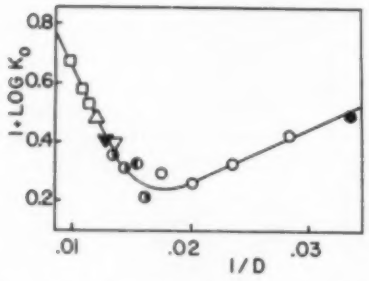

Fig. 2. Log k_o vs. 1/D for sodium reactants in solvent-water mixtures, indicated by; open square—glycine, open triangle—urea, solid inverted triangle—pure water, open inverted triangle—sucrose, circle, right side solid—methanol, circle, left side solid—t-butyl alcohol, open circle—isopropanol, solid circle—n-propanol.

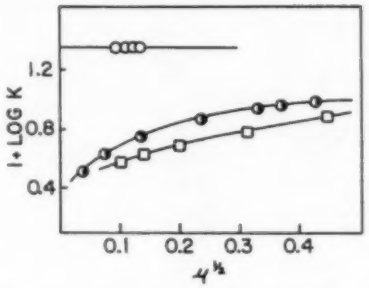

Fig. 3. Log k vs. $\mu^{1/2}$ for calcium reactants in 50% isopropanol—open circle, calcium in water—circle, right side solid, and sodium in water—open square.

taining 40 to 72% alcohol. Davis and LaMer suggested that a more satisfactory comparison of rate constants would be obtained if a mole fraction instead of a molar scale were used for the calculated k_o values. While such a corrected scale eliminates some of the scatter in the $D = 80$ portion of the curve its over-all shape as shown in Fig. 2 is not altered. It should be noted that the k_o values obtained with water and 30% I-PrOH fall on the middle part of the curve.

A reasonable explanation for the over-all data as shown is that in solvents of dielectric constants greater than 80 the salts which provide the reactant ions are completely dissociated and that reaction proceeds between "free" ions unaffected by ion association. The remainder of the plot manifests the increasing influence of cation charge on the reaction. The presence of alcohols, or other organic solvents, with water may tend to desolvate the ion species in solution and thus effect a mutual electrostatic attraction between oppositely charged ions.

According to Duncan and Kepert (16) an associated ion-pair could behave as a single entity or the constituent ions could retain their individual identities and charge influences. The observed rate constants for alkali and calcium salts appear to conform with such a dual behavior. If the symbolic structure, $M^{+n}S_2O_3^{n-2}$, is written for ion-pairs, their n—2 net charge and that for the critical complex formed between these species and bromoacetate ion govern the effect of ionic strength variation on the rate of reaction. The sign and magnitude of slopes from log k *vs.* $\mu^{1/2}$ plots should then reflect these effects. In plots like those shown in Fig. 1, the slopes were calculated from log k values and ionic strengths created from ion-pair contributions rather than "free" thiosulfate ions. The observed slopes are compared with those calculated from $2AZ_AZ_B$ in which Z_A is taken as −1. The agreement between the observed and calculated values is best for rates measured in 50, 60, and 72% alcoholic mixtures. The increasing deviation from the calculated results in 40 and 30% alcohol solvents is probably the result of partial rather than the complete association between thiosulfate ion and its cations assumed in these solvents. However, it is reasonable to expect that if the dissociation constants of the ion-pair species could be estimated for these solvents that a treatment similar to that given by Davies and Williams (8) could be utilized to bring the rate data in better conformity with theory. It also is interesting to note that the exclusion of ion-pairs in which the bromoacetate ion could be involved is justified on the basis of the good agreement with the assumed mechanism obtained with solvents of lower dielectric constants.

Figure 3 summarizes the results obtained with calcium salts as reactants in water and 50% isopropanol. The nonlinear curve with the data obtained in water suggests that increased concentration of the calcium salts favors ion-pair formation, and the log k *vs.* $\mu^{1/2}$ plot tends to level out as the concentration of ion-pairs increases. On the other hand, the data obtained with 50% alcohol show that the k values do not change with concentration of reactants used and the zero slope for the log k *vs.* $\mu^{1/2}$ plot reflects participation in reaction by an ion-pair with a zero net charge. It should be noted that when calcium thiosulfate is assumed to be associated that the ionic strengths calculated from its concentrations used in rate studies would not be too different from each other although the spread of concentration of this salt is significant. The data and Fig. 3 omit rate data obtained with this calcium system to which sodium chloride had been added in significant amounts, although the observed rate constants changed but little with these salt additions.

The behavior of ion-pairs in which the constituent ions retain their individual charge influences is manifest by the various k_o results calculated from the observed rates. These rate constants reflect all the energy contributions to the formation of the transition-state and are independent of ionic strength variations. The values for all the alkali metal systems are recorded in Table IV. It is apparent that with 50 and 60% alcohol the k_o results for the three alkali metal systems are significantly different and stand in the decreasing order of magnitude Cs > K> Na. In other solvents the data obtained also show that k_o values for potassium salts are greater than for sodium systems. In water the observed rates give a reversed order of k_o magnitudes.

It is also true that k_o for each alkali metal system is larger for reactions carried out in solvents con-

taining the greater amount of alcohol, starting at 40% alcohol, and that such k_o values appear to be proportional to $1/D$ in which D is the dielectric constant of the reaction medium.

The difference among the alkali metal k_o values from data obtained with a given solvent, and their increased values with solvents of lower dielectric constants, may be attributed to electrostatic effects derived from the independent influence of the constituent ions of the ion-pair taking part in reaction. These effects may be visualized if the reaction mechanism is represented by:

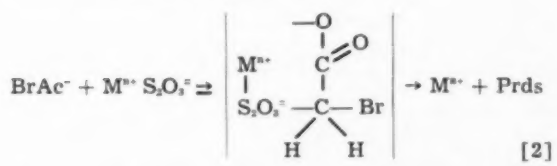

[2]

Expression [2] shows an intermediate complex in which an ion-pair is oriented with the bromoacetate ion. The orientation is effected by an electrostatic attraction between the cation of the ion-pair and the carboxylate structure of bromoacetate ion which in turn reduces the electron density at the alpha carbon position. The entry of thiosulfate ion into the transition-state thus is enhanced by this combined effect.

The apparent influence of the cation size may be accounted for if it is assumed that the constituent ions of the ion-pair are separated by their distance of closest approach when the intermediate complex is formed, although they may be separated otherwise at an undetermined distance before such a complex is created. The reactivity of the thiosulfate ion should then be least affected by a greater distance of separation between its center of charge and that of its associated cation. This condition is satisfied by the thiosulfate salt with the cation of largest radius and is consistent with the expectation that ions in solvents with the same dielectric constant should have electric field strengths proportional to $1/r$ if r is taken as the radius of the ion from the center of ion charge. The order of k_o values for the three alkali systems is thus the reverse of that for increased influence of cation in reducing the reactivity of the thiosulfate ion associated with it. If this argument is valid, the different k_o values for the three alkali metal systems in a given solvent, should be leveled to a common value if the effect of different cation size is cancelled. This may be accomplished by adjusting the k_o results to a common radius value. Table V records the results obtained when the k_o values of each alkali metal system is divided by the radius of its metal ion using the crystalline lattice ion radius for the latter value. The k_o/r ratios obtained by using the ion radii values in Angstrom units are, in effect, the rate constants obtained with salts having cation radii of 1.0Å. The observed data with 50 and 60% alcohol, which are complete for all three alkali metals, give individual k_o/r ratios which agree within 10% of the average of the three values obtained with each solvent.

The electrostatic effects manifest by the relationship between k_o values and the dielectric constants of the solvent mixtures used in reactions from which these k_o values were obtained can be leveled to a common dielectric constant value. Table V also shows the results of multiplying each k_o/r value by the dielectric constant of the solvent mixture in which rates were measured. The k_oD/r values are then, in effect, the rate constants for alkali metal salts having cations with the same radii and in solvents from which the effect of dielectric constant has been eliminated. The individual k_oD/r values are also within 10% of the average of all data obtained in solvents with 40 to 72% alcohol content. These results are all consistent with electrostatic contributions to the energy of formation of the transition-state complex derived from the cation influence on the reactivity of thiosulfate ion and its attraction to the carboxylate structure of the bromoacetate ion. The results from k_oD/r are possible only if the cation attraction to the carboxylate structure obeys the simple Coulomb attraction rule for oppositely charged species.

Corsaro (7) has reported data for reaction rates with systems containing equimolar amounts of bromoacetate-thiosulfate ions and thorium nitrate additions less than reactant ion concentrations. The reactions follow an apparent third order mechanism since they were second order with respect to thiosulfate ion concentration, and consistent third rate constants were calculated from the appropriate rate expression. The rate constants so obtained divided by the molar concentration of thorium nitrate used gave constant values over a wide range of thorium additions.

It would appear that one thorium ion is regenerated as two thiosulfate ions react and the order of the reaction thus is sustained. But this would require a mechanism in which two bromoacetate ions and two thiosulfate ions form a transition-state structure and is improbable. A possible mechanism can be represented by the following:

$$Th^{+4} + S_2O_3^{=} \rightleftarrows ThS_2O_3^{++} \qquad [3]$$

$$ThS_2O_3^{++} + S_2O_3^{=} \rightleftarrows ThS_2O_3^{++}S_2O_3^{=} \qquad [4]$$

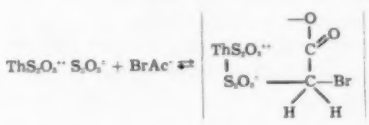

[5]

Expression [3] shows that one thiosulfate ion can form a complex ion with one thorium ion, or at least, an intimate ion-pair. This complex in turn can form the type of ion-pair which takes part in reaction in a manner similar to those which have been discussed.

The constancy of the rate constant/(Th) ratios up to thorium nitrate additions equal to that of sodium salts then may be interpreted as resulting from the fact that the complex ion, $ThS_2O_3^{++}$, is being regenerated during reaction. When the thorium concentration is in excess of sodium salts the rates fall off since then more complex ion, $ThS_2O_3^{++}$, is

being formed and less actual reactant, $ThS_2O_3^{++}-S_2O_3^{=}$, would be present. It may be argued that if this explanation is valid that the maximum in the rate constant value should appear at concentrations of added thorium nitrate equal to one half that of sodium reactants. However, this also would assume that all of the thorium and thiosulfate ions are involved in the formation of the species, $ThS_2O_3^{++}S_2O_3^{=}$. It is more probable that, while the species $ThS_2O_3^{++}$ is readily formed, $ThS_2O_3^{++}S_2O_3^{=}$ depends on an equilibrium shown by expression [4].

The steps shown in [3], [4], and [5] are over simplified. Solvation of all species is probably an important factor in reaction mechanism. Nevertheless the kinetic facts can be explained, at least in part, if the assumption that the ion-pair species as described take part in reaction.

Conclusions

The reaction between thiosulfate and bromoacetate ions may be complicated by the creation of associated ion pairs even in very dilute aqueous solutions. The effect of added alcohol to a reaction cannot be explained alone by a decrease of dielectric constant. Probably such additions have some dehydration effects which result in enhanced mutual electrostatic attraction between oppositely charged species. The various data reported in this investigation appear to justify the conclusion that an ion-pair may behave as a discrete entity and still retain the identity of its constituent ions.

Although it was postulated that the ions making up the pair may be at a distance of separation corresponding with that of closest approach, it was not intended that a conclusion should be drawn that such a condition prevails other than when an intermediate such as described by expression [2] is created. The actual transition-state probably occurs subsequent to the formation of the intermediate in which the ion-pair is shown.

The agreement between the observed slopes for log k *vs.* $\mu^{1/2}$ plots and those calculated by assuming the presence of ion pairs, $M^{+}S_2O_3^{=}$, may be taken as evidence for the participation of ion-pairs which behave as single entities. The apparent effect of cation size and that from the variation of dielectric constants of solvent media, is consistent with ion-pair behavior in which its constituent ions retain their cation charge influence, and thiosulfate ion its discrete reactivity, although modified by its association with cations.

The rate data for sodium systems containing thorium nitrate show to what extent the participation of complex ions or ion-pairs may modify a reaction mechanism.

The observed results, when ethyl bromoacetate is a reactant in place of bromoacetate salts, demonstrate a need to consider the effect of ion association in the study of displacement type reactions from which it is expected that a comparison of nucleophilic reactivities may be obtained. A review of such reactions by Streitweiser (24) clearly demonstrates this need.

Manuscript received Oct. 20, 1960; revised manuscript received March 15, 1961.

Any discussion of this paper will appear in a Discussion Section to be published in the June 1962 JOURNAL.

REFERENCES

1. J. N. Brönsted, *Z. Physik. Chem.*, **102**, 169 (1922).
2. N. Bjerrum, *ibid.*, **108**, 82 (1924).
3. G. Scatchard, *Chem. Revs.*, **10**, 229 (1932).
4. V. K. LaMer, *ibid.*, **10**, 179 (1932).
5. S. W. Benson, "The Foundations of Chemical Kinetics," Chap. 15, McGraw Hill Book Co., New York (1960).
6. E. S. Amis, "Kinetics of Chemical Change in Solution," Chap. 4, MacMillan Co., New York (1949).
7. G. Corsaro, R. Smith, and H. L. Stephens, *This Journal*, **105**, 229 (1958).
8. C. W. Davies and I. W. Williams, *Trans. Faraday Soc.*, **54**, 1547 (1958).
9. T. O. Denney and C. D. Monk, *ibid.*, **48**, 992 (1951).
10. E. W. C. Righellato and C. W. Davies, *ibid.*, **26**, 592 (1930).
11. I. L. Jenkins and C. D. Monk, *J. Am. Chem. Soc.*, **72**, 2645 (1950).
12. S. Winstein and R. Heck, *ibid.*, **74**, 5584 (1952).
13. S. Winstein *et al.*, *ibid.*, **78**, 328 (1956).
14. A. H. Fainberg and S. Winstein, *ibid.*, **78**, 2763 (1956).
15. W. J. Hamer, Editor, "The Structure of Electrolytic Solutions," Chap. 3, John Wiley & Sons, Inc., New York (1959).
16. *Ibid.*, Chap. 25.
17. V. K. LaMer and R. W. Fessenden, *J. Am. Chem. Soc.*, **54**, 2351 (1932).
18. A. R. Olsen and T. R. Simonsen, *J. Chem. Phys.*, **17**, 1167 (1949).
19. F. G. Ciapetta and H. M. Tomlinson, *J. Phys. Chem.*, **55**, 429 (1951).
20. V. K. LaMer, *Chem. Phys.*, **17**, 662 (1939).
21. A. N. Kappana, *J. Indian Chem. Soc.*, **33**, 3341 (1929).
22. H. G. Davis and V. K. LaMer, *J. Chem. Phys.*, **10**, 585 (1942).
23. G. Akerlof, *J. Am. Chem Soc.*, **54**, 4132 (1932).
24. A. Streitwieser, Jr., *Chem. Revs.*, **56**, No. 4 (1956). R. M. Fuoss, *J. Am. Chem. Soc.*, **79**, 9301 (1957).

Limiting Currents for the Reduction of the Tri-iodide Ion at a Rotating Platinum Disk Cathode

J. D. Newson and A. C. Riddiford

Department of Chemistry, The University of Southampton, Southampton, England

ABSTRACT

Limiting currents for the reduction of the tri-iodide ion have been determined with a rotating platinum disk cathode. The concentration of tri-iodide ion has been varied over the range 0.124-3.70 mM; the angular velocity of the disk, 50-200 rpm; the temperature, 25.0°-44.7°C; and the kinematic viscosity of the solution 0.00874-0.0555 cm^2 sec^{-1}. The results confirm the validity of Levich's theory for Prandtl numbers within the range 350-33,000.

In 1942, Levich solved the problem of mass-transport to the surface of a rotating disk from a solution containing not more than three ion species (1). A number of experimental investigations designed to check this theory have been published. These have been summarized by Gregory and Riddiford (2), who have shown that the observations are in excellent agreement with a slightly modified form of the theory. The experiments were confined, however, to a somewhat restricted range of conditions, and it is the purpose of the present paper to describe a more extensive check of this important theory.

To this end, the observations of Hogge and Kraichman (3) on the limiting currents for the reduction of tri-iodide ion have been confirmed and extended. The experimental results have thrown light on the kinetics of the iodine redox electrode process, and this aspect of the work is discussed in the following paper (4).

Experimental

Solutions.—ANALAR grade iodine and potassium iodide were used without further purification to prepare a stock solution 0.025M in tri-iodide ion and 0.1M in potassium iodide. The cell solutions were made up by diluting the requisite volume of stock solution with 0.1M potassium iodide solution. Commercial sucrose was used for increasing the viscosity of some of the solutions. The solutions were freed from oxygen by using cylinder nitrogen of normal grade ($O_2 < 0.05\%$).

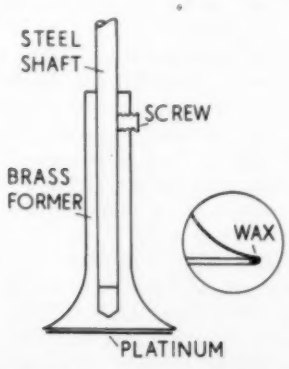

Fig. 1. The disk electrode. (Inset). Detail of edge

Disk electrode.—The form finally adopted is shown in Fig. 1. A stout platinum plate was soft soldered to a brass former with a long shank, and the plate was then machined true by turning the former on a shaft held in an accurately centered chuck. The former, and the edges of the platinum disk, were insulated with APIEZON wax applied as a benzene solution. Several chemical-resistant paints and lacquers were tried, but either they absorbed iodine rapidly from the solution, or would not adhere to the brass former.

Pinholes in the wax gave current/potential curves of unusual shape with high limiting currents, an effect that has been explained elsewhere (2). Pinholes were easily seen by immersing the disk in concentrated nitric acid, when they appeared as bright "brassy" specks. These were then painted over with the wax and left to dry. They occurred most frequently when the wax coat became old and brittle, or when it was still soft and the iodine could penetrate. The wax became sufficiently hard if left for 12 hr.

Normally, the disk was cleaned and polished between each series of runs by a very fine emery powder which was applied with a damp chamois leather kept for this purpose. Although this treatment was thought at first to be rather drastic, and indeed was sometimes omitted on this account, a careful comparison of the current/potential curves obtained showed that it was without significant effect on the rate of the surface reaction. The limiting currents, being dependent only on the apparent area, were also unaffected. The disk was stored under distilled water when not in use.

The disk was spun by mounting the former on a steel shaft which rotated in ball-races. Mounted in this way, the eccentricity amounted to less than 0.001 in., measured at the circumference of the disk. The disk radius was 1.56 cm, giving an apparent surface area of 7.64 cm^2.

Other electrodes.—The anode was formed from a stout sheet of platinum foil (5 x 5 in.) such that its surface area was some 20 times larger than that of the disk electrode, so ensuring that it remained

virtually unpolarized during the experimental runs.

The reference electrode was a silver/silver iodide electrode made according to Owen's description (5). It was filled with 0.1M potassium iodide solution, and capillary connection to the test solution was made at a point in the solution slightly above the lower (working) surface of the disk electrode. The test solutions were always 0.1M in potassium iodide, and the concentrations of tri-iodide ion studied were such that the liquid/liquid junction potential was negligible. It is of interest to note that, with this arrangement of the capillary connection, the potential of the working disk electrode measured against the reference electrode was independent of the position of the capillary junction, so long as this junction was above the plane of the lower surface of the disk. If this junction was lowered, however, an ohmic drop at once became apparent.

Other details.—The electrode vessel was cylindrical, and of 5.5 in. diameter such that the walls did not interfere with the flow about the disk (2). It was filled with about 1700 ml of solution.

Nitrogen was presaturated with iodine and water vapor by passing it through a solution of the same composition as the test solution, and at the same temperature. It was then passed over the surface of the test solution in the electrode vessel to maintain a slight positive pressure within the system.

During a run, the first reading taken was the open-circuit potential of the disk electrode measured against the reference electrode. Subsequent readings were obtained with various currents flowing, until the limiting current was reached. After this, a few readings of the disk potential were made in the reverse direction with decreasing current, and finally the open-circuit potential was checked. The observations made with progressively increasing currents always agreed closely with those made in the reverse direction. Steady readings were obtained with no appreciable time lag. Separate experiments showed that the residual currents for 0.1M potassium iodide solutions were negligible.

The kinematic viscosity of the solutions was measured with an Ostwald capillary viscometer. The necessary kinetic energy corrections were applied using Barr's method (6). The diffusion coefficient of the tri-iodide ion for given experimental conditions was measured using diaphragm cells of the same form as those described previously (2).

Results

Kinematic viscosity of the solutions.—The kinematic viscosity ν was determined for all the experimental solutions, and the observed values are reported in Tables I to III. Over the range investigated, ν does not vary significantly with change of tri-iodide concentration.

Diffusion coefficient of the tri-iodide ion.—The diffusion coefficient D of the tri-iodide ion was determined for all except three of the experimental solutions. The values for solutions 0.75M and 1.50M in sucrose at 25°C were obtained, respectively, by interpolation and extrapolation of a plot of log D against log ν. The value for a solution 1.0M in sucrose at 44.7°C was obtained by extrapolation of a plot of log D against $1/T$. The diffusion coefficient does not vary significantly with the concentration of the tri-iodide ion. The observed values are reported in Tables I to III.

Table I. Diffusion coefficient D of tri-iodide ion and kinematic viscosity ν for sucrose solutions at 25°C. All solutions 0.1M in iodide ion

Sucrose concentration, mole·liter^{-1}	$10^5 D$, cm^{2}sec^{-1}	$10^2 \nu$, cm^{2}sec^{-1}
0	1.13 (mean)	0.874
0.25	0.889, 0.891	1.08
0.50	0.682, 0.686, 0.686	1.36
0.75	—	1.79
1.00	0.379, 0.381	2.45
1.50	—	5.55

Table II. D and ν for the sucrose-free solutions at different temperatures

Temp, °C	$10^5 D$, cm^{2}sec^{-1}	$10^2 \nu$, cm^{2}sec^{-1}
25.0	1.13 (mean)	0.874
30.0	1.28, 1.27	0.787
35.0	—	0.715
35.2	1.41, 1.42	—
40.0	—	0.650
40.2	1.60, 1.60	—
45.0	—	0.595
45.2	1.73, 1.76	—

Table III. D and ν for the 1.0M sucrose solutions at different temperatures

Temp, °C	$10^5 D$, cm^{2}sec^{-1}	$10^2 \nu$, cm^{2}sec^{-1}
25.0	0.380 (mean)	2.45
30.2	0.429, 0.439	—
30.6	—	2.11
35.0	—	1.88
35.4	0.535, 0.522	—
40.0	—	1.66
41.7	0.644, 0.649	—
45.0	—	1.49

Limiting currents.—The limiting currents were obtained from plots of the current/potential curves. A typical set of curves is shown in Fig. 2, and it will be seen that determination of the limiting currents presents no difficulty.

The effect of varying the tri-iodide concentration over the range 0.124-3.70 mM (millimolar) was studied at 25°C. For each concentration, the effect of altering the angular velocity was measured, usually over the range 50-200 rpm. The observed limiting currents are shown in Table IV.

Next, the effect of varying the viscosity of the solution was studied at 25°C by adding sucrose to a solution 2.42 mM in tri-iodide ion. The concentration of sucrose was varied over the range 0 to 1.50M, and for each concentration the effect of varying the angular velocity of the disk was studied over the range 50-200 rpm. The observed results are shown in Table V.

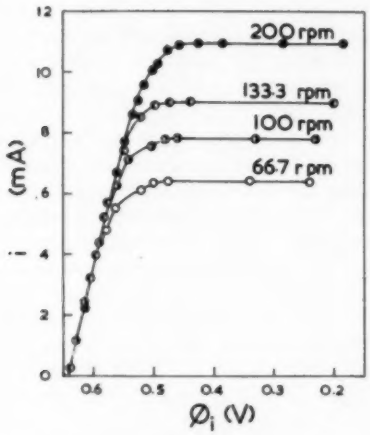

Fig. 2. Cathodic current/potential curves for a solution 2.47×10^{-3} M in I_3^- and 0.1M in I^- at 25°C. Potential expressed on decinormal silver/silver iodide scale. Apparent area of electrode = 7.64 cm².

Third, the cathodic limiting currents were determined as a function of temperature over the range 25.0°-44.5°C for a solution 2.45 mM in tri-iodide ion. In each case, the angular velocity of the disk was varied between 50 and 200 rpm. The observed results are given in Table VI.

Finally, the temperature coefficient was studied over the range 25.0°-44.7°C for 2.45 mM tri-iodide ion and 1.0M sucrose. Again, the effect of varying the angular velocity was studied at each temperature, and the observed results are shown in Table VII.

Discussion

These results require little comment. In Tables IV to VII, the calculated figures are theoretical limiting currents (2) computed from

$$i_{l\,lim} = 17.30 z A c D^{2/3} \nu^{-1/6} m^{1/2} I(\infty)^{-1} \text{ amp} \quad [1]$$

where z is the number of electrons involved in the electrochemical process, A is the apparent area of the working surface (cm²), c is the bulk concentration of the limiting solute species, namely, tri-iodide ion (mole liter⁻¹), D is the diffusion coefficient of this species (cm² sec⁻¹), ν is the kinematic viscosity of the solution (cm² sec⁻¹), m is the angular velocity of the disk (rpm) and $I(\infty)$ is given by the equation

Table IV. Cathodic limiting currents (ma) for tri-iodide reduction in 0.1M potassium iodide solution at 25°C

rpm		Tri-iodide concentration (millimolar) 0.124	0.241	0.617	1.24	2.47	3.70
44.4	obs				2.62		7.84
	calc				2.62		7.85
50	obs	0.280	0.537	1.39	2.75	5.50	
	calc	0.278	0.539	1.39	2.78	5.54	
66.7	obs	0.322	0.621	1.58	3.20	6.40	9.42
	calc	0.321	0.624	1.60	3.21	6.40	9.61
100	obs	0.390	0.760	1.94	3.90	7.80	11.62
	calc	0.393	0.764	1.96	3.93	7.84	11.77
133.3	obs	0.451	0.881	2.23	4.50	9.02	13.41
	calc	0.454	0.882	2.27	4.54	9.05	13.59
200	obs	0.550	1.06	2.73	5.61	10.98	16.38
	calc	0.556	1.08	2.77	5.56	11.08	16.65
400	obs	0.779		3.83	7.83		
	calc	0.785		3.92	7.85		

Table V. Cathodic limiting currents (ma) for tri-iodide reduction in 0.1M KI and 2.42 millimolar I_3^- with added sucrose at 25°C

rpm		Sucrose Concentration (mole·liter⁻¹) 0[a]	0.25	0.50	0.75	1.00	1.50
50	obs	5.50	4.50	3.65	2.90	2.19	1.18
	calc	5.54	4.50	3.65	2.89	2.24	1.17
66.7	obs	6.40	5.20	4.22	3.39	2.59	1.37
	calc	6.40	5.20	4.22	3.34	2.58	1.35
100	obs	7.80	6.34	5.13	4.10	3.16	1.67
	calc	7.84	6.38	5.16	4.09	3.17	1.65
133.3	obs	9.02	7.28	5.98	4.75	3.69	1.97
	calc	9.05	7.26	5.96	4.72	3.66	1.90
200	obs	10.98	8.90	7.28	5.80	4.51	2.37
	calc	11.08	9.01	7.31	5.78	4.48	2.33

[a] Tri-iodide 2.47 millimolar.

Table VI. Cathodic limiting currents (ma) for tri-iodide reduction in 0.1M KI at different temperatures

		Temp, °C 25.0	30.0	34.9	39.8	44.5
Tri-iodide conc., millimolar		2.47	2.46	2.46	2.45	2.45
rpm 50	obs	5.50	5.98	6.52	7.10	7.74
	calc	5.54	6.05	6.57	7.19	7.67
66.7	obs	6.40	6.96	7.54	8.20	8.86
	calc	6.40	6.99	7.59	8.30	8.85
100	obs	7.80	8.50	9.30	10.00	10.86
	calc	7.84	8.56	9.30	10.17	10.84
133.3	obs	9.00	9.80	10.70	11.56	12.41
	calc	9.05	9.88	10.74	11.73	12.50
200	obs	10.98	12.00	13.10	14.16	15.26
	calc	11.08	12.11	13.15	14.38	15.34

Table VII. Cathodic limiting currents (ma) for tri-iodide reduction in 0.1M KI and 1M sucrose at different temperatures

		Temp, °C 25.0	30.6	34.9	39.8	44.7
Tri-iodide conc., millimolar		2.42	2.46	2.46	2.45	2.45
rpm 50	obs	2.19	2.60	2.83		
	calc	2.24	2.63	2.92		
66.7	obs	2.59	3.00	3.30	3.80	4.05
	calc	2.58	3.04	3.37	3.81	4.26
100	obs	3.16	3.70	4.00	4.60	5.00
	calc	3.17	3.72	4.13	4.66	5.22
133.3	obs	3.69	4.25	4.64	5.22	5.70
	calc	3.66	4.29	4.77	5.38	6.03
200	obs	4.51	5.20	5.66	6.40	7.00
	calc	4.48	5.26	5.85	6.59	7.38

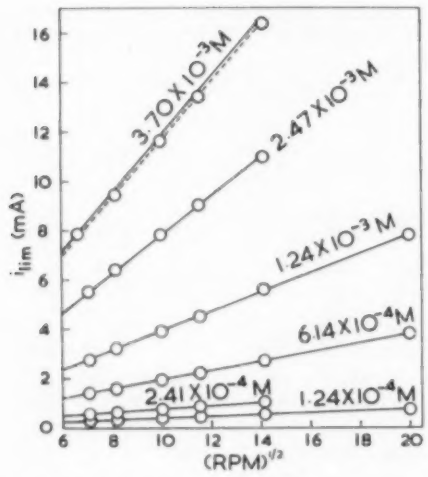

Fig. 3. Cathodic limiting currents for tri-iodide ion reduction in solutions 0.1M in I^- at 25°C at I_3^- concentrations, indicated on each line, vs. cathode angular velocity (r.p.m.) The solid lines are the theoretical slopes computed from equation [1]. The broken line shows the effect of correcting for electrical migration.

$$I(\infty) = 0.8934 + 0.316(D/\nu)^{0.58} \qquad [2]$$

Since the values of D and ν recorded in Tables I-III were measured at temperatures which, in some cases, differed slightly from those at which the current/potential curves were determined, the values required for Eq. [1] and [2] were obtained by interpolation in plots of log D and log ν, respectively, against $1/T$.

The observed and calculated values for the limiting currents (Tables IV to VII) agree to within ± 1% in most cases. At 25°C, for 3.70 mM tri-iodide ion, there is some indication of the onset of electrical migration (Fig. 3). Equation [1] only holds when the transport number of the critical ion species is effectively zero. In the present case, this will only be true provided the ratio c_a/c_i is smaller than a critical value, c_a and c_i being, respectively, the bulk concentrations of tri-iodide ion and iodide ion. Since the ratio of the observed limiting current to that calculated from Eq. [1] must be $1/(1 + t_a)$, where t_a is the transport number of the tri-iodide ion, a migratory contribution to the transport process will be shown by an observed limiting current which is smaller than the calculated value.

The observed results for the 3.70 mM tri-iodide ion support this view. The effect is small and may be assessed with sufficient accuracy by the following argument. We assume that the mobility of the tri-iodide ion is roughly the same as that of the iodide ion. Then, since the transport number of the iodide ion in 0.1M KI is 0.5117 at 25°C (7), $t_a \sim 0.51\ c_a/c_i$. For $c_a/c_i = 0.0370$, the migratory contribution will be of the order of 2%. The broken line in Fig. 3 shows that this correction accounts for the observed deviation. For all other cases in the present study, the correction is less than 1%, and hence smaller than the experimental error.

The results shown in Table V offer a number of points of interest. It will be noted that there is excellent agreement between theory and experiment over the wide viscosity range studied. Gregory and Riddiford (2) found agreement between theory and experiment for the range of Prandtl numbers 350-770. The present results extend this range to 33,000. The correction to Levich's theory becomes less important as the Prandtl number increases; it amounts to 3% for the sucrose-free solutions at 25°C, but is only 0.2% for the 1.50M sucrose solution at the same temperature. An important point is that natural convection is still negligible under these conditions. Moreover, the agreement between theory and experiment shows that there is no edge effect, *i.e.*, the diameter of the disk chosen is very much larger than the thickness of the transport boundary layer, as required by the theory.

The poorest agreement is found for the results shown in Table VII, particularly the value at 44.7°C. This is almost certainly due to an uncertainty in the value of D, obtained by extrapolation of the data recorded in Table III. Apart from this, there can be little doubt that the theory is valid over the extended range of experimental conditions reported in the present paper.

It seems probable that the measure of agreement between theory and experiment could be improved by reducing the eccentricity of the disk and by determining D with greater precision. In a study of the cathodic reduction of ferricyanide ion (8), using precision ground shafts and taking extreme care to mount the disk normal to the axis of the shaft, limiting currents have been obtained which are reproducible to within ±0.25%.

Acknowledgment

The authors record their thanks to Mr. E. W. Balson, B.Sc., for the readiness with which he gave assistance and practical advice, and to the University of Southampton for the provision of a maintenance grant to J. D. N.

Manuscript received Aug. 1, 1960; revised manuscript received March 13, 1961.

Any discussion of this paper will appear in a Discussion Section to be published in the June 1962 JOURNAL.

REFERENCES

1. V. Levich, *Acta Physicochim. U.R.S.S.*, **17**. 257 (1952).
2. D. P. Gregory and A. C. Riddiford, *J. Chem. Soc.*, **1956**, 3756.
3. E. A. Hogge and M. B. Kraichman, *J. Am. Chem. Soc.*, **76**, 1431 (1954).
4. J. D. Newson and A. C. Riddiford, *This Journal*, **108**, 699 (1961).
5. B. B. Owen, *J. Am. Chem. Soc.*, **57**, 1526 (1935).
6. G. Barr, "Monograph of Viscometry," Clarendon (1931).
7. L. J. Longsworth, *J. Am. Chem. Soc.*, **57**, 1185 (1935).
8. S. Azim and A. C. Riddiford, to be published.

The Kinetics of the Iodine Redox Process at Platinum Electrodes

J. D. Newson and A. C. Riddiford

Department of Chemistry, The University of Southampton, Southampton, England

ABSTRACT

Three paths for the iodine redox process at platinum electrodes are discussed with reference to stationary current/potential curves obtained for the cathodic reduction of the tri-iodide ion in potassium iodide solutions. It is shown that the process follows the path originally proposed by Vetter, the slow stage being the transfer of an electron from the platinum to an adsorbed iodine atom, and that the degree of reversibility of the process increases as the concentration ratio of tri-iodide to iodide is decreased. The apparent energy of activation for the over-all process is 5.3 kcal·mole^{-1} for solutions containing only potassium iodide and tri-iodide. The results, and those of other workers, indicate that the electrode surface is nonuniform.

Comparatively little work has been published on the kinetics of the iodine redox process at platinum electrodes. Vetter (1) has commented on work published prior to 1952, and has studied both the anodic and cathodic directions using 1*N* sulfuric acid as supporting electrolyte. Using the d-c stationary current/potential curve method, he found the reaction to be fast such that the nature of the redox process was largely obscured by the transport of iodine to and from the electrode. For this reason, he turned to an a-c method (2), and, from the determined dependence of the exchange current density on the concentrations of the iodide and tri-iodide ions, deduced a mechanism which may be symbolized as follows, where *S* denotes a surface site, the nature of which is to be established.

$$I^- + S = I{-}S + e^- \qquad [1]$$

$$I{-}S + I{-}S = I_2 + 2S \qquad [2]$$

$$I_2 + I^- = I_3^- \qquad [3]$$

The electron-transfer step [1] was identified as the slow stage.

Kolthoff and Jordan (3) have studied the oxidation of iodide ion at a platinum anode in solutions of pH 1, 4, and 8. They have reported that the process becomes increasingly irreversible as the pH of the solution increases. No mechanism was suggested by these authors.

Recently, however, Jordan and Javick (4) published a further study of the anodic oxidation of iodide ion, using 0.1M perchloric acid as supporting electrolyte, and have postulated that the process occurs directly through the two-electron transfer step [4]. The bulk concentration of iodide ion never ceeded 10^{-6}M in their experiments, such that the tri-iodide equilibrium [step 3] could be neglected (5).

$$2I^- = I_2 + 2e^- \qquad [4]$$

It is of interest to note that Frumkin and Tedoradse (6, 7), in an investigation of the reduction of chlorine at a platinum cathode, have considered the mechanism

$$Cl^- + S = Cl{-}S + e^- \qquad [5]$$

$$Cl{-}S + Cl{-}S = Cl_2 + 2S \qquad [6]$$

the analogue to Vetter's mechanism, and an alternative

$$Cl^- + S = Cl{-}S + e^- \qquad [7]$$

$$Cl^- + Cl{-}S = Cl_2 + S + e^- \qquad [8]$$

They point out that the second mechanism is analogous to the mechanism for hydrogen evolution by electrochemical desorption of hydrogen atoms. Indeed, both mechanisms are closely analogous to the two most strongly favored mechanisms for hydrogen evolution (8, 9). Frumkin and Tedoradse show that their results are in accord with the second of these two mechanisms.

These studies present several problems of interest, and in discussing them it will be convenient to generalize the mechanisms in the following way:

Path (*a*)

$$X^- + S = X{-}S + e^- \qquad [9]$$

$$X{-}S + X{-}S = X_2 + 2S \qquad [10]$$

$$(X_2 + X^- = X_3^-) \qquad [11]$$

Path (*b*)

$$X^- + S = X{-}S + e^- \qquad [12]$$

$$X^- + X{-}S = X_2 + S + e^- \qquad [13]$$

$$(X_2 + X^- = X_3^-) \qquad [14]$$

Path (*c*)

$$2X^- = X_2 + 2e^- \qquad [15]$$

$$(X_2 + X^- = X_3^-) \qquad [16]$$

where, for example, X^- can represent a halide ion.

Jordan (10) has criticized Vetter's conclusion that path (*a*) represents the course of the iodine redox process on the grounds that the dissociation of iodine in aqueous solution, if it occurred, would be too small to account for the observed currents. If, as seems probable, the iodine atoms are adsorbed on the platinum surface, this objection is invalid. Vet-

ter's conclusion may, however, be criticized on other grounds, since his results are not uniquely diagnostic of path (a). By varying c_3, the concentration of tri-iodide ion, while keeping c_1, the concentration of iodide ion, constant Vetter found the relation

$$(RT/\mathbf{F})\,(\partial \ln i_o/\partial \phi_o)_{c_1} = 0.78 \qquad [17]$$

where i_o is the observed exchange current, and ϕ_o is the equilibrium potential of the electrode. Conversely, he found dependence

$$(RT/\mathbf{F})\,(\partial \ln i_o/\partial \phi_o)_{c_3} = 0.13 \qquad [18]$$

and, by varying c_1 and c_3 so that ϕ_o remained constant

$$(\partial \ln i_o/\partial \ln c_1)_{\phi_o} = 1 \qquad [19]$$

These dependences show that, whatever the mechanism, there is a single rate-determining step. Application of the general equations[1] for the dependence of exchange currents on the concentrations of species participating in the electrode process (11) permits the calculation of the corresponding dependences for each step in paths (a), (b), and (c). These are shown in Table I, wherein i_{j_o} and α_j, respectively, are the exchange current and transfer coefficient for the j-th step.

Since $0 \leq \alpha_j \leq 1$, it is clear that Vetter's results are consistent with the view that the rate-determining step is the primary discharge process

$$I^- + S = I{-}S + e^-$$

with $\alpha = 0.78$, but they do not serve to distinguish between paths (a) and (b). This raises the interesting point that, if (b) is the path of the iodine redox process, then together with Frumkin and Tedoradse's work on the chlorine electrode one would expect the bromine electrode to follow the same course. On the other hand, if (a) represents the path for the iodine electrode, the study of the bromine electrode would then be a matter of considerable importance.

The disagreement between Vetter's conclusions and those of Jordan and Javick remains, however, to which may be added the point that the actual path might conceivably involve other species (*e.g.*, HOI, OI^-), this since the results of Kolthoff and Jordan (3) have not, as yet, been explained. In this communication, an attempt is made to resolve these problems by considering the course of the process in neutral solution at a rotating platinum disk cathode. The experimental details have been given in the preceding paper (12).

Table I. Dependence of exchange current on concentration C_1 of iodide and C_3 of tri-iodide ions for different paths

Path	Step	$\frac{RT}{\mathbf{F}}\left(\frac{\partial \ln i_{j_o}}{\partial \phi_o}\right)_{c_1}$	$\frac{RT}{\mathbf{F}}\left(\frac{\partial \ln i_{j_o}}{\partial \phi_o}\right)_{c_3}$	$\left(\frac{\partial \ln i_{j_o}}{\partial \ln c_1}\right)_{\phi_o}$
(a)	9	α_9	$\alpha_9 - 2/3$	1
	10	2	2/3	2
	11	2	0	3
(b)	12	α_{12}	$\alpha_{12} - 2/3$	1
	13	$1 + \alpha_{13}$	$\alpha_{13} - 1/3$	2
	14	2	0	3
(c)	15	$2\alpha_{15}$	$2\alpha_{15} - 4/3$	2
	16	2	0	3

[1] In the case of the iodine redox process, these equations will be valid provided that θ_o, the fraction of the surface available for the discharge of iodide ions, is potential-independent. It will be shown that this condition is satisfied for the rotating disk cathode used in the present study, and it is thought to be a reasonable assumption for Vetter's investigation.

Mechanism of the Process

Stationary current/potential curves were obtained for solutions 0.1M in potassium iodide with tri-iodide ion concentrations ranging from 1.24×10^{-4} to 3.70×10^{-3}M at 25°C. The large excess of iodide ion served to suppress ionic migration of the tri-iodide ion, and to ensure that the concentration of free iodine was negligible at all points in the system. Thus the over-all electrode process is quite simply

$$3I^- = I_3^- + 2e^- \qquad [20]$$

and the concentrations of the iodide ion and tri-iodide ion at the electrode surface ($\bar{c}_1$ and $\bar{c}_3$, respectively) can be computed from the expressions

$$\bar{c}_1/c_1 = 1 - i/i_{l_{1m,a}} \qquad [21]$$

$$\bar{c}_3/c_3 = 1 - i/i_{l_{1m,c}} \qquad [22]$$

c_1 and c_3 being the bulk concentrations of the ions. The current i is reckoned negative for net cathodic currents, and the cathodic limiting current $i_{l_{1m,c}}$ can be computed from the extended Levich theory (13). The anodic limiting current $i_{l_{1m,a}}$ is large, and can be computed with sufficient precision from the equation

$$i_{l_{1m,a}}/i_{l_{1m,c}} = -c_1/c_3(1 + 2t_+) \qquad [23]$$

where t_+ is the transport number of the potassium ion (14).

That, in general, the rate of the surface process was not very fast in comparison with the rates of the transport processes was shown in two ways. First, the data were tested against the reversible equation

$$\phi_i = \phi^\circ + (RT/2\mathbf{F}) \ln \bar{c}_3/\bar{c}_1^3 \qquad [24]$$

in which ϕ_i is the working potential of the electrode when it is sustaining a current i, and ϕ° is the standard electrode potential. Second, the observed initial slopes of the current/potential curves were compared with those computed from the expression (11)

$$(\partial\phi_i/\partial i)_{i=0} = (RT/2\mathbf{F})\,(\sum{}' \nu_j/i_{j_o} + 3/i_{l_{1m,a}} - 1/i_{l_{1m,c}}) \qquad [25]$$

on the assumption that $\sum{}' \nu_j/i_{j_o} = 0$, *i.e.*, that the ratio of the stoichiometric number ν_j for any step in the mechanism of the surface process to the exchange current for that step i_{j_o} is negligible in comparison with the transport terms. Except at the lowest tri-iodide ion concentrations (1.24×10^{-4}M and 2.41×10^{-4}M), linear plots were not obtained by using Eq. [24], and the observed values for $(\partial\phi_i/\partial i)_{i=0}$ were always larger than the reversible value.

At the lowest tri-iodide ion concentrations, the plots of ϕ_i against log $(\bar{c}_3/\bar{c}_1^3)$ were linear, but with slopes greater than 0.0296 v predicted by Eq. [24]. The slopes are shown in Table II, but it will be con-

Table II. Comparison of experimental results with Eq. [24]

$c_1 = 0.1M$, 25°C

c_3, mM·liter^{-1}	Angular velocity, rpm	Obs. slope, v	$\frac{0.0296}{\text{Obs. slope}}$
0.241	200	0.0452	0.655
0.124	400	0.0422	0.701
0.124	200	0.0387	0.764
0.124	100	0.0367	0.806

venient to defer discussion of these observations to the next section, which deals with Kolthoff and Jordan's observations (3).

The data for the runs at higher tri-iodide ion concentrations have been checked against the three mechanisms discussed in the previous section. For each mechanism, rate equations may be set up to correspond with rate control by each separate step, or by combinations of these steps. Considering path (*a*), step [9], for example,

$$i/\mathbf{F}A = k_{9,a} \exp(\alpha_9 \mathbf{F}\Delta\phi_i/RT)\bar{c}_i\bar{\theta}_o - k_{9,c} \exp(-(1-\alpha_9)\mathbf{F}\Delta\phi_i/RT)\bar{\theta} \quad [26]$$

where A is the area of the electrode and α_9 is the transfer coefficient for this step. $\Delta\phi_i$ denotes the difference $\phi_i - \phi^*$, where ϕ^* is a fixed value of the electrode potential which will be discussed, together with the anodic and cathodic rate constants ($k_{9,a}$ and $k_{9,c}$, respectively) in the following sections.[2] $\bar{\theta}_o$ is the fraction of the surface area available for the discharge of iodide ions when a current i is flowing through the electrode, and $\bar{\theta}$ is the fraction covered with adsorbed iodine atoms.

If step [9] determines the observed rate, then from steps [10] and [11]

$$\bar{\theta}/\bar{\theta}_o = (\bar{c}_2/\bar{c}_1)^{1/2}/(K_{10}K_{11})^{1/2} \quad [27]$$

where K_{10} and K_{11} are the respective equilibrium constants for these steps. From Eq. [26] and [27], at electrochemical equilibrium when $i = 0$ and $\phi_i = \phi_o$, the open-circuit potential,

$$k_{9,a} = k_{9,c}(K_{10}K_{11})^{-1/2} \exp(-\mathbf{F}\Delta\phi_o/RT)(c_2/c_1^*)^{1/2} \quad [28]$$

Substituting Eq. [27] and [28] into [26], and rearranging gives

$$\phi_i = (RT/(1-\alpha_9)\mathbf{F}) \ln Y + \phi^* + (RT/(1-\alpha_9)\mathbf{F}) \ln (Z/i) \quad [29]$$

where

$$Y = \mathbf{F}Ak_{9,c}\bar{\theta}_o(K_{10}K_{11})^{-1/2}(c_2/c_1)^{1/2} \quad [30]$$

$$Z = \exp(\eta\mathbf{F}/RT)(\bar{c}_1/c_1) - (\bar{c}_2/c_2)^{1/2}/(\bar{c}_1/c_1)^{1/2} \quad [31]$$

η being the overpotential ($= \phi_i - \phi_o$). Provided that $\bar{\theta}_o$ is potential-independent, the linearity or otherwise of the plot of ϕ_i against log (Z/i) forms one test of whether rate control by step [9] is possible.

[2] The use of concentrations in these rate equations may be defended on the grounds that the presence of a large excess of iodide ion ensures that the variation of the respective activity coefficients may be neglected. The latter may be regarded as incorporated in the appropriate rate and equilibrium constants.

Corresponding rate equations have been set up and tested for the other possibilities, and the results of these tests can be summarized as follows:

1. The nonelectron transfer steps [10], [11], [14], and [16] did not give linear plots, and rate control by these steps may therefore be ruled out.
2. Step [12] gave linear plots with $\alpha_{12} \geq 1$, and step [13] gave linear plots with $\alpha_{13} \sim 0$, so that rate control by these steps seems improbable.
3. Steps [9] and [15] both gave linear plots with $0 < \alpha < 1$, and are therefore possible explanations.
4. Tests for joint control by two steps gave nonlinear plots in the case of paths (*a*) and (*c*), and linear plots with improbable values for the transfer coefficient in the case of path (*b*).

This leaves, as possibilities, path (*a*) with step [9] rate-determining, or path (*c*) with control by step [15]. To distinguish between them, the experimental results were checked by Frumkin and Tedoradse's procedure (6). For a set of runs with the same tri-iodide ion concentration but differing speeds of stirring, and considering a fixed overpotential sufficiently high for the anodic component to be negligible, then if step [9] is rate-determining the relation between the current i_c which flows at this overpotential and the corresponding stirring speed will be

$$i_c^2 = i_{max}^2 - (i_{max}^2/B)(i_c/m^{1/2}) \quad [32]$$

where i_{max} is the maximum kinetic current which could flow at the given overpotential, m is the angular velocity of the disk, and $B = i_{11m,c}/m^{1/2}$. For step [15], on the other hand, (and, incidentally, for steps [12] and [13])

$$1/i_c = 1/i_{max} + 1/Bm^{1/2} \quad [33]$$

Figure 1 exemplifies the result of testing these equations. Both give linear plots, but the value of B obtained by use of Eq. [32] is 0.41, whereas Eq. [33] gives the value 0.49. From the theory of the rotating disk system (12), and by experiment, it is known that the value of B in this case is 0.393. There can be no doubt that the observed rate is, in fact, half-order

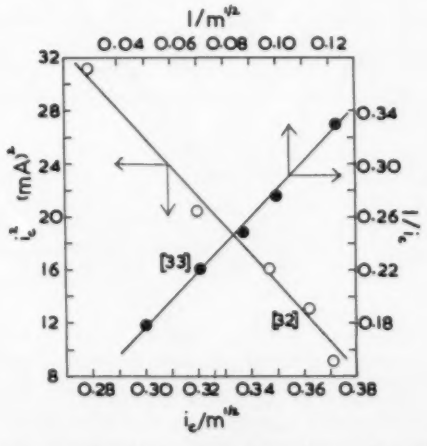

Fig. 1. Test of Eq. [32] and [33]. $[I^-] = 0.1M$, $[I_3^-] = 2.47 \times 10^{-3}M$, 25°C, $\eta = -0.07$ v.

with respect to tri-iodide ion, thus establishing Vetter's original mechanism (a) with rate control by the electron-transfer step.

This half-order dependence means that $\bar{\theta}$, the fraction of the surface covered by adsorbed iodine atoms, must approximate to zero, so that if $\bar{\theta}_0$, the fraction of the surface available for discharge, is regarded as equal to $1-\bar{\theta}$, then it will be independent of the electrode potential, as has been assumed in the above discussion. This point is considered in the following sections.

The half-order dependence also means that paths of the type considered by Rüetschi (15) for the hydrogen evolution reaction, and exemplified for the present system by the scheme

$$I^- + I - S = I_2 + S + e^- \quad [34]$$

$$I_2 + 2S = 2I - S \quad [35]$$

$$I_2 + I^- = I_3^- \quad [36]$$

are inapplicable. Mechanisms involving the participation of HOI or OI^- are similarly ruled out.

The fact that equally good linear kinetic plots were obtained for a number of possibilities, including postulated rate control by step [15] in path (c), suggests that Jordan and Javick's (4) method of testing their experimental results was not crucial. The excellent linearity of kinetic plots based on step [9], and those for steps [13] and [15] (for which this method of kinetic treatment is identical), are exemplified in Fig. 2, in which for steps [13] and [15],

$$Z' = \exp(2\mathbf{F}\eta/RT)(\bar{c}_i/c_i) - (\bar{c}_s/c_s)/(\bar{c}_i/c_i)^2 \quad [36a]$$

From Fig. 2, it will be noted that linearity obtains over the range of $i/i_{lim.c}$ from 0.03 to 0.88. This, together with Fig. 1, strongly suggests that step [9] is rate-controlling over the whole range of potentials studied.

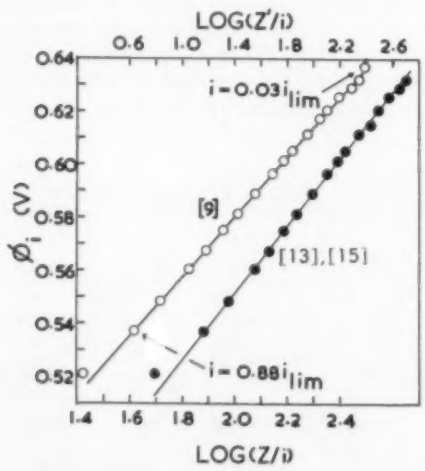

Fig. 2. Kinetic plots for cathodic polarization: (a) assuming rate control by step [9] (open circles, lower abscissae), (b) assuming rate control by step [13] or [15] (solid circles, upper abscissae). Z and Z' are defined by Eq. [31] and [36a], respectively. Open-circuit potential = 0.6395 v, potentials against decinormal silver/silver iodide reference electrode. $[I^-] = 0.1M$, $[I_2] = 2.47 \times 10^{-3}M$, 133.3 rpm, 25°C.

Oxidation of Iodide Ion

We now consider the results of Kolthoff and Jordan (3) for the anodic oxidation of iodide ion at 25°C. They observed two stages under the conditions investigated, occurring over different potential ranges, such that two limiting currents were found. Attention will be confined to the first stage, corresponding to the oxidation of iodide ion to iodine.

They found that the first stage could be expressed by the equation

$$\phi_i = \text{const.} + (0.0296/a)\log[i/(i_{lim.c} - i)^2] \quad [37]$$

where $i_{lim.c}$ is the lower limiting anodic current, and a is a constant. An equation of this form, with $a = 1$, is readily deduced for the over-all process [4] on the assumption that the process is reversible. From the plot of ϕ_i against $\log[i/(i_{lim.c} - i)^2]$, they found slopes approximating closely to the reversible value for solutions of pH 1.

For solutions of higher pH, however, their results gave slopes greater than 0.0296 v, or $a < 1$. According to Kolthoff and Lingane (16), a slope greater than the reversible value indicates a measure of irreversibility in the electrode process, an assumption accepted by other workers (17). In consequence, Kolthoff and Jordan concluded that the anodic oxidation of iodide ion becomes increasingly irreversible as the pH of the solution increases. No explanation appears to have been found for this, nor does the postulate fit in readily with any of the mechanistic paths discussed in the previous section.

In our view, the assumption is wrong since, irrespective of the magnitude of the slope, the form of Eq. [37] *implies* reversibility. On the other hand, once it is accepted that the electrode process is reversible under these experimental conditions, the following argument leads to the interesting conclusion that the electrode surface is nonuniform.

According to Audubert (18, 19) and Bonnemay (20, 21), nonuniformity of the surface of a solid electrode is sometimes shown by the sum of the anodic and cathodic transfer coefficients being less than unity when the electrode is sustaining a current,[3] although they must sum to unity at electrochemical equilibrium. Applying this concept to the iodine electrode process, Eq. [26] may be written (omitting the subscript 9)

$$i/\mathbf{F}A = k_a \exp(\bar{\alpha}\mathbf{F}\Delta\phi_i/RT)\,\bar{c}_i\,\bar{\theta}_0 - k_c \exp(-\bar{\beta}\mathbf{F}\Delta\phi_i/RT)\,\bar{\theta} \quad [38]$$

where $\bar{\alpha}$ and $\bar{\beta}$, respectively, are the anodic and cathodic transfer coefficients for the *working* electrode. At electrochemical equilibrium, $i = 0$, $\bar{\alpha} = \alpha$, $\bar{\beta} = \beta$, $\alpha + \beta = 1$ and the exchange current can be expressed[4]

[3] An alternative explanation, inapplicable in the present instance, is that the rate-determining step on the anodic side differs from the rate-determining step on the cathodic side.

[4] This implies that k_a and k_c, the rate constants at $\phi_i = \phi^*$ remain unaltered. The justification for this assumption will be apparent from the following sections.

$$i_o = \mathbf{F}Ak_c \exp(\alpha\mathbf{F}\Delta\phi_o/RT)\, c_1\theta_o = \mathbf{F}Ak_c \exp(-\beta\mathbf{F}\Delta\phi_o/RT)\theta \quad [39]$$

where ϕ_o is the open-circuit potential. From Eq. [38] and [39],

$$i/i_o = \exp[(\bar{\alpha}\Delta\phi_i - \alpha\Delta\phi_o)\mathbf{F}/RT](\bar{c}_1/c_1)(\bar{\theta}_o/\theta_o) - \exp[-(\bar{\beta}\Delta\phi_i - \beta\Delta\phi_o)\mathbf{F}/RT](\bar{\theta}/\theta) \quad [40]$$

At the low bulk iodide ion concentrations used by Kolthoff and Jordan, step [11] need not be considered, so that if step [10] is reversible,

$$\bar{\theta}/\theta = (\bar{\theta}_o/\theta_o)(\bar{c}_2/c_2)^{1/2} \quad [41]$$

where the subscript 2 refers to molecular iodine. Moreover, from the Nernst equation,

$$\phi_o = \phi_2^\circ + (RT/\mathbf{F}) \ln c_2^{1/2}/c_1 \quad [42]$$

where ϕ_2° is the standard potential for process [4].

Then if the rate of the electrode process is completely transport-controlled, i.e., if step [9] is also reversible, $i/i_o = 0$ and from Eq. [40]-[42],

$$\phi_i = \phi^* + (\phi_2^\circ - \phi^*)/(\bar{\alpha} + \bar{\beta}) + (RT/(\bar{\alpha} + \bar{\beta})\mathbf{F}) \ln \bar{c}_2^{1/2}/\bar{c}_1 \quad [43]$$

which becomes of the same form as Eq. [37] as c_2 approaches zero.

The corresponding expression for the over-all process [20] is

$$\phi_i = \phi^* + (\phi^\circ - \phi^*)/(\bar{\alpha} + \bar{\beta}) + (RT/(\bar{\alpha} + \bar{\beta})\mathbf{F}) \ln \bar{c}_3^{1/2}/\bar{c}_1^{3/2} \quad [44]$$

In the next section it is shown that $\phi^* \sim \phi^\circ$ for this process, so that Eq. [44] is of the same form as [24] except that the slope is $RT/(\bar{\alpha} + \bar{\beta})\mathbf{F}$. On this argument, the figures shown in the last column of Table II correspond to the sum $\bar{\alpha} + \bar{\beta}$. Thus it would appear that the electrode process becomes increasingly reversible as the ratio c_3/c_1 is decreased, a conclusion which is supported by the discussion of the exchange currents in the last section, and which fits Kolthoff and Jordan's results (3). The nonuniformity of the surface is also discussed in the last section of this paper.

Analysis of the Current/Potential Curves

For the irreversible cathodic runs, values of $1 - \alpha_o$, the transfer coefficient for the reduction of adsorbed iodine atoms, can be obtained from the slopes of the experimental plots of Eq. [29] and are reported in Tables III to VI. Examination of these values reveals that the transfer coefficient is insensitive to changes in temperature and viscosity. On the other hand, $1 - \alpha_o$ shows a marked dependence on the bulk concentration of tri-iodide ion, on the bulk concentration of iodide ion, and on the rate of stirring.

Table III. Values of $(1 - \alpha_o)$ for the nonviscous runs at 25°C

$c_1 = 0.1$M

c_3, mM·liter^{-1}	rpm 66.7	100	133.3	200	400
3.70	0.532	0.467	0.440	0.392	
2.47	0.573	0.548	0.520	0.471 0.493	
1.24	0.730	0.690	0.635	0.602	0.537
0.617			0.677	0.670	0.650

Table IV. Values of $(1 - \alpha_o)$ for the viscous runs at 25°C

$c_1 = 0.1$M, $c_3 = 2.42 \times 10^{-3}$M

Sucrose conc, mole·liter^{-1}	rpm 66.7	100	200
0.25	0.549	0.522	0.445
0.50		0.538	0.452
0.75		0.524	0.440
1.00		0.554	0.488
1.50		0.519	0.455

Table V. Values of $(1 - \alpha_o)$ for the nonviscous runs at higher temperatures

$c_1 = 0.1$M, $c_3 = 2.46 \times 10^{-3}$M

Temp, °C	rpm 100	133.3	200
30.0	0.533	0.523	0.483, 0.480
34.9	0.572	0.524	0.496, 0.485
39.8	0.567	0.535	0.493, 0.465
39.6*	0.972		

* $c_1 = 1.0$M.

Table VI. Values of $(1 - \alpha_o)$ for solutions 1.0M in sucrose at higher temperatures

$c_1 = 0.1$M, $c_3 = 2.45 \times 10^{-3}$M, 200 rpm

Temp, °C	$1 - \alpha_o$
30.6	0.461
34.9	0.493
39.9	0.480

The most probable explanation of these unusual observations is that Eq. [29] was derived by assuming that the electrode surface was uniform, i.e., that the anodic and cathodic transfer coefficients summed to unity. As discussed in the preceding section, however, there are good reasons for setting this assumption aside. A most informative way of freeing Eq. [29] from this assumption lies in the computation of the term Y on the right-hand side. If constant, Y can be obtained by the following extrapolation procedure.

Y should be constant for any series of runs in which the temperature and the ratio c_3/c_1 are maintained constant. If, in such a series, the linear plot from Eq. [29] is extrapolated back to $\log(Z/i) = 0$, the resulting values for the observed potential $\phi_{Z=i}$ should vary linearly with $1/(1 - \alpha_o)$

$$\phi_{Z=i} = (RT/(1 - \alpha_o)\mathbf{F}) \ln Y + \phi^* \quad [45]$$

From the slope of this plot, $Ak_c\bar{\theta}_o(K_{10}K_{11})^{-1/2}$ can be evaluated, and the constancy of this composite term for different series of runs (i.e., differing c_3/c_1) at the same temperature then affords a check of the validity of the arguments developed in the preceding

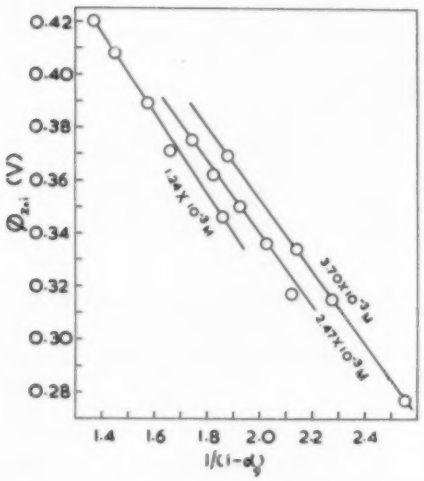

Fig. 3. Test of Eq. [45] at 25°C. $[I^-] = 0.1M$, $[I_3^-]$ as shown on plots, potentials expressed on decinormal silver/silver iodide scale.

sections. Moreover, the plot offers a means for determining the characteristic potential ϕ^*.

For the purpose of this check, the most extensive data are provided by the nonviscous runs at 25°C (see Table III). Figure 3 shows the plot of Eq. [45] for three series of runs taken from Table III. The slopes differ for each series. Nevertheless the values obtained for $Ak_{0,c}\overline{\theta_0}(K_{10}K_{11})^{-1/2}$, and for ϕ^*, are satisfactorily constant, as will be seen from Table VII. The area of the electrode has been left in this composite term since the actual surface area of the working disk electrode is not known. The constancy of the term confirms that $\overline{\theta_0}$ is potential-independent.

The mean value obtained for ϕ^* from these series is +0.626 v on the decinormal silver/silver iodide scale, or +0.540 v on the hydrogen scale. This is very close to the value of the standard potential for the tri-iodide/iodide redox electrode (22), +0.535 v, and can be identified as the value of the potential for which the free energy of activation is the same for the anodic and cathodic directions. It follows (23-25) that the standard entropy change for the rate-determining step is very small, *ca.* 0.4 e.u., in conformity with the view that the slow stage in the process is electron-transfer between the platinum surface and an adsorbed iodide ion or iodine atom.

The Rate Constants

Values for the composite term $Ak_{0,c}\overline{\theta_0}(K_{10}K_{11})^{-1/2}$ obtained from three series of nonviscous runs at 25°C have been reported in Table VII. Under the other experimental conditions investigated (12) there are fewer members to each series of runs, and consequently there is more uncertainty attached to the values of ϕ^* obtained by extrapolation. Where extrapolation is possible, however, the values so obtained suggest that ϕ^* is practically constant.

This is to be expected if the rate-determining step is, in fact, electron transfer to an adsorbed iodine atom. The variation in the potential of the decinormal silver/silver iodide electrode amounts to no more than 3 mv over the temperature range studied (26), and for the runs in which the viscosity of the solution was altered by adding sucrose it would seem that the liquid/liquid junction potential between the solution and the reference electrode is small. For these reasons, a constant value of $\phi^* = 0.626$ v on the silver/silver iodide reference scale has been assumed for all the remaining runs. Values of the composite rate constant have been computed from Eq. [45], and the mean values are reported in Tables VIII to X.

Table VII. Check of Eq. [45]

$c_1 = 0.1M$, 25°C. Potentials *vs.* decinormal silver/silver iodide reference electrode.

c_3, mM·liter^{-1}	rpm	$\phi_{z=i}$, v	$Ak_{0,c}\overline{\theta_0}(K_{10}K_{11})^{-1/2}$, mole/sec^{-1}	ϕ^*, v
3.70	200	0.277	2.63×10^{-7}	0.626
	133.3	0.315		
	100	0.334		
	66.7	0.369		
2.47	200	0.336	2.52×10^{-7}	0.626
		0.317		
	133.3	0.350		
	100	0.362		
	66.7	0.375		
1.24	400	0.346	2.63×10^{-7}	0.627
	200	0.371		
	133.3	0.389		
	100	0.408		
	66.7	0.420		

Table VIII. Composite rate constants for viscous runs at 25°C

$c_1 = 0.1M$, $c_3 = 2.42 \times 10^{-3}M$

Sucrose conc, mole·liter^{-1}	$Ak_{0,c}\overline{\theta_0}(K_{10}K_{11})^{-1/2}$ mole/sec^{-1}	ϵ
0.25	1.86×10^{-7}	76.7
0.50	1.51×10^{-7}	74.7
0.75	1.20×10^{-7}	72.7
1.00	8.1×10^{-8}	70.8
1.50	4.1×10^{-8}	66.8

Table IX. Composite rate constants for the nonviscous runs at higher temperatures

$c_1 = 0.1M$, $c_3 = 2.46 \times 10^{-3}M$

Temp, °C	$Ak_{0,c}\overline{\theta_0}(K_{10}K_{11})^{-1/2}$ mole·sec^{-1}	$Ak_{0,c}\overline{\theta_0}/K_{10}^{1/2}$
30.0	3.10×10^{-7}	2.58×10^{-4}
34.5	3.57×10^{-7}	2.85×10^{-4}
39.6	3.98×10^{-7}	3.03×10^{-4}

Table X. Composite rate constants for solutions 1.0M in sucrose at higher temperatures

$c_1 = 0.1M$, $c_3 = 2.45 \times 10^{-3}M$

Temp, °C	$Ak_{0,c}\overline{\theta_0}(K_{10}K_{11})^{-1/2}$ mole·sec^{-1}
30.6	9.5×10^{-8}
34.9	1.2×10^{-7}
39.9	1.0×10^{-7}

At 25°C, the value of K_{11} is 7.68×10^5 cm³ mole⁻¹ (27) so that from Table VII $Ak_{9,c}\theta_o/K_{10}^{1/2} = 2.27 \times 10^{-4}$ mole$^{1/2}$ cm$^{3/2}$ sec^{-1}. The corresponding values for the nonviscous runs at higher temperatures are shown in Table IX. Lack of knowledge of the actual surface area A, of θ_o and of K_{10} prevent the detailed analysis of the composite rate constant. It seems likely, however, that $A\theta_o$ will not vary significantly with change in the experimental conditions, so that variation in the composite term will be mainly due to variation in the product $k_{9,c}(K_{10}K_{11})^{-1/2}$ or, having allowed for K_{11}, in the product $k_{9,c}/K_{10}^{1/2}$. The values for $Ak_{9,c}\theta_o(K_{10}K_{11})^{-1/2}$ correspond to an apparent energy of activation of 5.3 kcal mole⁻¹ for the nonviscous runs. Correcting for the known temperature coefficient of K_{11} (27) alters this value to 3.7 kcal mole⁻¹. The values recorded in Table X for the runs in 1.0M sucrose solutions are too uncertain to permit the estimation of an apparent energy of activation, the probable reason being the uncertainty in the limiting currents.

Considering the data reported in Table VIII for the viscous runs at 25°C, it is evident that the rate constant decreases with increasing sucrose concentration. The third column of the table shows the bulk dielectric constant ϵ of the solution (ignoring the presence of electrolytes) computed from data listed by Harned and Owen (28), and it will be seen that the decrease in the rate constant is reflected by a decrease in ϵ.

Exchange Currents

If step [9] is solely rate-determining, then from Eq. [25],

$$(\partial\phi_i/\partial i)_{i=0} = (RT/2\mathbf{F})(2/i_{9,o} + 3/i_{11m,d} - 1/i_{11m,c}) \quad [46]$$

from which the exchange current may be computed. Alternatively $i_{9,o}$ could be calculated from the expression

$$i_{9,o} = \mathbf{F}Ak_{9,c}\theta_o(K_{10}K_{11})^{-1/2} \exp(-(1-\alpha_9)\mathbf{F}\Delta\phi_o/RT)(c_2/c_1)^{1/2} \quad [47]$$

The difference $\Delta\phi_o = \phi_o - \phi^*$ is rather small for most of the experimental conditions, however, so that the values of $i_{9,o}$ computed from Eq. [47] are not in general so reliable as those computed from Eq. [46]. Table XI shows the comparison for two runs, and it will be seen that the values of $i_{9,o}$ are close, particularly in the case when the difference $\Delta\phi_o$ amounted to 68 mv. This implies that the assumption that step [9] controls the rate of the surface process is justified. Values computed from Eq. [46] for all the cathodic runs are collected in Tables XII-XV.

Table XI. Exchange currents computed from Eq. [46] and [47]. Apparent electrode area 7.64 cm²

c_1 mole·liter⁻¹	10^3c_2	Temp, °C	rpm	$\Delta\phi_o$, v	$i_{9,o}$, ma [46]	$i_{9,o}$, ma [47]
0.1	3.70	25.0	200	0.0175	3.27	3.75
1.0	2.27	39.6	200	0.0680	21.6	21.4

Table XII. Exchange currents for the non-viscous runs at 25°C

c_2, mM·liter⁻¹	$c_1 = 0.1$M Mean $i_{9,o}$, ma	$\lvert i_{11m,c}\rvert/i_{9,o}$ (rpm)$^{1/2}$
3.70	3.17	0.37
2.47	2.64	0.30
1.24	2.62	0.15
0.617	2.59	0.075
0.241	2.52	0.030
0.124	1.94	0.020

Table XIII. Exchange currents for the viscous runs at 25°C

$c_1 = 0.1$M, $c_2 = 2.42 \times 10^{-3}$M

Sucrose conc, mole/liter⁻¹	Mean $i_{9,o}$, ma	$\lvert i_{11m,c}\rvert/i_{9,o}$ (rpm)$^{1/2}$
0.25	2.33	0.27
0.50	1.99	0.26
0.75	1.50	0.27
1.00	1.21	0.26
1.50	0.63	0.27

Table XIV. Exchange currents for the nonviscous runs at higher temperatures

$c_1 = 0.1$M, $c_2 = 2.46 \times 10^{-3}$M

Temp, °C	Mean $i_{9,o}$, ma	$\lvert i_{11m,c}\rvert/i_{9,o}$ (rpm)$^{1/2}$
30.0	3.44	0.25
34.9	3.80	0.24
39.8	4.04	0.25
39.6*	24.1	0.042

* $c_1 = 1.0$M.

Table XV. Exchange currents for the 1.0M sucrose solutions at higher temperatures

$c_1 = 0.1$M, $c_2 = 2.45 \times 10^{-3}$M

Temp, °C	Mean $i_{9,o}$, ma	$\lvert i_{11m,c}\rvert/i_{9,o}$ (rpm)$^{1/2}$
30.6	1.31	0.28
34.9	1.71	0.23
39.9	1.50	0.30

The exchange current density is a good criterion of the reversibility of an electrode process in cases where the surface process is so slow that the transport processes exert no influence on the observed rate. For faster reactions, however, a preferable criterion is that the magnitude of the limiting current divided by the square root of the rate of stirring should be much smaller than the exchange current, [cf. Jordan, ref. (29)] or in the present case

$$\lvert i_{11m,c}\rvert/i_{9,o}\,(\text{rpm})^{1/2} \sim 0 \quad [48]$$

Values of this ratio are shown in Tables XII-XV. From Table XII, it will be seen that the process approaches reversibility as the concentration of triiodide ion is decreased until, at concentrations below *ca.* 2.4×10^{-4}M, no satisfactory kinetic plots can be obtained. Instead, as previously discussed, the experimental results satisfy equations of the form [44], as shown in Table II. This effect is shown particularly clearly by the fact that raising the concentration of iodide ion from 0.1 M to 1.0 M increases the exchange current from 4.04 to 24.1 ma. The

ratio $i_{lim.c}/i_{s.c}(rpm)^{1/2}$ drops from 0.25 to 0.042. Apart from this concentration ratio, it will be seen that no other experimental factor has any appreciable effect on the degree of reversibility.

From Tables XII-XV, it is seen that $i_{s.c}$ falls within the range 0.6-4.0 ma. For 1*N* sulfuric acid solutions, when the process is nearly reversible, Vetter (1, 2) found values of the exchange current density of the order 10-100 ma cm^{-2}. These figures were based on the apparent area of the electrode. On the same basis, the corresponding exchange current densities for the present study are 0.08-0.52 ma cm^{-2}, and are much lower than Vetter's values, as would be expected. The difference is broadly attributable to a variation in the uniformity of the electrode surface.

There are several possible reasons why a solid electrode may behave in a nonuniform fashion, but as yet there is little evidence in favor of one particular explanation for any given electrode (30). In the case of the iodine redox process, Vetter (2) found it necessary to assume that only about 60% of the surface of his platinum electrode was effective for electron transfer, *i.e.*, that the exchange current density was greater on certain surface sites than on others. In a subsequent study (31), he has shown that, with platinum wire electrodes which have been etched by cleansing in warm chromic acid, the effective surface may be reduced to 30% of the total surface area. Llopis, Fernández-Biarge, and Pérez-Fernández (32) attribute these results to inactivity of the electrodes used by Vetter, which in turn were more active than those used in the present investigation.

This inactivity may well be connected with the observations that oxide films may be formed on platinum electrodes either by anodic polarization, or by treatment with strong oxidants (33, 34). The formation by anodic polarization is dependent on the pH of the solution, and it would thus appear that an explanation of Kolthoff and Jordan's results (3), and the present results, might be sought on this basis. In this connection, it is significant that "inactive" platinum electrodes show the same behavior as platinum electrodes which have been "poisoned" by the action of polysulfide solutions (32).

A more detailed investigation of the nature of the surface sites responsible for the anodic and cathodic partial currents is, however, desirable. Clearly, it is not sufficient simply to regard a certain fraction of the surface as being inactive. The results are strongly suggestive of the view that the anodic and cathodic sites differ.

Conclusion

The results leave little doubt that the process follows the path originally postulated by Vetter (2), with slow electron transfer to an adsorbed iodine atom as the rate-determining step.

Since Frumkin and Tedoradse's results (6, 7) indicate that the chlorine electrode process follows path (b), it is clear that the study of the bromine electrode is a matter of some importance. This is now under investigation.

Acknowledgment

We thank Professor A. N. Frumkin for providing further information connected with the published observations on the chlorine electrode (6, 7), and Professor J. Jordan for permitting us to see a manuscript copy of his paper (10) in advance of publication.

Manuscript received Aug. 1, 1960; revised manuscript received March 13, 1961.

Any discussion of this paper will appear in a Discussion Section to be published in the June 1962 JOURNAL.

REFERENCES

1. K. J. Vetter, *Z. physik. Chem.*, **199**, 22 (1952).
2. K. J. Vetter, *ibid.*, **199**, 285 (1952).
3. I. M. Kolthoff and J. Jordan, *J. Am. Chem. Soc.*, **75**, 1571 (1953).
4. J. Jordan and R. A. Javick, *ibid.*, **80**, 1264 (1958).
5. J. Jordan, Private communication.
6. A. N. Frumkin and G. Tedoradse, *Z. Elektrochem.*, **62**, 251 (1958).
7. A. N. Frumkin and G. Tedoradse, *Doklady Akad. Nauk S.S.S.R.*, **118**, 530 (1958).
8. J. O'M. Bockris, "Modern Aspects of Electrochemistry," Vol. 1, Butterworths, London (1955).
9. J. O'M. Bockris and H. Mauser, *Can. J. Chem.*, **37**, 475 (1959).
10. J. Jordan, *Trans. Symposium on Electrode Processes (1959)*, in course of publication.
11. A. C. Riddiford, *J. Chem. Soc.*, **1960**, 1175.
12. J. D. Newson and A. C. Riddiford, *This Journal*, **108**, 695 (1961).
13. D. P. Gregory and A. C. Riddiford, *J. Chem. Soc.*, **1956**, 3756.
14. L. G. Longsworth, *J. Am. Chem. Soc.*, **57**, 1185 (1935).
15. P. Rüetschi, *This Journal*, **106**, 819 (1959).
16. I. M. Kolthoff and J. J. Lingane, "Polarography," 2nd ed., Vol. 1, p. 202, Interscience Publishers Inc., New York (1952).
17. D. J. Ferrett and C. S. G. Phillips, *Trans. Faraday Soc.*, **51**, 390 (1955).
18. R. Audubert, *J. Phys. Rad.*, **3**, 81 (1942).
19. R. Audubert, *Discussions Faraday Soc.*, **1**, 72 (1947).
20. M. Bonnemay, *C. R. Acad. Sci, Paris*, **222**, 793, 1222 (1946); **223**, 76 (1946).
21. M. Bonnemay, *J. Chim. Phys.*, **44**, 187 (1947).
22. A. C. Riddiford, *Z. Elektrochem.*, **61**, 752 (1957).
23. M. I. Tempkin, *Zhur. fiz. Khim.*, **22**, 1081 (1948).
24. J. E. B. Randles, *Trans. Faraday Soc*, **48**, 828 (1952).
25. R. Parsons, *ibid.*, **54**, 1053 (1958).
26. B. B. Owen, *J. Am. Chem. Soc.*, **57**, 1526 (1935).
27. M. Davies and E. Gwynne, *ibid.*, **74**, 2748 (1952).
28. H. S. Harned and B. B. Owen, "The Physical Chemistry of Electrolytic Solutions," 3rd ed., p. 161, Reinhold Publishing Corp., New York (1958).
29. J. Jordan, *Anal. Chem.*, **27**, 1708 (1955); **28**, 522 (1956).
30. A. C. Riddiford, "Surface Phenomena in Chemistry and Biology," J. F. Danielli, K. G. A. Pankhurst and A. C. Riddiford, Editors, p. 224, Pergamon Press, New York (1958).
31. K. J. Vetter, *Z. physik. Chem.*, **199**, 300 (1952).
32. J. Llopis, J. Fernández-Biarge, and M. Pérez-Fernández, *Acta Electrochim.*, **1**, 130 (1959).
33. I. M. Kolthoff and N. Tanaka, *Anal. Chem.*, **26**, 632 (1954).
34. F. C. Anson and J. J. Lingane, *J. Am. Chem. Soc.*, **79**, 4901 (1957).

Technical Notes

Barrel Plating by Means of Electroless Palladium

R. N. Rhoda

Research Laboratory, The International Nickel Company, Inc., Bayonne, New Jersey

This process for the electroless deposition of palladium and the bath employed in the process were first discussed in April, 1959 (1); all are now the subject of a patent (2). Further refinements in the operating procedure and in the bath formulations are reported here.

Barrel Plating

Electroless plating may be done by suspending specimens in the plating bath or by tumbling in a nonperforated barrel. It is considered that its main application will involve the plating of large numbers of small parts, and hence we have focused our recent work on barrel plating. An advantage of this method is the self-polishing of the pieces during tumbling in the barrel. Operating conditions of the suspension and barrel methods are much the same.

The chemical ingredients reported in the earlier paper (1) have been augmented and now include these materials:

Solvents (aqueous): ammonium hydroxide, ammonium hydroxide plus ammonium chloride, ethylamine, and N-aminoethyl ethanolamine.

Stabilizers: ammonium chloride, ammonium nitrate, ammonium sulfate, acetone, disodium salt of EDTA (ethylenediammine-tetraacetic acid), methyl ethyl ketone, and 2-2′ thiodiethanol.

Palladium is conveniently supplied as the chloride of the soluble tetrammine amine complex and is added to new baths and as make-up in aqueous solution containing a small quantity of the solvent. Of the solvents ammonium hydroxide is the least expensive and is readily available; it has been used in most of our work. The stabilizer inhibits solution decomposition and several types of compounds perform satisfactorily. On a weight basis the disodium salt of EDTA is more effective than the inorganic stabilizers or the ketones. The best stabilizer of the is 2-2′ thiodiethanol, but the color of the palladium deposits from these baths tends to be dull, perhaps because of the sulfide group in this compound. No reducer other than hydrazine has been found which will produce metallic deposits of palladium.

The aim of this new work was to operate the barrel plating operation to achieve as high a rate of plating as possible without encountering spontaneous decomposition of the bath during either plating or subsequent storage of the solution at room temperature. Most of the barrel plating was done within these limits:

Palladium concentration: 2.5-20 g/l in a solution containing 8.0 g/l Na_2 EDTA and 280 g/l ammonium hydroxide

Temperature: 25°-45°C

Load: 100 small electrical connectors with a total surface area of 560 cm^2

Solution volume: 700 ml

Rate of hydrazine additions: as 1M solution, 4-24 ml/hr (0.1-0.8 g N_2H_4/hr).

Under our experimental conditions it was determined that at any specific palladium concentration and operating temperature there was a rate of hydrazine addition beyond which spontaneous decomposition of the system might occur; these are given in Table I. In general at low concentrations and temperatures more rapid rates of hydrazine addition are tolerated. Increasing the surface area of the load allows hydrazine to be added at proportionally higher rates.

The plating rates were determined for a large number of combinations within the limitations of Table I. These rates increase with an increase in temperature; an increase of 10°C almost doubles the rate of reaction. These rates also increase with increasing rates of addition of hydrazine; this increase is small at 25° and greater at 45°C. Increasing the palladium concentration causes the rate of reaction to increase at 25°, but has little effect at 45°C. Maximum plating rates which emerge from these various possibilities are low compared to attainable electrodeposition rates. Within the permissible addition rates and concentrations of Table I the plating rates fall into these ranges: at 25°C, 12-33 μ in./hr; at

Table I. Maximum addition rates of reducer

Solution volume: 700 ml
Load: 560 cm^2 (100 connectors)
Addition interval: 15 min

Palladium concentration, g/l	Temp, °C	Maximum addition rate, g/15 min	Maximum addition rate, Ml of 1M Solution/15 min
5	25	0.160	5
	35	0.096	3
	45	0.096	3
10	25	0.128	4
	35	0.096	3
	45	0.096	3
20	25	0.096	3
	35	0.064	2
	45	0.032	1

Table II. General schemes for pretreatment of substrates for electroless palladium plating

Substrate	Form	Pretreatment
Aluminum	Sheet	$H_2SO_4 + HNO_3$ etch
Carbon	Rods	N_2H_4 soak
Gold	Immersion plate	1:1 HCl dip
	Sheet	None
Graphite	Rods	N_2H_4 soak
Kovar	Wire	1:1 HCl + $PdCl_2$ dip
Molybdenum	Wire	Chromic acid
Nickel	Bright plate	Cathodic clean, then 1:1 HCl + $PdCl_2$ dip
	Dull plate	Cathodic clean, then 1:1 HCl dip
	Sheet	Cathodic clean, then 1:1 HCl dip
Palladium	Electroplate	1:1 HCl dip
Silver	Plate	Cathodic clean, then 1:1 HCl dip
Tantalum	Sheet	H_3PO_4
Titanium	Sheet	Alkaline soak then $CrCl_3$ + HF dip (patented process)

35°C, 33-78 μ in./hr; at 45°C, 50-95 μ in./hr. The highest plating rates were achieved at 45°C at the addition rate of 0.096 g of hydrazine/15 min at a palladium concentration of 10 g/l. For this set of conditions 0.1 mil of palladium can be deposited in about 1¼ hr.

The above rates were achieved for short periods of operation during which the plating solution was not significantly exhausted. Plating runs under longer operating conditions require modification in technique. The addition of hydrazine at a constant rate results in a slow increase in the ratio of excess hydrazine to palladium ions in the solution, and this leads ultimately to decomposition during the run or during subsequent storage of the solutions. Diminishing the addition rate of hydrazine with time has proven satisfactory and has not greatly changed the long-time rate of deposition. One can envision that any commercial application of this process would involve continuous make-up of the palladium concentration of the solution along with the addition of hydrazine so that the rate of reaction would remain constant during the entire run.

The amount of palladium deposited by a given quantity of hydrazine was found to vary with the operating conditions. A series of plating runs at various temperatures was performed at a palladium level of 10 g/l, a load of 560 cm² of surface, a plating volume of 700 ml, and an addition rate of 3 ml of 1M hydrazine/15 min. The amount of palladium deposited per unit of hydrazine in short time runs was found to be: at 25°C, 0.059 g/ml; at 35°C, 0.122 g/ml; at 45°C, 0.184 g/ml. These quantities also have been approached in long-time runs. If the equation

$$2Pd(NH_3)_4^{++} + N_2H_4 + 4OH^- \xrightarrow[\text{surface}]{\text{catalytic}} 2Pd^\circ + 8NH_3 + N_2 + 4H_2O$$

is correct this amount should theoretically be 0.213 g/ml.

The stability of used solutions during storage conditions is important in industrial applications. Solutions stored at room temperature appear to be stable if the palladium content is 0.0023M (0.25 g/l) in solutions containing higher concentrations of hydrazine, but are stable at higher concentrations of palladium if the hydrazine concentration is below 0.001M (0.032 g/l). Refrigeration of these plating solutions also prevents decomposition, but this may not be practical on a large scale. A number of spent solutions have been stored, replenished with palladium solution, and reused without difficulty.

Applications

Palladium deposited by barrel plating has been found to be ductile, pure, and adherent on suitable prepared substrates. The pretreatment scheme for some selected substrates is given in Table II.

Manuscript received Oct. 28, 1960; revised manuscript received March 7, 1961. This paper was prepared for delivery before the Houston Meeting, Oct. 9-13, 1960.

Any discussion of this paper will appear in a Discussion Section to be published in the June 1962 JOURNAL.

REFERENCES

1. R. N. Rhoda, *Trans. Inst. Metal Finishing*, **36**, 82 (1959).
2. R. N. Rhoda and A. M. Madison, U.S. Pat. 2,915,406, Dec. 1, 1959.

A Displacement Copper System for the Soldering of "Pure" Aluminum

Sheldon L. Matlow[1]

Intellux, Inc., Santa Barbara, California

A number of methods are available for the electroplating of solderable metals onto aluminum (1, 2). Recently a method of displacement plating of copper onto the α-phase of the aluminum-silicon system was reported (3). It was considered of interest, therefore, to develop a method of displacement plating copper onto "pure" aluminum. The designation "pure" is taken here to signify reagent grade purity. Since the ultimate goal of this study was the development of a convenient technique for the soldering of aluminum, no attention was given to the various factors considered when the plating is to be used as such. Thus, the entrainment of a fluxing material in the pores of the copper was of great utility. If the copper were to be used as a coating material, the entrained material would make the plating unsuitable.

Experimental

Materials used.—The aluminum was obtained from Baker and Adamson in the form of B & S gauge No. 14 wire, and is the A.C.S. reagent grade. After plating, the wires were "tinned" by dipping in a 200°C solder pot containing 60/40 Tin-Lead solder. It was found that no flux is necessary. Material entrained in the channels acts as a very efficient flux. The fluxing material is volatile as is shown by the evolution of gas during the solder-dipping operation. In order to retain the fluxing material long enough to obtain proper fluxing, it was found necessary to dip the wires into the solder quickly. However, once the wire is in the liquid solder, the soldering procedure is quite insensitive with respect to soldering time. In the testing procedure the "tinned" wires were soldered with 62 mil 60/40 solder cored with "Resin-Five" flux (Kester Solder Co., Chicago, Illinois).

Test procedure.— The "tinned" wires were soldered together with a ¼ in. overlap. One end was clamped in a vise. The other end was connected to a 0-50 lb spring scale. A force was applied slowly to the scale with the wires parallel to the floor. The reading of the scale when the joint yielded or when one of the wires broke was recorded. The scale reading was used as the measure of the solder bond strength.

Experimental results.—The procedure found to yield the greatest bond strengths consists of the following steps:

1. Degreasing. The wires were given a preliminary degreasing in 90°C perchloroethylene for 10-15 min, followed by an absolute methanol rinse and a deionized water rinse at room temperature;
2. Oxide removal. The gross oxide layer was removed by a room temperature dip in a 10*N* NaOH solution for 30 sec, followed by a deionized water rinse at room temperature;
3. "Sensitizing." The cleaned wires were given a 10-sec room temperature dip in 1.5 g $CuCl_2 \cdot 2H_2O$/100 ml H_2O to which two drops of concentrated HCl were added to clarify the solution;
4. Plating. The "sensitized" wires were placed directly into a room temperature bath of 14 g $CuCl_2 \cdot 2H_2O$/100 ml conc. aqueous NH_3 for 10 min; after the plating operation the wires are rinsed in deionized water and blown dry with filtered compressed air.

The reason for the necessity of the "sensitizing" treatment is not known; however, it was found that, without it, the ammoniacal copper plating was quite spotty. The ammoniacal copper was found to be necessary since the acidified copper does not adhere to the wire. If $CuSO_4$ is used in place of the $CuCl_2$, the plating does not adhere. The reason for the extreme difference in behavior between the sulfate and the chloride is not known. It is possible, however, that there is sufficient complexing with the chloride ion to slow down the rate enough to reduce the mossiness of the film.

The parameters investigated were: concentration of sodium hydroxide, time in sodium hydroxide, concentration of $CuCl_2 \cdot 2H_2O$ for "sensitizing," time in "sensitizer," concentration of $CuCl_2 \cdot 2H_2O$ in concentrated aqueous NH_3 and time in plating solution. The system was found to be remarkably insensitive to the variation of the parameters. An example of

Table I. Variable—concentration of ammoniacal $CuCl_2$

1. Concentration of NaOH = 10*N*; time in NaOH = 30 sec.
2. 1.5 g $CuCl_2 \cdot 2H_2O$/100 ml H_2O; time in "sensitizer" = 10 sec.
3. Time in ammoniacal $CuCl_2$ = 10 min.

	$CuCl_2 \cdot 2H_2O$/100 ml NH_4OH (conc.)					
	8 g	10 g	12 g	14 g	16 g	18 g
Strength in lb	Did not solder	23	20	26	24	17
		23	23	25	25	18
		21	25	25	25	16
		26	25	25	24	18
		24	22	25	20	19
		23				
Avg		23±1	23±2	25±0	24±1	18±1

[1] This report is based on studies made by the investigator while with the Semiconductor Division of the Hoffman Electronics Corp., El Monte, Calif.

this insensitivity is shown in Table I where the results for the variation of plating time are listed. These data represent the extremes of the variations observed.

Manuscript received Oct. 21, 1960; revised manuscript received Feb. 14, 1961. This paper was prepared for delivery before the Houston Meeting, Oct. 9-13, 1960.

Any discussion of this paper will appear in a Discussion Section to be published in the June 1962 JOURNAL.

REFERENCES

1. J. T. N. Atkinson, *This Journal*, **105**, 24 (1958).
2. R. F. Hafer, in "Metal Finishing Guidebook-Directory," 27th ed., p. 279, Metals and Plastics Publications, New Jersey (1959).
3. S. L. Matlow and H. J. Gould, *This Journal*, **108**, 198 (1961).

Measurement of Thickness of Electroplates Taking Advantage of the Impedance Change in the Stripping Cell

U. H. Narayanan, K. Sundararajan, and M. S. Kasabekar

Central Electrochemical Research Institute, Karaikudi, India

Of the various methods that are in vogue for the measurement of thickness of electroplated coatings, the anodic stripping method has been given considerable attention in recent years. Electronic instruments (1,2) have been devised to indicate exactly when the coating has been dissolved out, and the time taken for the dissolution of the coating is recorded automatically.

The present note describes a novel method based on the fact that the stripping cell impedance is altered suddenly at the moment when the coating is dissolved out completely. This method can be considered as an application of the "polarization titration" technique of Franck (3) or what is more appropriately referred to later (4, 5) as impedance titration.

The principle involved is essentially the same as for the anodic stripping method except that a small alternating current of about 1.5 ma (rms) was superimposed over the electrolyzing current. The alternating voltage across the cell was adjusted to a value of 150 mv (rms). When the stripping was just over, the ripple voltage across the cell suddenly changes due to a change in the impedance of the system. The drift in the a-c voltage across the cell during stripping was not greater than 10 mv (rms). This sudden change in the a-c voltage across the cell was made use of in actuating a relay by means

Table I

Amount of a-c ripple superimposed, mv, rms		Cd/Cu 150	Cd/Ms 150	Cr/Cu 150
Solutions used (6)		5% $KClO_3$ + 0.75% conc. HCl	5% $KClO_3$ + 0.75% conc. HCl	10% NaOH + 1.0M potassium chromate
D-C electrolyzing current, ma		10	10	8
Change in the ripple after stripping, mv, rms		150-180	150-250	150-120
Counter readings:	1	6467	2985	5418
	2	6481	2990	4655
	3	6322	3012	5187
	4	6368	2968	5018
	5	6340	2984	4166
(1000 counts of 50 cps pulses take 20 sec)	6	6457	2986	4377
	7	6371	3007	5274
	8	6387	3094	5410
	9	6387	3054	5423
	10	6447	3096	5266
	11	6300	2990	4124
	12	6405	3099	5378
Average thickness:				
(*a*) As calculated from the experimental results		0.226 thou	0.489 thou	0.112 thou
(*b*) As checked from microscopic measurements		0.211 thou	0.510 thou	0.105 thou
Precision obtainable*		±1.5%	±1.5%	±7%

* The precision obtainable corresponds to a maximum deviation from the mean at 99% confidence limit. The values indicated include both the error in the measurement and the error due to nonuniformity in the thickness of the coatings. In the case of chromium, the error is mostly due to nonuniformity of the coating.

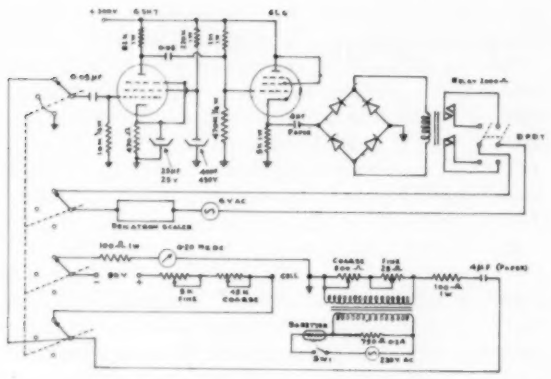

Fig. 1. Circuit diagram of electronic thickness measurement meter based on admittance change.

of a suitable electronic circuit as shown in Fig. 1. The relay stopped a Dekatron Scaler which was started at the same time as the constant current was switched on. The scaler was capable of measuring time to an accuracy of 0.02 of a second. It would be possible to arrange to read the thickness of the coating directly on the counting device by feeding a signal of proper frequency to the scaler. An advantage of this method lies in the fact that it involves a-c amplification and multistage amplification becomes easy.

The method and the instrument was put to test for chromium plating on copper base and for cadmium coatings on mild steel and copper. The data are presented in Table I.

Acknowledgment

The authors are grateful to Professor K. S. G. Doss, Director, Central Electrochemical Research Institute, for his keen interest and helpful suggestions in this work.

Manuscript received Oct. 3, 1960; revised manuscript received March 2, 1961.

Anv discussion of this paper will appear in a Discussion Section to be published in the June 1962 JOURNAL.

REFERENCES

1. H. J. Francis, *J. (and Trans.) Electrochem. Soc.*, **93**, 79 (1948).
2. S. Satyanarayana and D. L. Roy, *J. Sci. Ind. Res.*, **18A**, 75 (1959).
3. U. F. Franck, *Z. Elektrochem. Ber. Bunsen, Physki. Chem.*, **62**, No. 3 (1958).
4. K. Sundararajan and U. H. Narayanan, Unpublished work.
5. K. S. Narayanan and H. C. Gaur, To be published.
6. P. B. Mathur and M. L. Bhaskara Rao., To be published.

On the Theory of Electroluminescence Deterioration

P. M. Jaffe

Research Department, Westinghouse Electric Corporation, Bloomfield, New Jersey

It is well known that the output of an electroluminescent (EL) phosphor decreases with increasing operating time (1-4). In general, the luminescence appears to decrease in two steps, an initial rapid decrease followed by a slower decrease (4). In order to gain some understanding of the mechanism involved in this deterioration, glow curves were measured after increasing periods of operation of an EL cell. Thornton (3) has also studied glow curves of deteriorated phosphors, but he only examined a fresh and a well-aged phosphor.

The phosphor studied was a ZnS:Cu,Cl powder phosphor having green emission and showing relatively poor maintenance of output; similar results were also obtained with green ZnS:Cu,Br. The phosphor was incorporated in an EL cell, 5 mils thick, with plastic dielectric. The front electrode was tin oxide-coated glass and the back electrode was an evaporated layer of aluminum. The maintenance of output was measured at 4000 cps, 150 v rms. Glow curves were taken after field excitation (no ultraviolet used) at liquid nitrogen temperature, at 4000 cps, 150 v, in order to utilize the same phosphor volume as was involved in the maintenance determination; the phosphors were exposed to infrared radiation at room temperature in order to empty deep traps prior to cooling to liquid nitrogen temperature. The heating rate was 10-12°C/min.

The maintenance of this phosphor, as determined in a dry box having less than 5% relative humidity, is shown in Fig. 1.[1] Glow curves were taken after 0, 96, 600, and 1000 hr of operation and are shown in Fig. 2, curves A, B, C, and D, respectively. The glow curves have been normalized on the low temperature peak. Only the salient features will be considered here.

All the curves have in common a pronounced glow peak located around −145°C. The zero-hour glow

[1] Thornton (4) has shown that the maintenance is independent of humidity for a relative humidity less than 30%.

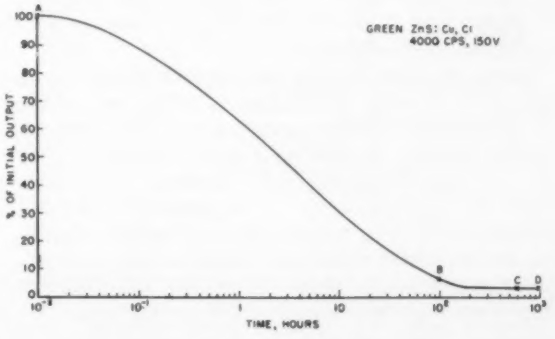

Fig. 1. Maintenance curve for a green electroluminescent ZnS:Cu,Cl powder phosphor.

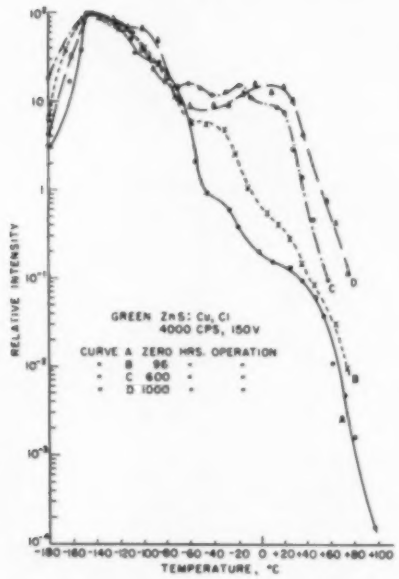

Fig. 2. Glow curves of the electroluminescent ZnS:Cu, Cl phosphor used in this study obtained after increasing periods of operation corresponding to points, A, B, C, and D of Fig. 1.

curve shows, in addition to the −145°C glow peak, several glow peaks (shoulders) at higher temperatures. In the 96-hr glow curve the −50°C glow peak has increased considerably relative to the −145°C peak. The 600-hr glow curve shows a further increase in the amplitude of the −50°C peak (actually measured at −60°C but this shift was due to the use of a slightly faster heating rate) and a very large increase in the intensity of the + 30°C peak. The 1000-hr glow curve shows a further increase in the amplitude of the +30°C peak while there is a slight decrease in the −50°C glow peak.

The important thing to note in these glow curves is that at the time when the phosphor has shown almost its maximum deterioration, point B in Fig. 1, the +30°C peak is not very pronounced, but there has been a marked increase in the −50°C peak.

Both Thornton (1, 3) and Roberts (2) have presented theories describing the electroluminescence deterioration mechanism. Neither theory, however, seems to explain the present glow curve data. The following hypothesis is advanced which explains Thornton's (1, 3, 4) and Robert's (2) data as well as the data presented here.

Under the influence of the applied electric field, the donor (halogen) is induced to diffuse away from its equilibrium position near the acceptor (copper) leaving behind in its place a sulfur vacancy, $V_s^{\cdot}$ or $(V_s^{\cdot})_n$ [using Hoogenstraaten's notation (5)].[3] This sulfur vacancy gives rise to the glow peak located around −50°C (5). The ultimate fate of this diffusing coactivator is not known at this time. It is this postulated diffusion of the donor with the resultant trap formation which causes the initial rapid decrease in light output (6). The slower component of the deterioration can be explained either by field-enhanced diffusion of oxygen into the lattice from the surface, eventually filling the sulfur vacancy left by the halide as suggested by Thornton (3),[3] and/or by the gross association of sulfur vacancies (7), $(V_s^{\cdot})_n$, where presumably $n > 2$. Either of these two hypotheses will explain the +30°C shoulder (peak) and is consistent with the data reported here.

If diffusion of the coactivator is important, then the use of Br or I as coactivator in place of Cl should result in improved maintenance since, other factors being equal, the larger the ionic size the slower the diffusion rate of the coactivator. This is illustrated by the following two experiments:

1. Phosphors containing the raw mix composition 0.1 atomic % Cu, 0.3 atomic % halide (Cl, Br, or I) result in the sequence of improved maintenance of Cl (green) < Br (green) < I (blue).[4] This is in spite of the fact that blue electroluminescent Cl- or Br-coactivated phosphors have much poorer maintenance than the corresponding green-emitting phosphors (4). This difference is not due to increased halogen retention (4) in the order Cl-Br-I since chemical analysis shows that the I-coactivated phosphor has less halide than either of the other two samples.

2. If the best-maintaining green EL ZnS:Cu,Cl and ZnS:Cu,Br phosphors prepared in this laboratory are compared, the latter phosphors are much better (by a factor of at least 5) in half-life; *i.e.*, the time needed to reach 50% of the initial output.

It should be mentioned that other factors influence the maintenance of electroluminescence such as the presence of moisture (4, 8), particle size (4), etc. It is felt, however, that anion diffusion is one of the major factors in deterioration.

Acknowledgments

The writer would like to thank Mr. G. Scanlon for his experimental aid in this project, Dr. W. A. Thornton for the many valuable discussions held with him, and Dr. H. F. Ivey for reading the manuscript and suggesting several improvements.

Manuscript received Feb. 6, 1961.

Any discussion of this paper will appear in a Discussion Section to be published in the June 1962 JOURNAL.

REFERENCES

1. W. A. Thornton, *Bull. Am. Phys. Soc.*, II, **1**, 30 (1956); *J. Appl. Phys.*, **28**, 313 (1957).
2. S. Roberts, *J. Appl. Phys.*, **28**, 262 (1957).
3. W. A. Thornton, "Solid State Physics in Electronics and Telecommunications," vol. 4, p. 658, Academic Press, New York (1960).
4. W. A. Thornton, *This Journal*, **107**, 895 (1960).
5. W. Hoogenstraaten, *ibid.*, **100**, 356 (1956).
6. W. A. Thornton, *Phys. Rev.*, **102**, 38 (1956).
7. W. Reichardt and G. Tappe, *Z. Naturforsch.*, **13**, 57 (1958).
8. I. L. Smith, R. Potter, and M. Aven, Paper presented at Electrochemical Society Meeting, Chicago, May 1-5, 1960.

[3] The idea of field-induced diffusion of the coactivator has also been postulated by Thornton (1, 3) and by Roberts (2) but utilizing a different mechanism from that presented here.

[4] Hoogenstraaten (5) has correlated this peak (actually at 45°C in his paper) with the presence of oxygen.

[4] Green EL ZnS:Cu,I apparently cannot be made, at least with normal methods of preparation.

The Use of Thermoelectric Effects during Crystal Growth

J. R. O'Connor[1]

Electronic Material Sciences Laboratory, Air Force Cambridge Research Laboratories, L. G. Hanscom Field, Bedford, Massachusetts

At a solid-liquid interface Peltier heat $\mathbf{J}\ \alpha\ T_m$ is either absorbed or evolved on the passage of a current density $\pm\ \mathbf{J}$. The quantity α is the difference between the absolute Seebeck coefficient of the solid and liquid phases at their melting point T_m. Ioffe (1) has suggested the use of Peltier cooling for an isothermal crystallization process and Pfann *et al.* (2) have used the effect to produce p-n junctions in Ge. This paper will consider only the use of Peltier cooling to increase the steady-state rate of crystallization V cm^3 sec^{-1} of a semiconductor growing from a melt. The rate V is given by $V = Af$ where A cm^2 is the cross-section area and f cm sec^{-1} is a linear growth rate. There are two specific areas where Peltier effects could be helpful: (*a*) for thermoelectric materials of low thermal conductivity k it is desirable to grow as large a crystal as possible for a given low growth rate, *i.e.*, the increase in V is given by $\Delta V = f\,\Delta A$; and (*b*) for the growth of films and dendrites (3) it is necessary to be able to produce large growth rates. In this case ΔV is given by $A\,\Delta f$.

Thermoelectric Effects

Consider the experimental apparatus of Fig. 1. A horizontal boat of length $S + L$ contains a solid in contact with its melt at $x = 0$. A heat source at $x = -L$ and a sink at $x = S$ provide the constant temperatures T_L and T_s, respectively. These contacts also allow a d-c current $\mathbf{J}A$ to be passed through the interface. For $\mathbf{J} = 0$, the interface is assumed to be stationary at $x = 0$ and the net heat flux across the interface is zero. That is

$$k_{s,m}\,G_s - k_{l,m}\,G_l = 0 \qquad [1]$$

where G is a thermal gradient at the interface and the subscripts s, l, and m refer to solid, liquid, and melting point, respectively. For $\mathbf{J} > 0$, the gradients in both the solid and liquid will change so as to satisfy Domenicali's equation (4) for a homogeneous material.

$$\nabla \cdot k\,\nabla T + \rho \mathbf{J} \cdot \mathbf{J} - \tau \mathbf{J} \cdot \nabla T = 0 \qquad [2]$$

A solution (5) to Eq. [2] for the solid phase is

$$k_{s,m}(G'_s - G_s) = \pm\, N_T \mathbf{J} < \tau_s > \Delta T_s - N_J \mathbf{J}^2 S < \rho_s > \qquad [3]$$

where G'_s is the new thermal gradient, ρ_s is the resistivity, τ_s is the Thomson coefficient, N_J and N_T represent the fraction of Joule and Thomson heats flowing into the interface and $\Delta T_s \equiv T_m - T_s$.

Each term of Eq. [3] is expressed in watts cm^{-2}. Values for N_J and N_T can be computed from

$$1 - N_{J,T} = \int_{T_s}^{T_m} \int_{T_s}^{T} F(T)dT\,dT / \Delta T_s \int_{T_s}^{T_m} F(T)dT \qquad [4]$$

where: $F(T) = \rho_s(T)\,k_s(T)$ for N_J; and, $F(T) = \tau_s(T)$ for N_T. Values for $N_{J,T}$ for various functions $F(T)$ are plotted against $t \equiv T_m/T_s$ in Fig. 2.

The current $\mathbf{J}A$ will move the interface to a new

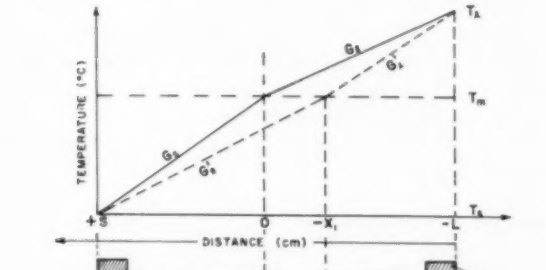

Fig. 1. Schematic diagram of the solid-liquid system. The G's are the themal gradients for $\mathbf{J}=0$. For $\mathbf{J}>0$ the G''s change to the G's.

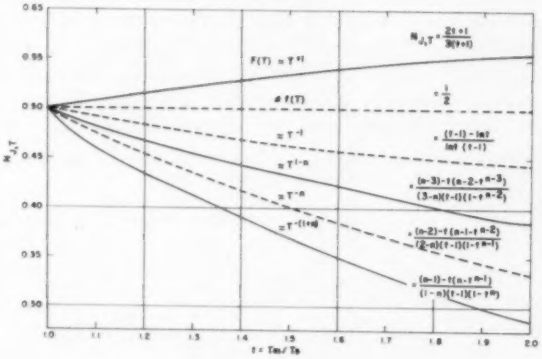

Fig. 2. Values of N_J and N_T for various temperature distributions F(T) are plotted as a function of $t \equiv T_m/T_s$. The quantity n is a constant that appears in the expression $\rho_s(T) = \rho_{s,m}\,(T_m/T)^n$. The expressions for N_J and N_T are only valid for values of t such that T_s is greater than the intrinsic conduction temperature. The curves were plotted using a value of $n = 3$.

[1] Present address: M.I.T. Lincoln Laboratory, Lexington, Mass.

equilibrium position $-x_1$, which is defined by $k_{s,m} G'_s - k_{l,m} G'_l = -\mathbf{J} \alpha T_m$, or allow the solid to be withdrawn at an increased rate Δf[2]. It is assumed that the melt is replenished at $x = -L$ so as to fix the interface at $x = 0$. The increase in the growth rate is given by

$$\Delta f = \mathbf{J}[\alpha T_m - \mathbf{J}(N_J < \rho_s > S + \tfrac{1}{2} \rho_l L) + N_T < \tau_s > \Delta T_s]/jdH \qquad [5]$$

where d g cm^{-3} is the density of the solid (at $T = T_m$), H cal g^{-1} is the latent heat and $j = 4.184$ converts calories to joules. In deriving Eq. [5] it has been assumed that: (a) the properties of the liquid are metallic so that $<\rho_l> = \rho_l$, $\tau_l = T d\alpha_l/dT \approx 0$ and $N_J = \tfrac{1}{2}$; (b) the heat carried by the moving interface is negligible; (c) the boundary conditions of Eq. [1] are not changed; and, [d] the Thomson, Peltier, and Joule heats remain uncoupled. Equation [5] can be differentiated to yield an optimum current density J_o given by

$$J_o = \frac{\alpha T_m + N_T < \tau_s > \Delta T_s}{2 N_J < \rho_s > S + \rho_l L} \qquad [6]$$

This current density will produce a maximum change in the growth rate, given by

$$\Delta f_{max} = J_o^2 (N_J < \rho_s > S + \tfrac{1}{2} \rho_l L)/jdH \qquad [7]$$

Values of the material parameters that appear in Eq. [6] and [7] are given for some semiconductors in Table I. The thermoelectric properties of the III-V materials were computed from the data of Blum (6, 7).

Effect of Thermal Conductivity on Peltier Cooling

The temperature distribution in the solid as well as values for N_J and $<\rho_s>$ will depend on the temperature dependence of k_s. For most semiconductors above the intrinsic temperature $k_s(T)$ can be expressed by $k_s(T) = (k_s)_{ph} + (k_s)_{el} \approx A/T + BT$. The temperature distribution in the solid, for a given set of boundary conditions, will depend on the relative magnitudes of A and B. Three limiting cases exist namely: (a) $k_s(T) \sim T^{-1}$; (b) $k_s(T) \sim T$; and, (c) $k_s(T) \neq f(T)$. For each of these cases an analytic expression can be obtained for the product $N_J <\rho_s>$ by using Eq. [4] and the expression $S <\rho_s> = \int_0^{T_m} \rho_s(x)dx = \int_{T_s}^{T_m} \rho_s(T)(dx/dT)dT$. For the case $k_s(T) =$ constant the product $N_J <\rho_s>$ is simply $\rho_{s,m} t/2$. For either of the other two cases $N_J <\rho_s>$ does not differ from this value by more than 4% (for $t \leq 2$). Physically the situation is as follows: a large thermal gradient in the solid increases Joule heating, but allows a smaller fraction of this heat to return to the interface. A small thermal gradient does just the opposite.

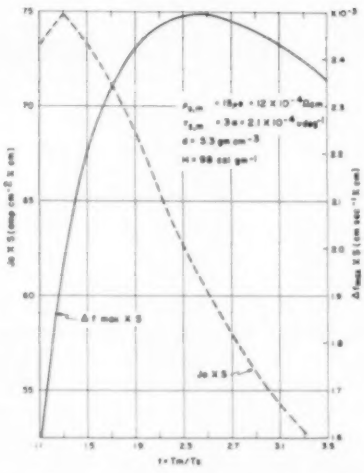

Fig. 3. Functions Δf_{max} and J_o vs. t are plotted using the material constants of Ge. A maximum in the current density occurs at $t = 1.3$. The quantity $\Delta f_{max} S$ is a maximum at $t = 2.4$. For Ge and a value of $S = 2$ cm this value of t is equivalent to a large thermal gradient of $\sim 350°$ cm^{-1}.

For most materials $\tau_s(T) \sim T^{-1}$ and the relation $\tau_s = \tau_{s,m} T_m/T$ is valid. The factor $N_J < \tau_s > \Delta T_s$ is equivalent to $\tau_{s,m}(1 - \ln t)/t - 1)$ which is independent of k_s. Equations [6] and [7] are, therefore, not dependent on the temperature dependence of k_s. These equations are plotted as a function of t in Fig. 3. The function $J_o S$ is a maximum when t satisfies the expression

$$[\ln \tau\,(2t - 1) - (t - 1)]/(t - 1)^2 = 1 + \alpha/\tau_{s,m}$$

For large $\tau_{s,m}$ the ratio $\alpha/\tau_{s,m} \to 0$ so that t is ≈ 2, i.e., it is desirable to use a large temperature gradient equal to T_s/S in order to use the maximum current density. As $\tau_{s,m}$ decreases the optimum value of t decreases. For Ge $\alpha/\tau_{s,m} \approx 1/3$ and $J_o S$ is a maximum at $t = 1 + 1/3$.

[2] Note that if the interface had been moving at a constant rate f_o for $J = 0$ the rate is now given by $f = f_o + \Delta f$.

Table I. Properties of some semiconductors at the melting point[1]

	T_m, °K	d, g cm^{-3}	H, cal g^{-1}	$\rho_{s,m} \times 10^6$, ohm-cm	$\rho_l \times 10^6$, ohm-cm	$\alpha \times 10^6$, v deg^{-1}	$\tau_{s,m} \times 10^6$, v deg^{-1}	J_o, amp cm^{-2}	Δf_{max}, cm sec^{-1}
Si	1693	2.3	336	3300	165	58	170	17	3×10^{-4} (1.1 cm/hr)
Ge	1209	5.3	98	1200	63	70	210	40	1×10^{-3} (3.6 cm/hr)
GaSb	993	7.0	63	5200	25	30	130	4	4×10^{-5} (0.1 cm/hr)
InSb	796	5.8	51	410	102	235	125	195	16×10^{-3} (58 cm/hr)

[1] The values of J_o and Δf_{max} were computed using the following values: $N_J = N_T = \tfrac{1}{2}$; $S = L = 2$ cm; and $\Delta T_s = 200$°K.

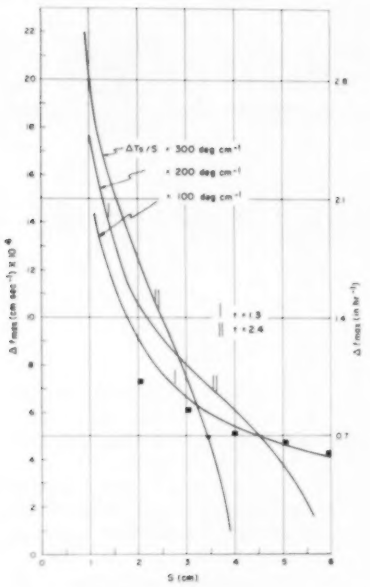

Fig. 4. Maximum growth rate of Ge due to Peltier effects is plotted as a function of distance S from the interface for various thermal gradients. Curves are plotted using the data of Fig. 3. The experimental points are the averages of at least three sets of data and should lie on the curve $\Delta T_o/S = 100°$ cm^{-1}.

Experimental Procedure

Several Ge crystals were grown from the melt by the Czochralski method under the following conditions: a Cu plated <111> seed was held in a Mo holder and rotated at 30 rpm; the linear growth rate was maintained constant at $f_o = 0.1$ cm hr^{-1}; the initial steady-state cross-section area of the crystals was ~0.8 cm^2; and a large melt was contained in a graphite crucible. The vertical temperature gradient in the growing ingot was ~100° cm^{-1}. The Mo seed holder was rotated in a Hg contact so that a d-c current J_oA could be passed through the solid-liquid interface. This current would be maintained until the area reached a new steady-state value. At this point the d-c voltage E was removed and the ingot returned to thermal equilibrium (with $J = 0$). This process would be repeated several times using a value of J_o from Fig. 3. After the ingot was removed from the furnace the area changes ΔA were measured and values of Δf_{max} were computed from the relation $\Delta f_{max} = f_o \Delta A/A$. Average values of Δf_{max} *vs.* S are plotted in Fig. 4. These values should lie on the curve for $\Delta T_o/S = 100°$ cm^{-1}. Plots of Δf_{max} *vs.* S are also shown for $\Delta T_o/S = 200°$ and 300° cm^{-1}.

Discussion

The agreement between theory and experiment for Δf_{max} *vs.* S is satisfactory for large values of S. For small values of S the experimental values of Δf_{max} are low. This may be due in part to Joule and/or Peltier heating at the interface between the seed and its holder.

The effect of steady-state Peltier cooling for a material like Ge is quite small. This is due primarily to the low value of α/dH. Table I, however, shows that this ratio is high for some compounds, *e.g.*, InSb. For these materials Peltier effects can be appreciable and may prove useful for various methods of crystal growth.

For any material Fig. 3 and 4 show that in order to obtain appreciable Peltier cooling it is necessary to keep S small and ΔT_o as large as possible. However, this requires a cooled, ohmic contact to be maintained near the interface. This contact will in general limit the efficiency of the process.

Acknowledgments

The writer is grateful to W. A. McLaughlin for most of the experimental data and to A. C. Yang for several helpful discussions.

Manuscript received Nov. 28, 1960; revised manuscript received March 10, 1961.

Any discussion of this paper will appear in a Discussion Section to be published in the June 1962 JOURNAL.

REFERENCES

1. A. F. Ioffe, *Zhur. Tekh. Fiz.*, **26**, 478 (1956).
2. W. G. Pfann, K. E. Benson, and J. H. Werwick, *J. Electronics*, **2**, 597 (1957).
3. E. Billig, *Proc. Roy. Soc. (London)*, **A229**, 346 (1955).
4. C. A. Domenicali, *J. Appl. Phys.*, **25**, 1310 (1954).
5. J. R. O'Connor, *ibid.*, **31**, 1690 (1960).
6. A. I. Blum, *Soviet Phys.-Solid State*, **5**, 696 (1959).
7. A. I. Blum and G. P. Ryabtsova, *ibid.*, **5**, 692 (1959).

Brief Communication

Germanium-Doped Gallium Arsenide Tunnel Diodes

R. Solomon[1]

Hughes Semiconductor Division

and R. Newman[2] and N. R. Kyle

Semiconductor Materials Department, Hughes Research Laboratories, Newport Beach, California

This communication describes a method for the preparation of degenerate p-type GaAs using germanium as the dopant. Tunnel diodes fabricated from this material exhibit electrical characteristics identical to those fabricated from Zn-doped material.

Recent work (1-4) has indicated that group IV elements have an amphoteric electrical behavior in III-V compounds. For example, germanium will act as either a donor or an acceptor in GaAs depending on whether it occupies, respectively, a gallium or an arsenic site in the lattice. The net electrical activity of the germanium will be determined by the fraction of germanium atoms at each of the two sites. The fraction of donors will be increased by any growth condition which maximizes the ratio gallium vacancies/arsenic vacancies. The fraction of acceptors will be increased similarly by a condition which minimizes this ratio. It is a relatively simple matter to minimize this ratio by growing GaAs from a gallium-rich solution, thereby forcing Ge to be predominantly an acceptor.

In our experiments, small crystals of GaAs were grown by cooling melts consisting of 90 parts (by weight) gallium, 6 parts arsenic, and from 3 to 15 parts germanium. The question as to the optimum proportions of the elements was not explored, nor were attempts made to produce large single crystal ingots. The GaAs grows in the form of platelets, approximately 4 mm on a side, with exceptionally flat faces. The platelets are separated from the gallium matrix by boiling in dilute HNO_3.

The tunnel diodes were fabricated using a gold plated Kovar tab for the base contact and a tin-tellurium pellet for the junction. Table I shows some representative parameters for the best diodes which have been prepared. Table II shows the dependence of the peak current densities on the per cent germanium added to the melt. The estimated carrier densities for the base region are derived from a comparison of the observed values of peak current density for Ge-doped and Zn-doped diodes.

[1] Present address: Varian Associates, Palo Alto, Calif.

[2] Present address: Aeronutronic Division, Ford Motor Company, Newport Beach, Calif.

Table I. Electrical characteristics for Ge-doped GaAs tunnel diodes with 15% Ge in the melt

J_p	= 15,000 amp/cm^2
I_p/I_v	= 15:1
V_v	= 1.0 v
V_p	= 0.1 v
r_s	= 2-3 ohms

Table II. Dependence of peak current density on the germanium concentration in the melt

% Ge	J_p, amp/cm^2	Estimated hole-conc.
3	50	10^{19}/cm^3
8	2×10^3	2×10^{19}
15	1.5×10^4	5×10^{19}

The small crystal size of the Ge-doped material precluded direct Hall measurement. It will be noted that the estimated carrier density is approximately proportional to the concentration of Ge in the melt. This may indicate both a constant segregation coefficient and a constant ratio of acceptor to donor activity for the Ge over the concentration range employed.

Because of the amphoteric behavior of germanium in GaAs, it is expected that this material would make an interesting starting point into an investigation of the observed instability in the I-V characteristic of GaAs tunnel diodes. Such an investigation is in progress at this laboratory.

Manuscript received Feb. 2, 1961. This research was supported by the U. S. Army Signal Corps.

Any discussion of this paper will appear in a Discussion Section to be published in the June 1962 JOURNAL.

REFERENCES

1. C. Kohn, S. A. Kulin, and B. L. Averbach, *Phys. Rev.*, **108**. 965 (1957).
2. O. G. Folberts and E. Schillman, *Z. Naturforsch.*, **12a**, 943 (1957).
3. J. M. Whelan, J. D. Struthers, and J. A. Ditzenberger, "Properties of Elemental and Compound Semiconductors," H. C. Gatos, Editor, pp. 141-154, Interscience Publishers, New York (1960).
4. J. O. McCauldin and R. Harada, *J. Appl. Phys.*, **31**, 2065 (1960).

Feature Section

The Changing Pattern of Industrial Research

Presidential Address*

Ralph A. Schaefer

Most industrial research organizations are actively engaged in studying natural or physical phenomena. These investigations are for the orderly accumulation, integration, and evaluation of new and old data which may have a pronounced influence on the economic life of the corporation. Research laboratories have become the distinguishing hallmark of progressive American business. Annual reports, press releases, and public addresses of corporation officials invariably extol the importance of research to the well-being of the company. Research is, in reality, creating something that does not now physically exist. These research laboratories are charged with the responsibility of bringing something into being which previously existed only in the minds of men. To be commercially successful, this something must fill a real or apparent human need, and desire must be pursued by the corporation that has both technological and distribution competence. Research studies in a free and competitive society have become synonymous with industrial stability and growth.

Research and development activities are big business. In 1959, our national research and development expenditures approached 12½ billion dollars, which is equivalent to approximately 2.6% of the gross national product. This sum is nearly twice the amount expended five years ago, and it is expected that this rate of increase will continue. Since there is considerable difficulty in separating research and development activities, because of their functional overlap, both are included. With time, it is very probable that the distinction between them will disappear.

During that same interval, the employment of technically trained personnel increased eight times faster than our total labor force. Although there may be individual company exceptions concerning the effectiveness of research, the funds employed generally appear to have been well spent.

As expected, any corporate function which has expanded rapidly will exert a significant influence on both the present and the future images of the corporation. Industrial research is no exception, for the academic freedom to study items arising from personal interest and curiosity has been replaced largely by programmed research. Also, this research activity is being integrated into the over-all business functions of industrial enterprise. Thus, the individual research worker, along with his ideas, has tended to be lost in the total group effort. As a result, most organized industrial research can be described as "team" or "directed" research. By definition, this type of work is an organized search for the solution of a well-defined technical problem without attempting to restrict the field of exploration. It is well established that directed research is the most economical procedure for creating products which do not exist.

As professional scientists and engineers, we can feel justifiably proud of the part that our respective technical disciplines have played in solving the problem of production. The solution of this problem appears even more dramatic when one paints the production picture against the background of history, for the application of known physical science data to the production of useful products has moved us from an economy of scarcity, which existed from the beginning of time, to one of superabundance in less than five generations. This period can be conveniently divided into two parts—the earlier 80 years, which can be attributed to the efforts of the individual research worker and "wood shed" inventor, and the latter forty years which can be credited to "team" research.

History of Organized Corporate Research

The father of organized and directed research was Thomas A. Edison, who, late in the 19th century, employed a paid staff of research workers or experimenters for the specific purpose of developing new products. Thus, he became the first research administrator to schedule and plan investigations to solve technical problems on proposed products which, when created, would serve a useful purpose. American industry began 30 years later to adopt the principle of planned research as a technique to speed the flow of new products. Another contributing factor, which favored large-scale investigations, was the scarcities created by World War I.

As with any social trend, the transition from one mode of operation to another is never complete. Thus, one can compare the creativity statistically on the basis of patents issued, from the research workers of highly organized industrial research laboratories to individuals, or small company research workers. For the period 1940-1960, Maurice Crews, Assistant Patent Commissioner, published his findings on this comparison. His data showed that 60% of the most important patents issued during that time were on ideas from individuals or small organizations, which filed only 40% of the patent applications. Further, the Crews report pointed out that in the same period over-all research and development activities had increased 6 to 12 times, depending on the particular industry, while patent applications increased only 15%. On the other hand, the published technical literature, both original researches and review articles, independent of inventions or patents, was produced principally by universities and large industrial research and development organizations.

Those data show quite clearly that the size of a research organization does not, as some sociologists claim, automatically increase creativeness by cross-fertilization

* Delivered at the Indianapolis Meeting, May 2, 1961.

of ideas within a group having various technical disciplines. Perhaps this means that the old adage "Necessity is the mother of invention" is as true today as when it was written some 300 years ago. Certainly, the individual research worker observes the need to create a product or process more clearly because of proximity to the problem than does his counterpart in a large organization, and he may act more effectively on these stimuli. Similarly, it is well known that under wartime conditions a nation can force progress because of the real and apparent need to win over the enemy.

Along with the apparent loss of individual creativity as indicated by inventions, a number of publicized personnel surveys have indicated that a majority of scientifically trained people in the physical sciences feel that management misuses their talents and misunderstands their needs and desires, and that they are poorly compensated, psychologically if not financially. In their opinion, management's only interest is to direct research for the generation of profit, rather than to provide them with some sort of extension curricula having academic freedom. To fit the concept that the best research is the least directed, the contenders of this thinking point to the individual creative scientists and engineers of the 18th and 19th centuries who made substantial technical contributions. While that is true, I seriously doubt that today we would have synthetic fibers, plastics, or atomic energy if the development of those products had depended on the individual efforts of purely academic scientists and engineers.

An additional item of growing concern in research planning is the high casualty ratio of technical ideas to worth-while products, processes, or services. Even with good preliminary technical review, only one in 550 initial ideas which pass the first screening will ever establish a market position and generate profits for the owners. On the one hand, there is continually rising research and development cost and on the other, decreasing creativity.

Social Implications of Technical Advances

During the Middle Ages, it was alleged that one of the principal reasons for killing common criminals was insufficient food, shelter, and clothing to support a noncontributing member of society. Contrast that with today, when we have four to five million people drawing unemployment compensation because our economy cannot utilize the fruits of its labors. We have sufficient technical capability to produce a superabundance of the necessities, plus the luxuries of life, but we do not have an adequate understanding of the social sciences involving human behavior and marketing to accomplish a more uniform distribution of our productive capacity. The problem appears to be one of closing the gap between production and consumption. Our current heavy military expenditures tend to hide the real extent of this gulf. When one compares the thousands of generations who faced continual privation and starvation with two or three generations enjoying plenty, it is understandable that this new era will require painful social adjustments. The beneficial effects of new products will not accomplish their purpose of raising overall living standards unless the physical and social sciences can solve their common problems with facts rather than opinions. We all desire more goods and services, but we don't know how to coordinate their technical production with their distribution.

Physical-Social Science Team

As already indicated, one of the major obstacles to more rapid technical advancement is our limited knowledge of human behavior. We need to develop our social science knowledge so that we can describe human behavior in the same scientific terms we now use to describe the behavior of an atom. Countless thousands of experimental observations have been made over the years to gain our present knowledge in physical science and engineering. It is sheer nonsense to expect that a comparable knowledge of social science and human reactions to new products will be acquired more easily.

At the present time, motivation research and marketing management are developing rapidly as an important segment of the social science field concerned with the distribution aspects of production. This area of scientific study is approximately two generations behind those of the physical sciences. To date, most of this data, which can be classified as market research, has been concerned primarily with the techniques of amassing and analyzing data rather than the factors we should study to clarify problems in human behavior. In other words, the scientific method of measuring, testing, and evaluating data is just beginning to show up in the social science spectra.

The Product Planner

In order to coordinate technical and marketing studies for maximum productivity with minimum risk, American industry is giving corporate stature to the product planner. Corporations are rapidly approaching the time when merely to create new products or improve present ones and leave their marketing to chance is not enough for survival, much less for growth. Every company in our industrial complex must fight to maintain or improve its market position against all other contenders. In reality, the product planner strives to anticipate the impact on human behavior of a product that has not yet been born. He charts technical data, interprets, and attempts to predict the social acceptance of new products in the distribution channels, before the corporation commits large sums to create products, processes, or services which people do not choose to buy. Generally speaking, nontechnically trained individuals are assuming leadership in directing this new industrial forward look. In most corporations, the product planner will be an individual trained in the social sciences or in liberal arts rather than in the physical sciences.

There appears to be a mental resistance among engineering-trained individuals against developing themselves for appointment to these key management positions. If we, who are trained in the physical sciences, do not accept the challenge to aid in solving the distribution problems with the same aggressive ingenuity that solved the production problem, then I fear that future research administrators will be trained in the art and science of distribution, rather than in the science of mathematics and its related fields.

About 25 years ago, a sales representative of a large chemical company approached a potential customer with a new product. After some preliminary investigations, the potential customer found the product to be unsuitable because of its limited solubility in any of the common solvents. On reporting this fact sometime later to the sales representative, he observed, "Well, we have developed a product that don't melt, don't dissolve, and don't sell." Now, some 20 years later, the product has established a market position because of those and other unique properties. However, I am quite sure that those who created and developed the product were both frustrated and disgusted at the time by the poor marketing results obtained by their employer. Certainly, the chance marketing of unsuccessful new products does

nothing for the morale of scientists and engineers whose ingenuity created them. If products are well planned and evaluated simultaneously in both technical and marketing areas, so that all weaknesses are eliminated early in gestation, creativity will be stimulated in the research laboratories. To quote Alexandre Dumas, "Nothing succeeds like success." For research administration is similar to a general's philosophy of battle—he fights to win. No scientist or engineer wants to see his or another's creation fail in the market place, especially when the fault is not his. Scientifically trained individuals coordinating the technical problems in both physical and social areas involving new product growth will tend to close the alleged gulf between the scientist and management. Their spokesmen can understand and interpret both points of view.

Technical Centers of Tomorrow

The technical center of the next generation is not likely to be a mere experimental research and development laboratory in the sense of creating new products. Rather it will become the corporate intelligence and nerve center for product stability and growth. Product distribution knowledge will be the nerve center which will control and guide the entire research and development activity. Both market and production considerations will influence the technical projects as they progress through the laboratory. Thus, marketing will become the sensing device responsible for direction of the technical centers toward products which will benefit the user and will be purchased at profitable price levels. To attain these objectives calls for extensive product planning, since good research is approximately 90% inspiration and only about 10% perspiration, or, if you will, 90% brain and 10% brawn. The social or human reactions to these new products will be evaluated at the beginning of the new-product cycle and will continue to influence the product from the cradle to a successful product launching or the grave. With research costs taking an increasing bite of the corporation's profits, the productivity of the laboratory will ultimately determine whether the corporation sustains itself and grows or slips backward in the competitive battle for survival.

Technical Society Contributions

Only a small number of technical societies have recognized that both production and distribution knowledge are essential to substantial new product growth. Most of the technical and engineering societies have viewed marketing data as current events or light reading. Publications of original physical science researches are generally considered on a higher intellectual plane than social science studies. It should be remembered that many of our physical science articles and publications of 50 or 75 years ago were not up to present research quality standards. Scientific progress resembles that of individuals—we think first as children then as adults. In the medical field, doctors are learning that both medicine and psychology are required to maintain the physical and mental health of their patients. Likewise, an industrial organization needs the knowledge of both physical and social scientists to provide the necessary information for corporate stability and product growth.

The Electrochemical Society

Over the years, our Society has demonstrated technical leadership in the electrochemical field. At the present time, an appointed committee of the Society is studying the problems involved in creating and financing a third publication. This publication would provide a medium for the convention papers that neither appear in the JOURNAL nor are compiled later in total or in part into monographs. It is my earnest hope that this publication will become a reality.

Once this publication has been established, the Society should encourage the presentation at conventions, and subsequent publication, of papers from the distribution field as well as from the technical areas of electrochemistry. In this way, our Society will be providing greater educational opportunities to its members. A broader knowledge of these interrelationships between engineering and distribution will permit the more economical flow of new products into the channels of distribution, where the results of our efforts are ultimately going to be measured. In the future, I, for one, hope that we, as scientists and engineers, will play an ever-increasing role in developing a more scientific approach to the problems of distribution.

FUTURE MEETINGS OF
The Electrochemical Society

Detroit, Mich., October 1, 2, 3, 4, and 5, 1961
Headquarters at the Statler Hotel
Sessions will be scheduled on
Batteries, Corrosion (including a Symposium on Surface Structure vs. Corrosion Behavior), Battery–Corrosion Joint Symposium on Fused Salt Corrosion, Electrodeposition (including symposia on Addition Agents and on Electrodeposited Magnetic Films), Electronics (Semiconductors), Electro-Organics, and Electrothermics and Metallurgy
(*See* August JOURNAL for complete program)

★ ★ ★

Los Angeles, Calif., May 6, 7, 8, 9, and 10, 1962
Headquarters at the Statler Hilton Hotel
Sessions probably will be scheduled on
Electric Insulation, Electronics (including Luminescence and Semiconductors), Electrothermics and Metallurgy, Industrial Electrolytics, and Theoretical Electrochemistry

★ ★ ★

Boston, Mass., September 16, 17, 18, 19, and 20, 1962
Headquarters at the Statler Hilton Hotel

★ ★ ★

Pittsburgh, Pa., April 14, 15, 16, 17, and 18, 1963
Headquarters at the Penn Sheraton Hotel

★ ★ ★

New York, N. Y., September 29, 30, and October 1, 2, and 3, 1963
Headquarters at the New Yorker Hotel

★ ★ ★

Toronto, Ont., Canada, May 3, 4, 5, 6, and 7, 1964
Headquarters at the Royal York Hotel

Papers are now being solicited for the meeting to be held in Los Angeles, Calif., May 6-10, 1962. Triplicate copies of each abstract (*not exceeding 75 words in length*) are due at Society Headquarters, 1860 Broadway, New York 23, N. Y., *not later than December 15, 1961* in order to be included in the program. *Please indicate on abstract for which Division's symposium the paper is to be scheduled, and underline the name of the author who will present the paper.* No paper will be placed on the program unless one of the authors, or a qualified person designated by the authors, has agreed to present it in person. An author who wishes his paper considered for publication in the JOURNAL should send triplicate copies of the manuscript to the Managing Editor of the JOURNAL, 1860 Broadway, New York 23, N. Y.

Presentation of a paper at a technical meeting of the Society does not guarantee publication in the JOURNAL. However, all papers so presented become the property of The Electrochemical Society, and may not be published elsewhere, either in whole or in part, unless permission for release is requested of and granted by the Editor. Papers already published elsewhere, or submitted for publication elsewhere, are not acceptable for oral presentation except on invitation by a Divisional program Chairman.

Current Affairs

Annual Report of the Board of Directors, April 1, 1960–March 31, 1961

(Presented at Society Business Meeting, Indianapolis, May 2, 1961)

Your Board of Directors has the following matters of special interest to bring to the attention of members of the Society.

Amendments to Constitution

Our attention has been called to the fact that the Articles of Incorporation of the Society, under the Membership Corporation Law of the State of New York, provides for the election of 19 members on its Board of Directors. For the past several years, we have been operating under a Constitution providing for 18 elected members, and an amendment will be submitted to our Annual Meeting today to provide for an increase in the number of Directors in order to comply with the provisions of our Articles of Incorporation.

Young Author's Prize and Francis Mills Turner Memorial Award for 1959

Young Author's Prize.—Dr. Franz A. Posey of the Oak Ridge National Laboratory, Oak Ridge, Tenn., was awarded the Young Author's Prize for 1959 for his paper entitled "Kinetic Studies on Corrosion Systems, I. Polyelectrodes under Activation Control" which appeared in the July 1959 issue of the JOURNAL.

Turner Memorial Award.—Dr. Robert G. Carlson, General Electric Co., Evendale, Ohio, was awarded the Francis Mills Turner Memorial Award for 1959 for his paper entitled "Tungsten Zone Melting by Electron Bombardment" which appeared in the January 1959 issue of the JOURNAL.

Honorable Mention.—Mr. Donald M. Smyth, Sprague Electric Co., North Adams, Mass., received Honorable Mention for 1959 for his paper "The Silver/Silver Chloride/Chlorine Solid Electrolytic Cell" which appeared in the August 1959 issue of the JOURNAL.

The winners of these Awards for 1960 will be announced at our Banquet this evening. [Further details will appear in the August 1961 JOURNAL.]

Assistance Awards for 1961

On recommendation of the Honors and Awards Committee, the Board of Directors approved of three Summer Assistance Awards for the period June-September 1961 to a fellow or teaching assistant pursuing work between a degree of B.S. and Ph.D. on a subject in the field of interest to The Electrochemical Society. These Awards are intended to cover a period for which the recipients have no financial support. [The recipients of the Assistance Awards for 1961 will be announced in the August 1961 JOURNAL.]

Society Finances

Special action was taken during the past year to augment Society income in order to cope with inflation and to carry on the Society's expanded program of activities and services to members. Active Membership Dues were increased from $15.00 to $20.00; Sustaining Membership Dues from $100.00 to $135.00; Nonmember Journal Subscription from $18.00 to $24.00; and Guest Registration Fee to our National Meetings from $13.00 to $20.00. It will be noted that all concerned have shared in these increases of an equitable basis. These are our principal sources of income.

Colin Garfield Fink Fellowship

Your Board of Directors is pleased to announce the acceptance of the contribution of $1000.00 from Dr. and Mrs. Henry B. Linford for the establishment of the Colin Garfield Fink Fellowship, and desires at this time, on behalf of the members of the Society, to express to Dr. and Mrs. Linford its sincere appreciation for this generous contribution and the purpose for which it will be used. [Further details will appear in a later issue of the JOURNAL.]

Society Organizational Structure

During the past several years, your Board of Directors has been increasingly concerned with improving the organizational structure of our Society so as to better serve the interests of its members. Our National Office is assuming increasing duties and responsibilities. Our Publication Committee at present is concerned with surveying areas of communication in order to more expeditiously disseminate information with respect to latest scientific and technical developments, and a special Technical Survey Committee has been appointed to review our technical development. All of these projects hold promise for the future growth and development of the Society.

Another project which the Board at present is considering is a review of the Bylaws of our various Divisions so as to bring about some degree of uniformity of procedures in all areas of interest. Efforts are being made in cooperation wtih our Divisional Officers to plan symposia two or three years in advance and to disseminate symposia subjects among all Divisions so that, in the event a mutuality of interest exists in a particular subject, an opportunity will be available for joint sponsorship.

National Convention Committee

During the past year, the Board of Directors approved an amendment to the Bylaws of the Society to provide for a permanent National Convention Committee. National Meetings of the Society are becoming larger and assuming such increasing importance that it was felt desirable to organize this on a National basis. This Committee will work in close relationship with our various host Sections, and the accumulated experience of our National Office will be placed at their disposal in organizing future National Meetings of the Society.

Ralph A. Schaefer, *Chairman*

Annual Report of the Secretary, April 1, 1960-March 31, 1961

(Presented at Society Business Meeting, Indianapolis, May 2, 1961)

It is a pleasure to review the progress which has been made by our Society for the fiscal year ending March 31, 1961.

Membership

The membership of the Society is at an all-time high with 3333 members. This compares with the previous year's total of 3124 and shows a net increase of 209.

Patron and Sustaining Membership

Corporate support in the form of Sustaining Memberships showed a net loss of 12 during the past year. The business recession undoubtedly accounted for some of the losses, while others are due to withdrawal of concerns whose business has changed to the extent that they no longer have a major interest in electrochemical industries.

Special Symposia

At our Indianapolis Meeting this week, a special symposium on Electrochemical Measurements and Instrumentation is being arranged by our Theoretical Division and is being supported by a grant from the National Science Foundation. Six speakers from overseas will present papers and participate in this meeting.

Journal of the Society

The JOURNAL of the Society continues to experience a continued period of growth, and our budget for the period 1961-1962 contains an increased appropriation in order to keep abreast of papers which have been cleared for publication.

Monographs and Special Publications

During the past year, the publication "Surface Chemistry of Metals and Semiconductors" containing the papers presented at our Columbus Meeting came off the press and now is being distributed. Others previously approved and now in various stages of production include: "Metal Iodides and Iodide Metals," "Primary Batteries," "Electrode Processes," "Iron Ores," "Rhenium," "Modern Electroplating" (Revised Edition), "High-Temperature Technology" (Revised Edition).

Consideration also is being given by the Corrosion Division and the Publication Committee to bringing the "Corrosion Handbook" up to date.

Edward Goodrich Acheson Award

On recommendation of the Honors and Awards Committee, Dr. Henry B. Linford was approved as the 1960 recipient of the Edward Goodrich Acheson Gold Medal and Prize.

Return Group Visit to the U.S.S.R.

It will be recalled that at our Chicago Meeting in the spring of 1960 the Society welcomed a delegation of scientists from the Soviet Union, including Professor Frumkin who was presented with the 1959 Palladium Medal Award. As a result of this visit, a delegation of four scientists from our country is at present in the Soviet Union on a return visit.

Second International Conferences on Passivity

An organizing committee has been appointed for the Second International Conference on Passivity which will be held in Canada in the fall of 1962. This Conference will be sponsored by our Society, the Faraday Society, and the Deutsche Bunsen-Gesellschaft. Our Society's representatives on the organization committee will be Dr. Morris Cohen, Dr. Norman Hackerman, and Dr. H. H. Uhlig. Papers presented at this Conference will be published in a special edition of the JOURNAL.

National Office

In accordance with the directives of our Board of Directors and the National Convention Committee established by our Board, Mr. Shannon, our Executive Secretary, has taken on the added responsibility of making the necessary hotel arrangements for conventions ten years in advance, to assure the availability of suitable facilities on the desired dates. All this is being done with the cooperation and assistance of Local Committees.

In closing, I would like to take this opportunity once again to commend our Executive Secretary and his staff for the excellent job they are doing at the National Office. Despite the fact that Mr. Shannon and his staff have accepted added responsibility during the past year, the office has continued to provide efficient, effective, and considerate service to the membership in all its functions.

Ivor E. Campbell, *Secretary*

Manuscripts and Abstracts for Spring 1962 Meeting

Papers are now being solicited for the Spring Meeting of the Society, to be held at the Statler Hilton Hotel in Los Angeles, Calif., May 6, 7, 8, 9, and 10, 1962. Technical Sessions probably will be scheduled on Electric Insulation, Electronics (including Luminescence and Semiconductors), Electrothermics and Metallurgy, Industrial Electrolytics, and Theoretical Electrochemistry.

To be considered for this meeting, triplicate copies of abstracts (*not exceeding 75 words in length*) must be received at Society Headquarters, 1860 Broadway, New York 23, N. Y., *not later than December 15, 1961. Please indicate on abstract for which Division's symposium the paper is to be scheduled and underline the name of the author who will present the paper.* No paper will be placed on the program unless one of the authors, or a qualified person designated by the authors, has agreed to present it in person. An author who wishes his paper considered for publication in the JOURNAL should send triplicate copies of the manuscript to the Managing Editor of the JOURNAL, 1860 Broadway, New York 23, N. Y.

Presentation of a paper at a technical meeting of the Society does not guarantee publication in the JOURNAL. However, all papers so presented become the property of The Electrochemical Society, and may not be published elsewhere, either in whole or in part, unless permission for release is requested of and granted by the Editor. Papers already published elsewhere, or submitted for publication elsewhere, are not acceptable for oral presentation except on invitation by a Divisional program Chairman.

Financial Statement of The Electrochemical Society, Inc.

Statement of Income and Expenses
April 1, 1960-March 31, 1961

	Budget 1960-1961 adjusted	General Fund	Society Reserve Fund
Income			
General Fund			
Membership Dues	$ 45,000	$ 56,125.04	
Patron and Sustaining Memberships	22,000	23,840.00	
Reprints	5,000	6,790.47	
Nonmember Journal Subscriptions	24,000	37,786.73	
Office Sale Journal and Publications	500	916.87	
Advertising	15,000	11,152.12	
Bound Volumes	3,000	2,165.60	
Conventions	9,000	10,070.76	
Interest Earned on General Funds	750	943.71	
	$124.250	$149,791.30	
Society Reserve Fund			
Nonmember Journal Subscriptions	$ 4,800		$ 5,198.70
Nonmember Convention Registrations	3,000		2,928.00
Monograph Royalties	2,500		2,549.82
Income from Investments	3,300		5,217.42
	$ 13,600		$15,893.94
Expenses			
Print and Mail Journal	$ 55,000	$ 54,161.08	
Salaries	57,400	57,058.18	
Rent	5,400	5,400.00	
Postage, Supplies, and Miscellaneous	8,000	9,406.08	
Bound Volumes	3,000	3,305.97	
Local Sections and Divisions	1,500	1,119.50	
Membership Directory	800	1,101.00	
Young Author's Prize	100	100.00	
New York Office Travel	4,000	3,277.53	
Presidential Office Fund	2,000	49.90	
Conventions: Program Booklets	2,200	1,542.40	
Materials, Supplies, Postage	2,000	2,054.53	
	$141,400		
Contingency Fund—1% Estimated Income	1,200		
	$142,600	$138,576.17	
Special Appropriation			
Joint Symposium Chicago Meeting	500		360.00
	$ 13,100		$15,533.94
Excess Income Over Expenses General Fund	−18,350	$ 11,215.13	
Income Credited to Society Reserve Fund	13,100	15,533.94	
Excess Income Over Expenses	−5,250	$ 26,749.07	
Capital Investments from General Fund Surplus			
New Office Equipment (Cumulative)	$ 600		
New Mailing Plate Machine	1,800		

Balance Sheet at March 31, 1961
Statement of Assets

Cash			
Chemical Bank New York Trust Company			
Electronics Division Monograph Fund		$ 427.29	
Corrosion Division Monograph Fund		1,770.80	
Electrodeposition Division Monograph Fund		1,600.05	
Electrothermics & Metallurgy Monograph Fund		1,529.82	
Theoretical Division Monograph Fund		1,858.97	
New Capital Equipment		315.98	
Colin Garfield Fink Fellowship Fund		273.75	
Consolidated Fellowship Fund		832.23	
Society Reserve Fund		11,523.32	
General Fund		5,913.79	
		$ 26,046.00	
Petty Cash Fund		103.36	
U.S.A. Treasury Bills—General Fund		19,916.70	
Excelsior Savings Bank—General Fund		9,362.06	
Greenwich Savings Bank—General Fund		9,667.48	
Chase Manhattan Bank Savings Account—General Fund		9,801.57	
First National City Bank Savings Account General Fund		10,055.83	$ 84,953.00
Investments (Value 3/31/61)			
Edward Goodrich Acheson Fund Securities	$ 38,739.01		
Savings Account	913.40	39,652.41	
F. M. Becket Memorial Award Fund Securities	20,926.56		
Savings Account	1,264.39	22,190.95	
Consolidated Fellowship Fund Securities		45,027.36	
Colin Fink Fellowship Fund Securities		730.00	
Joseph W. Richards Memorial Fund Savings Account		829.75	
Edward Weston Fellowship Fund Hanover Bank	524.77		
Securities	15,670.46	16,195.23	
General Portfolio of Investments Corrosion Division: Corrosion Handbook	19,935.88		
Stress Corrosion	260.00		
Electrodeposition Division	1,000.00		
Electrothermics & Metallurgy	4,000.00		
Society Reserve Fund	127,118.22	152,314.10	276,939.80
Other Assets			
Convention Advance		1,000.00	
Accounts Receivable		3,530.66	
Furniture and Fixtures	13,117.41		
Less Reserve for Depreciation	719.54	12,397.87	
Inventory		3,573.40	20,501.93
			$382,394.73

Statement of Liabilities and Surpluses

Liabilities

Accounts Payable	$ 5,004.25	
Deferred Income India Section	90.46	
Overseas Subscription Payable (DBG and Faraday)	2,013.49	
Life Memberships	2,268.21	
Federal and State Taxes Withheld	1,536.65	$ 10,913.06

Surpluses

Special Funds			
Edward Goodrich Acheson Fund	39,652.41		
F. M. Becket Memorial Award Fund	22,190.95		
Consolidated Fellowship Fund	45,859.59		
Colin Fink Fellowship Fund	1,003.75		
Joseph W. Richards Memorial Fund	829.75		
Edward Weston Fellowship Fund	16,195.23	125,731.68	
Division Monograph Funds			
Corrosion	21,966.68		
Electrodeposition	2,600.05		
Electronics	427.29		
Electrothermics & Metallurgy	5,529.82		
Theoretical	1,858.97	32,382.81	
Society Reserve Fund			
Surplus	123,107.60		
Net Income Received	15,533.94	138,641.54	
General Fund			
Surplus	65,045.91		
New Capital Equipment	315.98		
	65,361.89		
Less Advances:			
Electro-Organic Chemistry 500.00			
Technology of Columbium 481.65			
Vacuum-Metallurgy 113.94			
10-Year Index (1952-1961) 755.79	1,851.38		
	63,510.51		
Excess Income Over Expenses	11,215.13	74,725.64	371,481.67
			$382,394.73

General Portfolio of Investments

Value of Securities 3/31/60		$117,888.27
Additional Investments		
Society Reserve Fund:		
Interest and Dividend Shares	1,404.02	
New Purchases	11,027.36	12,431.38
Increased Value Securities 3/31/61		21,994.45
FUND VALUE 3/31/61		$152,314.10

Society Reserve Fund

Equity Value in General Portfolio 3/31/60			$ 92,692.39
Additional Investments			
*Interest and Dividend Shares	1,404.02		
New Purchases	11,027.36		12,431.38
Increased Value Securities 3/31/61			21,994.45
Equity Value in General Portfolio 3/31/61			$127,118.22
*Bank Credit Balance 3/31/60		8,420.76	
*Cash Dividends	3,813.40		
*Monograph Royalties	2,549.82		
*Convention Registration Fees	2,928.00		
*Journal Subscriptions	5,198.70	14,489.92	
		22,910.68	
Less New Securities Purchased	11,027.36		
Less Special Symposium Expense	360.00	11,387.36	
Bank Credit Balance 3/31/61			11,523.32
FUND VALUE 3/31/61			$138,641.54

*Total Income from Sources Indicated $15,893.94

Division Monograph Funds

Corrosion Division

Equity Value in General Portfolio 3/31/60			$ 20,195.88
Bank Credit Balance 3/31/60	1,899.65		
Monograph Royalties	1,814.55	3,714.20	
Palladium Medal Expense	1,100.00		
Corrosion Research Council	743.40		
Petty Cash Advance	100.00	1,943.40	
Bank Credit Balance 3/31/61			1,770.80
FUND VALUE 3/31/61			$ 21,966.68

Electrothermics and Metallurgy Division

Equity Value in General Portfolio 3/31/60		4,000.00
Bank Credit Balance 3/31/60	879.60	
Monograph Royalties	650.22	
Bank Credit Balance 3/31/61		1,529.82
FUND VALUE 3/31/61		$ 5,529.82

Electrodeposition Division

Equity Value in General Portfolio 3/31/60		1,000.00
Bank Credit Balance 3/31/60	1,449.57	
Monograph Royalties	150.48	
Bank Credit Balance 3/31/61		1,600.05
FUND VALUE 3/31/61		$ 2,600.05

Electronics Division

Bank Credit Balance 3/31/60	137.44	
Monograph Royalties	289.85	
Bank Credit Balance 3/31/61		$ 427.29

Theoretical Electrochemistry Division

Bank Credit Balance 3/31/60	1,546.20	
Monograph Royalties	312.77	
Bank Credit Balance 3/31/61		$ 1,858.97

Special Funds

Edward Goodrich Acheson Fund

Value Securities 3/31/60		$33,977.12
New Securities Purchased		1,972.94
		35,950.06
Increased Value Securities 3/31/61		2,788.95
Value of Securities 3/31/61		$ 38,739.01
Savings Account Balance 3/31/60	3,564.17	
Dividends from Investments	1,497.49	
Interest on Savings Account	91.94	
	5,153.60	
Less Purchase Securities	1,972.94	
Acheson Award Expenses	2,267.26	4,240.20
Savings Account Balance 3/31/61		913.40
FUND VALUE 3/31/61		$ 39,652.41

Consolidated Fellowship Fund

Value Securities 3/31/60		$ 39,118.69
Dividend Shares		1,252.00
		40,370.69
Less Securities Sold		23.30
		40,347.39
Increased Value Securities 3/31/61		4,679.97
Value Securities 3/31/61		$ 45,027.36
Bank Credit Balance 3/31/60	$ 250.00	
Cash Dividends	1,225.60	
Securities Sold	23.30	
	1,498.90	
Less 1960 Assistance Award	666.67	
Bank Credit Balance 3/31/61		832.23
FUND VALUE 3/31/61		$ 45,859.59

F. M. Becket Memorial Award Fund

Value Securities 3/31/60		$15,297.37
New Securities Purchased		688.00
Increased Value Securities 3/31/61		4,941.19
Value Securities 3/31/61		$ 20,926.56
Savings Account Balance 3/31/60	$ 1,364.45	
Dividends on Investments	546.32	
Interest Accrued	41.62	
	1,952.39	
Less New Securities Purchased	688.00	
Savings Account Balance 3/31/61		1,264.39
FUND VALUE 3/31/61		$ 22,190.95

Colin Garfield Fink Fellowship Fund

Securities Contributed December 1960	$ 732.50	
Less Value 3/31/61	2.50	
Value of Securities 3/31/61		$ 730.00
Cash Donated	$ 267.50	
Dividend on Investment	6.25	
Bank Credit Balance 3/31/61		273.75
FUND VALUE 3/31/61		$ 1,003.75

Edward Weston Fellowship Fund

Value Securities 3/31/60	$14,428.22	
Increased Value Securities 3/31/61	1,242.24	
Value of Securities 3/31/61		$ 15,670.46
Dividends on Investments	$ 524.77	
Checking Account Balance 3/31/61		524.77
FUND VALUE 3/31/61		$ 16,195.23

Joseph W. Richards Memorial Fund

Savings Account Balance 3/31/60	$ 799.49	
Interest Accrued	30.26	
FUND VALUE 3/31/61		$ 829.75

Certificate of Audit

I have examined the balance sheet and statement of income and expenses of The Electrochemical Society, Incorporated, for the period April 1, 1960 to March 31, 1961. My examination was made in accordance with generally accepted auditing standards and, accordingly, included such tests of the accounting records as were considered necessary.

In my opinion, the balance sheet and statement of income and expenses present fairly the financial position of The Electrochemical Society, Incorporated, at March 31, 1961, in conformity with generally accepted accounting principles applied on a basis consistent with that of the preceding year.

(Signed) N. W. Marinelli, *Auditor*

Section News

Council of Local Sections

At the Indianapolis Meeting of the Society, April 29-May 3, 1961, the following were elected officers of the Council of Local Sections for the year 1961-1962:

Chairman—J. C. White (Washington-Baltimore), 4205 Woodberry St., University Park, Hyattsville, Md.; 1-year term

Vice-Chairman—R. F. Bechtold (San Francisco), 3725 Bon Homme Way, Concord, Calif.; 1-year term

Secretary—S. W. Scott (Niagara Falls), 1097-98th St., Niagara Falls, N. Y.; 1-year term

Representative on Board of Directors—A. J. Cornish (Pittsburgh), Westinghouse Research Labs., Beulah Rd., Churchill Boro., Pittsburgh, Pa.; 2-year term

N. C. Cahoon (Cleveland) still has one year to serve of his term as Representative on the Board of Directors.

R. F. Bechtold, *Secretary*

Detroit Section

At the Annual Meeting of the Detroit Section on May 9, the following officers were elected for the 1961-1962 season:

Chairman—Seward E. Beacom, General Motors Corp., Research Labs., 12 Mile & Mound Rds., Warren, Mich.

1st Vice-Chairman (Program)—A. Albert Johnson, Metal & Thermit Co., 1700 E. Nine Mile Rd., Ferndale, Mich.

2nd Vice-Chairman (Membership)—Leland M. Morse, Dept. of

Electrochemistry, Central Engineering Div., Chrysler Corp., 12800 Oakland, Highland Park 3, Mich.

Secretary-Treasurer—Ann G. Piken, Bendix Corp., Research Lab. Div., Southfield, Mich.

Councilor—A. Edward Remick, Dept. of Chemistry, Wayne State University, Detroit, Mich.

The term of Councilor Frank Passal, who was elected a year ago, extends through this coming year.

The Detroit Section recently amended its Bylaws to add a new class of membership, that of Honorary Detroit Section Member, to be awarded as a recognition of long years of service to the Section and the science of electrochemistry.

Ann G. Piken, *Sec.-Treas.*

New York Metropolitan Section

The Section's final technical meeting of the year was held at Victor's Restaurant in New York City on April 19, 1961. Speaker of the evening was Richard N. Rhoda, supervisor of the Platinum Metals Section, Research Lab., International Nickel Co., Inc. Dr. Rhoda discussed the first successful methods for the electroless deposition of thick coatings of palladium.

Palladium can be deposited on properly prepared substrates by chemical reduction of a complex palladium salt. This salt is dissolved in ammonium hydroxide containing a stabilizing agent, and a solution of hydrazine is used as the reducing agent. Deposition begins when the article to be plated is immersed. Since the process is catalytic and the palladium deposit is a catalyst, deposition continues until the ingredients are exhausted or the article is removed. Coatings up to 2.5 mils thick have been produced by this method on geometrically complex surfaces.

Dr. Rhoda discussed operating conditions for barrel plating and the precautions to be taken to prevent spontaneous decomposition of the bath during plating or storage. He also mentioned possible applications of the coatings in the electronic and chemical industries.

J. L. Everhart

Pacific Northwest Section

As a result of a recent letter ballot of Pacific Northwest Section membership for the office of Secretary-Treasurer to fill a vacancy arising from the resignation of Dr. Lawrence Young from this post, the following are the current officers (1961-1962) of the Section:

Chairman—Henry J. Wittrock, Dept of Metallurgical Research, Kaiser Aluminum & Chemical Corp., Spokane 69, Wash.

Vice-Chairman—Glen C. Ware, 1343 Alta Vista Dr., Corvallis, Ore.

Secretary-Treasurer — John A. Ayres, 1419 Wright Ave., Richland, Wash.

H. J. Wittrock, *Chairman*

Pittsburgh Section

The annual joint meeting of the Pittsburgh Branch of the American Electroplaters' Society and the Pittsburgh Section of The Electrochemical Society was held on April 12 at the Gateway Plaza in Pittsburgh, Pa.

C. L. Faust, chief, Electrochemical Engineering, Battelle Memorial Institute, Columbus, spoke on "Some Metallurgical Aspects of Protective Coatings for High Temperatures." Slides were used to show that the surface of a material was not necessarily the same as the bulk, and he described the effects of various methods of surface preparation on the electrodeposit placed on it. He pointed out that the type of plating bath in which the surface is coated will affect its performance.

After a brief description of the difficulties encountered when using plated parts at high temperatures, such as the formation of brittle alloys or evaporation of the bulk material through the coating, Dr. Faust reported several instances where preplating the surface with some other material prevented the undesirable reactions from taking place.

As an additional note of interest, the ECS Pittsburgh Section has participated in the Buhl Planetarium School Science Fair this year, and presented a reward of $25.00 to one of the high school students in the Pittsburgh area. The Section also makes an annual award of $50.00 to a graduate student engaged in electrochemical research in the Pittsburgh area. This year, the recipient of the award is E. G. Coleman of the Carnegie Institute of Technology. Mr. Coleman will present a résumé of his research at the Spring Meeting of the Pittsburgh Section on May 19, at which time he will be presented with his award.

E. J. Smith, *Sec.-Treas.*

San Francisco Section

At the March 29 meeting of the San Francisco Section, in the Men's Faculty Club, University of California, Berkeley, Dr. Ralph Schaefer spoke in two capacities. As President of the Society, he discussed the Society's growth and its publications. As a scientist, he listed eight areas of future development in electrochemistry, and considered in particular the present and future activities in electrodeposition.

Various problems in this field, such as unsatisfactory throwing power and roughness of deposit, have led to specific experimental work which he discussed. Such experiments have led to improved knowledge and control of relevant variables in the electrodeposition process.

Worden Waring, *Vice-Chairman*

Notice to Members and Subscribers

(Re Changes of Address)

To insure receipt of each issue of the JOURNAL, please be sure to give us your old address, as well as your new one, when you move. Our records are filed by states and cities, not by individual names. The Post Office does not forward magazines.

We should have this information *by the 16th of the month* to avoid delays in receipt of the next issue.

New Members

In May 1961, the following were elected to membership in The Electrochemical Society by the Admissions Committee:

Active Members

W. A. Albers, Jr., Research Labs., Bendix Corp., Southfield, Mich. (Electronics—Semiconductors)

F. C. Anson, California Institute of Technology, Pasadena, Calif. (Battery, Electro-Organic, Theoretical Electrochemistry)

G. R. Argue, Texas Research & Electronics; Mail add: 1606 Salem Dr., Richardson, Texas (Electronics—Semiconductors)

K. M. Arnold, General Telephone & Electronics Lab., Bayside, N. Y. (Electronics)

R. H. Atkinson, Westinghouse Electric Corp.; Mail add: 62 Oakwood

By action of the Board of Directors of the Society, all prospective members must include first year's dues with their applications for membership.

Also, please note that, if sponsors sign the application form itself, processing can be expedited considerably.

Court, Fanwood, N. J. (Electrothermics & Metallurgy)

S. S. Baird, Texas Instruments, Inc.; Mail add: 506 Lois Lane, Richardson, Texas (Corrosion, Electronics—Semiconductors, Theoretical Electrochemistry)

E. P. Barbaro, Westinghouse Electric Corp.; Mail add: 15 Circle Dr., Delmont, Pa. (Electronics—Semiconductors)

R. D. Bedi, Metal & Thermit Corp.; Mail add: 21900 Blackstone, Oak Park 37, Mich. (Corrosion, Electrodeposition)

Irvin Berman, U. S. Air Force Research Center-CRRCSA-1; Mail add: 172 Redington St., Swampscott, Mass. (Electronics—Semiconductors)

David Boies, Armour Research Foundation, Illinois Institute of Technology; Mail add: 10605 S. Wood St., Chicago 43, Ill. (Battery, Corrosion)

J. F. Brady, McDonnell Aircraft Corp.; Mail add: 211 W. Jewel, Kirkwood 22, Mo. (Electrodeposition)

R. A. Broker, Union Carbide Metals Co., Mail add: 708 Ward St., Devola, Marietta, Ohio (Industrial Electrolytic)

M. G. Cowart, P. R. Mallory & Co., Inc.; Mail add: 309 S. Division St., Du Quoin, Ill. (Electronics)

G. R. Dimeler, Sun Oil Co.; Mail add: 1333 Memory Lane, West Chester, Pa. (Battery Theoretical Electrochemistry)

F. M. Donahue, Jr., Stanford Research Institute; Mail add: 1718-C Meridian Ave., South Pasadena, Calif. (Battery, Corrosion, Theoretical Electrochemistry)

D. A. Duffy, General Chemical Div., Allied Chemical Corp., P. O. Box 70, Morristown, N. J. (Electronics)

S. R. Faris, Socony Mobil Oil Co., Inc., Box 900, Dallas, Texas (Battery, Electro-Organic)

S. S. Fry, Fansteel Metallurgical Corp.; Mail add: 1648 Victoria, North Chicago, Ill. (Electric Insulation, Electronics—Semiconductors)

L. R. Griffith, California Research Corp.; Mail add: 852 Gelston Place, El Cerrito, Calif. (Battery, Theoretical Electrochemistry)

Charles Grun, Yardney Electric Corp.; Mail add: 86-25 Van Wyck Expressway, Jamaica 35, N. Y. (Battery)

E. D. Haidemenakis, R.C.A. Semiconductor and Materials Div.; Mail add: 77 Chester Circle, New Brunswick, N. J. (Electronics—Semiconductors and Luminescence)

M. S. Hall, Physical Research Dept., National Cash Register Co., Dayton 9, Ohio (Electronics—Luminescence)

K. R. Hill, P. R. Mallory & Co., Inc., 3029 E. Washington St., Indianapolis, Ind. (Battery, Electro-Organic, Theoretical Electrochemistry)

J. F. Hinton, Leeds & Northrup Co., Research and Development; Mail add: 214 S. Jessup St., Philadelphia 7, Pa. (Electronics)

J. R. S. Johnson, Transitron Electronic Corp.; Mail add: 213 Humphrey St., Marblehead, Mass. (Electric Insulation)

P. A. Joyner, Minneapolis-Honeywell Regulator Co., 2754 4th Ave. S., Minneapolis, Minn. (Battery)

S. W. Kessler, Jr., R.C.A.; Mail add: Box 305, R.D. 1, White Haven, Pa. (Electronics—Semiconductors)

Mary P. King, Melpar, Inc.; Mail add: 24 S. Old Glebe Rd., Arlington 4, Va. (Electronics—Semiconductors and Luminescence, Electrothermics & Metallurgy)

H. W. Koren, Airborne Instruments Lab., Div. Cutler-Hammer; Mail add: 9 Cider Mill Lane, Huntington, L. I., N. Y. (Electronics—Semiconductors)

M. L. Loehr, Burroughs Corp., Research Center; Mail add: Stafford House, 5555 Wissahickon Ave., Philadelphia 44, Pa. (Electronics—Semiconductors)

A. E. Lyall, Gulton Industries, Inc.; Mail add: 262 Clinton Ave., North Plainfield, N. J. (Battery)

R. T. Macdonald, California Research Corp., 576 Standard Ave., Richmond, Calif. (Battery, Theoretical Electrochemistry)

Alfred Mayer, R.C.A. Semiconductor Div.; Mail add: 819 Penn Place, Plainfield, N. J. (Electronics—Semiconductors)

R. F. Merkert, Union Carbide Metals Co.; Mail add: 231 Callodine Ave., Buffalo 26, N. Y. (Electrothermics & Metallurgy)

L. C. Moore, Electric Storage Battery Co., Missile Battery Div., P. O. Box 11301, Raleigh, N. C. (Battery)

W. J. Musgrave, John E. Fast & Co.; Mail add: 731 Prospect Ave., Winnetka, Ill. (Electric Insulation)

M. J. Nelson, Pennsalt Chemicals Corp.; Mail add: 750 Conifer Lane, Calvert City, Ky. (Industrial Electrolytic)

W. E. Parker, Speer Carbon Co., Packard Rd., Niagara Falls, N. Y. Industrial Electrolytic)

R. B. Penland, Kaiser Aluminum & Chemical Corp., Dept. of Metallurgical Research, Spokane 69, Wash. (Corrosion, Electrodeposition, Theoretical Electrochemistry)

R. A. Perfetto, Westinghouse Electric Corp.; Mail add: 604 Hillside Dr., Pittsburgh 35, Pa. (Electronics—Semiconductors)

Robert Pikovnik, General Electric Co.; Mail add: 3646 Freemont Rd., South Euclid 21, Ohio (Electronics—Luminescence)

G. E. Pittman, Texas Instruments, Inc., Box 5012, Sta. 9, Dallas 22, Texas (Electronics—Semiconductors)

W. M. Portnoy, Texas Instruments, Inc., Box 5012, Dallas 22, Texas (Electronics—Semiconductors)

J. E. Powderly, Eagle-Pitcher Co.; Mail add: 1118 Elm, Miami, Okla. (Electronics—Semiconductors)

R. M. Roe, U. S. Naval Research Lab.; Mail add: 6705-41st Ave., University Park, Md.

Theoretical Division Enlarged Abstract Booklet Spring 1961

The Theoretical Electrochemistry Division has available a number of copies of the "Enlarged Abstract" booklet containing 1000-word abstracts of papers presented before the Theoretical Division symposia during the Indianapolis Spring Meeting of the Society, April 30 to May 3, 1961.

The booklet contains about 100 pages and includes the abstracts of the Symposium on Electrochemical Instrumentation which was sponsored by the National Science Foundation. Six foreign speakers participated at this meeting.

The price is $2.50 per copy. Checks should be made payable to: Theoretical Division, The Electrochemical Society. Booklets are available from:

P. Rüetschi
Electric Storage Battery Co.
Research Center
Yardley, Pa.

F. N. Ruehlen, Phillips Petroleum Co.; Mail add: 1446 Elm, Bartlesville, Okla. (Battery)

M. J. Schlatter, California Research Corp., 576 Standard Ave., Richmond, Calif. (Battery, Electro-Organic, Theoretical Electrochemistry)

J. B. Schroeder, Ohio Semiconductors Inc.; Mail add: 1615 Hess Blvd., Columbus 12, Ohio (Electronics—Semiconductors)

R. S. Shwartz, I.B.M. Corp., Boardman Rd., Poughkeepsie, N. Y. Electronics—Semiconductors)

K. E. Shull, Philadelphia Suburban Water Co., 762 Lancaster Ave., Bryn Mawr, Pa. (Industrial Electrolytic)

S. M. Sokalski, Allied Research Products, Inc., Mail add: 23460 Manistee, Oak Park 37, Mich. (Electrodeposition)

A. D. Squitero, International Nickel Co., Inc. 67 Wall St., New York 5, N. Y. (Electrodeposition)

M. E. Stanton, Delco Radio Div., General Motors Corp.; Mail add: 400 S. 139 West, Kokomo, Ind. (Electronics)

Toshihiko Suzuki, Westinghouse Electric Corp., Semiconductor Dept.; Mail add: 307 S. Maple Ave., Greensburgh, Pa. (Electronics—Semiconductors)

C. E. Tirrell, Ionics Inc.; Mail add: 55 Willow Rd., Nahant, Mass.

G. H. Turner, Consolidated Mining & Smelting Co. of Canada Ltd.; Mail add: Box 362, Trail, B. C., Canada (Electronics—Semiconductors)

R. W. Vreeland, P. R. Mallory & Co., Inc., Indianapolis 6, Ind. (Electronics)

G. G. Wald, Lockheed Aircraft Corp., Burbank, Calif. (Corrosion)

J. E. Wardill, Mining & Chemical Products Ltd.; Mail add: Englefield Lodge, Middle Hill, Egham, Surrey, England (Electronics—Semiconductors, Electrothermics & Metallurgy)

A. J. Warner, Aerovox Corp., Box 147, Marion, Mass. (Electric Insulation)

Harry Weisberg, R.C.A.; Mail add: 65 Yeager Ave., Forty Fort, Pa. (Electronics—Semiconductors)

C. E. Welch, Jr., Sprague Electric Co., Lansing, N. C. (Electrodeposition, Electronics)

C. L. Wellington, Wellington Electronics Inc.; Mail add: 274 Van Nostrand Ave., Englewood, N. J. (Electric Insulation, Industrial Electrolytic)

F. G. Will, General Electric Co.; Mail add: 410 Robinson St., Schenectady, N. Y. (Theoretical Electrochemistry)

I. W. Wolf, General Electric Co.; Mail add: 9 Damson Rd., Liverpool, N. Y. (Electrodeposition, Electronics—Luminescence, Electro-Organic, Theoretical Electrochemistry)

T. J. Yu, Korea Storage Battery Co.; Mail add: 396 Tapsimri-Dong, Tongdaemoon-Ku, Seoul, Korea (Battery)

M. I. Zwelling, Line Materials Industries; Mail add: 2040 Norwood Blvd., Zanesville, Ohio (Electric Insulation)

Associate Members

B. S. Baker, Lockheed Aircraft Corp.; Mail add: 609 Grand Fir Ave., Sunnyvale, Calif. (Battery, Theoretical Electrochemistry)

W. A. Beaton, Sylvania Electric Co.; Mail add:: 19 Linden St., Lynn, Mass. (Electronics)

V. O. Hinkle, Jr., Texas Instruments, Inc.; Mail add: 1214 Magnolia Dr., Richardson, Texas (Electronics)

P. C. Whitman, General Electric Co.; Mail add: R.D. 1, Route 5, Weedsport, N. Y. (Electronics)

Student Associate Members

D. R. Rhodes, 314 B, Noyes Lab., University of Illinois, Urbana, Ill. Theoretical Electrochemistry)

K. I. Vasu, Dept. of Inorganic and Physical Chemistry, Indian Institute of Science, Bangalore 12, India (Corrosion, Electrodeposition, Electrothermics & Metallurgy, Theoretical Electrochemistry)

E. L. Vetor, Purdue University; Mail add: R.R. 1, Yorktown, Ind. (Battery)

Reinstatement to Active Membership

G. G. Hatch, W. S. Atkinson & Associates Ltd., 33 Price St., Toronto 5, Ont., Canada (Electrothermics & Metallurgy)

Transfers to Active Membership

R. W. Stiegler, Jr., Texas Instruments, Inc., P. O. Box 5012, Dallas, Texas (Electronics—Semiconductors)

D. R. Wolter, Ray-O-Vac Co., 525 University Ave., Madison, Wis. (Battery)

Z. A. Foroulis, Esso Research & Engineering Co., P. O. Box 209, Madison, N. J. (Corrosion, Electronics—Semiconductors, Theoretical Electrochemistry)

Allen Gover, Texas Instruments, Inc.; Mail add: 1707 "O" Ave., Plano, Texas (Electronics—Semiconductors and Luminescence, Electrothermics & Metallurgy, Theoretical Electrochemistry)

H. H. Jennison, Jr., P. R. Mallory & Co., Inc.; Mail add: 840 S. Washington, Du Quoin, Ill. (Electronics—Semiconductors)

D. H. Jurden, Strategic-Udy Metallurgy Ltd., 3527 Stanley Ave., P. O. Box 300, Niagara Falls, Ont., Canada (Electrothermics & Metallurgy)

J. B. Lounsbury, Chemical Physics Section, Armour Research Foundation, 10 W. 35 St., Chicago 16, Ill.

Siego Matsuda, Cambridge Metal Research Inc., Natick Industrial Center, Natick, Mass. (Corrosion, Electrothermics & Metallurgy)

George Schick, Bell Telephone Labs., Inc.; Mail add: 351 Broad St., Newark 4, N. J. (Corrosion)

Personals

Donald H. Bissell has been named chairman of the board of Chromium Corp. of America, New York City. Mr. Bissell, who has been with the

December 1961 Discussion Section

A Discussion Section, covering papers published in the January-June 1961 JOURNALS, is scheduled for publication in the December 1961 issue. Any discussion which did not reach the Editor in time for the June 1961 Discussion Section will be included in the December 1961 issue.

Those who plan to contribute remarks for this Discussion Section should submit their comments or questions in triplicate to the Managing Editor of the JOURNAL, 1860 Broadway, New York 23. N. Y., *not later than September 1, 1961.* All discussion will be forwarded to the author(s) for reply before being printed in the JOURNAL.

firm for more than 35 years, formerly was president and chief executive officer. He has been instrumental in the growth of industrial chromium plating and in the development of many of today's established engineering practices.

Norman Craig, a member of the Electrochemistry Section of the National Bureau of Standards, Washington, D. C., has been awarded the U. S. Dept. of Commerce Gold Medal for Exceptional Service. He was cited for "outstanding work in the accurate determination of the faraday, an important fundamental constant of physics and chemistry."

Herbert A. Laitinen, professor of analytical chemistry at the University of Illinois, Urbana, is the winner of the American Chemical Society's 1961 Fisher Award in Analytical Chemistry for his fundamental contributions in electroanalytical chemistry. He gave his award address on March 22 before the Division of Analytical Chemistry at the 139th ACS National Meeting in St. Louis. In addition to being active in the teaching and research fields, Dr. Laitinen is secretary of the Commission on Electrochemical Data of the Analytical Section of the International Union of Pure and Applied Chemistry; a member of the Advisory Panel, Bureau of Standards, Chemistry Division I; editor of Monographs and Special Publications of The Electrochemical Society; and assistant editor of *Analytica Chimica Acta*. In 1960, Dr. Laitnen published "Chemical Analysis," his first solely authored textbook.

George H. Morrison, formerly head of inorganic and analytical chemistry at General Telephone & Electronics Labs., Inc., Bayside, N. Y., becomes professor of chemistry at Cornell University, Ithaca, N. Y., as of July. He also will be in charge of the analytical program of the Materials Science Center at Cornell.

Lincoln T. Work has been elected president of the Chemists' Club, New York City, for 1961-1962.

News Items

ECS Detroit Meeting, October 1961

The Detroit Section of The Electrochemical Society, being host to the National Meeting in October, wishes to point out that tickets to several excellent sports events may be obtained.

On October 1, 1961, the Detroit Lions will play San Francisco in Detroit, and the University of Michigan will meet U.C.L.A. on September 30 and Army on October 7 in Ann Arbor. Orders for tickets to the Detroit—San Francisco game may be placed by sending a check for $3.50 to Detroit Football Co., 1401 Michigan Ave., Detroit 16, Mich., after July 1. The University of Michigan tickets at $5.00 apiece may be obtained by writing Ticket Dept., Ferry Field, Ann Arbor, Mich. It is to be noted that Detroit is the home of the Detroit Tigers who may provide a sports spectacular about the time of the Meeting.

James P. Hoare, *Publicity Chairman*
ESC 1961 Fall Meeting

New ECS Sustaining Members

Hewlett-Packard Company, Palo Alto, Calif., recently became a Sustaining Member of The Electrochemical Society.

U. S. Steel Corporation, Pittsburgh, Pa., became a Sustaining Member of the Society as of January 1961.

International Symposium on Ultrapure Materials

An International Symposium entitled "Reinststoffe in Wissenschaft und Technik" has been announced, to be held in Dresden, East Germany, November 30 to December 2, 1961. The Symposium is sponsored by the Chemische Gesellschaft, the Gesellschaft Deutscher Berg- und Hüttenleute, and the Physikalische Gesellschaft, all of the Eastern Deutsche Demokratischen Republik. Foreign workers in the field are invited to attend and to submit 15-minute papers for presentation. Details may be obtained from Professor E. Rexer, Institut für Angewandte Physik der Reinststoffe Dresden, Winterbergstrasse 28, Dresden A 20.

Fuel, Heat Cells Open 15th Annual Power Sources Conference

Direct generation of electricity from fuel and heat is coming of age. The rapid development of fuel cells and thermal cells for the creation of electricity to the point of field testing with electronic equipment was emphasized at the 15th Annual Power Sources Conference, sponsored by the U. S. Army Signal Research and Development Lab., Fort Monmouth, N. J., May 9-11, at the Shelburne Hotel, Atlantic City, N. J.

For the first time, the Conference devoted an entire day to fuel cells —batteries that consume fuel without heat or open flames to produce electricity without the moving parts of conventional generators. Half a day was devoted to thermal energy conversion—direct generation of electricity from heat.

A spokesman for the Laboratory's Power Sources Division, host at the Conference, said that despite some previous claims, fuel cells consuming such exotic fuels as hydrogen, oxygen, and hydrogen peroxide, as well as more common substances such as hydrocarbons and alcohol, are not ready for general use.

Rather, he said, they have reached the stage where they can be tested under rugged field conditions as power sources for electrical and electronic equipment that previously used chemical batteries or power-driven mechanical generators. The same is true, he added, of thermal units that turn the heat of burning fuel directly into electricity without the necessity of going through a steam, gasoline, or diesel engine.

In addition to fuel and thermal batteries, solar energy conversion, primary, and secondary conventional batteries were subjects of discussion at the Conference. Development of reliable high-rate zinc-silver-oxide batteries for missiles was announced, as were the latest developments in radiation-resistant solar cells for satellite power. High-rate batteries release large jolts of power for relatively short periods.

Chairman of the Conference was Arthur F. Daniel, director of the Power Sources Division in the Laboratory.

18th International Congress of Pure and Applied Chemistry

Final arrangements have been concluded on the program of the 18th International Congress of Pure and Applied Chemistry to be held in Montreal, Canada, August 6-12, 1961.

Complete details are available in the recently published third circular, which is available from the Secretary, 18th International Congress of Pure and Applied Chemistry, National Research Council, Ottawa, Ont., Canada.

Announcement has been made of the title of the plenary lecture to be given by Academician N. N. Semenov, Moscow, U.S.S.R. It is: "Certain Chemical Reactions at Reduced Temperatures and Related Problems of Energy Transfer." [For titles of the

other plenary and sectional lectures, *see* p. 91C of the April 1961 JOURNAL.]

The third circular also gives the preliminary program for the 21st Conference of the Union of Pure and Applied Chemistry, business session of the Congress, on August 2 to 5, at the University of Montreal.

Ultralow-Conductivity Water

Applying an electrophoretic ion-exclusion technique, the National Bureau of Standards (1) recently succeeded in preparing water of extremely low ion content. The water obtained has an electrical conductivity of 0.039×10^{-6} ohm^{-1} at 18°C, indicating a residual ion content which is equivalent to a sodium chloride concentration of 1 ppb. Containing less than one third of the ionic impurities of the water prepared by Kohlrausch and Heydweiller in their historic purification experiments, this water approaches the theoretical conductivity—and ideal purity—more closely than any values previously reported in the literature.

The present research, undertaken by Wolfgang Haller and H. C. Duecker of the Bureau's staff, was part of a study on ion diffusion. In designing the purification procedure, two principal considerations were involved. First, instead of using multiple distillation as in the classic experiments, an electrophoretic procedure was applied. In this way, purest water was obtained in two hours, while, in the best previous study, 36 consecutive vacuum distillations were required. Second, the purification apparatus was designed to recirculate the purified water continuously through the electric field, thus immediately removing any ions which might originate from the walls of the apparatus and contaminate the already purified water.

By this kinetic method, it is possible to maintain the purity of the water if a container material with very low ion-release is used. While fused silica containers which had been exposed to water for ten years were utilized in former purifications, high-density polyethylene, platinum, and borosilicate glass which had been exposed to steam for a number of hours just before purification were found suitable for the present experiments. The steam condenses in the apparatus, thus rinsing its internal surfaces with a stream of freshly distilled water. At the temperature of this treatment, the diffusion of ions from the glass—which is the main potential source of ionic impurities—is many times faster than at the temperatures at which the apparatus is used, resulting in an effective depletion of the surface regions of the glass from objectionable ions.

Reference

1. For further technical information, *see* "Ultra Low-Conductivity Water by Electrophoretic Ion Exclusion," by Wolfgang Haller and H. C. Duecker, *J. Research NBS*, **64A** (Phys. and Chem.), 527 (Nov.-Dec. 1960).

Burgess Battery Expands Line of Mercury Cells and Batteries

Expansion of Burgess Battery Co.'s line of mercury cells and batteries into a full selection for wide-range industrial, instrument, and electronic applications requiring constant voltage power sources was announced recently.

From the 17 basic types of mercury cells in the complete Burgess line, a virtually unlimited variety of multiple-cell batteries now can be designed to meet varying specifications for space, weight, voltage, battery life, or other special conditions, according to Dr. Joseph J. Coleman, vice-president of engineering.

The greatly expanded mercury cell line is a further extension of the company's lines of batteries, which previously included more than 3000 different types of dry cells, nickel-cadmium, and reserve batteries—together comprising the widest range of batteries offered by any U.S. battery manufacturer.

"Burgess long has been the industry leader in designing and manufacturing special purpose batteries for military, industrial, and scientific uses," Dr. Coleman declared. "By extending our design and consultation service on special batteries to the mercury battery field, we can assure designers of electronic and electrical products complete assistance in meeting all special battery needs," he explained.

Mercury batteries primarily are specified when a constant voltage level is of prime importance. The new Burgess batteries and cells operate either intermittently or continuously through a wide range of temperature and pressure conditions, providing energy uniformly and dependably after many months or extended periods of storage.

In addition to the basic standard cells and multiple cell batteries, more than 60 types of Burgess mercury batteries are available on special order, and others can be designed to customers' specifications, the company noted.

Complete technical data on the standard and special order lines, as well as special consultation on design problems, can be obtained by writing Engineering Dept., Burgess Battery Co., Freeport, Ill.

Book Reviews

Viscoelastic Properties of Polymers, by John D. Ferry. Published by John Wiley & Sons, Inc., New York City, 1961. 482 pages; $15.00.

This is a highly specialized and highly mathematical treatment of a science which cuts across several conventional fields, although even the less mathematically trained reader will find much material which

Brief Communications

The JOURNAL accepts short technical reports having unusual importance or timely interest, where speed of publication is a consideration. The communication may summarize results of important research justifying announcement before such time as a more detailed manuscript can be published. Consideration also will be given to reports of significant unfinished research which the author cannot pursue further, but the results of which are of potential use to others. Comments on papers already published in the JOURNAL should be reserved for the Discussion Section published biannually.

Submit communications in triplicate, typewritten double-spaced, to the Editor, Journal of The Electrochemical Society, 1860 Broadway, New York 23, N. Y.

will increase his understanding of the flow properties of many of our important commercial materials.

The nature of viscoelastic behavior is explained with illustrations in the field of high polymers. The exact interrelations among the viscoelastic functions are explored with the help of the classic Maxwell and Voigt mechanical analogies. Methods of exact and approximate calculation are followed by experimental methods used for the study of viscoelastic liquids, soft and hard viscoelastic solids, and fibers.

The basic molecular theory underlying the rheology of linear and cross-linked polymeric systems is discussed. Both the rubbery state of matter and the glassy state, as well as the transition zone from rubber-like to glass-like consistency, are given much attention. Phenomena found in concentrated polymer solutions, plasticized polymers, and gels are compared.

The glareless finish of the paper in this book is commendable. It greatly reduces the strain on the eyes of the reader.

Henry S. Myers

Thermoelectricity. Edited by Paul H. Egli. Published by John Wiley & Sons, Inc., New York City, 1960. 407 pages; $10.00.

Most of the chapters of this book were presented at the Conference on Thermoelectricity sponsored by the Naval Research Laboratory in September 1958 and are somewhat dated. The four sections of the book are: I. Fundamental Concepts in Thermoelectricity, II. Basic Parameters in Thermoelectricity, III. Chemical and Physical Properties of Materials at High Temperatures, IV. Measurement of Material Properties.

The 23 chapters in the four sections provide much specific guidance for engineers and scientists working in the field, and an excellent overall view for those wishing introduction to this new field.

S. C. Hyman

Meetings of Other Organizations

Oct. 4-6—National Association of Corrosion Engineers, Western Regional Conference, Hotel Multnomah, Portland, Ore.

Oct. 9-11—National Association of Corrosion Engineers, North Central Regional Conference, Chase-Park Plaza Hotel, St. Louis, Mo.

Oct. 9-13—American Rocket Society, Space Flight Report to the Nation, New York Coliseum, New York, N. Y.

Oct. 30-Nov. 2—National Association of Corrosion Engineers, Northeast Regional Conference, Hotel Statler, New York, N. Y.

Announcements from Publishers

"Electronic Packaging with Resins: A Practical Guide for Materials and Manufacturing Techniques," by Charles A. Harper. Published by McGraw-Hill Book Co., New York City, 1961. 360 pages; $11.00.

"Germanium and Silicon," Selective Bibliography SB-437,* 10 cents.

"Antimony, Bismuth, Gallium, Indium, Selenium, and Tellurium," Selective Bibliography SB-438,* 10 cents.

"Low Temperature Research on Materials," Selective Bibliography SB-451,* 10 cents.

"High Temperature Research," Selective Bibliography SB-453,* 10 cents.

"Molten and Fused Salts," Selective Bibliography SB-425,* 10 cents.

"Hydrolysis of Water-Saturated Chlorofluorocarbons in the Presence of Metals and the Associated Corrosion," Feb. 1961. AEC Report K-1461,* 20 pages; 50 cents.

"Oxidation Potential of the Ce (III): Ce (IV) Couple as a Function of Temperature in Perchloric Acid Solutions—Thermodynamic Properties," Aug. 1960. AEC Report UCRL-9332,* 46 pages; $1.00.

"High-Temperature Metallurgy and Heat-Resistant Alloys." Selective Bibliography SB-452,* 34 pages; 10 cents.

"Thermistors and Resistors." Selective Bibliography SB-429*; 10 cents.

"Thermopiles and Thermocouples." Selective Bibliography SB-430*; 10 cents.

"Thermionics and Cathodes." Selective Bibliography SB-431*; 10 cents.

"Ferroelectricity and Ferromagnetism." Selective Bibliography SB-434*; 10 cents.

"Review of Research and Development at the Idaho Chemical Processing Plant on the Electrolytic Dissolution of Nuclear Fuel," Feb. 1961. AEC Report IDO-14535,* 57 pages; $1.25.

"Cut the Cost of Producing Ferrosilicon in Electric Furnaces," Oct. 1960, Moscow. Translation of an article by Ya. S. Shchedrovitskiy and Yu. S. Maksimov in the Russian-language journal *Stal'* (Steel), No. 10. Translation 61-11684,* 12 pages; 50 cents.

"Gas Atmosphere Effects on Materials," R. A. Baughman, General Electric Co., for Wright Air Development Div., U. S. Air Force, May 1960. Report PB 161 980,* 232 pages; $3.50.

"Recent Developments in Casting Resins and Technology for Electrical Encapsulation Applications," Plastics Technical Evaluation Center, Picatinny Arsenal, N. J., for Dept. of Defense, Nov. 1960. Report PB 171 034,* 34 pages.

"Nitrogen Tetroxide Corrosion Studies," C. W. Alley and others, Allied Chemical Corp., for Wright Air Development Div., U. S. Air Force, July 1960. Report PB 171 301,* 40 pages; $1.75.

"The Determination of the Effects of Elevated Temperatures on the Stress Corrosion Behavior of Structural Materials," F. A. Crossley and others, Armour Research Foundation of Illinois Institute of Technology, for Wright Air Development Div., U. S. Air Force, May 1960. Report PB 161 962,* 53 pages; $1.50.

"Research Investigation to Determine the Optimum Conditions for Growing Single Crystals of Selected Borides, Silicides, and Carbides," A. D. Kiffer, Linde Co. of Union Carbide Corp., for Wright Air Development Div., U. S. Air Force, April 1960. Report PB 161 792,* 24 pages; $1.00.

"Peltier Effects for Crystal Growing," Louis L. Thomas, Research Chemicals Div. of Nuclear Corp. of America, for Wright Air Development Div., U. S. Air Force, May 1960. Report PB 161 985,* 45 pages; $1.50.

* Order from Office of Technical Services, Business and Defense Services Administration, U.S. Dept. of Commerce, Washington 25, D. C.

"Second Status Report on Fuel Cells," B. R. Stein and E. M. Cohn, Office of the Chief of Research and Development, Dept. of the Army, Dec. 1960. Report PB 171 155,* 80 pages; 75 cents.

"Compliant Electrodes for Dielectric Measurements," Andrew R. Blanck, Feltman Research Labs., Picatinny Arsenal, U. S. Army, Aug. 1960. Report PB 161 670,* 15 pages; 50 cents.

"Synthesis and Purification of Dielectric Materials," W. C. Divens, and others, Westinghouse Electric Corp., for Wright Air Development Div., U. S. Air Force, Sept. 1960. Report PB 171 364,* 77 pages; $2.00.

"Electroanalytical Method for the Determination of Carbon and Hydrogen in Organic Compounds," H. S. Haber and K. W. Gardiner, Bell & Howell Research Center, for Wright Air Development Div., U. S. Air Force, Sept. 1960. Report PB 171 409,* 26 pages; 75 cents.

"Corrosion of Materials by Lithium at Elevated Temperatures," E. E. Hoffman, Union Carbide Corp., for U. S. Atomic Energy Commission. Report ORNL-2924,* 147 pages; $2.75.

"Fundamental Studies of the Chemistry and Physics of Organic Materials Adsorbed on Metal Substrates," H. A. Roth, R. F. Lumb, and C. M. Doede, Quantum Inc., for Wright Air Development Div., U. S. Air Force, April 1960. Report PB 161 840,* 149 pages; $2.75.

"A Study of the Effects of Surface Films on the Mechanical Properties of Metals," I. R. Kramer, Martin Co., for Wright Air Development Div., U. S. Air Force, July 1960. Report PB 171 150,* 34 pages; $1.00.

* Order from Office of Technical Services, Business and Defense Services Administration, U.S. Dept. of Commerce, Washington 25, D. C.

Advertiser's Index

Anaconda American Brass Company 128C

Bell Telephone Laboratories, Inc. 127C

Great Lakes Carbon Corp., Electrode Division ..... Cover 2

New Products

High-Throw, Bright-Nickel Plating Process. Metal & Thermit Corp. has announced a new process for plating bright nickel deposits. The process, a Watts-type bath that can be used with either air or mechanical agitation, gives high-brilliance deposits with excellent brightening rates and outstanding chromium receptivity. Further information and technical data available from Metal & Thermit Corp., General Offices, Rahway, N. J.

Alumon "D," a new simplified method of plating on aluminum utilizing a dilute zincate solution, has been developed by Enthone, Inc., 442 Elm St., New Haven 8, Conn., subsidiary of American Smelting and Refining Co. The new zincating bath is made up at a concentration of only 1 lb/gal of Alumon "D" salts.

Subminiature Four-Layer Diode. Shockley Transistor unit of Clevite Transistor, Stanford Industrial Park, Palo Alto, Calif., has announced a new subminiature "glass" package for its four-layer diode. The new diode, designated as Type E, is capable of handling 10 amp pulses or 150 ma of continuous current, three times the capacity of the nearest comparable type of four-layer diode.

Oxide-Removing "Dip." Electroplating onto copper and copper-alloy printed circuits is said to be substantially improved by Deoxyde, which reportedly removes oxides, light soils, fingermarks, and similar plating deterrents, through a simple dipping operation. The new formulation is said to clean without affecting plating resists, or etching copper circuits, thus promoting reject-free production of subsequent electroplating operations. A product bulletin giving details and applications data is available from the manufacturer, The Meaker Co., subsidiary of Sel-Rex Corp., Nutley, N. J.

Literature from Industry

MacDermid Alumetex Process for preparing aluminum alloys for electroplating, which can be used to plate all commonly electroplated metals on all aluminum alloys, is fully described in Technical Data Sheet No. 13, a six-page usage and instruction sheet prepared by MacDermid Inc., Waterbury, Conn.

Raytheon Co. Catalog. More than 150 different silicon diffused rectifiers are described in a new six-page catalog available free from Warren Schoonmaker, Semiconductor Div., Raytheon Co., 215 First Ave., Needham, Mass.

"The Corrosion Resistance of Zirconium." This 14-page book contains detailed graphs for over 100 highly corrosive media in concentrations up to 100% and temperatures up to 400°F. Available from Zirconium Association, 2130 Keith Bldg., Cleveland 15, Ohio.

Employment Situations

Positions Available

Four challenging research positions for experienced surface chemists, in fully-equipped laboratory devoted to research and development on aluminum and copper alloys, involving: A. Electrochemical kinetics, adsorption, and oxide film structure investigations related to finishing processes. B. Studies of interfacial surface reactions between polymeric resins and metal oxide surfaces relating to strength and permanence of joints in the adhesive bonding of metals. C. Mechanisms relating to surface phenomena, associated with liquid metal-solid metal inter-action as applied to soldering and brazing. D. Surface and electrochemical reactions effecting the kinetics of general, localized, and stress corrosion processes. Pleasant living, with access to major university. Send reply to R. H. Endriss, Personnel Manager, Olin Mathieson Chemical Corp., 125 Munson St., New Haven, Conn.

Solid-State Chemists — Research and development group seeks chemist or chemical physicist for solid-state work on cathodoluminescent and electroluminescent materials, photoconductors, and chemicals for electronic applications. Candidates should have Ph.D. or equivalent and be capable of independent work. Unexperienced as well as experienced candidates will be considered. Modern and well-equipped laboratories, in northeastern Pennsylvania. Publication of work encouraged. Send résumé to: D. F. Fortney, Technical Services, Chemical and Metallurgical Division, Sylvania Electric Products Inc., Towanda, Pa.

The Electrochemical Society

INSTRUCTIONS TO AUTHORS OF PAPERS

(Revised as of 1/1/61)

Address all correspondence to the Editor, JOURNAL OF THE ELECTROCHEMICAL SOCIETY, 1860 BROADWAY, NEW YORK 23, N. Y.

GENERAL

Manuscripts must be submitted in triplicate to expedite review. They should be typewritten, double-spaced, with 2½-4 cm margins.

Title should be brief, followed by the author's name and business or university connection. Authors should be as brief as is consistent with clarity and should omit introductory or explanatory material which may be regarded as familiar to specialists in the particular field. Proprietary and trade names should be avoided if possible; if used, they should be capitalized to protect the owners' rights.

Authors may suggest qualified reviewers for their papers, but the JOURNAL reserves the right of final choice.

TYPES OF ARTICLES

Technical Articles must describe original research of basic nature and must have adequate scientific depth. Articles of wide diversity of interest are appropriate, but subjects primarily covered in other specialized journals (*e.g.*, analytical or nuclear chemistry) are not considered appropriate. An ***Abstract*** of about 100 words should state the scope of the paper and summarize its results. Suitable headings and subheadings should be included, but sections should not be numbered. Articles in recent issues of the JOURNAL should be consulted for current style.

Technical Notes are used for reporting briefer research, developmental work, process technology; new or improved devices, materials, techniques, or processes which do not involve more basic scientific study. No abstract is required.

Brief Communications are used only to report new information of scientific or technological importance which warrants rapid dissemination.

ILLUSTRATIONS

Drawings and ***Graphs*** ordinarily will be reduced to column width, 8.3 cm, and after such reduction should have lettering no less than 0.15 cm high. Lettering must be of letter-guide quality. India ink on tracing cloth or paper is preferred, but India ink on coordinate paper with blue ruling is acceptable. The sample graph shown on the reverse page conforms to suggestions of the American Standards Association (ASA Report Y15.1-1959).

Photographs should be used sparingly, must be glossy prints, and should be mailed with protection against folding. ***Micrographs*** should have a labeled length unit drawn or pasted on the picture.

Captions for figures (including photographs) must be included on a separate sheet. Captions and figure numbers must *not* appear in the body of the figure; they will be removed if they do.

Numerical Data should not be duplicated in tables and figures.

EQUATIONS

Mathematical Equations should be written on a single line if possible, and parentheses, brackets, the solidus (/), negative exponents, etc., may be used freely for this purpose. Authors are urged to consult Chapter VI of the "Style Manual" of the American Institute of Physics (available for $1.00 at American Institute of Physics, 57 East 55 St., New York 22, N. Y.) and to follow the patterns described there.

SYMBOLS

If more than a few ***Symbols*** are used, they should be defined in a list at the end of the paper, with units given. For example:

$a, b \ldots$ = empirical constants of Brown equation

f_i^* = fugacity of pure ith component, atm

D_v = volume diffusion coefficient, cm^2/sec

ABBREVIATIONS

The AIP "Style Manual" referred to here gives a suitable list of common ***Abbreviations***. Units usually will be abbreviated without periods throughout the text, as sec, min, hr, cm, mm, etc.

UNITS

Metric Units should be used throughout, unless English units are clearly more appropriate in the area of discussion.

POTENTIAL SIGNS

Electrode Potentials: Authors are urged to state and make use of the polarity of test electrodes with respect to the reference electrode used, *i.e.*, Zn is normally negative, Cu normally positive with respect to the standard hydrogen electrode. The sign for the emf of a cell should conform to the free energy change of the chemical reaction as written or implied, in accordance with the definition $\Delta G = -nFE$. These suggestions agree with the IUPAC conventions adopted in 1953. If any other convention is used, it should be stated clearly and used consistently throughout the manuscript.

REFERENCES

Literature References should be listed on a separate sheet at the end of the paper in the order in which they are cited in the text. Authors' initials must be given, and the style and abbreviations adopted by *Chemical Abstracts* should be used. Any recent issue of the JOURNAL may be consulted.

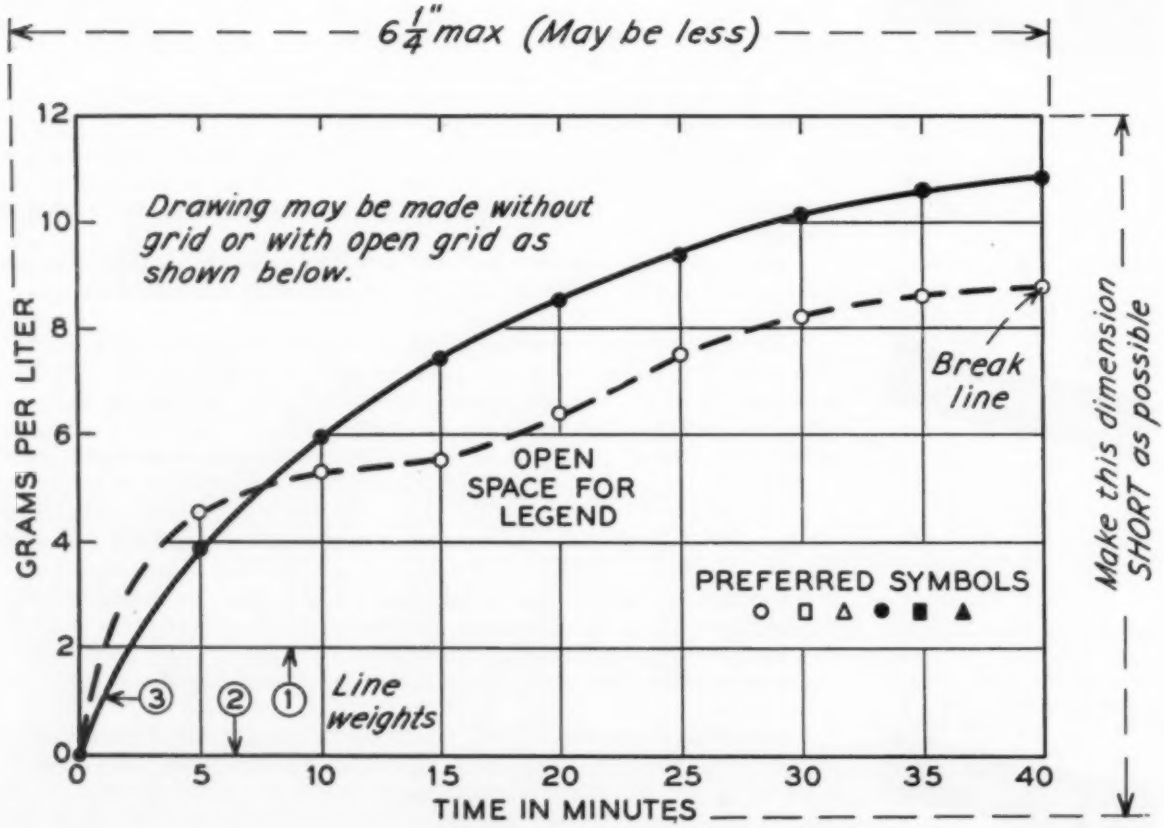

Remarks: Line weight 2 is used for borders and zero lines. When several curves are shown, each may be numbered and described in the caption. Lettering shown is approximately ⅛ in. In plotting current or potential as ordinate, increasing negative values should go down.

SAMPLE CURVE DRAWING FOR REDUCTION TO $\frac{1}{2}$ SIZE

The Electrochemical Society

Patron Members

Aluminum Co. of Canada, Ltd., Montreal, Que., Canada
International Nickel Co., Inc., New York, N. Y.
Olin Mathieson Chemical Corp., Chemicals Div., Industrial Chemicals Development Dept., Niagara Falls, N. Y.
Union Carbide Corp.
Divisions:
Union Carbide Metals Co., New York, N. Y.
National Carbon Co., New York, N. Y.
Westinghouse Electric Corp., Pittsburgh, Pa.

Sustaining Members

Air Reduction Co., Inc., New York, N. Y.
Ajax Electro Metallurgical Corp., Philadelphia, Pa.
Allen-Bradley Co., Milwaukee, Wis.
Allied Chemical Corp.
Solvay Process Div., Syracuse, N. Y.
General Chemical Div., Morristown, N. J.
Alloy Steel Products Co., Inc., Linden, N. J.
Aluminum Co. of America, New Kensington, Pa.
American Metal Climax, Inc., New York, N. Y.
American Potash & Chemical Corp., Los Angeles, Calif. (2 memberships)
American Smelting and Refining Co., South Plainfield, N. J.
American Zinc Co. of Illinois, East St. Louis, Ill.
American Zinc, Lead & Smelting Co., St. Louis, Mo.
American Zinc Oxide Co., Columbus, Ohio
M. Ames Chemical Works, Inc., Glens Falls, N. Y.
Armco Steel Corp., Middletown, Ohio
Basic Inc., Maple Grove, Ohio
Bell Telephone Laboratories, Inc., New York, N. Y. (2 memberships)
Bethlehem Steel Co., Bethlehem, Pa. (2 memberships)
Boeing Airplane Co., Seattle, Wash.
Burgess Battery Co., Freeport, Ill. (4 memberships)
Canadian Industries Ltd., Montreal, Que., Canada
Carborundum Co., Niagara Falls, N. Y.
Catalyst Research Corp., Baltimore, Md.
Columbian Carbon Co., New York, N. Y.
Columbia-Southern Chemical Corp., Pittsburgh, Pa.
Consolidated Mining & Smelting Co. of Canada, Ltd., Trail, B. C., Canada (2 memberships)
Continental Can Co., Inc., Chicago, Ill.
Cooper Metallurgical Associates, Cleveland, Ohio
Corning Glass Works, Corning, N. Y.
Diamond Alkali Co., Painesville, Ohio
Dow Chemical Co., Midland, Mich.
Wilbur B. Driver Co., Newark, N. J. (2 memberships)
E. I. du Pont de Nemours & Co., Inc., Wilmington, Del.
Eagle-Picher Co., Chemical Div., Joplin, Mo.
Eastman Kodak Co., Rochester, N. Y.
Thomas A. Edison Research Laboratory, Div. of McGraw-Edison Co., West Orange, N. J.
Electric Auto-Lite Co., Toledo, Ohio
C & D Division, Conshohocken, Pa.
Electric Storage Battery Co., Yardley, Pa.
Englehard Industries, Inc., Newark, N. J. (2 memberships)
The Eppley Laboratory, Inc., Newport, R. I. (2 memberships)
Exmet Corp., Tuckahoe, N. Y.
Fairchild Semiconductor Corp., Palo Alto, Calif.
Food Machinery & Chemical Corp.
Becco Chemical Div., Buffalo, N. Y.
Westvaco Chlor-Alkali Div., South Charleston, W. Va.
Foote Mineral Co., Paoli, Pa.
Ford Motor Co., Dearborn, Mich.
General Electric Co., Schenectady, N. Y.
Chemistry & Chemical Engineering Component, General Engineering Laboratory
Chemistry Research Dept.
General Physics Research Dept.
Metallurgy & Ceramics Research Dept.
Aircraft Accessory Turbine Dept., West Lynn, Mass.
General Instrument Corp., Newark, N. J.

(Sustaining Members cont'd)

General Motors Corp.
Delco-Remy Div., Anderson, Ind.
Guide Lamp Div., Anderson, Ind.
Research Laboratories Div., Warren, Mich.
General Telephone & Electronics Laboratories Inc., Bayside, N. Y. (2 memberships)
Gillette Safety Razor Co., Boston, Mass.
Globe-Union, Inc., Milwaukee, Wis.
Gould-National Batteries, Inc., Minneapolis, Minn.
Grace Electronic Chemicals, Inc., Baltimore, Md.
Great Lakes Carbon Corp., New York, N. Y.
Hanson-Van Winkle-Munning Co., Matawan, N. J. (2 memberships)
Harshaw Chemical Co., Cleveland, Ohio (2 memberships)
Hercules Powder Co., Wilmington, Del.
Hewlett-Packard Co., Palo Alto, Calif.
Hill Cross Co., Inc., West New York, N. J.
Hoffman Electronics Corp., Semiconductor Div., El Monte, Calif. (2 memberships)
Hooker Chemical Corp., Niagara Falls, N. Y. (3 memberships)
Hughes Aircraft Co., Culver City, Calif.
International Business Machines Corp., Yorktown Heights, N. Y.
International Minerals & Chemical Corp., Skokie, Ill.
ITT Federal Laboratories, Div. of International Telephone & Telegraph Corp., Nutley, N. J.
Jones & Laughlin Steel Corp., Pittsburgh, Pa.
K. W. Battery Co., Skokie, Ill.
Kaiser Aluminum & Chemical Corp.
Div. of Chemical Research, Permanente, Calif.
Div. of Metallurgical Research, Spokane, Wash.
Kawecki Chemical Co., Boyertown, Pa.
Kennecott Copper Corp., New York, N. Y.
Libbey-Owens-Ford Glass Co., Toledo, Ohio
Mallinckrodt Chemical Works, St. Louis, Mo.
P. R. Mallory & Co., Indianapolis, Ind.
Merck & Co., Inc., Rahway, N. J.
Metal & Thermit Corp., Detroit, Mich.
Miles Chemical Co., Div of Miles Laboratories, Inc., Elkhart, Ind.
Minnesota Mining & Manufacturing Co., St. Paul, Minn.
Monsanto Chemical Co., St. Louis, Mo.
Motorola, Inc., Chicago, Ill.
National Cash Register Co., Dayton, Ohio
National Lead Co., New York, N. Y.
National Research Corp., Cambridge, Mass.
National Steel Corp., Weirton, W. Va.
North American Aviation, Inc., Rocketdyne Div., Canoga Park, Calif.
Northern Electric Co., Montreal, Que., Canada
Norton Co., Worcester, Mass.
Ovitron Corp., Long Island City, N. Y.
Peerless Roll Leaf Co., Inc., Union City, N. J.
Pennsalt Chemicals Corp., Philadelphia, Pa.
Phelps Dodge Refining Corp., Maspeth, N. Y.
Philco Corp., Philadelphia, Pa.
Philips Laboratories, Inc., Irvington-on-Hudson, N. Y.
Potash Co. of America, Carlsbad, N. Mex.
Radio Corp. of America
Tube Div., Harrison, N. J.
RCA Victor Record Div., Indianapolis, Ind.
Ray-O-Vac Co., Madison, Wis.
Raytheon Co., Waltham, Mass.
Reynolds Metals Co., Richmond, Va.
Rheem Semiconductor Corp., Mountain View, Calif.
Schering Corporation, Bloomfield, N. J.
Shawinigan Chemicals Ltd., Montreal, Que., Canada
Speer Carbon Co.
International Graphite & Electrode Div., St. Marys, Pa.
Sprague Electric Co., North Adams, Mass.
Stackpole Carbon Co., St. Marys, Pa.
Stauffer Chemical Co., New York, N. Y.
Tennessee Products & Chemical Corp., Nashville, Tenn.
Texas Instruments, Inc., Dallas, Texas
Metals and Controls Corp., Attleboro, Mass.
Three Point One Four Corp., Yonkers, N. Y.
Titanium Metals Corp. of America, Henderson, Nev.
Tung-Sol Electric Inc., Newark, N. J.
Udylite Corp., Detroit, Mich. (4 memberships)
Universal-Cyclops Steel Corp., Bridgeville, Pa.
Upjohn Co., Kalamazoo, Mich.
U. S. Steel Corp., Pittsburgh, Pa.
Victor Chemical Works, Chicago, Ill.
Western Electric Co., Inc., Chicago, Ill.
Wyandotte Chemicals Corp., Wyandotte, Mich.
Yardney Electric Corp., New York, N. Y.